UNIVERSIDADE DE LISBOA
FACULDADE DE CIÊNCIAS

UNIVERSITY OF ST. ANDREWS
SCHOOL OF BIOLOGY

Investigation of fin whales using ocean-bottom recordings

Doutoramento em Ciências do Mar

Andreia Filipa da Silva Pereira

Tese orientada por:
Prof. Doutor Luis Manuel Henriques Marques Matias
Prof. Doutor Len Thomas
Prof. Doutor Peter Tyack

Documento especialmente elaborado para a obtenção do grau de doutor

2018

UNIVERSIDADE DE LISBOA
FACULDADE DE CIÊNCIAS

UNIVERSITY OF ST. ANDREWS
SCHOOL OF BIOLOGY

Investigation of fin whales using ocean-bottom recordings

Doutoramento em Ciências do Mar

Andreia Filipa da Silva Pereira

Tese orientada por:
Prof. Doutor Luis Manuel Henriques Marques Matias, Prof. Doutor Len Thomas, Prof. Doutor Peter Tyack

Júri:

Presidente:

- Doutor João Manuel de Almeida Serra, Professor Catedrático, Faculdade de Ciências da Universidade de Lisboa

Vogais:

- Doutor Peter Lloyd Tyack, Professor, School of Biology da Universidade of St. Andrews, Escócia (orientador)
- Doutor Tiago André Lamas Oliveira Marques, Research Fellow, School of Mathematics and Statistics da Universidade of St. Andrews, Escócia
- Doutor Manuel Eduardo dos Santos, Professor Associado, Instituto Universitário de Ciências Psicológicas, Sociais e da Vida - ISPA
- Doutora Cristina Brito, Investigadora FCT, Faculdade de Ciências Sociais e Humanas da Universidade Nova de Lisboa
- Doutora Maria Paula Pompeu de Miranda Rodrigues de Teves Costa, Professora Auxiliar, Faculdade de Ciências da Universidade de Lisboa
- Doutora Susana Inês da Silva Custódio, Professora Auxiliar, Faculdade de Ciências da Universidade de Lisboa

Documento especialmente elaborado para a obtenção do grau de doutor

Fundação para a Ciência e a Tecnologia (SFRH/BD/52554/2014), from the Doctoral Programme - PD/143/2012 - Lisbon Doctoral School on Earth System Science, Instituto Dom Luiz (IDL)

2018

ACKNOWLEDGMENTS

My academic career has gone through several life-changing moments and this thesis was one of those occasions. From studying the behaviour of big cats and dogs, to analysing photographs of dorsal fins of bottlenose dolphins of an African country (São Tomé and Príncipe), I was always looking for opportunities where I could learn more about wildlife and where I could develop different skills to help protect biodiversity. For this thesis I had to learn a lot about concepts and scientific areas that were far away from my "comfort zone". Suddenly, I had to learn about seismic waves and several seismic methods, sound propagation and passive acoustic monitoring of cetaceans. The animals that I was used to seeing in person or in photographs were transformed into numbers and acoustic signals. It was really an adventure and I could not have been happier with this experience! I could not have done this without the help and support of my supervisors, friends and colleagues.

To Professor Luis Matias, thank you for your incredible support and guidance. I am very grateful for your patience with my lack of knowledge and your assistance in every step of this thesis.

To Professor Len Thomas and Peter Tyack, who guided me through the treacherous waters of statistics and bioacoustics. Also, thank you for having me in St. Andrews and for the opportunities to learn more about these two scientific areas that were almost foreign to me.

To Danielle Harris, you were the real MVP. Without all of your help and guidance in every single step of this thesis I could not have done this. I could not thank you enough.

To professor Pedro Miranda, the head of Instituto Dom Luiz and program director of the Earthsystems doctoral school, I am very grateful for giving me the opportunity to take this PhD.

To my "esteemed colleagues" Mariana Santos e Vânia Lima, thank you for all of the conversations, jokes and support. It seems that we actually end this thing…

To my "coop friends" Cláudia Faustino, Jesus Alcazar, Martin Dobry who transformed my first long period in St. Andrews into an awesome time! It was the first time I was by myself and far away from my family for such a long time and with you three the time went by so quickly! Thank you!

To the Matthews, Marlene and Denis, thank you for having me in your home! You were my saviours in my last period in St. Andrews. I am extremely grateful for your kindness (I'm sorry that my last months were so busy and I couldn't be a better company).

To Kit Kovacs and Christian Lydersen, I am extremely grateful for giving me the opportunity to travel to Svalbard and be a part of your team in one of your scientific ship surveys. Although my body wasn't cooperating with my mind (damn you seasickness), it was a travel of a lifetime! I will never forget the beautiful landscape and my first time being so close to a blue whale! Thank you José Luis for being a part of this journey to Svalbard with me and taking care of the OBS.

To Tiago Marques, I am extremely grateful for helping me with distance sampling and taking the time to evaluate my progress throughout the years, in the annual seminars.

To Inês Carvalho and Cristina Brito, who were the driving forces of my academic career in cetacean ecology and conservation. Thank you for taking me into your team and for always being there for me.

To my family, especially my mother who continues to give me unconditional support. Although there were times when I felt I was not going to end this, my mother never doubt me. *Obrigada mãezinha!*

And finally but not the least, to my partner in crime, Francisco Martinho, thank you for your omnipresence and support.

ABSTRACT

Instruments used for seismic monitoring (OBS) have been recording baleen whales along with the target data. These long-term datasets provide valuable information for the study of large cetaceans that would otherwise be difficult to obtain due to economic and logistic reasons. Fin whales are classified as 'Endangered' species and therefore knowledge about population size and spatial and temporal distribution patterns is essential for good management strategies. In Portugal, sightings of fin whales off mainland waters are rare and are insufficient to assess any kind of trend. In this context, seismic datasets may become one of the primary sources of information on a year-round basis. The general aim of this thesis was to demonstrate the use of acoustic datasets, collected for non-biological focussed studies, such as seismic data, to study fin whales. Between September 2007 and August 2008 a network of 24 OBS was deployed off southwest Portugal with the main aim to obtain data to study the microseismicity originating from potential tsunami sources. During this time fin whale sounds were also recorded. The main acoustic signal produced by fin whales used in this thesis was the 20-Hz call. A detection process to detect the 20-Hz call was developed (Chapter 2) and the resulting dataset of automatic detections was used to: 1) estimate a relative location, i.e. a range from the recording instrument, of the automatic detections with the single-station method and develop a classification scheme that help deciding if a detection was from a 20-Hz call and if the range estimates were inside the critical area of the single station (Chapter 3); 2) characterize the 20-Hz call and assess the existence of different acoustic groups (Chapter 4); 3) obtain an average fin whale density and abundance (Chapter 5); and 4) assess the impact of acoustic interference on the 20-Hz call and infer about the depth of the calling fin whale (Chapter 6). This thesis showed how OBS data can be used in different types of studies about fin whales and provide valuable information for cetacean conservation.

Keywords: Ocean-bottom seismometer (OBS), fin whale, cetacean, bioacoustics, wildlife conservartion

RESUMO

Em sismologia, as estações sísmicas de fundo oceânico (OBS), são geralmente utilizadas para caracterizar a estrutura da Terra, localizar terramotos e registar ruído antropogénico. Dependendo das configurações dos instrumentos e parâmetros de registo, alguns OBS podem fornecer registos acústicos de longa duração e cobrir extensas áreas geográficas. A baixa taxa de amostragem a que os instrumentos de observação sísmica de longa duração gravam, entre 40 a 100 Hz, permite que registam não só os dados-alvo, como também sinais biológicos de baixa frequência, como certos sons de baleias de barbas. As duas espécies de baleias de barbas que produzem os sons de frequência mais baixa são a baleia-azul (*Balaenoptera musculus*) e a baleia-comum (*Balaenoptera physalus*). Ambas foram caçadas de forma intensiva durante o século XX e algumas das suas populações foram severamente reduzidas. As duas espécies apresentam distribuições geográficas extensas e hábitos pelágicos, o que dificulta a sua monitorização sistemática. Por isto, dados acústicos adquiridos por OBS podem fornecer informação valiosa sobre a distribuição espacial e abundância das populações.

Esta tese teve como objectivo principal demonstrar o uso de conjuntos de dados colectados para estudos não biológicos, como o caso de dados sísmicos, para estudar baleias-comuns a sudoeste de Portugal. Em Portugal, apesar das baleias-comuns apresentarem um estatuto de conservação “Ameçado”, informação-base sobre a ocorrência desta espécie é escassa e existem poucos recursos para executar estudos de longa duração. Neste contexto, conjuntos de dados sísmicos podem tornar-se numa das fontes de informação principais obtidas ao longo do ano, permitindo a avaliação da presença de baleias que vocalizam, distribuição, abundância e possíveis tendências. Várias questões sobre a ocorrência e estrutura populacional da baleia-comum em Portugal continental permanecem por responder. Esta tese traz uma abordagem multidisciplinar ao estudo da baleia-comum, utilizando métodos da sismologia, acústica, ecologia e estatística. Entre 2007 e 2008, um conjunto de 24 OBS foi colocado no fundo oceânico, a sudoeste de Portugal, com o objectivo principal de colectar dados para o estudo da microssismicidade originada por potenciais fontes de tsunamis. Durante este período, sinais acústicos produzidos por baleias-comuns também foram registados.

No Capítulo 2 pretendeu-se desenvolver um processo de detecção da vocalização mais comum produzida pela baleia-comum, a vocalização de 20-Hz. Um algoritmo para detecção, que incluiu uma correlação cruzada normalizada entre um modelo da vocalização de 20-Hz e a forma de onda dos registos acústicos, foi incluído no software de sísmica

SEISAN. O algoritmo foi executado diversas vezes com configurações diferentes, criando vários “detectores”. A precisão dos detectores foi avaliada usando uma subamostra aleatória sistemática dos registos acústicos dos OBS. Os resultados mostraram que existiam diferentes detectores adequados, dependendo dos objectivos da análise em particular. Em primeiro lugar, um detector mostrou ser mais adequado para estudos que visavam estimativas da abundância, nas quais o objectivo principal é detectar vocalizações acima de um limite dos parâmetros incluídos no algoritmo. Houve ainda um segundo detector que demonstrou ser mais adequado para avaliar o comportamento e movimentos de pequena-escala do animal que está a vocalizar; neste caso as configurações do detector foram optimizadas para detectar o máximo de vocalizações possíveis produzidas por um animal e excluir vocalizações de outros animais. Uma vez que o segundo detector com uma pequena correcção era adequado para vários tipos de estudos incluídos nesta tese, este foi o escolhido para ser aplicado a toda a extensão dos registos acústicos dos OBS. A aplicação do detector resultou num conjunto de dados de detecções automáticas que foi utilizado nos capítulos seguintes.

No Capítulo 3, um método sísmico para estimar a localização de terramotos a partir de um único instrumento, o método de estação-única, foi utilizado para localizar vocalizações de 20-Hz de baleia-comum de uma subamostra representativa dos registos acústicos dos OBS. Foram também consideradas correcções para contabilizar as influências da velocidade do som na coluna de água e a estrutura de velocidade na camada superficial do fundo oceânico. Apesar de já ter sido demonstrado o uso deste método em providenciar estimativas de localização de vocalizações de baleia-comum em estudos anteriores a esta tese, era ainda necessário esforços adicionais sobre a classificação das estimativas de localização. Vários parâmetros incluídos no algoritmo relacionados com a localização das vocalizações foram avaliados a aplicou-se um esquema de classificação ao conjunto de dados de detecções automáticas obtido no Capítulo 2. Dois conjuntos de dados de detecções foram produzidos através de duas abordagens diferentes para manter vocalizações próximas dos OBS. Foi necessária uma consideração especial relativamente às vocalizações próximas dos OBS porque consistem em dados cruciais para a obtenção de estimativas de abundância confiáveis através do método de amostragem por distâncias (Capítulo 5).

O Capítulo 4 incluiu uma caracterização acústica da vocalização de 20-Hz da baleia-comum, obtida através da medição de parâmetros espectrais e temporais do sinal. A existência de um ou mais grupos acústicos foi também avaliada através de uma análise hierárquica. A comparação dos resultados com estudos publicados revelou a presença de dois conjuntos de características acústicas: um conjunto de características acústicas associadas a baleias-comuns do Mar Mediterrâneo e um segundo conjunto de características

acústicas associadas a baleias-comuns do oceano Atlântico Norte. A identificação do primeiro grupo teve algumas incertezas uma vez que a verificação manual das detecções apenas permitiu confirmar a sua presença num mês da amostra dos registos acústicos. No entanto, houve uma ocasião, com verificação manual, em que os dois conjuntos de características acústicas foram registados em simultâneo. Adicionalmente, uma pesquisa automática dos intervalos entre vocalizações dos dois grupos acústicos revelou que o intervalo associado ao primeiro grupo (Mediterrâneo) foi também registado noutros meses para além daquele em que foi feita a sua verificação manual.

No Capítulo 5 foi possível obter estimativas médias de densidade (número de animais por unidade de área) e abundância (número de animais na área de estudo) de baleia-comum, através da análise de amostragem por distâncias e utilizando as detecções da vocalização de 20-Hz. Antes da análise de amostragem por distâncias, foi executada uma avaliação inicial da adequabilidade dos dois conjuntos de dados de detecções obtidos no Capítulo 3. O conjunto de dados de detecções com o melhor ajuste do modelo da probabilidade de detecção de uma vocalização, o qual é incluído nas estimativas de densidade média de vocalizações, foi o escolhido para as análises seguintes do Capítulo. A densidade média da vocalização de 20-Hz foi transformada em densidade média de baleia-comum utilizando uma taxa de produção da vocalização obtida a partir de dados publicados. Assumindo que a estimativa de densidade média de baleia-comum obtida seria representativa da área de estudo à volta dos OBS, a abundância média de baleia-comum foi estimada através da divisão da densidade média pela área de estudo.

No Capítulo 6 pretendeu-se utilizar o efeito de espelho de Lloyd para inferir a profundidade da baleia que está a vocalizar. Através da utilização de um conjunto de vocalizações de 20-Hz de baleia-comum, o estudo teve como objectivo: 1) demonstrar e analisar as diferenças nas características das vocalizações que ocorrem devido ao efeito de espelho de Lloyd; e 2) estimar a profundidade da baleia que está a vocalizar. A partir do espectrograma, foram identificadas diferentes características espectrais das vocalizações no mesmo conjunto de sinais. Os resultados sugeriram que algumas características medidas nas vocalizações de baleia-comum poderiam estar relacionadas com o efeito de espelho de Lloyd. A inferência da profundidade da baleia que está a vocalizar foi obtida através da comparação de modelos de perda de transmissão do sinal com as observações. Os modelos de perda de transmissão do sinal consideraram o efeito de espelho de Lloyd para uma vocalização de baleia-comum produzida perto da superfície e registada no fundo oceânico por um OBS. A inferência da profundidade da baleia que está a vocalizar não foi simples e foi necessário

avaliar a profundidade usando apenas uma parte específica do conjunto de vocalizações, onde a interferência do efeito de espelho de Lloyd era mais pronunciada.

Nesta tese foram demonstrados diversos estudos biológicos que podem ser realizados através dos registos acústicos de OBS. Os resultados desta tese fornecem informação sobre uma espécie ameaçada e que é pouco estudada em águas Portuguesas. A extensa cobertura espacial dos OBS e os diversos tipos de informação que podem ser obtidos através dos seus registos demonstram que os OBS são ferramentas valiosas na conservação de cetáceos.

Palavras-chave: Estação sísmica de fundo oceânico (OBS), baleia-comum, cetáceo, bioacústica, conservação da vida selvagem

TABLE OF CONTENTS

Chapter 1

GENERAL INTRODUCTION

1.1. Monitoring cetaceans

Cetaceans (dolphins, porpoises and whales) have a long history of association with humans. Some species because of their distribution and their behaviour have stayed elusive. But other species either because of their close proximity with human activity or because of their economic potential have been targets of human exploitation for a long period. Their long and lasting relationship with humans, low reproductive rates, and long lifespan, make them susceptible to changes in the environment – they do not recover quickly and the impacts can be difficult to assess at short-time scales. Therefore, although cetaceans can be a difficult group to study, their long-term exposure to ecosystem disturbances makes them a crucial group to study and to protect. Active management and consistent monitoring of cetaceans are crucial tasks to protect their future. Knowledge of stock structure, population size and spatial and temporal patterns is essential for good management strategies.

In order to assess the status of a species and to identify conservation priorities, it is necessary to determine how that species is divided into stocks. The term “stock” has been used to refer to biological and management units (Wang, 2002). Wang (2002) defines a management stock as a “group of conspecific individuals that are managed separately”. A biological stock is “characterized by no or low levels of genetic exchange” and can also be designated as a population or subpopulation (Wang, 2002). Although the identification of management stocks was initially influenced by economic and political interests (Wang, 2002), the recent approach also takes in consideration biological aspects of the species, such as spatial distribution, abundance and genetic differentiation. Therefore, in recent years the term “stock” is considered a combination of both management and biological units (NMFS, 2014; IUCN, 2017; IWC, 2018). In this thesis, a stock is defined as a ‘group of individuals of the same species that are demographically, but not necessarily genetically isolated’ (Taylor *et al.*, 2005; Clapham *et al.*, 2008). A stock can also be referred as a population. The identification and assessment of stocks requires consistent monitoring of several biological parameters.

Traditionally, cetacean monitoring has been accomplished by visual surveying. Such surveys find the species of interest either from land, aircrafts or on-board ships following a sampling strategy. When researchers encounter animals, they collect data by observing the animals such as species present, an estimate of the number of animals, age group (adult, juvenile, and calf), and behaviour. However, visual surveying is influenced by several factors such as sea conditions, time of day, amount of time that animals spend at the surface, remoteness of the surveyed area, and human and financial resources. Acoustic monitoring of cetaceans provides a method of observation that can supplement or replace visual methods and give important information for stock assessment. Currently, researchers have been deploying both fixed and towed acoustic instruments for dedicated cetacean surveys (Mellinger *et al.*, 2007; Zimmer, 2014). Additional fixed passive acoustic datasets acquired for non-biological purposes have also been providing crucial data, as they contain sounds of several cetacean species, depending on the instrument sampling rate. Networks of hydrophones of navies and other governmental agencies and organizations, such as the U.S. National Oceanic and Atmospheric Administration (NOAA) or the Preparatory Commission for the Comprehensive Nuclear-Test-Ban Treaty Organization (CTBTO), are spread throughout the world's oceans and have been crucial resources for cetacean studies.

1.2. Ocean-bottom seismometers

In seismology, ocean-bottom seismometers (OBS) are regularly used to characterize earth structure, locate earthquakes and record anthropogenic sounds (Frank and Ferris, 2011; Wilcock, 2012). OBS experiments can be long-term (for passive monitoring) or short-term (usually for active seismic surveys). The long-term OBS deployments will be the only ones discussed in the following paragraphs.

The most complete OBS have two sensors: 1) a seismometer that includes three velocity sensors, two horizontal (X, Y) and one vertical (Z), which are placed perpendicular to one another; and 2) a hydrophone (H). In some cases, the hydrophone is not deployed.

OBS are deployed from a research vessel in a precise location and then free fall to the seafloor. Depending on the current speed, the OBS stay in a nearby location during the monitoring period with the seismometer in direct contact with the seafloor. On some occasions, the seismometer can also be buried on the seafloor with a help of a remote

operated vehicle (ROV) (Wilcock, 2012). The hydrophone is placed in the water above the seafloor, tied to the OBS frame or floating a few meters above it.

An earthquake or any other type of disturbance in the earth's crust or in the water layer, causes the release of energy that is propagated by seismic waves. When particles move in the same direction that the energy is traveling, in a longitudinal motion, alternating from compression to expansion, they are being subject to a pressure wave. Because these waves are the first to arrive at a seismic station, they are also known as primary waves or P-waves. P-waves travel in all types of media; solid and fluids (liquid and gas). In the last two media they are also known as sound or acoustic waves. The secondary S-waves move particles in a direction perpendicular to the propagation of energy. They do not cause volume changes of the material through which they propagate, they shear it. Because liquids and gases cannot transmit shear stress, S-waves only propagate in solid media. When seismic waves arrive at the OBS, they cause the seismometer to move and the hydrophone records the associated pressure change. The magnitude of the ground motion (particle velocity) is converted into an electrical signal that is recorded by the OBS along with the time of the waves. In hydrophones, the pressure changes caused by the waves are transformed into electrical signals by a piezoelectric transducer.

OBS deployed for long-term observations have a typical sampling rate between 40 Hz, for recording regional and global earthquakes, and 100 Hz, for local earthquakes (Havskov and Ottemöller, 1999). Based on the Nyquist-Shannon sampling theorem, this means that with the current recording systems that operate with over-sampling, the 100 Hz OBS can accurately record signals up to ~45 Hz. Because of their low sampling rate, OBS can record continuously for long periods of time. Seismic data are usually archived in a Standard for the Exchange of Earthquake Data (SEED) format (IRIS, 2017). The SEED format is an international standard format that allows the easy exchange of seismic time series between institutions and research groups.

The OBS sensor configuration and recording parameters depend on the aim of the study, environmental settings and on the decisions made by the researchers. Most OBS are deployed in isolation from one another (e.g. Wilcock, 2012; Harris *et al.*, 2013; Brodie and Dunn, 2014) but others can be linked by a cable that connects them to a station (Iwase, 2015). OBS have been deployed at depths between 2 000-6 000 meters (Wilcock, 2012; Harris *et al.*, 2013; Brodie and Dunn, 2014; Iwase, 2015; Dréo *et al.*, 2018). OBS can be separated by hundreds of kilometres (Brodie and Dunn, 2014) or they can have a short spacing of 3 kilometres (Wilcock, 2012). The former network was a part a project that aimed to investigate

the processes that occur at the tectonic plate boundaries, in the Southwest Pacific Ocean (Wei *et al.*, 2012). The latter network spacing was designed to locate microearthquakes associated with hydrothermal heat extraction from a crustal magma chamber, in the Northeastern Pacific Ocean (Wilcock *et al.*, 2009). Shallow deployments of OBS for long term monitoring are less common due to the risk of losing the instrument package by trawling.

OBS are usually placed near tectonic boundaries or in areas with intense seismic activity, mostly in offshore waters. The growing interest in marine geophysics and acoustics has led to an increase in the numbers of OBS deployed across the world's oceans. For example, Figure 1 shows the Global Seismographic Network (GSN), which is a cooperative partnership between the Incorporated Research Institutions for Seismology (IRIS) and the U.S. Geological Survey (USGS), coordinated with the international community. It is an extensive network of seismic stations that include OBS that are spread throughout the world. Currently, there are hundreds of OBS collecting data for specific studies that also provide long-term and large-scale recordings of secondary data that can be useful for other types of research (e.g. investigating the oceanic infra-gravity waves (Rawat *et al.*, 2014) or the meteorological storms (Davy *et al.*, 2014)).

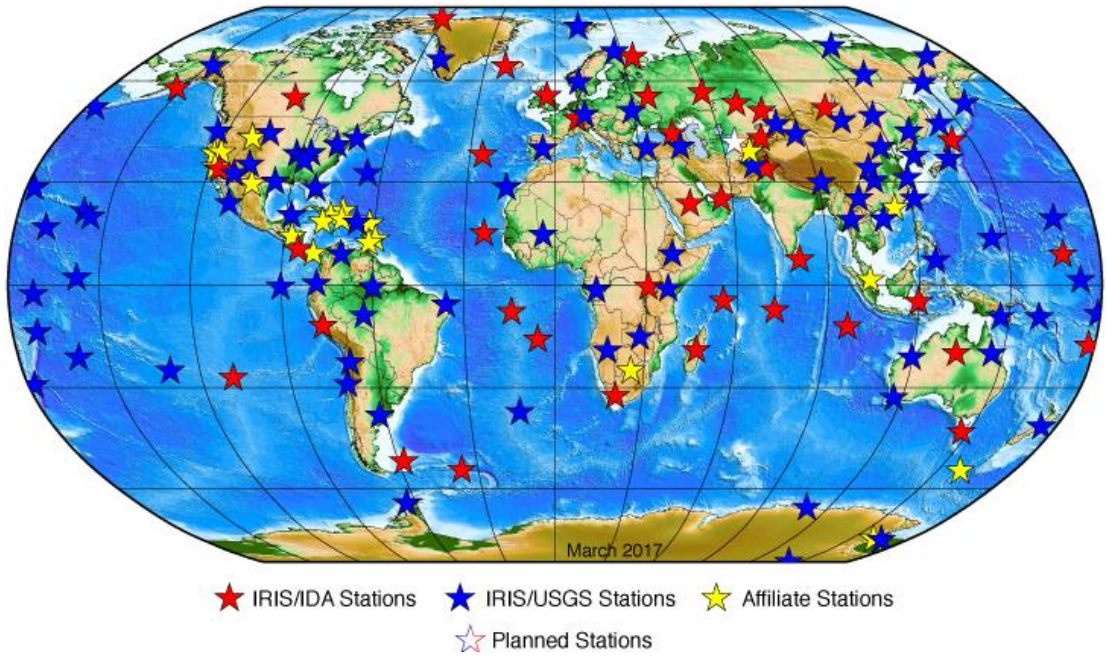

Figure 1. Distribution of the GSN by March 2017. In: IRIS retrieved in 21st February 2018 from https://www.iris.edu/. Copyright 2017 by IRIS.

In the useful frequency band for OBS that record at a 100 Hz sampling rate (0-45 Hz), in addition to natural earthquakes, other acoustic signals produced by different types of sources can also be found (Wilcock *et al.*, 2014): 1) anthropogenic sounds, mostly shipping,

but also sounds from energy extraction, seismic air guns, and ocean science; 2) weather, such as tidal currents, surface wind interactions, ice; and 3) marine mammals. Bryde's (*Balaenoptera edeni*) and sei (*Balaenoptera borealis*) whales produce low frequency sounds but their acoustic behaviour is poorly described (Rankin and Barlow, 2007; Baumgartner *et al.*, 2008). The two cetacean species that produce some of the loudest and the lowest frequency sounds are the blue (*Balaenoptera musculus*) and fin (*Balaenoptera physalus*) whales (Richardson *et al.*, 1995; Mellinger *et al.*, 2007). These two species were intensively hunted in the 20th century and some of their stocks were severely depleted (Clapham and Baker, 2002). Both species have extensive distribution ranges and pelagic habits, which hinder their systematic monitoring. Therefore, acoustic data acquired by OBS may provide valuable information about the spatial distribution and abundance of stocks of these species.

OBS have been used to answer a variety of ecological and behavioural questions about baleen whales. McDonald *et al.* (1995) were probably the first to show the use of OBS in the study of large cetaceans. They were able to detect blue and fin whale calls in the vertical channel of the seismometer and track them. They also analysed effects of anthropogenic and natural sound sources in the behaviour of the tracked whales. Oleson *et al.* (2007) used OBS to assess the temporal distribution of different types of blue whale calls in southern California. OBS were used for a period of time while their main recording instruments were removed from the study area. Sound source levels for 20-Hz fin whale calls were measured from the vertical channel of seismometers in the Northeast Pacific Ocean (Weirathmueller *et al.*, 2012). Brodie and Dunn (2014) detected various baleen whale calls recorded in the vertical channel of the seismometers, such as blue, fin and Bryde's whales in the Lau Basin, southwest Pacific Ocean. They analysed the occurrence patterns of several signals from these species. Most studies focus on the movements of fin and blue whales. Positions of the calling whales have been estimated by different types of location techniques with data collected from OBS (e.g. Rebull *et al.*, 2006; Wilcock, 2012; Harris *et al.*, 2013; Dréo *et al.*, 2018).

Density estimation methods have also been applied to OBS data. Harris *et al.* (2013) demonstrated the use of distance sampling (using the location and number of detected signals) to obtain fin whale call density estimates with data from one day. If a call rate of the detected signal is available, then the signal density estimate can be transformed into animal density (e.g., Buckland, 2006).

1.3. Fin whale ecology

Fin whales are a cosmopolitan species and are found mostly in offshore waters. Although their migratory behaviour is not so well understood as other mysticete species, it is assumed that they spend the summer feeding in high-latitude productive areas, also known as 'feeding' or 'summer' grounds, and spend the winter in tropical or sub-tropical areas for reproductive purposes, also referred to as 'winter' or 'breeding' grounds (Kellogg, 1929). There are some exceptions, as this seasonal latitudinal movement seems to be oversimplistic in describing fin whale movement (Geijer *et al.*, 2016). In some occasions, only part of the population may migrate or some individuals might show different migration patterns (Geijer *et al.*, 2016). For example, fin whales have shown year-round residency in low-latitude areas, such as in the Gulf of California (Urban *et al.*, 2005), in the Mediterranean Sea (Notarbartolo di Sciara *et al.*, 2003) and in East China Sea (Mizroch *et al.*, 2009). Other fin whale populations have also remained year-round around their high-latitude areas, such as in the Gulf of Maine, Gulf of St Lawrence and Nova Scotia (Delarue *et al.*, 2009). Although the main migratory behaviour is also observed, fin whales show more of a continuum of migratory strategies that seem to reflect local adaptations (Geijer *et al.*, 2016).

The habitat of fin whales is mostly pelagic, and their spatial distribution seems to be influenced by prey distribution and oceanographic conditions that influence prey density (Cotté *et al.*, 2009; Druon *et al.*, 2012). In the North Atlantic, their preferred prey is the northern krill (*Meganyctiphanes norvegica*), but they also feed on other species of planktonic crustaceans, schooling fishes and even small squid (Aguilar, 2002). Fin whales feed by lunge feeding, in which they dive down to a certain depth, where there is high prey density. At depths usually greater than 100 meters (Acevedo-Gutiérrez *et al.*, 2002), they perform several lunges, engulfing large amounts of water and filter prey through their keratinized plates called baleen (Goldbogen *et al.*, 2006, 2007). After the lunging process they come to the surface to breathe. The deepest feeding dives known for fin whales were recorded inside the Mediterranean, in the Ligurian Sea, exceeding 470 meters (Panigada *et al.*, 1999). In the North Atlantic, reproductive activities are more predominant during the winter period, mostly in December and January (Lockyer, 1984; Aguilar, 2002)

Globally, fin whales are classified as an "Endangered" species by the International Union for Conservation of Nature (IUCN) because of a global population decline by more than 70%, as the result of the intensive whaling activities during the 19th and 20th centuries (Reilly *et al.*, 2013). The conservation status of fin whales around Europe is considered "Near Threatened", although there are still no recent quantitative data that could support this (IUCN,

2007). The International Whaling Commission (IWC) executed an extensive assessment of the North Atlantic fin whales in 1991 and an update for the northern part of the Atlantic in 2006 (Reilly *et al.*, 2013). Based mainly on catch data, the IWC divides fin whales in the North Atlantic into seven stocks (Donovan, 1991): Nova Scotia; Newfoundland-Labrador; West Greenland; East Greenland-Iceland; North Norway; West Norway-Faeroe Islands; British Isles-Spain-Portugal (Fig. 2). However, these units are not discrete as there is evidence of a degree of interchange between them (IWC, 2007; Castellote *et al.*, 2011). The accepted abundance estimates by the IWC do not cover all of the stocks and some stock-specific estimates can be considered dated, such as the number of 17,355 animals (Coefficient of Variation CV of 0.27) for the Spain-Portugal-British Isles unit obtained in 1989 (Buckland *et al.*, 1992). Within the Mediterranean Sea, the population was estimated in 1991 from surveys covering much of the western basin at 3,583 (CV of 0.27) (Forcada *et al.*, 1996).

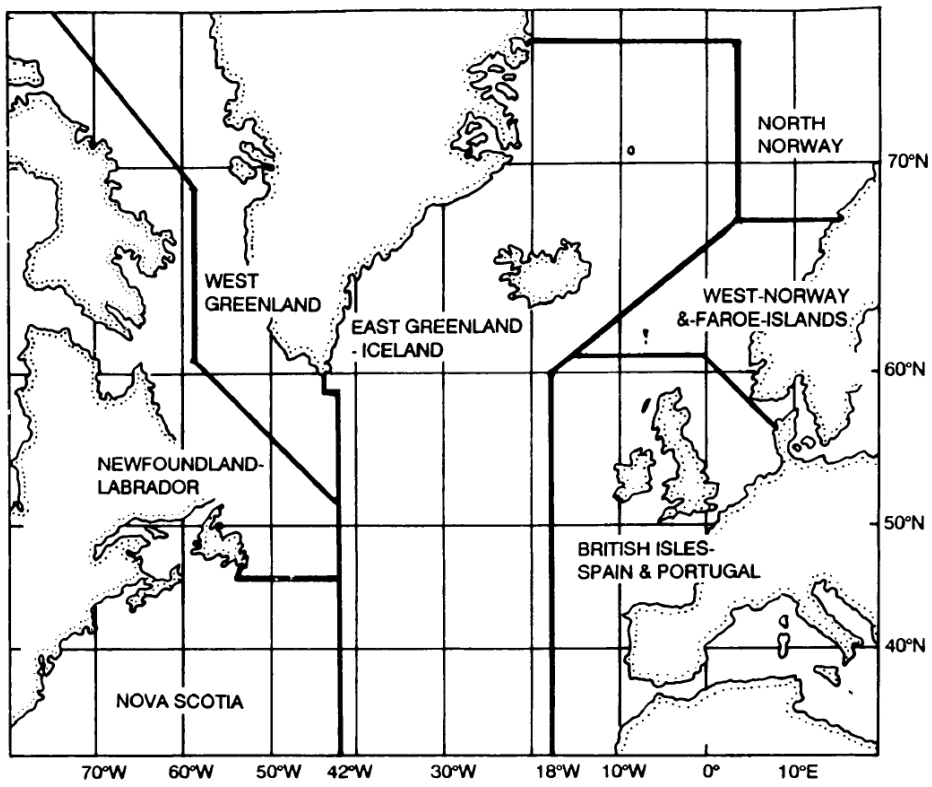

Figure 2. Fin whale stocks for the North Atlantic defined by the IWC. Adapted from "A review of IWC stock boundaries," by G.P. Donovan, 1991, Report of the International Whaling Commission 13, 39–68. Copyright by the International Whaling Commission.

Despite the close proximity, fin whales in the Mediterranean Sea are considered a subdivision of the British Isles-Spain-Portugal stock and are listed as a "Vulnerable" population by the IUCN (Panigada and Notarbartolo di Sciara, 2012). In the Mediterranean Sea, acoustic (Clark, 1995; Clark *et al.*, 2002) and visual (Gannier and Ganiier, 1993) data show that fin

whales are recorded throughout the year. They travel to highly productive areas to feed during the summer, but their winter distribution is still uncertain, as they probably disperse over the Mediterranean Sea (Notarbartolo di Sciara *et al.*, 2003). Adult individuals with calves are sighted throughout the year in the Mediterranean Sea (Notarbartolo di Sciara *et al.*, 2003).

Berubé *et al.* (1998) found significant levels of divergence and heterogeneity in mitochondrial and nuclear DNA between eastern North Atlantic fin whales and Mediterranean fin whales. This division is also confirmed by differences in the levels of organochlorine pollutant concentrations (Aguilar *et al.*, 2002) and stable isotopes (Giménez *et al.*, 2013). Acoustic studies also reveal the occurrence of two distinct groups, one identified as being from the North Atlantic Ocean and other from the Mediterranean Sea (Castellote *et al.*, 2011). Although there is an increasing amount of evidence of the division between these two groups, the degree of overlap and interchange between them is still subject of great discussion. Historical records suggested that some individuals from the North Atlantic Ocean would enter the Mediterranean Sea (Notarbartolo di Sciara *et al.*, 2003). Recent studies confirm this movement and also show that some fin whales from the Mediterranean Sea travel towards the North Atlantic Ocean (Raga and Pantoja, 2004; Gauffier *et al.*, 2009). Satellite tagged data showed that the Mediterranean-North Atlantic movement might be limited. From 8 tagged whales in the north-western Mediterranean Sea, only one whale crossed the Strait of Gibraltar and travelled up to central Portugal (Cotté *et al.*, 2009). From 7 tagged whales in the Ligurian Sea, 5 remained in the area during winter and only 2 individuals travelled south-west towards the Balearic Islands (Panigada *et al.*, 2013). However, both of the satellite telemetry studies were undertaken with a small sample of animals and results might not be representative. For management purposes, the Strait of Gibraltar is considered the border between Mediterranean and North Atlantic fin whales (e.g. IWC, 2007; Panigada and Notarbartolo di Sciara, 2012). Acoustic data show that the two different acoustic groups, North Atlantic Ocean and Mediterranean Sea have a degree of overlap (Castellote *et al.*, 2011). However, because only males are believed to produce sequences of the 20-Hz call (Croll *et al.*, 2002), which was the call type used in Castellote *et al.* (2011) and is described more fully below, this overlap would only be indicative of the males in the population. Palsbøll *et al.* (2004) estimated an exchange of two females per generation between the subdivision of the Mediterranean Sea and the North Atlantic Ocean but they didn't clarify whether this interaction was unidirectional or bidirectional.

In the south of the Iberian Peninsula, fin whales were once abundant and occurred on a year-round basis (Sanpera and Aguilar, 1992). They were actively hunted in the 1920s with about 7 000 individuals taken from the area (Reilly *et al.*, 2013). Hunting activities ceased in

1986 after the IWC moratorium, but the recent numbers of fin whales in the area are still small, compared to the past abundance (Clapham *et al.*, 2008). In Portugal, fin whales have a national conservation status of “Endangered” but there are no data that support this, other than the global assessment (Queiroz *et al.*, 2006). Whaling data from the 20th century suggest that fin whales were abundant in Portuguese mainland waters as they were the most caught cetacean species (Sanpera and Aguilar, 1992). Strandings data from 1526 until 1977, for the continental coast of Portugal, show they were one of the most stranded large cetacean species (Sousa and Brito, 2011). Recent sightings in mainland waters are sparse and are insufficient to assess any kind of trend.

For example, between 2010 and 2014 whale-watching activities in the south of continental Portugal only recorded 4 sightings of fin whales (Laborde *et al.*, 2015). However, data collected were limited because vessels did not go beyond 10 nautical miles from shore.

In the Azores and Madeira archipelagos fin whales are seen throughout the year, but are more common during spring and summer, probably as they travel to their northern feeding grounds (Queiroz *et al.*, 2006; Silva *et al.*, 2013). Feeding activities have also been documented off South Portugal, in the Gorringe Bank (Martinho, 2015), in the vicinity of the Azores islands (Visser *et al.*, 2011) and around Madeira (Gordon *et al.*, 1995). Waters around the Azores archipelago seem to function as temporary feeding areas for whales that migrate up to the summer area in eastern Greenland-western Iceland (Silva *et al.*, 2013). Fin whales from the subdivision of the Mediterranean Sea or the North Atlantic Ocean could occur in continental Portuguese waters. However, without an identification of observed whales, the occurrence and distribution of fin whales in Portuguese waters remains uncertain.

1.4. Fin whale acoustics

Fin whales produce fairly simple acoustic signals between 15 and 142 Hz that include the following sounds: 20-Hz calls, low frequency narrow band calls called backbeats, rumbles, higher frequency sounds that are mostly upsweeps (around 100 Hz), and non-vocal impulsive sounds (Watkins, 1981). The most common and the most studied fin whale sound is the “20-Hz call”, also known as “regular” call (Clark *et al.*, 2002). This signal is a ~1 second, downward sweeping tone between 30 and 15 Hz (Watkins *et al.*, 1987). Because of its frequent production and its use in most studies, the 20-Hz call will be the focus of the following description. Twenty Hz calls are produced in sequences and/or bouts but they can also be produced individually (Watkins, 1981). Usually fin whales produce series of 20-Hz calls, called

sequences that are separated by two types of periods of silence: rests, which can last between 1–20 minutes, and longer gaps, lasting between 20 minutes and 2 hours (Watkins *et al.*, 1987; Delarue *et al.*, 2009; Soule and Wilcock, 2012). Within a sequence, individual calls are separated by stereotyped intervals (called the inter-call interval, ICI), measured from the beginning of a signal to the beginning of the next one (Watkins *et al.*, 1987). Sequences form bouts (also known as 'songs') that are separated by periods of silence greater than 2 hours (Fig. 3). Backbeats are relatively constant in frequency (between 18 and 20 Hz) and last ~0.8 seconds (Clark *et al.*, 2002). Usually backbeats are also produced within sequences, alternating with 20-Hz calls or with repetition.

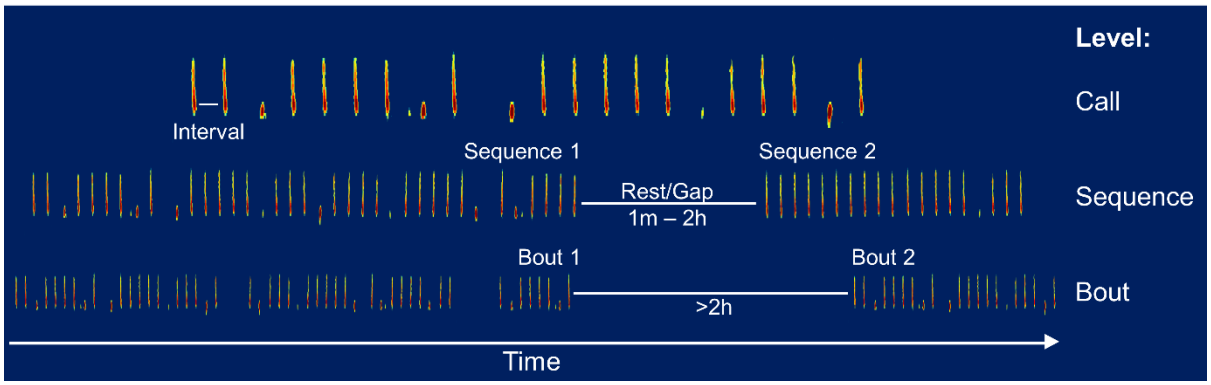

Figure 3. Structure of fin whale acoustic sounds.

The 20-Hz call is likely used for local and long-distance communication (Watkins, 1981). Sound source levels for this signal are relatively similar across different oceans and show the following ranges: 160-186 dB re 1µPa at 1 m in the western north Atlantic (Watkins *et al.*, 1987), 159-189 dB re 1µPa at 1 m in the Northeast Pacific Ocean (Charif *et al.*, 2002; Weirathmueller *et al.*, 2012) and 189 dB re: 1µPa at 1 m in the Southern Ocean (Širović *et al.*, 2007). Theoretically, this signal could be heard out to a distance of hundreds and possibly thousands of kilometres (Širović *et al.*, 2007). When 20-Hz calls are produced in sequences, the sound source level is fairly constant (Weirathmueller *et al.*, 2012). Fin whales usually stay at shallow depths when producing acoustical signals (Watkins, 1981). From a total of 10 tagged whales, Stimpert *et al.* (2015) found that higher call rates were produced during dives of about 10-15 meters, with little body movement, body pointing downwards, and moderate body roll. Calling whales were also more likely to be travelling and in groups. The study by *Croll et al.* (2002) suggests that that bouts are only produced by male fin whales (Croll *et al.*, 2002). They combined acoustic location and molecular techniques to identify the sex of the calling whale and found that although there was a 1:1 overall sex ratio (21 males and 22 females), only males vocalized at the time of the study period. However, the number of fin whales that vocalized was very small (only 9 whales and all males). The production of fin

whale bouts is seasonal and it peaks during the fall and winter months (Thompson and Friedl, 1982; Watkins *et al.*, 2000; Stafford *et al.*, 2007), which coincide with the breeding season. Because of this, it is suggested that these signals may be used by males to advertise areas with high density of prey to females (Payne and Webb, 1971; Croll *et al.*, 2002; Clark and Gagnon, 2004).

The production of the various types of signals and their characteristics vary across geographical areas (e.g. Watkins *et al.*, 1987, Hatch and Clark, 2004; Castellote *et al.*, 2011, Oleson *et al.*, 2014). The 20-Hz call is recorded worldwide and its features and bout structure show the most discriminatory power among different regions that may correspond to some degree of population differentiation (Hatch and Clark, 2004). Backbeats and higher frequency upsweeps are less frequent and seem to be produced more in the Atlantic Ocean (Hatch and Clark, 2004). Hatch and Clark (2004) found differences in the median frequency of the 20-Hz call between the Gulf of California and other areas of the Pacific and the North Atlantic. At a smaller spatial scale, Castellote *et al.* (2011) found differences in the frequency bandwidth of the 20-Hz call between North Atlantic and Mediterranean fin whales. Some call features might show a level of variability that could come from acoustic interference or differences in measurement settings that result from a researcher's decision (for example, spectrograms can be produced at different temporal and frequency resolutions). However, the inter-call interval is the most reliable and most distinct feature of the 20-Hz call. It is typically consistent within a bout of an individual but it has showed differences between areas (e.g. Castellote *et al.*, 2011; Hatch and Clark, 2004; Delarue *et al.*, 2009). Despite the great utility of the inter-call interval to show geographical differences between fin whales, it is a feature that needs long-term monitoring because it may show inter- and intra-annual changes in some areas (Morano *et al.*, 2012; Oleson *et al.*, 2014).

1.5. Thesis outline

The general aim of this thesis was to demonstrate the use of acoustic datasets, collected for non-biological focussed studies, such as seismic data, to study fin whales. In Portugal, although fin whales are listed as "Endangered" species, background information about the occurrence of this species is scarce and there are few resources to undertake long-term studies. In this context, seismic datasets may become one of the primary sources of information on a year-round basis, allowing the assessment of presence of calling fin whales, their distribution, abundance status and possible trends. Several questions regarding fin whale occurrence, stock structure and characteristics off Portuguese waters remain

unanswered. Between September 2007 and August 2008 a network of 24 OBS was deployed off southwest Portugal with the main aim to obtain data to study the microseismicity originating from potential tsunami sources. During this time fin whale sounds were also recorded. This thesis brings a multidisciplinary approach to the study of fin whales, using methods from seismology, acoustics, ecology and statistics.

Chapter 2 focuses on the detection process of the 20-Hz fin whale call. A detection algorithm, which included a normalized cross-correlation between the waveform of the recordings and a template of the call, was added to the seismic software *SEISAN*. The algorithm was run multiple times with different settings (creating several "detectors"). The accuracy of the detectors was evaluated, using a systematic random subsample of the acoustic recordings of the OBS. The results showed that different detectors were optimal, depending on the goals of a particular analysis. Firstly, one detector was more suitable for studies aimed at abundance estimation, where the main goal was to detect calls above a given detection threshold with both false and missed detections being accounted in abundance estimation methods (e.g. Marques *et* al., 2013). Secondly, there was another detector that was more suitable for assessing fine-scale movement and behaviour of a given calling animal; in this case, the detector settings were optimised to detect as many calls produced by an individual animal as possible, as well as excluding calls from other animals. Because the second detector with a minor correction was suitable for several types of studies included in this thesis it was the one applied to the entire span of the recordings of the OBS. The application of the detector resulted in a dataset of automatic detections that was used in the following chapters.

In **Chapter 3**, a standard seismological method for estimating earthquake location from a single instrument, the single-station method (Roberts *et al.*, 1989), was used to locate 20-Hz fin whale calls from a representative subsample of the recordings. Corrections to account for the influences of the sound speed in the water layer and the velocity structure in the top strata of the seabed were considered. Although the use of this method to provide location estimates had been already demonstrated (Harris *et al.*, 2013; Matias and Harris, 2015), there was still additional work to be done on the classification of the location estimates. Different parameters of the algorithm related to the location of the calls were assessed and a classification scheme was applied to the entire dataset of automatic detections. In addition, two datasets of automatic detections were produced with different approaches to retain close calls, which are crucial for reliable estimates of Chapter 5.

Chapter 4 includes an acoustic characterization of the 20-Hz fin whale calls, obtained by the measurement of spectral and temporal parameters of the signal. The existence of one or more acoustic groups was also evaluated by a hierarchical clustering analysis. The comparison of the results with published studies revealed the presence of two sets of acoustic characteristics: one set related with fin whales from the Mediterranean Sea and a second set related with fin whales from the North Atlantic Ocean. There were some uncertainties about the identification of group 1 (Mediterranean) as it was based in a subsample with manual verification of only one month. However, there was one occasion, confirmed by manual inspection of the spectrogram, when these two groups of acoustic characteristics were recorded simultaneously. A further automatic search of the inter-call interval of the two acoustic groups suggested that group 1 was also present in other months.

Chapter 5 presents the average density (number of animals per unit area) and abundance (number of animals in the study area) estimates of fin whales using the 20-Hz calls and distance sampling analysis. Prior to the distance sampling analysis, there was an initial assessment of the suitability of two datasets developed in Chapter 3. The one with the best fit of the detection probability model, which is used to estimate an average call density, was the one used in further analysis of Chapter 5. The average call density was transformed in a fin whale density by using a cue rate obtained from published work (Stimpert *et al.*, 2015). Assuming that the fin whale density estimate is representative of the area around the OBS, the average fin whale abundance was obtained by dividing the average density by the study area.

Chapter 6 covers the use of the Lloyd's Mirror Effect (LME) to infer the depth of a calling whale. Using a bout of the 20-Hz fin whale calls with estimated ranges, the study aimed to: 1) show and analyse differences of call features due to the LME; and 2) estimate the depth of the calling whale. The spectrogram showed that different spectral characteristics of the calls could be identified within the same bout. Transmission loss models considering the LME for a fin whale call generated close to the surface and recorded at the seafloor by an instrument were developed. Inference of depths of calling whale was undertaken by comparing the transmission loss models with observations. However, it was not a straightforward task and the depth needed to be assessed using only a specific part of the bout where the interference was more pronounced.

Chapter 7 summarizes the results of this thesis and highlights future research directions. It also provides a general discussion on the use of OBS in the study of large cetaceans and their contribution to cetacean conservation.

1.6. REFERENCES

Acevedo, A., Croll, D. A., and Tershy, B. R. (**2002**). “High feeding costs limit dive time in the largest whales,” The Journal of Experimental Biology **205**, 1747–1753.

Aguilar, A. (**2002**). “Fin whale (*Balaenoptera physalus*),” in Encyclopedia of Marine Mammals, edited by W.F. Perrin, B. Würsig, and J.G.M. Thewissen (Academic Press, San Diego, USA), pp. 435–438.

Aguilar, A., Borrell, A., and Reijnders, P. J. H. (**2002**). “Geographical and temporal variation in levels of organochlorine contaminants in marine mammals,” Marine Environmental Research **53**, 425–452.

Baumgartner, M. F., Van Parijs, S. M., Wenzel, F. W., Tremblay, C. J., Carter Esch, H., and Warde, A. M. (**2008**). “Low frequency vocalizations attributed to Sei whales (*Balaenoptera borealis*),” Journal of the Acoustical Society of America **124**, 1339–1349.

Bérubé, M., Aguilar, A., Dendanto, D., Larsen, F., Notarbartolo di Sciara, G., Sears, R., et al. (**1998**). “Population genetic structure of North Atlantic, Mediterranean Sea and Sea of Cortez fin whales, *Balaenoptera physalus*, (Linnaeus 1758): Analysis of mitochondrial and nuclear loci,” Molecular Ecology **7**, 585–599.

Brodie, D. C., and Dunn, R. A. (**2014**). "Low frequency baleen whale calls detected on ocean-bottom seismometers in the Lau basin, southwest Pacific Ocean," Journal of the Acoustical Society of America **137**, 53–62.

Buckland, S. T. (**2006**). “Point transect surveys for songbirds: robust methodologies,” The Auk, **123**, 345–357.

Buckland, S. T., Cattanach, K. L. and Lens, S. (**1992**). “Fin whale abundance in the eastern North Atlantic, estimated from Spanish NASS-89 data,” Reports of the International Whaling Commission **42**, 457–460.

Castellote, M., Clark, C. W., and Lammers, M. O. (**2011**). “Fin whale (*Balaenoptera physalus*) population identity in the western Mediterranean Sea,” Marine Mammal Science **28**, 325–344.

Charif, R. A., Mellinger, K. J., Dunsmore, K. M., Fristrup, K. M., and Clark, C. W. (**2002**). “Estimated source levels of fin whale (*Balaenoptera physalus*) vocalizations: adjustments for surface interference,” Marine Mammal Science **18**, 81–98.

Clapham, P. J., Aguilar, A., and Hatch, L. T. (**2008**). "Determining spatial and temporal scales for management: lessons from whaling," Marine Mammal Science **24**, 183–201.

Clapham, P. J. and Baker, C. S. (**2002**). “Modern whaling,” in Encyclopedia of Marine Mammals, edited by W.F. Perrin, B. Würsig, and J.G.M. Thewissen (Academic Press, San Diego, USA), pp. 1328–1332.

Clark, C. W. (**1995**). “Application of U.S. Navy underwater hydrophone arrays for scientific research on whales,” Report of the International Whaling Commission **45**, 210–212.

Clark, C. W., Borsani, F., and Notarbartolo di Sciara, G. (**2002**). “Vocal activity of fin whales, *Balaenoptera physalus*, in the Ligurian Sea,” Marine Mammal Science **18**, 281–285.

Clark, C. W., and Gagnon, G. J. (**2004**). “Low-frequency vocal behaviors of baleen whales in the North Atlantic: Insights from integrated undersea surveillance system detections, locations, and tracking from 1992 to 1996,” U.S. Navy Journal of Underwater Acoustics **52**, 609–640.

Cotté, C., Guinet, C., Taupier-Letage, I., Mate, B., and Petiau, E. (**2009**). “Scale dependent habitat use by a large free-ranging predator, the Mediterranean fin whale,” Deep-Sea Research I **56**, 801–811.

Croll, D., Clark, C. W., Acevedo, A., Tershy, B., Flores, S., Gedamke, J., and Urban, J. (**2002**). “Only male fin whales sing loud songs,” Nature (London) **117**, 809.

Davy, C., Barruol, G., Fontaine, F. R., Sigloch, K., and Stutzmann, E. (**2014**). “Tracking major storms from microseismic and hydroacoustic observations on the seafloor,” Geophysical Research Letters **41**, 8825–8831.

Delarue, J., Todd, S. K., VanParijs, S. M., and DiIorio, L. (**2009**). “Geographic variation in Northwest Atlantic fin whale (*Balaenoptera physalus*) song: Implications for stock structure assessment,” Journal of the Acoustical Society of America **125**, 1774–1782.

Donovan, G. P. (**1991**). A review of IWC stock boundaries. Report of the International Whaling Commission **13**, 39–68.

Dréo, R., Bouffaut, L., Guillon, L., Labat, V., Barruol, G., and Boudraa, A. O. (**2018**). “Antartic blue whale location with ocean bottom seismometers in southern Indian Ocean,” UACE2017 - 4th Underwater Acoustics Conference and Exhibition, 87–92.

Druon, J. N., Panigada, S., David, L., Gannier, A., Mayol, P., Arcangeli, A., Cañadas, A., Laran, S., di Méglio, N., and Gauffier, P. (**2012**). “Potential feeding habitat of fin whales in the western Mediterranean Sea: an environmental niche model,” Marine Ecology Progress Series **464**, 289–306.

Forcada, J., Aguilar, A., Hammond, P., Pastor, X., and Aguilar, R. (**1996**). “Distribution and abundance of fin whales (*Balaenoptera physalus*) in the western Mediterranean sea during the summer,” Journal of Zoology **238**, 23–34.

Frank, S. D., and Ferris, A. N. (**2011**). "Analysis and location of blue whale vocalizations in the Solomon Sea using waveform amplitude data," Journal of the Acoustical Society of America **130**, 731–736.

Gannier, A. and Gannier, O. (**1993**). “The winter presence of the fin whale in the liguro provençal basin: preliminary study,” European Research on Cetaceans **7**, 131–134.

Gauffier, P., Verborgh, P., Andreu, E., Esteban, R., Medina, B., Gallego, P., and de Stephanis, R. (**2009**). “An update on fin whales (*Balaenoptera physalus*) migration through intense maritime traffic in the Strait of Gibraltar,” Paper presented to the IWC Scientific Committee, Madeira, Portugal, May, Paper No. SC/61/BC6 pp. 1–4.

Geijer, C. K. A., Notarbartolo di Sciara, G., and Panigada, S. (**2016**). "Mysticete migration revisited: are Mediterranean fin whales an anomaly?," Mammal Review **46**, 284–296.

Giménez, J., Gómez-Campos, E., Borrell, A., Cardona, L., and Aguilar, A. (**2013**). “Isotopic evidence of limited exchange between Mediterranean and eastern North Atlantic fin whales,” Rapid Communications in Mass Spectrometry **27**, 1801.

Goldbogen, J. A., Calambokidis, J., Shadwick, R. E., Oleson, E. M., McDonald, M. A., and Hildebrand, J. A. (**2006**). "Kinematics of foraging dives and lunge-feeding in fin whales," Journal of Experimental Biology **209**, 1231–1244.

Goldbogen, J. A., Pyenson, N. D., and Shadwick, R. E. (**2007**). "Big gulps require high drag for fin whale lunge feeding," Marine Ecology Progress Series **349**, 289–301.

Gordon, J. C. D., Steiner, L., and Martins, H. R. (**1995**). "Observations of fin whales (*Balaenoptera physalus* L., 1758) around the central north Atlantic islands of the Azores and Madeira. Arquipélago," Life and Marine Sciences **13A**, 79–84.

Harris, D., Matias, L., Thomas, L., Harwood, J., and Geissler, W. H. (**2013**). "Applying distance sampling to fin whale calls recorded by single seismic instruments in the Northeast Atlantic," Journal of the Acoustical Society of America **134**, 3522–3535.

Hatch, L. T., and Clark, C. W. (**2004**). "Acoustic differentiation between fin whales in both the North Atlantic and North Pacific Oceans, and integration with genetic estimates of divergence," Paper presented to the IWC Scientific Committee, Sorrento, Italy, July, Paper No. SC/56/SD6, pp. 1–37.

Havskov J., Ottemöller L. (**2010**). *Routine Data Processing in Earthquake Seismology* (Springer Science+Business Media B.V., Dordrecht, The Netherlands).

Incorporated Research Institutions for Seismology, IRIS (**2011**). Washington, USA, http://www.iris.edu/manuals/rdseed.htm (Last viewed 24th February, 2018).

International Union for Conservation of Nature, IUCN (**2017**). The IUCN Red List of Threatened Species. Version 2017.3, Cambridge, UK, http://www.iucnredlist.org (Last viewed 14th February, 2018).

IUCN SSC Cetacean Specialist Group, European Mammal Assessment team. (**2007**). *Balaenoptera physalus*, regional assessment. in IUCN 2017. IUCN Red List of Threatened Species. Version 2017.3, Cambridge, UK, http://www.iucnredlist.org (Downloaded 31th January, 2018).

International Whaling Commission, IWC (**2018**). Cambridge, UK, https://iwc.int/estimate (Last viewed 30th January, 2018).

IWC. (**2007**). “Report of the Joint NAMMCO/IWC Scientific Workshop on the Catch History, Stock Structure and Abundance of North Atlantic Fin Whales, 23-26 March 2006, Reykjavík, Iceland,” Journal of Cetacean Research Management **9**, 451–68.

Iwase, R. (**2015**). "Fin whale vocalizations observed with ocean bottom seismometers of cabled observatories off east Japan Pacific Ocean," Japanese Journal of Applied Physics **54**, 07HG01–07HG03.

Kellogg, R. (**1929**). “What is known of the migrations of some of the whalebone whales,” Smithsonian Institution Annual Report **1929**, 467–494.

Laborde, M. I., Cid, A., Fonseca, C., and Castro, J. (**2015**) "Baleen whales in southern Portugal: new insights," Abstract WW-01 presented at the 2015 European Cetacean Society, 23-25 March, St Julian’s Bay, Malta.

Lockyer, C. (**1984**). Review of baleen whale (Mysticeti) reproduction and implications for management in Reproduction in whales, dolphins and porpoises, Report of the International Whaling Commission, Special Issue 6, edited by W.F. Perrin, R.L. Brownell, and D.P. DeMaster, (International Whaling Commission, Cambridge, UK), pp. 27–50.

Marques, T. A., Thomas, L., Martin, S. W., Mellinger, D. K., Ward, J., Moretti, D., Harris. D., and Tyack, P. (**2013**). “Estimating animal population density using passive acoustics,” Biological Reviews **88**, 287–309.

Martinho, F. (**2015**). (personal communication).

Matias, L., and Harris, D. (**2015**) "A single-station method for the detection, classification and location of fin whale calls using ocean-bottom seismic stations," Journal of the Acoustical Society of America **138**, 504–520.

McDonald, M. A., Hildebrand, J. A., and Webb, S. C. (**1995**). “Blue and fin whales observed on a seafloor array in the Northeast Pacific,” Journal of the Acoustical Society of America **98**, 712–721.

Mellinger, D. K., Stafford, K. M., Moore, S. E., Dziak, R. P., and Matsumoto, H. (**2007**) "An Overview of Fixed Passive Acoustic Observation Methods for Cetaceans," Oceanography **20**, 36–45.

Mizroch, S. A., Rice, D. W., Zwiefelhofer, D., Waite, J., and Perryman, W. L. (**2009**). "Distribution and movements of fin whales in the North Pacific Ocean," Mammal Review **39**, 193–227.

Morano, J. L., Salisbury, D. P., Rice, A. N., Conklin, K. L., Falk, K. L., and Clark C. W. (**2012**) "Seasonal and geographical patterns of fin whale song in the western North Atlantic Ocean," Journal of the Acoustical Society of America **132**, 1207–1212.

National Marine Fisheries Service, NMFS. (**2004**). A Requirements Plan for Improving the Understanding of the Status of U.S. Protected Marine Species. Report of the NOAA Fisheries National Task Force for Improving Marine Mammal and Turtle Stock Assessments. U.S. Dep. Commerce, NOAA Tech. Memo. NMFS-F/SPO-63, pp. 1–112.

Notarbartolo di Sciara, G., Zanardelli, M., Jahoda, M., Panigada, S. and Airoldi, S. (**2003**). "The fin whale *Balaenoptera physalus* (L. 1758) in the Mediterranean Sea," Mammal Review **33**, 105–150.

Oleson, E. M., Širović, A., Bayless, A. R., and Hildebrand, J. A. (**2014**). "Synchronous seasonal change in fin whale song in the North Pacific," PLoS ONE **9**, e115678.

Oleson, E. M., Wiggins, S., and Hildebrand, J. A. (**2007**). "Temporal separation of blue whale call types on a southern California feeding ground," Animal Behaviour **74**, 881−894.

Palsbøll, P. J., Bérubé, M., Aguilar, A., Notarbartolo di Sciara, G., and Nielsen, R. (**2004**). "Discerning between recurrent gene flow and recente divergence under a finite-site mutation model applied to North Atlantic and Mediterranean fin whales (*Balaenoptera physalus*) populations," Evolution (Lawrence, Kans.) **58**, 670–675.

Panigada, S., Lauriano, G., Zanardelli, M., Pierantonio, N., Donovan, G., Zerbini, A. et al. (**2013**) "Satellite tracking of fin whales in the Pelagos Sanctuary (western Mediterranean Sea)," European Research on Cetaceans **27**, 3–15.

Panigada, S. and Notarbartolo di Sciara, G. (**2012**). *Balaenoptera physalus*. in: IUCN 2017. IUCN Red List of Threatened Species. Version 2017.3, http://www.iucnredlist.org (Downloaded 31th January, 2018).

Panigada, S., Zanardelli, M., Canese, S., and Jahoda, M. (**1999**). "How deep can baleen whales dive?," Marine Ecology Progress Series **187**, 309–311.

Payne, R. S., and Webb, D. (**1971**). "Orientation by means of long range acoustic signaling in baleen whales," Annuals of the New York Academy of Sciences **188**, 110–141.

Queiroz, A. I., Alves, P. C., Barroso, I., Beja, P., Fernandes, M., Freitas, L., et al. (**2006**). "*Balaenoptera physalus* Baleia-comum," in Livro Vermelho dos Vertebrados de Portugal edited by M.J. Cabral, J. Almeida, P.R. Almeida, T. Dellinger, N. Ferrand de Almeida, M.E. Oliveira et al. (Instituto da Conservação da Natureza/Assírio & Alvim, Lisboa, Portugal) pp. 511-512.

Raga, J.A., and Pantoja, J. (**2004**). Proyecto Mediterráneo: Zonas de especial interés para la conservación de los cetáceos en el Mediterráneo espańol (Organismo Autónomo Parques Nacionales, Madrid, Spain) pp. 1–119.

Rankin, S. and Barlow, J., (**2007**). "Vocalizations of the sei whale *Balaenoptera borealis* off the Hawaiian Islands," Bioacoustics **16**, 137–145.

Rawat, A., Ardhuin, F., Ballu, V., Crawford, W., Corela, C., and Aucan, J. (**2014**). "Infragravity waves across the oceans," Geophysical Research Letters **41**, 7957–7963.

Rebull, O. G., Cusí J. D., Fernández M. R., and Muset J. G. (**2006**). "Tracking fin whale calls offshore the Galicia Margin, north east Atlantic ocean," Journal of the Acoustical Society of America **120**, 2077–2085.

Reilly, S. B., Bannister, J. L., Best, P. B., Brown, M., Brownell Jr., R. L., Butterworth, D. S., et al. (**2013**). "*Balaenoptera physalus*," in IUCN 2017. IUCN Red List of Threatened Species. Version 2017.3, http://www.iucnredlist.org (Downloaded 31th January, 2018).

Richardson, W. J., Greene, J. C. R., Malme, C. I., and Thomson, D. H. (**1995**) *Marine Mammals and Noise* (Academic Press, San Diego, USA).

Roberts, R. G., Christoffersson, A., and Cassidy, F. (**1989**). “Real time events detection, phase identification and source location estimation using single station component seismic data and a small PC,” Geophysical Journal International **97**, 471–480.

Sanpera, C., and Aguilar, A. (**1992**). "Modern whaling off the Iberian Peninsula during the 20th century," Reports of the International Whaling Commission **42**, 723–730.

Silva, M. A., Prieto, R., Jonsen, I., Baumgartner, M. F., and Santos, R. S. (**2013**). “North Atlantic blue and fin whales suspend their spring migration to forage in middle latitudes: building up energy reserves for the journey?,” Plos One **8**, e76507.

Širović, A., Hildebrand, J. A., and Wiggins, S. M. (**2007**). “Blue and fin whale call source levels and propagation range in the Southern Ocean,” Journal of the Acoustical Society of America **122**, 1208–1215.

Soule, D. C., and Wilcock, J. S. (**2013**). “Fin whale tracks recorded by a seismic network on the Juan de Fuca Ridge, Northeast Pacific Ocean,” Journal of the Acoustical Society of America **133**, 1751–1761.

Sousa, A., and Brito, C. (**2011**). "Historical strandings of cetaceans on the Portuguese coast: anecdotes, people and naturalists," Marine Biodiversity Records **4**, e102.

Stafford, K. M., Mellinger, D. K., Moore, S. E., and Fox, C. G. (**2007**). “Seasonal variability and detection range modeling of baleen whale calls in the Gulf of Alaska, 1999–2002,” Journal of the Acoustical Society of America **122**, 3378–3390.

Taylor, B. L. (**2005**). “Identifying units to conserve,” in Marine Mammal Research: Conservation Beyond Crisis, edited by J.E. Reynolds III, W.F. Perrin, R.R. Reeves, S. Montgomery, and T.J. Ragen (The John Hopkins University Press, Baltimore, USA), pp. 146–164.

Thompson, P. O., and Friedl, W. A. (**1982**). “A long-term study of low frequency sound from several species of whales off Oahu,” HawaiiCetology **45**, 1–19.

Urban, R. J., Rojas-Bracho, L., Guerrero-Ruiz, M., JaramilloleGorreta, A., and Findley, L. T. (**2005**). “Cetacean diversity and conservation in the Gulf of California,” in Biodiversity, Ecosystems, and Conservation in Northern Mexico, edited by J.E. Cartron, G. Ceballos, and R.S. Felger (Oxford University Press, New York, USA), pp. 276–297.

Visser, F., Hartman, K. L., Pierce, G. J., Valavanis, V. D., and Huisman, J. (**2011**). “Timing of migratory baleen whales at the Azores in relation to the North Atlantic spring bloom. Marine Ecology Progress Series **440**, 267–279.

Wang, J. Y. (**2002)** "Stock Identity," in Encyclopedia of Marine Mammals, edited by W.F. Perrin, B. Würsig, and J.G.M. Thewissen (Academic Press, San Diego, USA), pp. 1189–1192.

Watkins, W. A. (**1981**). “Activities and Underwater Sounds of Fin Whales,” Scientific Reports of the Whales Research institute **93**, 83–117.

Watkins, W. A., Daher, M. A., Reppucci, G. M., George, J. E., Martin, D. L., DiMarzio, N. A., and Gannon, D. P. (**2000**). “Seasonality and distribution of whale calls in the North Pacific,” Oceanography **13**, 62–67.

Watkins, W. A., Tyack, P., and Moore, K. E. (**1987**). “The 20-Hz signals of finback whales (*Balaenoptera physalus*),” Journal of the Acoustical Society of America **82**, 1901–1912.

Wei, S. S., Wiens, D. A., Webb, S. C., Blackman, D. K., Dunn, R. A., and Conder, J. A. (**2012**). “Shear velocity structure of the Tonga arc and Lau backarc basin from Rayleigh wave tomography,” Abstract T53E-03 presented at the 2012 Fall Meeting, American Geophysical Union, 3–7 December, San Francisco, USA.

Weirathmueller, M. J., Wilcock, W. S. D., and Soule, D. C. (**2012**). “Source levels of fin whale 20Hz pulses measured in the Northeast Pacific Ocean,” Journal of the Acoustical Society of America **133**, 741–749.

Wilcock, W. S. D. (**2012**). “Tracking fin whales in the northeast Pacific Ocean with a seafloor seismic network,” Journal of the Acoustical Society of America **132**, 2408–2419.

Wilcock, W. S. D., Hooft, E. E. E., Toomey, D. R., McGill, P. R., Barclay, A. H., Stakes, D. S., and Ramirez, T. M. (**2009**). “The role of magma injection in localizing black smoker activity,” Nature Geoscience **2**, 509–513.

Wilcock, W. S. D., Stafford, K. M., Andrew, R. K., and Odom, R. I. (**2014**). "Sounds in the Ocean at 1–100 Hz," The Annual Review of Marine Science **6**, 117–140.

Zimmer, W. X. Z. (**2011**). *Passive Acoustic Monitoring of Cetaceans* (Cambridge University Press, New York, USA).

Chapter 2

DETECTION OF 20-HZ FIN WHALE CALLS FROM OBS DATA OFF SOUTHWEST PORTUGAL

2.1. INTRODUCTION

Most cetacean species are highly vocal and use several types of sounds for their daily activities, such as communication, navigation, feeding, and breeding, among others (Richardson *et al.*, 1995). The form of energy that propagates most efficiently in the water is sound. Light is absorbed much more strongly in water than in air and only reaches a depth of about 200 meters in clear ocean waters (Lammers and Oswald, 2015). Because of this, sound is a very important component in the life of cetaceans. The long range over which the acoustic signals produced by cetaceans can be detected makes them useful for research. Some of these signals show constant characteristics that allow researchers to identify signals at a species level (e.g. Watkins, 1981) and sometimes at an individual level (e.g. Tyack, 1997).

Acoustic data can provide information about the occurrence, distribution and some insights into the behaviour of a species. It is possible to assess the presence of a species in a particular area and the use of a habitat at different time scales, from hours to years (Nowacek *et al.*, 2016). For example, acoustic signals can reveal information about group differentiation and cohesion, which was observed in killer whales and sperm whales (e.g. Ford, 1989; Rendell *et al.*, 2012). Behavioural changes caused by anthropogenic pressure can also be assessed (e.g. Soto *et al.*, 2006; Castellote *et al.*, 2012). If a signal production rate is available, acoustic data can also be used to estimate abundance using several types of methods (e.g. Marques *et al.*, 2009). If signal location is possible, acoustic data can also be used to locate and track animals and to determine seasonal movements (e.g. Clark *et al.*, 1996; Stafford *et al.*, 2001; Wiggins *et al.*, 2005). Some mobile or fixed instruments can record sound over months, or even years (Mellinger *et al.*, 2007). The sounds produced by cetaceans can be found by manual scanning of a spectrogram, but in most cases the size of the recordings is so vast that this task becomes very labour intensive and expensive.

The analysis of large-scale acoustic datasets involves automated methods to find the sounds of interest. A variety of automated detection techniques are available, including

matched filtering, spectrogram correlation, energy summation, and neural networks (Stafford *et al.*, 1998; Mellinger and Clark, 2000; Mellinger, 2004; Mellinger *et al.*, 2004). The most widespread techniques are matched filtering and spectrogram correlation, in which a correlation of the signal waveform or a spectrogram with a template is calculated. Depending on the selected detection technique, there are several parameters that control whether a detection is made. Such parameters include a correlation threshold, a buffer time between detections or a threshold of quality related aspects, such as signal-to-noise ratio. A detection is only made when the set of these criteria are met. These criteria depend on the aim of the study in which the acoustic data are being used. If for example, the aim of the study is to detect the presence of a rare species, then a set of criteria that maximize the probability of detecting that species would be needed, even if that meant obtaining a large number of false detections. If the aim is to obtain specific information about a species that produces a signal frequently and has already established acoustic characteristics, then the parameters could be more selective. If the goal is to capture different classes of the same signal, then the template or the detector should be broad enough to allow some variance in the acoustic characteristics of that signal. In studies where the aim is to track a calling animal, it may not be necessary to detect all calls as long as the direction and the changes of tracks are being well represented. In this case, calls from a secondary animal that is not the target of detection and false detections should be as minimal as possible. If the aim is to use the acoustic data with a specific analysis method such as distance sampling, then the automated detector parameters need to be adjusted to the assumptions and requirements of that method (see Chapter 5 for more detail). Optimal thresholds of the parameters can be identified with receiver operating characteristic (ROC) curves, which are tools to assess the performance of a detector by comparing false detections with true detections (Zimmer, 2014).

A previous study used part of the acoustic recordings of this thesis in order to test and improve a particular location method, the single-station method (which is described in detail in Chapter 3) (Matias and Harris, 2015). Another study demonstrated the use of the range estimates of the signals to the recording instruments obtained with the single-station method in animal abundance methods (Harris *et al.*, 2013). In both studies, the 20-Hz fin whale call was detected using a matched-filter with a modified cross-correlation equation and a waveform template. Matias and Harris (2015) detected fin whale calls and air gun shots with an automated detector and showed a performance analysis of that detector. However, the performance analysis was undertaken with only one day of data.

In this thesis, the acoustic dataset of automatic detections were used to: 1) estimate the localition (Chapter 3) and depth (Chapter 6) of the calling fin whale; 2) characterize the most frequent signal produced by fin whales and assess the existence of acoustic groups

(Chapter 4); and 2) produce abundance estimates of fin whales (Chapter 5). In this chapter, the 20-Hz fin whale call was detected using a waveform matched filtering technique. The performance of different automated detectors was evaluated using a subsample of the acoustic data. The detector that showed the best balance between the number of true positives (correct detections) and the number of false positives (incorrect detections) was the one applied to the full extension of the acoustic recordings.

2.2. METHODS

2.2.1. Recording instruments, deployment and study area

Between September 2007 and August 2008 a network of 24 OBS was deployed off southwest Portugal, in an area that encompasses the southwest Iberian margin (Fig. 1). The instruments were part of the NEAREST (Integrated Observations from **Near** Shore Sourc**es** of **T**sunamis: Towards an Early Warning System) seismic monitoring project that aimed to investigate the local seismicity and the Earth structure in the source region of the Lisbon Earthquake and tsunami of 1755 (Silva *et al.*, 2017). This earthquake was possibly the most destructive event recorded in western Europe in historical time and completely devastated the city of Lisbon (e.g. Zitellini *et al.*, 2001). The deployment area hosts the Eurasia-Africa plate boundary and it is an active tectonic zone (e.g. Gràcia *et al.*, 2003). Some parts of the area are characterized by irregular topography and the existence of seamounts, such as the Gorringe Bank and others have smoother topography, with extensive abyssal plains. The instruments were placed on the seafloor at varying depths that ranged from 1.993 km to 5.100 km. The extent of the instrument array stretched up to 311.1 km (between OBS01 and OBS16). Instruments were typically placed ~ 30 km apart e.g., there was 32.3 km between OBS24 and OBS25.

The most western OBS (1, 2, 5, 8 and 11, Fig. 1) were inside the Gorringe Bank Special Area of Conservation. According to the national legislation *Diário da República n.º 148/2015, Série I de 2015-07-31*, inside this protected area there are two types of habitats (reefs and sandbanks) and at least two species (bottlenose dolphin and loggerhead turtle) of community interest (Presidência do Conselho de Ministros, 2015). The habitats and the species are listed in the 1992 European Union Directive on the conservation of natural habitats and of wild fauna and flora (European Commission, 1992), which requires member states of the European Union to establish Special Areas for Conservation to protect the listed species and habitats.

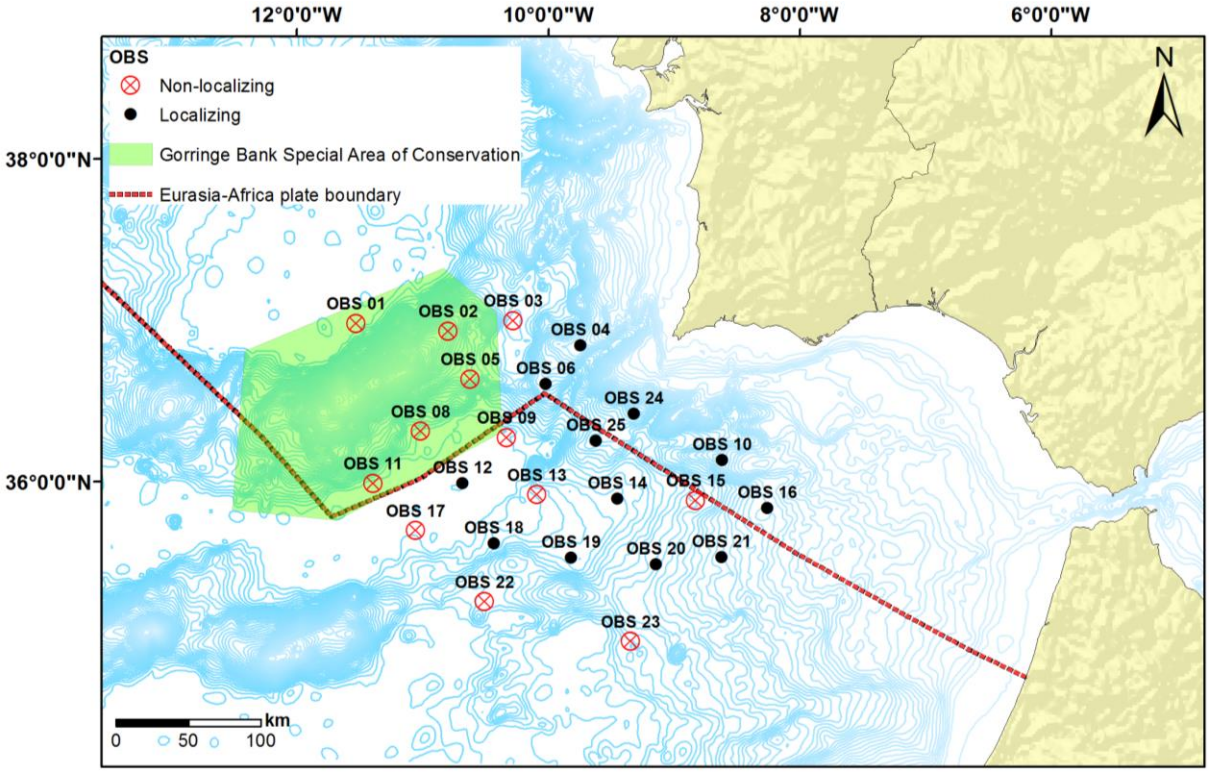

Figure 1. Location of the seismic monitoring array off southwest Portugal.

Each OBS was equipped with: 1) a 3-component Güralp CMG-40T broadband seismometer with flat velocity response of 0.017-50 Hz that registered the ground motion on the seafloor, 2) a HighTechInc. HTI-04/01/-PCA/ULF hydrophone with a response band of 0.017–8 kHz and –194 dB re. 1V/μPa sensitivity that registered pressure levels, and 3) an acquisition system with SEND Geolon MCS with 20 Gbytes of hard disk that saved the data. The OBS included 3 channels from the seismometer (two channels for the horizontal components, X and Y, and one channel for the vertical component, Z) and 1 channel from the hydrophone (H), all with a sampling rate of 100 Hz (Carrara *et al.*, 2008). The acquisition system settings ensured that seismic velocity recorded between 0.017 and 40 Hz and pressure recorded from 0.1 to 40 Hz without attenuation (Harris *et al.*, 2013). The recorded data were saved as four single channel files in a SEED format. Each seismometers were equipped with a levelling mechanism, which initiated a few hours after deployment, to level the vertical components after the arrival at the seafloor (Corela, 2014). During the monitoring period, the levelling action occurred every 15 days. More details on the sensors and recording system can be found in Corela (2014).

The recording period was not equal across all OBS. In some OBS, some components of the seismometers did not work properly at varying times (Table I). Instruments that did not have all three components of the seismometer working, which are required to obtain a location estimate of the detections (see Chapter 3), were designated as “non-localizing/NON LOC”

OBS. Instruments with all working components and that could provide a location estimate of the detections were designated “localizing/LOC” OBS. In addition, in the beginning of September there were several days when air gun experiments were undertaken (Somoza et al. 2007). These days were removed from the dataset and the start of the study period was set as 10th of September 2007 and the finish was 11th August 2008.

Table I – Details about the deployment and working period of each OBS used in this study.

OBS NO.	OBS DEPTH (km)	WORKING COMPONENTS	START	FINISH	NO. OF DAYS MONITORED
OBS 01	5.100	Z,Y, H	30-08-2007	12-06-2008	288
OBS02	2.270	Y, H	30-08-2007	31-07-2008	337
OBS 03	3.932	Z,Y, H	29-08-2007	31-07-2008	338
OBS 04	1.993	X, Y, Z, H	14-09-2007	25-06-2008	286
OBS 05	3.095	Z,Y, H	30-08-2007	23-06-2008	299
OBS 06	2.956	X (from Feb ’08), Y, Z, H	29-08-2007	20-07-2008	327
OBS 08	4.671	Z,Y, H	31-08-2007	09-08-2008	345
OBS 09	4.811	Z,Y, H	30-08-2007	29-04-2008	244
OBS 10	2.067	X, Y, Z, H	02-09-2007	29-06-2008	302
OBS11	4.855	Y, H	30-08-2007	02-05-2008	247
OBS 12	4.860	X, Y, Z, H	01-09-2007	20-07-2008	324
OBS 13	4.494	Z,Y, H	31-08-2007	14-07-2008	319
OBS 14	4.212	X, Y, Z, H	02-09-2007	04-08-2008	338
OBS 15	3.357	X, Z, H	01-09-2007	07-04-2008	220
OBS 16	2.069	X, Y, Z, H	01-09-2007	07-07-2008	311
OBS 17	4.873	Z,Y, H	30-08-2007	28-05-2008	273
OBS 18	4.605	X, Y, Z, H	01-09-2007	07-07-2008	311
OBS 19	4.287	X, Y, Z, H	01-09-2007	07-07-2008	311
OBS 20	3.449	X, Y, Z, H	01-09-2007	07-07-2008	311
OBS 21	2.566	X, Y, Z, H	01-09-2007	07-07-2008	311
OBS 22	4.095	Z,Y, H	31-08-2007	24-07-2008	329
OBS 23	3.747	Z,Y, H	31-08-2007	28-06-2008	303
OBS 24	2.439	X, Y, Z, H	29-11-2007	11-08-2008	257
OBS 25	3.234	X, Y, Z, H	24-11-2007	11-08-2008	262

2.2.2. Pre-processing of the data and the detection algorithm in SEISAN

The original data was provided in miniseed, a common format in seismology for data exchange. For analysis, the data was converted to the SEISAN format (Havskov and Ottemöller, 2008) and split into 4 files of 6 hours duration for each day and instrument.

The target signal of the detection process was the 20-Hz fin whale call, already described in Chapter 1. This call is a highly stereotyped downsweeping tone that starts at ~30

Hz and drops to ~15 Hz in ~1 second (Watkins *et al.*, 1987). Usually, the 20-Hz fin whale call is produced in sequences that are grouped in bouts that can last for hours, which eases the sound detection process.

The detection algorithm was based on a matched filter that uses a master waveform that can be either a synthetic signal or can be obtained from the data by identifying one of the loudest and highest signal-to-noise ratio (SNR) calls. The master waveform was selected by visualizing spectrograms of the Z-channel in TRITON (Wiggins, 2003). The sound file of the Z-channel used to create the spectrogram was filtered between 2 and 40 Hz using a Butterworth eight-pole bandpass filter. The Z-channel was the preferred channel to use for automated detection of fin whale calls because, when compared to the H-channel, the Z-channel showed higher amplitudes with higher levels of SNR, which was also observed in other published studies (e.g. McDonald *et al.*, 1995).

Spectrograms were calculated using a discrete Fourier transform with a Hanning window (window length of 256 samples with an overlap of 95%). Brightness and contrast settings were adjusted to produce the best visual image. The entire frequency range (0–50 Hz) was displayed for all spectrograms. The search for a suitable master waveform was undertaken based on days where the highest vocal activity was expected (in winter) and where previous detections of fin whale calls were already registered (e.g. Harris *et al.*, 2013; Corela, 2014). The template was selected to have acoustic characteristics in time and frequency similar to those previously published and described in the text above for 20-Hz fin whale call and with a window of low background noise. When 20-Hz calls are produced in sequences, the sound source is fairly constant (Weirathmueller *et al.*, 2012). As such, the template selected also had high amplitude, in order to cover a wide range of amplitude levels. After the master waveform was selected in TRITON, the master waveform was finally extracted in SEISAN and saved for the analysis.

The application of the matched filter using a standard expression for the normalized correlation (C_{xy}^{S}) between two arbitrary time series x_i and y_i is as follows:

$$C_{xy}^{S} = \frac{\sum x_i y_i}{\sqrt{\sum x_i^2 \sum y_i^2}} \qquad \text{Eq. 1}$$

The trigger time was taken as the time that maximizes this function. The normalized cross-correlation varied between -1 and +1 for perfectly anti-correlated or correlated signals. This function was not affected by the differences in amplitudes between two similar signals, $C_{xy}^{S}(x_i, \alpha y_i) = C_{xy}^{S}(x_i, y_i)$.

Matias and Harris (2015) noted Eq. 1 resulted in a very large number of detections with high correlations but very small absolute amplitude (equivalent to very small SNR). Although this is not important for the detection process, signals with small SNR values needed to be considered at the location estimation stage. Both signal detection and location estimation were performed by the application *wavwhaleh*. The single station method used in further analysis (see Chapter 3), provides reliable estimates of locations inside a critical range, (defined in Chapter 3). Outside the critical range, the method generates spurious range estimates. Signals with small amplitudes are likely to be generated further away from the recording instrument. Therefore, to avoid a large number of detections with potentially unreliable range estimates, a modified normalized cross-correlation C_{xy}^{M} was also tested:

$$C_{xy}^{M} = \left(\sqrt{2} \frac{\sum x_i y_i}{\sqrt{(\sum {x_i}^2)^2 + (\sum {y_i}^2)^2}} \right)^{M} \qquad \text{Eq. 2}$$

where M is a constant to be chosen by the analyst.
If $x_i = y_i$ this equation also gives a value of one, as Eq. 1, but when one time series is attenuated by a factor, e.g., $y_i = Ax_i$ then:

$$C_{xy}^{M} = \left(\sqrt{2} \frac{1}{\sqrt{A^2 + \frac{1}{A^2}}} \right)^{M} \qquad \text{Eq. 3}$$

Applying Eq. 2, the resulting correlation values of signals that differ in amplitude, even if they are perfectly correlated, are degraded.

Several parameters that influence the detection process were set and used by *wavwhaleh* (Table II). Other parameters related with the location method were also set but they will be discussed in Chapter 3. Different values of the parameters were tested and each set of parameters was defined as a “detector”.

Table II – Definitions of each parameter set for the detection process.

Parameter	Definition
Main Channel	Component of the seismometer to use for the cross-correlation between the master template. Either channels H or Z are accepted. Channel H is the default.
Cross-correlation equation	Choice of the equation to calculate the cross-correlation between two time series: = 1 Uses the traditional cross-correlation that over-estimates small triggers (Eq. 1). = 0 Uses the modified one that attenuates correlation values with amplitude of the signal (Eq. 2). Default. = 2 Identical to "0" but powered to (M)
Power of cross-correlation equation (M)	Power of cross-correlation, when using option 2 of the cross-correlation equation. Default is 1.
Correlation threshold	Minimum correlation value between the master template and channel waveform to accept a triggered event as a detection.
Buffer time	Minimum time between consecutive triggers to accept them as different detections.
Filter	Application (1 for application/0 no filter) of filter defined by a frequency range. The filter is recursive and can be band-pass (two frequencies defined), low-pass (upper limit frequency only) and high-pass (lower limit frequency only). The filter is a Butterworth type with 4 poles and 2 passes (8 poles total) for zero phase.

A detection was registered whenever the cross-correlation between the master template and the waveform of the recording exceeded the correlation threshold. The correlation threshold used for all detectors was set to a very low value of 0.2. A buffer time of 0.3 seconds was defined to avoid triggering mainly on closely spaced calls due to multipath arrivals. If a second detection was encountered within the buffer time of another detection, the detection with the highest correlation value was selected. The trigger time of a detection was defined as the time where the maximum cross-correlation value occurred. For all detections, several diagnostic parameters were computed, some related with the location estimates (see Chapter 3) and others related with the quality of the detected signal: correlation value, trigger time, channel amplitudes and SNR. The SNR was computed by the signal root square (RMS) and the noise RMS. The time window for the computation of the noise RMS has the same size as the signal's and precedes the trigger. The time window was defined by the duration of the master waveform.

2.2.3. Subsample

A total of 9 detectors of the *wavwhaleh* algorithm were tested with a systematic random subsample of the acoustic recordings in order to have the best representation of the time period and instruments. Because of time constraints it was not possible to check all detections made in all of the recordings for the 9 detectors. A subsample was defined in order to review manually all detections made and therefore assess the performance of each detector (see performance analysis below). The start day of the subsample was selected randomly, between 1 and 9, after the period when air gun shots were produced for a seismic experiment of the NEAREST project. Then a day was selected every 9 days to serve as a sample. The spacing of 9 days allowed a representation of ~11% of the dataset in the analysis. The selected days could contain fin whale bouts or could have other signals and/or noise. Each day was manually scanned for high SNR bouts using spectrograms and the days with the presence of fin whale bouts were marked for use in further analysis. There were 556 sampled days, 62 of which had potentially high SNR bouts. However, because of time constraints, only 30 of the marked days were randomly subsampled and analysed further.

For each of the 30 marked days, one hour of each bout was manually checked, considering 5 signal classes (Table III and Annex I) resulting in a 30-hour subsample (Table IV). In addition, the times of each signal were manually identified. The 20-Hz call was classified either as 1) being part of a main bout (20-Hz call), 2) produced in a secondary bout (auxiliary call), or 3) an arrival from multiple paths (multipaths). If there was uncertainty about whether an observed signal was a 20-Hz call, then the signal was classified as “unsure”. The class of unsure signals was only related with the 20-Hz call. The backbeat, another low frequency sound produced by fin whales, was also identified. During this hour there were also periods of silence of varying lengths when different types of false positives, which are defined below in the performance analysis description (2.2.4), could be recorded. The trigger times obtained in the automatic detection process using the same 30 hours were then compared with the manual times obtained with the visual scan of the subsample.

Table III – Description of the classes of signals identified in the subsample (spectrograms of each class can be found in Annex I).

Type of call	Description
20-Hz call	20-Hz call from the main bout (Fig. 1 in Annex I). Signals that showed a varying frequency interval between 15 and 30 Hz and a duration around 1 second. Amplitude of these signals was always above 500 counts. Signals of this class showed constant intervals between them, mostly from 10 to 15 seconds.
Backbeat	Backbeat from the main bout (Fig. 2 in Annex I). Backbeats were considered to have smaller spectrum bandwidth and a lower median frequency than 20-Hz calls. They were considered to be narrow-band signals between 15 to 18 Hz and almost always produced in between 20-Hz calls.
Auxiliary	Signals (either 20-Hz calls or backbeats) from possibly other animals (Fig. 3 in Annex I).
Multipath	Small amplitude signals that resembled 20-Hz/backbeats and were produced very close the main calls (Fig. 4 in Annex I). When there was only one animal calling, these close faint signals were considered multipaths. If potential multipaths were observed when there was more than one animal calling, in order to asses if it was a multipath or a second whale, the structure of the bout was also considered.
Unsure	Signals with low amplitude (below 500 counts) and low spectral intensity or signals, where it was not clear if they were 20-Hz calls (whether from the main bout or an auxiliary bout) (Fig. 5 in Annex I).
Other	Discrete signals not related with fin whale vocal activity recorded in the OBS, such as far ranging air guns, levelling of the OBS, and other whale species (Fig. 6 in Annex I).

Table IV – Summary of the subsample used in the overall performance analysis (2.2.4). All detections were manually identified. Shaded grey samples were from OBS that had all the 3-components working (localizing OBS) and were used in the analysis of Chapter 3. Main 20-Hz and main backbeats (bb) were signals produced in a main bout and aux 20-Hz and aux bb were produced in an auxiliary bout.

#	OBS	DATE	HOUR	Main 20-Hz	Main bb	Aux 20-Hz	Aux bb	Multipath	Unsure
1	17	02-11-2007	19:00:00	156	24	0	0	2	0
2	5	02-11-2007	03:00:00	206	18	0	0	47	0
3	5	11-11-2007	05:00:00	183	48	0	0	0	0
4	10	20-11-2007	04:00:00	100	52	0	0	18	0
5	4	20-11-2007	21:00:00	223	10	28	27	13	0
6	14	20-11-2007	12:00:00	169	27	0	0	58	0
7	12	29-11-2007	02:00:00	251	6	122	6	0	5
8	9	29-11-2007	02:00:00	117	15	120	18	0	0
9	16	08-12-2007	23:00:00	81	47	49	4	0	20
10	14	08-12-2007	21:00:00	210	28	26	5	0	10
11	3	08-12-2007	15:00:00	91	78	154	12	0	4
12	5	17-12-2007	12:00:00	180	37	42	4	0	0
13	3	17-12-2007	02:00:00	138	53	0	0	0	0
14	6	17-12-2007	04:00:00	199	12	43	9	0	0
15	13	26-12-2007	04:00:00	106	31	0	0	0	0
16	4	26-12-2007	00:00:00	187	41	1	1	0	3
17	25	04-01-2008	19:00:00	167	0	0	0	0	4
18	10	04-01-2008	06:00:00	124	0	33	0	8	0
19	20	04-01-2008	10:00:00	119	24	170	13	0	0
20	16	04-01-2008	13:00:00	208	28	0	0	13	0
21	13	22-01-2008	11:00:00	214	29	4	6	0	9
22	25	22-01-2008	11:00:00	180	20	32	1	4	0
23	5	22-01-2008	04:00:00	149	47	17	3	0	0
24	12	22-01-2008	19:00:00	152	55	0	0	12	0
25	12	31-01-2008	09:00:00	111	18	7	5	0	2
26	9	31-01-2008	07:00:00	140	49	62	58	0	0
27	24	31-01-2008	16:00:00	182	29	60	6	4	0
28	6	31-01-2008	11:00:00	74	9	0	0	0	2
29	5	09-02-2008	20:00:00	153	36	0	0	0	0
30	12	07-03-2008	18:00:00	165	48	13	3	13	0
TOTAL	**-**	**-**	**-**	**4 735**	**919**	**983**	**181**	**192**	**59**

2.2.4. Performance analysis

Automated methods for detecting acoustic signals facilitate the use of acoustic data, as detections are usually obtained very quickly and in a format almost 'ready to use'. However, it is necessary to assess the performance of the detectors, i.e., how well each detector can detect the signal of interest. There are several signals that could falsely trigger the detector, such as human-made noise and non-target biological sounds produced by other species. In some analyses, such as abundance estimation, the number of false detections can be accounted for by considering a false positive rate. Other studies where acoustic measurements are used to represent geographical differences between stocks, or where behavioural patterns are assessed, the variability caused by false positives should be minimal. A performance analysis was undertaken, in which several parameters were calculated (Mellinger *et al.*, 2016).

1. **True positive rate (correct detections):** Number of correct detections, including both main and auxiliary 20-Hz calls, i.e. true positives (a) divided by the total number of the 20-Hz calls, which is the number of true positives (a) and the number of missed 20-Hz calls (b).

$$True\ Positive\ Rate = \frac{a}{a+b} \qquad \text{Eq. 4}$$

2. **False positive rate:** Number of detections that are not from the desired signal which is the 20-Hz fin whale call, i.e. false positives (c) divided by the total number detections, which is the number of true positives (a) and the number of false positives (c). If some of the false positives show a seasonality pattern, then the detector could present more detections in the presence of that signal and therefore be biased. The presence of false detections should be random. The assessment of the seasonality of the false positives was considered as the subsample was representative for all study periods and the sampled time period consisted of one hour of each day that contained periods with whales and periods of silence where noise and other signals could trigger the detector.

$$False\ Positive\ Rate = \frac{c}{a+c} \qquad \text{Eq. 5}$$

3. **Missed calls:** Number of desired signals, the 20-Hz fin whale call that were not detected, i.e. missed signals (b) divided by the total number of 20-Hz fin whale calls (a + b). Quality-related parameters calculated by the algorithm, such as SNR, channel amplitude and cross-correlation, were evaluated in order to assess the possible causes for the missed calls.

$$Missed\ call\ rate = \frac{b}{a+b} \qquad \text{Eq. 6}$$

4. **Receiver Operating Curve (ROC) Curve:** Plot of the relationship between the false positive rate (%) (along the X axis) and the true positive rate (%) (along the Y axis) for a range of cross correlation thresholds. It represents how well the detectors are able to detect the signal in the presence of noise. A detector that shows an optimal performance is located at the top-left of the plot and is characterized by a balance between a low rate of false positives and a high rate of true positives.

The detection algorithm was built in a seismological software that was not designed to detect biological signals. The performance of the best detector was compared with a widely-used software by bioacousticians, Ishmael (Mellinger, 2002), in order to have a performance reference. In this software, there are several types of detectors, but the one used in this comparison was the matched filtering, which cross-correlates a stored signal (a .wav file, referred to as "template") with the signal waveform. The settings of the detector in Ishmael were set in a sequential procedure in order to maximize the number of true positives with the lowest number of false positives. In the first step, the detector was the most conservative, detecting as many signals as possible both true and false positives. The next combinations were set in order to retain as many true positives as possible minimizing the number of false positives. The change in the settings of the detector stopped when the rate of true positives decreased. When Ishmael is detecting a sound in a recording, it creates a detection function, which represents the likelihood that the target signal is present at each point in time, measured in arbitrary units. This detection function is different from the detection function that is defined for distance sampling analysis (which is included in Chapter 5). The detection function continuously updates through time and it shows high peaks when there are signals that are similar with the template. The crucial aspect of the detection process is the height of the detection function relative to a threshold. When the detection function exceeds this threshold for a specified length of time, a discrete detection event is recorded.

After the performance analysis and the identification of the most balanced set of characteristics, the chosen detector was applied to the recordings of the entire study period and instruments.

2.3. RESULTS

A total of 9 detectors were tested in the 30-hour subsample. Only 20-Hz calls, either from the main bout or auxiliary bouts were considered as true positives. Backbeats, multipaths, unsure signals and other detections were considered as false positives. From a visual inspection of the spectrograms of the 30-hour subsample, there was a total of 5 718 20-Hz calls, 4 735 from the main bouts and 983 that were auxiliary calls (Table III). A total of 1 351 other signals from different classes (backbeats, multipaths and unsure signals) was also manually found. Table V shows a summary of characteristics of each detector and the detection results. The maximum true positive rate of 99.3% was registered by detector 6. The minimum true positive rate was 58.4% with detector 3 for the lowest cross-correlation threshold investigated (0.2).

The use of the vertical channel Z (detectors 1-6) produced better results than the use of the hydrophone channel (detectors 8 and 9). Although the detectors with the hydrophone showed a high rate of true positives, they also showed a relatively high rate of false positives. Applying a filter with a broad frequency range defined by the frequency characteristics of the 20-Hz call increased the number of detections and also improved the performance (detectors 2, 4, and 6), allowing a higher rate of true positives.

The traditional cross-correlation equation used in detector 1 resulted in a rate of true positives that was improved with the application of a filter in detector 2 (from 65.5% to 87.5%). However, the application of the filter also increased the rate of false positives (from 77.7% to 90.6%). The modified cross-correlation equation was expected to be more selective, as it considered signal amplitude in the correlation value discarding the faintest triggers. As expected, the use of the modified cross-correlation in detector 3 decreased the rate of true positives, possibly discarding the low amplitude calls. The rate of false positives also decreased considerably. However, when the filter was applied with the modified cross-correlation powered to 1 (detector 4), there was a steep increase in the rate of true positives and the rate of false positives continued to be low. When using half of the power of the modified cross-correlation in detector 5, the rate of true positives continued to increase but in this case the rate of false positives showed a steep increase.

*Table V – Detector parameters varied during detector performance assessment, and corresponding results. All detectors were run with a correlation threshold of 0.2 *Values between brackets are detector 4 with a correlation threshold of 0.1*

Detector →	**1**	**2**	**3**	**4***	**5**	**6**	**8**	**9**
Parameters and results ↓								
Main channel	Z	Z	Z	Z	Z	Z	H	H
Cross-correlation equation	1	1	0	0	2	2	0	2
Power of cross-correlation equation	-	-	1	1	0.5	0.5	1	0.5
Filter (Yes/No)	0	1	0	1	0	1	1	1
Lower frequency	-	4	-	4	-	4	4	4
Upper frequency	-	40	-	40	-	40	40	40
Buffer time	0.3	0.3	0.3	0.3	0.3	0.3	0.3	0.3
Minimum correlation	0.2	0.3	0.2	0.2(0.1)	0.2	0.2	0.2	0.3
True Positive rate (%)	65.5	87.5	58.4	87.0(98.7)	82.6	99.3	88.4	97.9
Main 20-Hz calls (%)	68.1	89.3	63.8	92.1(99.6)	84.4	99.8	91.4	98.5
Auxiliary 20-Hz calls (%)	52.9	79.0	32.3	62.6(94.2)	74.1	96.9	73.9	94.8
False positive rate (%)	77.7	90.6	5.4	8.9(58.5)	90.0	90.7	40.2	88.5
Missed call rate (%)	34.5	12.5	41.6	13.0(1.3)	17.4	0.7	11.6	2.1

The ROC curve allows a more detailed look at the performance of each detector at different levels of the correlation threshold (c_min) (Fig. 2). The detector with a modified normalized cross-correlation powered to 0.5 and a filter of 4-40 Hz (detector 6) resulted in the highest rate of true positives but it also showed the highest rate of false positives. To correctly detect 99.3% of the 20-Hz calls, 90.7% of detections were false detections. This means that the modified cross-correlation with a power of 0.5 produced a high number of detections. The detector that showed the best performance, i.e. the one with the best balance between the number of true positives and false positives, was the one with a modified cross-correlation powered to 1 and a filter between 4 and 40 Hz (detector 4). At a correlation threshold of 0.2, the detector showed a high true positive rate of 87.0% with the smallest rate of false positives (8.9%). At a correlation threshold of 0.5, the modified cross-correlation equation with a power of 0.5 in detector 6 produced the same results obtained with a power of 1 for a lower correlation threshold (detector 4). The modified cross-correlation powered to 1 with the lowest correlation threshold possible (0.1) (detector 4) also showed similar results to the modified cross-

correlation equation with a power of 0.5 with correlation values of ~0.4 (detector 6). The third best performance was obtained with a detector in Ishmael. At low detection function thresholds, Ishmael showed the second lowest rate of false positives. Regarding Ishmael, there were two false positives that showed high values of the detection function (Fig. 3) and had an impact on the ROC curve of the detector.

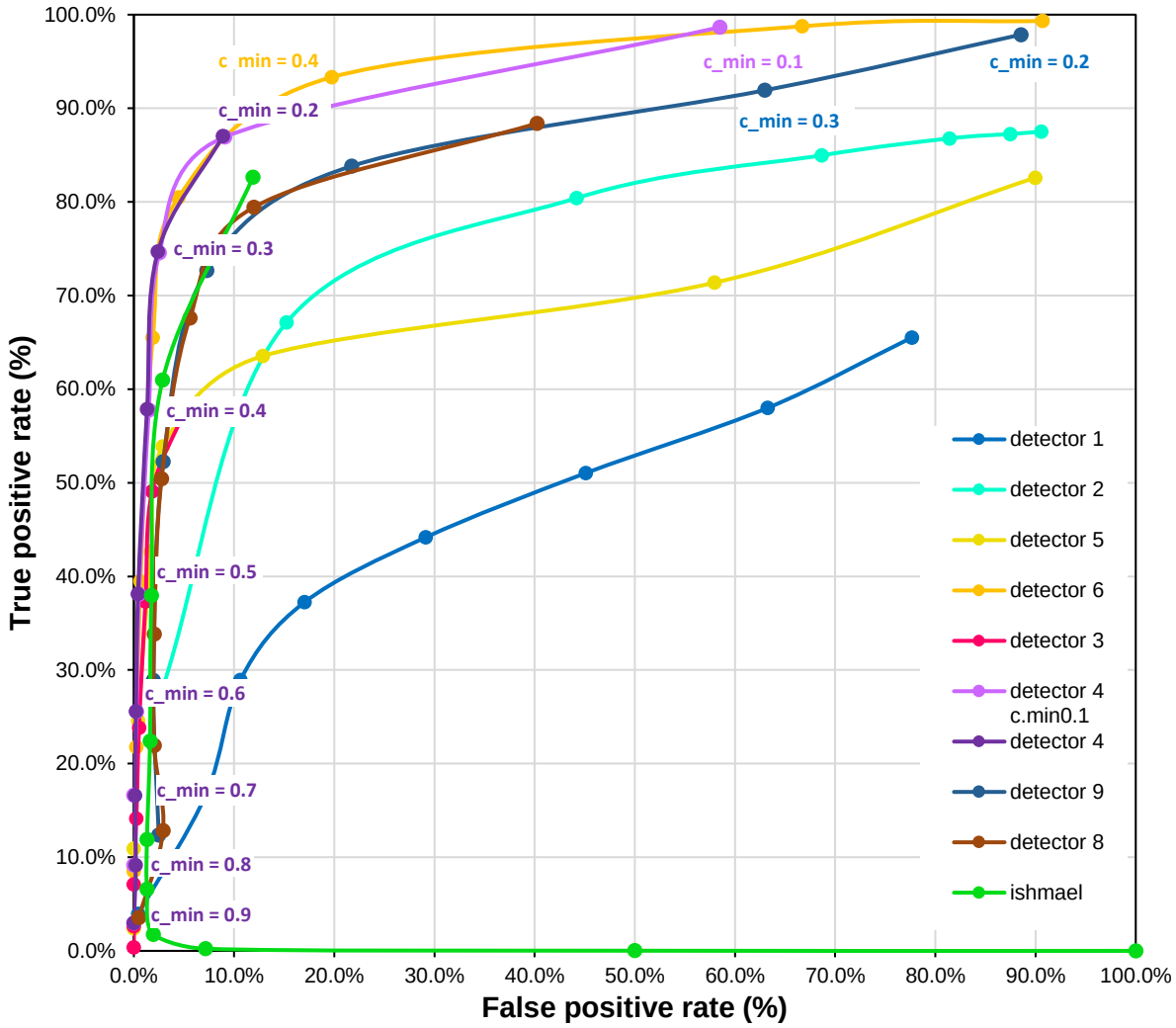

Figure 2. Receiver operating characteristic (ROC) curve for each detector used in the detection process of 20-Hz calls in the 30-hour subsample (n = 5 718). For reference purposes, correlation values (c_min) of the ROC curve for detectors 1, 4 and 6 are shown.

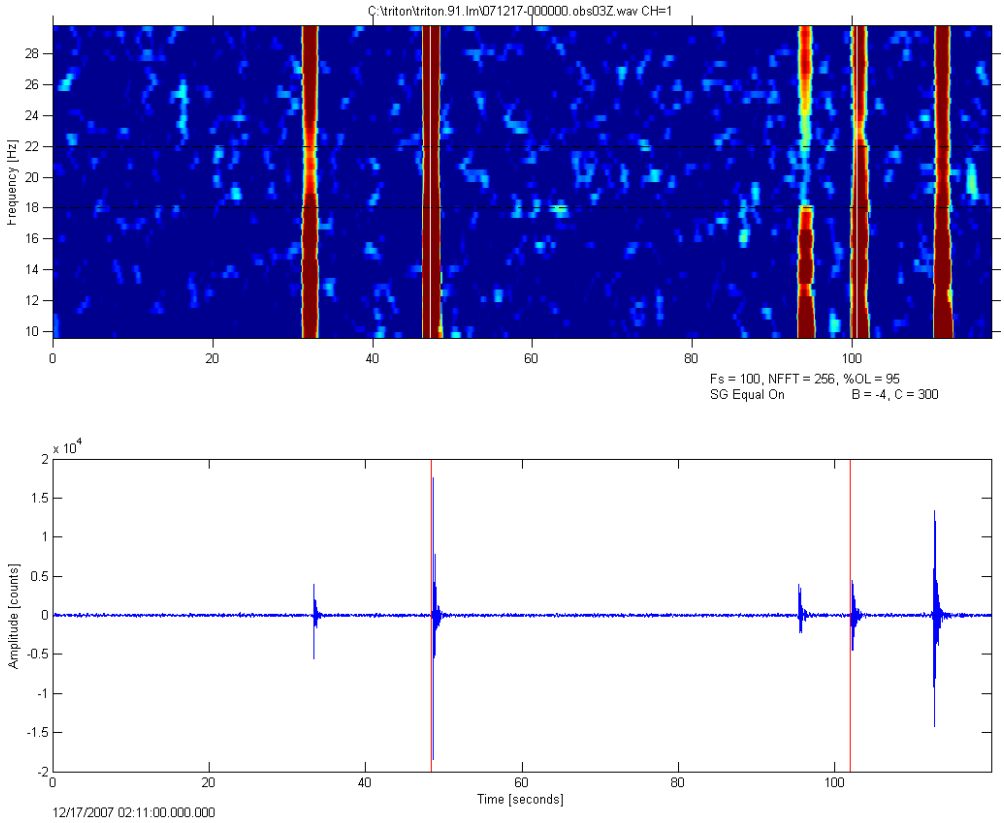

Figure 3. False positives obtained with a detector in Ishmael and that showed the highest values of the detection function. Vertical lines in white (top) and in red (bottom) represent the trigger times obtained in Ishmael. Spectrogram and waveform of 2 minutes recorded on OBS03 on 17/12/2007, at 2:11:00 obtained with TRITON.

To understand better the performance of the best detector, detector 4, the amplitude of the Z-channel and the SNR of the 20-Hz calls was plotted (Fig. 4). Missed calls from detector 4 presented small amplitudes and small SNR.

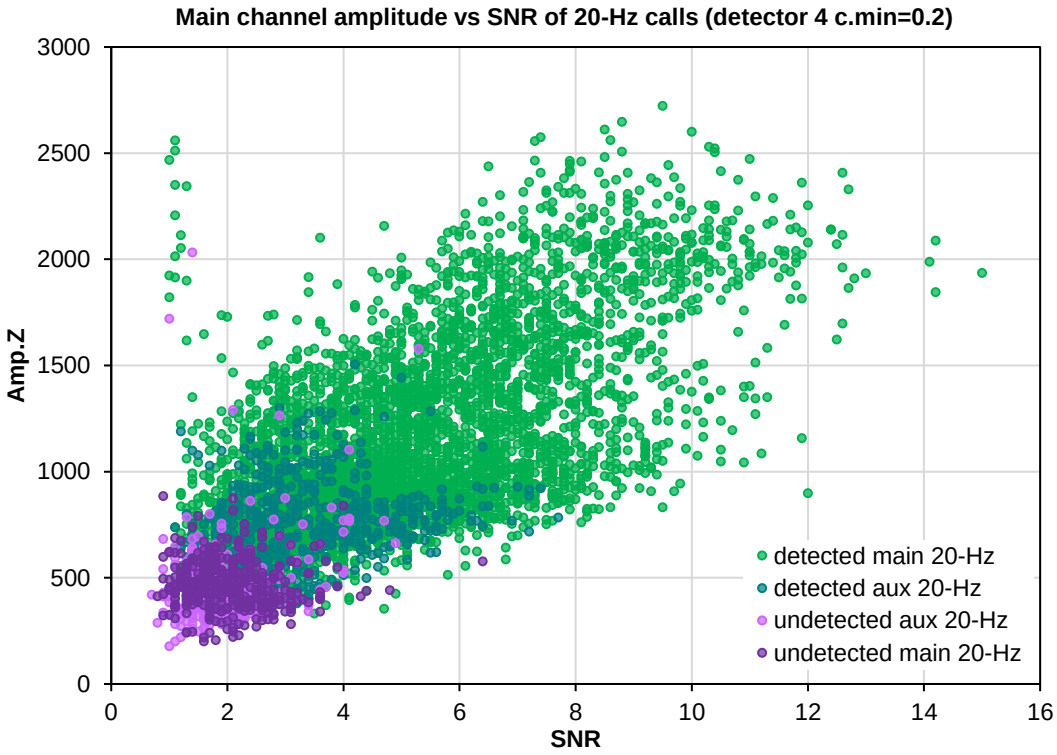

Figure 4. Z-channel amplitude (Amp.Z) with signal-to-noise ratio (SNR) of all 20-Hz calls in the subsample used for detector performance analysis (n = 5 718).

Examples of the spectrograms of some of the missed calls of detector 4 (Fig. 5) confirmed that most of them had low SNR, suggesting they could have been produced far away from the recording instruments (Fig. 5A) and other calls were missed because they presented some evidence of acoustic interference (Fig.5B, see Chapter 6) that the matched filter could not account for. The time resolution of the spectrograms in Fig. 4 was altered in each spectrogram in order to highlight why calls were missed by the detector.

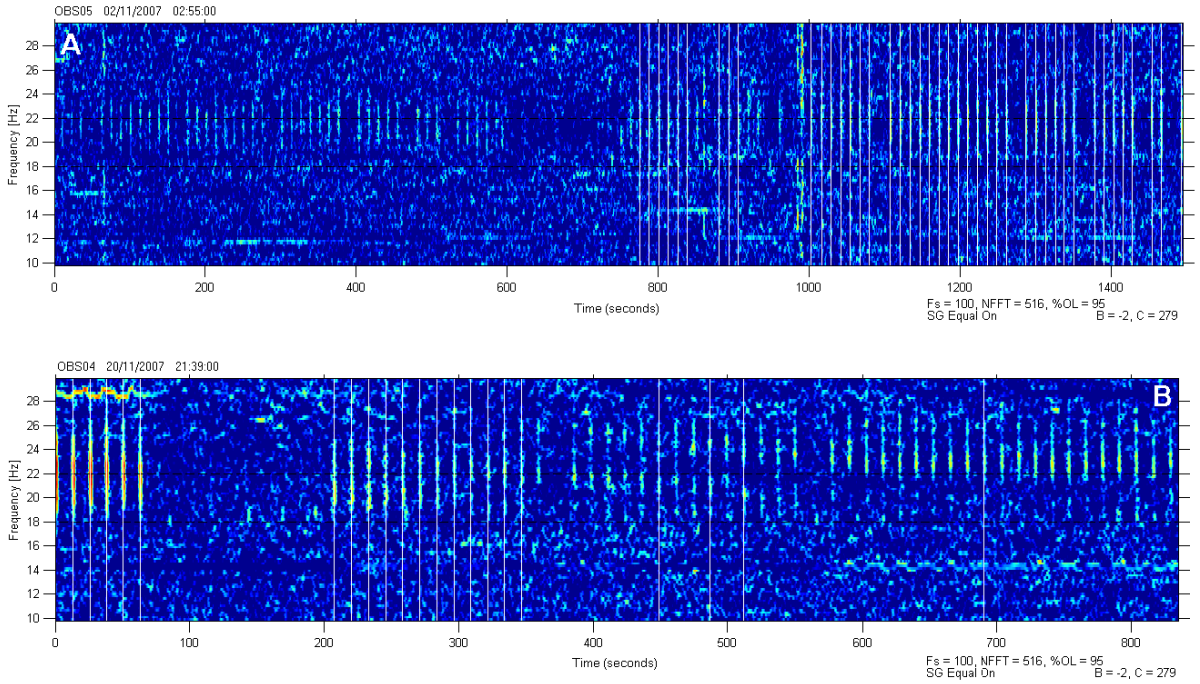

Figure 5. Examples of spectrograms with missed calls: A) Calls with low SNR, recorded in OBS05 on 02/11/2007 at 02:55:00; B) Calls with potential acoustic interference (see Chapter 6 for a more detailed visual description), recorded in OBS04, 20/11/2007 at 21:39:00. Vertical white lines represent the automatic detections made with detector 4.

Most false positives seemed to be produced by noise (Fig. 6) and few seemed to be caused by the levelling of the OBS (Fig. 7). Every 15 days, a gimbal system included in each seismometer performed the levelling of the vertical component which resulted in a series of strong signals that are were recorded on the seismometer and not on the hydrophone channel. On some occasions there was also a single false positive, also known as singleton (Fig. 8). The origin of the singletons is still unclear. They are described as Short Duration Events (SDE) and they may have a geological origin, they can be caused by fish bumps or by the sudden slip of the instrument frame. These events are described in detail in Corela (2014).

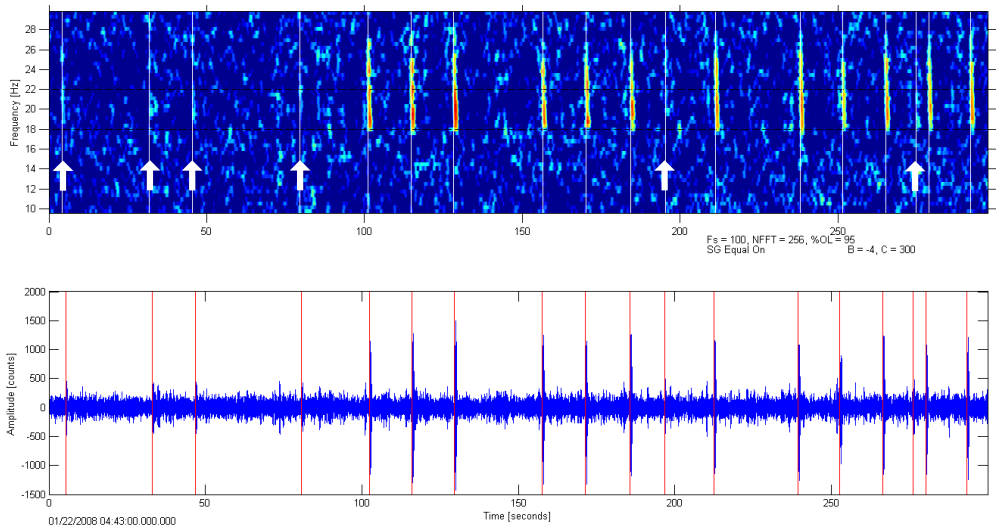

Figure 6. Spectrogram of 5 minutes of the recording on OBS05, 22/01/2008 at 4:43:00, showing the several detections (vertical red line) and false positives (white arrow).

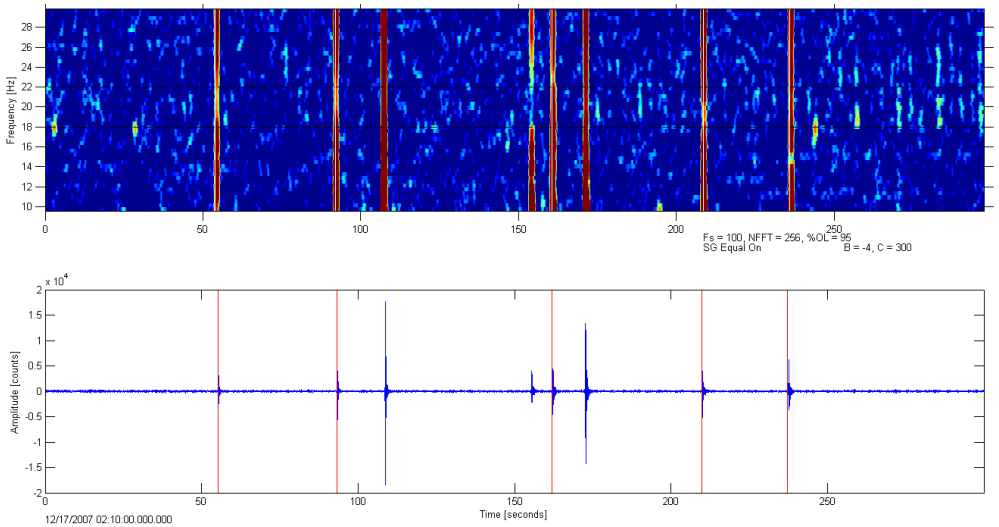

Figure 7. Spectrogram of 5 minutes of the recording on OBS03, 17/12/2007 at 2:10:00, showing the levelling of the OBS which was detected.

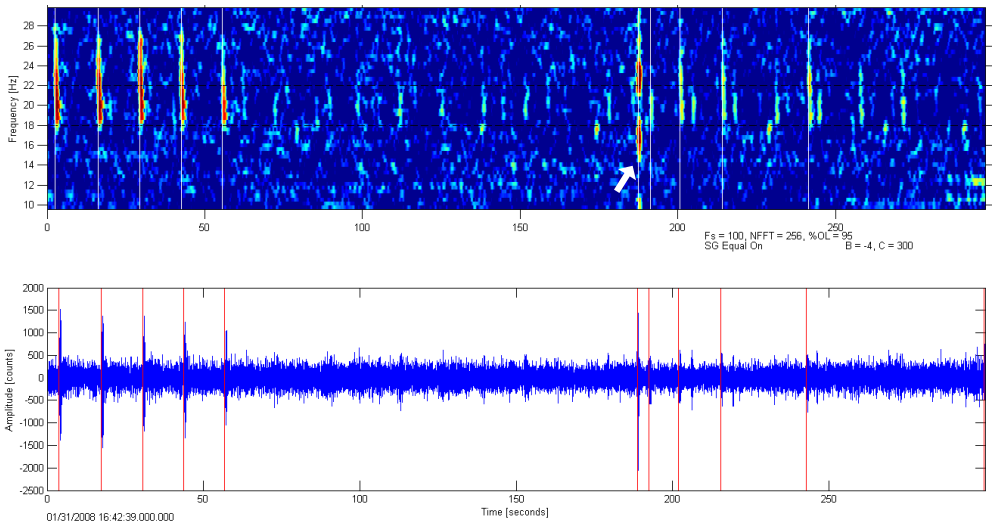

Figure 8. Spectrogram of 5 minutes of the recording on OBS24, 31/01/2008 at 16:42:39, showing an unsure signal (white arrow) that was identified as a false positive and were identified as a singleton.

Running the detector on the full dataset

The application of detector 4 in all recordings of all OBS resulted in a total of 2 918.312 detections (Table VI). All chapters of the thesis that include automatic detections used the totality (Chapter 3) or a subsample (Chapter 4 and 5) of these detections.

Table VI – Summary of detections with detector 4 for all OBS during their recording period. Non-localizing OBS are shaded grey. OBS06 started recording without the three components working properly (NON LOC) but after February 2008 all the channels that enable a location of a detected signal were working (LOC).

OBS NO.	Start date	Finish date	Number of days surveyed	Total number of detections
1	10-09-2007	12-06-2008	277	482 195
3	10-09-2007	31-07-2008	326	122 488
4	15-09-2007	25-06-2008	285	113 714
5	10-09-2007	23-06-2008	288	263 155
6	14-02-2008	20-07-2008	158	145 338(NON LOC)+7 327(LOC)
8	10-09-2007	10-08-2008	336	48 975
9	10-09-2007	29-04-2008	233	134 654
10	10-09-2007	29-06-2008	294	141 885
12	10-09-2007	20-07-2008	315	151 924
13	10-09-2007	14-07-2008	309	107 506
14	17-09-2007	20-07-2008	308	128 498
15	01-09-2007	07-04-2008	220	112
16	10-09-2007	07-07-2008	302	92 546
17	10-09-2007	28-05-2008	262	478 678
18	10-09-2007	17-07-2008	312	125 700
19	10-09-2007	17-07-2008	312	96 606
20	10-09-2007	12-07-2008	307	68 294
24	29-11-2007	11-08-2008	256	135 857
25	29-11-2007	11-08-2008	256	72 860
TOTAL	**-**	**-**	**-**	**2 918.312**

2.4. DISCUSSION

Automatic signal detection is a critical stage in the passive acoustic monitoring of cetaceans. Several parameters affect the choice of a detector but the main aspects to consider are the characteristics of the signal and the purpose of the resulting detections. Fin whales produce fairly simple acoustic signals in a repeated fashion (Watkins *et al.*, 1987) that eases the detection process. Energy-based (e.g. Clark *et al.*, 2002) and matched-filter, both based on the waveform (Harris *et al.*, 2013) and spectrogram (Delarue *et al.*, 2009; Castellote *et al.*, 2011) detection methods have been used to detect 20-Hz fin whale calls. In this acoustic dataset, the 20-Hz fin whale calls have been detected using a matched-filter with a modified cross-correlation equation (Harris *et al.*, 2013; Matias and Harris 2015). In Harris *et al.* (2013), the aim of the detection process was to obtain a small sample of calls in order to test a seismological method to locate the calls and to demonstrate its use in distance sampling methods. Although the detector used showed good results, its performance was only assessed with a small sample of one day. In this thesis, the aim of the detection process was to obtain a dataset of automatic detections that could be used in different types of studies: acoustic characterization and abundance estimates.

One of the key aspects of a widely used method to obtain abundance estimates, distance sampling, is that target signals very close to the recording instrument are more likely to be detected than those that are farther away (Buckland *et al.*, 2001). The average probability of detecting a signal is used to obtain an estimate of the number of signals per unit area, density, which in turn is used to calculate the number of signals in a study area, i.e. abundance (see Chapter 5). If a production rate of that signal is available, then the signal density can be transformed into animal density. The shape of the function that predicts the detectability of a call as a function of distance, the detection function, at near zero distances affects the average probability of detection (Thomas *et al.*, 2002). In order to have a reliable density estimate, it is crucial that the detection function at near zero distances has a “shoulder” which is obtained by the detection of close signals (Buckland *et al.*, 2001). In that case, the most suitable detector would be one with broad characteristics that would maximize the number of correct detections. This in turn could also maximize the number of false positives, but distance sampling can account for the rate of false positives in the estimates (Marques *et al.*, 2013). In studies about acoustic characterization, calls are usually used to represent geographical differences among groups (e.g. Hatch and Clark, 2004). In this case, the only concern would be obtaining a reliable representation of the acoustic differences with the least influence possible of false positives.

A total of 9 detectors were tested in a representative subsample at low correlation thresholds (0.2) in order to assess their performance. Five used the vertical channel of the seismometer and two used the hydrophone as the main channel for detection. Most detectors with the Z-channel produced better results than the detectors with the H-channel. McDonald *et al.* (1995) and Brodie and Dunn (2014) also found that the vertical channel of the seismometer was better suited for detection methods because it presented higher SNR values. The master waveform used in the matched filtering detection technique also affects the detection results. When there is variation between the target signals of detection, or when the background noise is not white (e.g. there is a high level of ship noise), the results of the matched filtering technique are less optimal (Mellinger *et al.*, 2016). The 20-Hz fin whale calls are highly stereotyped and when produced in sequences their sound source stays fairly constant (Watkins *et al.*, 1987; Weirathmueller *et al.*, 2013). The effectiveness of the detectors also relies on these two key aspects (highly stereotyped and constant source level signal) of the 20-Hz fin whale call. Although the detection process presented in this chapter focused on the 20-Hz fin whale call, efforts to develop a detection routine for backbeats was also undertaken. Because backbeats vary considerably in amplitude, the detection based on a matched filtering technique for this signal worked less well.

There were two detectors that were considered optimal, i.e. produced the number of detections suitable for specific aims, depending on the aim of the study. One detector (detector 6) showed a 99.3% rate of true positives but it also showed a high (90.7%) rate of false positives. The other detector (detector 4) presented a lower rate of true positives of 87.0% but it also showed one of the lowest rate of false positives 8.9%. Both used the modified normalized cross-correlation equation with the Z component of the seismometer as the main channel, a filter between 4 and 40 Hz and a buffer time of 0.3 seconds. The only difference was the power of the equation: detector 4 was set with a power of 1 and detector 6 was set with a power of 0.5. The ROC curve showed that at different correlation thresholds for each detector they behaved similarly. Detector 4 was the most balanced detector with the potential to be used in the two types of biological studies that follow this chapter. For standard distance sampling analysis, calls at or close to the recording point should be detected. Calls produced far away from the recording instrument have a small influence on the detection function that is used to estimate the detection probability that in turn is used to obtain an abundance estimate (see Chapter 5). The plot of the Z-channel amplitude with SNR of the calls for detector 4 showed that missed calls had a small amplitude and small SNR. These characteristics suggest that missed calls were potentially produced at far away ranges from the OBS and possibly outside the critical area for location estimates when using the single station method proposed by Harris *et al.* (2013) and Matias and Harris (2015). Other location methods are available and

provide location estimates outside this critical range, such as multipath and multi-sensor techniques (e.g. Rebull *et al.*, 2006; Wilcock, 2012). However, the aim of this thesis was to show the use of seismic datasets and methods to study fin whales. The single-station method is a widely used location method in seismology and has shown to provide reliable estimates of range of fin whale calls (Matias and Harris, 2015). Detector 4 retained calls with high levels of correlation and SNR with the smallest number of false positives. Therefore, the use of the single-station method to locate fin whale calls together with detector 4 in the detection process was considered as a correct approach.

The final task of the study in this chapter was to apply a detector to the full dataset of recordings and instruments. After testing a series of detectors with a representative sub-sample of the data, two detectors were identified as candidates for that task.

Detector 6 produced a high number of detections to obtain the 99.3% rate of true positives in a 30-hour subsample. The full dataset represented 11 months of recording for 24 instruments. The detections produced by detector 6 for the full dataset of recordings might not be suitable to manage as too many detections, mostly false positives, could result from its application. Detector 4 not only presented the most balanced performance of all detectors but it also provided a full dataset of detections that was manageable and could be used in studies of the following chapters. For each following chapter, detections were classified (Chapter 3 and 5) or further filtered (Chapter 4) based on the aim of each study. In conclusion, it was possible to obtain a balanced detector that showed efficiency in acquiring a useful dataset for different types of studies.

2.5. REFERENCES

Brodie, D. C., and Dunn, R. A. (**2014**). "Low frequency baleen whale calls detected on ocean-bottom seismometers in the Lau basin, southwest Pacific Ocean," Journal of the Acoustical Society of America **137**, 53–62.

Buckland, S. T., Anderson, D. R., Burnham, K. P., Laake, J. L., Borchers, D. L., and Thomas, L. (**2001**). *Introduction to Distance Sampling* (Oxford University Press, Oxford, UK), 432 pp.

Castellote, M., Clark, C. W., and Lammers, M. O. (**2012**). "Acoustic and behavioural changes by fin whales (*Balaenoptera physalus*) in response to shipping and airgun noise," Biological Conservation **147**, 115–122.

Castellote, M., Clark, C. W., and Lammers, M. O. (**2011**). "Fin whale (*Balaenoptera physalus*) population identity in the western Mediterranean Sea," Marine Mammal Science **28**, 325–344.

Carrara, G., Matias, L., Geissler, W., D'Oriano, F., Lagalante, M., Cianchini, G., et al. (**2008**). "NEAREST 2008 cruise preliminary report r/v Urania," http://nearest.bo.ismar.cnr.it/documentation/nearest-2008-preliminary-report (Last viewed February, 2018).

Clark, C. W., Borsani, F., and Notarbartolo di Sciara, G. (**2002**). "Vocal activity of fin whales, *Balaenoptera physalus*, in the Ligurian Sea," Marine Mammal Science **18**, 281–285.

Clark, C. W., Charif, R., Mitchell, S., and Colby, J. (**1996**). "Distribution and behavior of the bowhead whale, *Balaena mysticetus*, based on analysis of acoustic data collected during the 1993 spring migration off point barrow, Alaska. Reports of the International Whaling Commission **46**, 541–552.

Corela, C. J. C. (**2014**). "Ocean Bottom Seismic noise: applications for the crust knowledge, interaction ocean-atmosphere and instrumental behaviour," Ph.D. dissertation, University of Lisbon, Lisbon, Portugal.

Delarue, J., Todd, S. K., VanParijs, S. M., and DiIorio, L. (**2009**). "Geographic variation in Northwest Atlantic fin whale (*Balaenoptera physalus*) song: Implications for stock structure assessment," Journal of the Acoustical Society of America **125**, 1774–1782.

European Commission (**1992**). Council Directive 92/43/EEC on the conservation of natural habitats and of wild fauna and flora. European Community Gazette **206**, 1–50.

Ford, J. K. B. (**1989**). “Acoustic behaviour of resident killer whales (Orcinus orca) off Vancouver Island, British Columbia,” Canadian Journal of Zoology **67**, 727–745.

Gràcia, E., Dañobeitia, J., Vergés, J., and Parsifal Team (**2003**) "Mapping active faults offshore Portugal (36ºN–38ºN): Implications for seismic hazard assessment along the southwest Iberian margin," Geology **31**, 83–86.

Harris, D., Matias, L., Thomas, L., Harwood, J., and Geissler, W. H. (**2013**). “Applying distance sampling to fin whale calls recorded by single seismic instruments in the Northeast Atlantic,” Journal of the Acoustical Society of America **134**, 3522–3535.

Hatch, L. T., and Clark, C. W. (**2004**). “Acoustic differentiation between fin whales in both the North Atlantic and North Pacific Oceans, and integration with genetic estimates of divergence,” Paper presented to the IWC Scientific Committee, Sorrento, Italy, July, Paper No. SC/56/SD6, pp. 1–37.

Havskov, J., and Ottemöller, L. (1999). “SeisAn Earthquake analysis software,” Seismological Research Letters 70. http://www.seismosoc.org/publications/SRL/SRL_70/srl_70-5_es.html (Last viewed 12th February 2018).

Lammers, M. O., and Oswald, J. N. (**2015**) “Analyzing the acoustic communication of dolphins,” in Dolphin Communication and Cognition: Past, Present, and Future, edited by D. L. Herzing and C. M. Johnson (The MIT Press, Cambridge, USA, London, England), pp. 107–139.

Marques, T. A., Thomas, L., Martin, S. W., Mellinger, D. K., Ward, J., Moretti, D., Harris. D., and Tyack, P. (**2013**). “Estimating animal population density using passive acoustics,” Biological Reviews **88**, 287–309.

Marques, T. A., Thomas, L., Ward, J., DiMarzio, N., and Tyack, P. L. (**2009**). “Estimating cetacean population density using fixed passive acoustic sensors: An example with Blainville’s beaked whales,” Journal of the Acoustical Society of America **125**, 1982–1994.

Matias, L., and Harris, D. (**2015**) "A single-station method for the detection, classification and location of fin whale calls using ocean-bottom seismic stations," Journal of the Acoustical Society of America **138**, 504–520.

McDonald, M. A., Hildebrand, J. A., and Webb, S. C. (**1995**). “Blue and fin whales observed on a seafloor array in the Northeast Pacific,” Journal of the Acoustical Society of America **98**, 712–721.

Mellinger, D. K. (**2004**). “A comparison of methods for detecting right whale calls,” Canadian Acoustics **32**, 55–65.

Mellinger D. K. (**2002**) ISHMAEL: Integrated system for holistic multi-channel acoustic exploration and location. Pacific Marine Environmental Laboratory, Newport, OR. http://www.bioacoustics.us/ishmael.html (Last viewed 12th February 2018).

Mellinger, D. K., and Clark, C. W. (**2000**). “Recognizing transient low frequency whale sounds by spectrogram correlation,” Journal of the Acoustical Society of America **107**, 3518–3529.

Mellinger, D. K., Roch, M. A., Nosal, E. M., Klinck, H. (**2016**). "Signal processing," in Listening in the Ocean: New Discoveries and Insights on Marine Life from Autonomous Passive Acoustic Recorders, edited by W.W.L. Au and M.O. Lammers (Springer-Verlag New York, New York, USA), pp. 359–409.

Mellinger, D.K., Stafford, K. M., Moore, S. E., Munger, L., and Fox, C. G. (**2004**). “Detection of North Pacific right whale (*Eubalaena japonica*) calls in the Gulf of Alaska,” Marine Mammal Science **20**, 872–879.

Nowacek, D. P., Christiansen, F., Bejder, L., Goldbogen, J. A., Friedlaender, A. S. (**2016**). "Studying cetacean behaviour: new technological approaches and conservation applications," Animal Behaviour **120**, 235–244.

Presidência do Conselho de Ministros. (**2015**). *Diário da República n.º 148/2015, Série I de 2015-07-31* (Lisbon, Portugal), pp. 5181–5183 https://dre.pt/web/guest/home/-/dre/69920312/details/maximized?p_auth=sZsIw13j (Last viewed 31st January 2018).

Rebull, O. G., Cusí J. D., Fernández M. R., and Muset J. G. (**2006**). “Tracking fin whale calls offshore the Galicia Margin, north east Atlantic ocean,” Journal of the Acoustical Society of America **120**, 2077–2085.

Rendell, L., Mesnick, S. L., Dalebout, M. L., Burtenshaw, J., and Whitehead, H. (**2012**). "Can Genetic Differences Explain Vocal Dialect Variation in Sperm Whales, Physeter macrocephalus?,"Behavior Genetics **42**, 332–43.

Richardson, W. J., Greene, J. C. R., Malme, C. I., and Thomson, D. H. (**1995**) *Marine Mammals and Noise* (Academic Press, San Diego, USA).

Silva, S. D. M. M. F. (**2017**). “Strain partitioning and the seismicity distribution within a transpressive plate boundary: SW Iberia-NW Nubia,” Ph.D. dissertation, University of Lisbon, Lisbon, Portugal.

Soto, N. A., Johnson, M., Madsen, P. T., Tyack, P. L., Bocconcelli, A., and Borsani, J. F. (**2006**). "Does intense ship noise disrupt foraging in deep-diving cuvier’s beaked whales (*Ziphius cavirostris*)?," Marine Mammal Science **22**, 690-699.

Stafford, K. M., Fox, C. G., and Clark, D. S. (**1998**). “Long-range acoustic detection and location of blue whale calls in the northeast Pacific Ocean,” Journal of the Acoustical Society of America **104**, 3616-3625.

Stafford, K. M., Nieukirk, S. L., and Fox, C. G. (**2001**). “Geographic and seasonal variation of blue whale calls in the North Pacific,” Journal of Cetacean Research and Management **3**, 65–76.

Thomas, L., Buckland, S. T, Burnham, K. P., Anderson, D. R., Laake, J. L., Borchers, D. L., and Strindberg, S. (**2002**). "Distance sampling," in Encyclopedia of Environmetrics edited by A.H. El-Shaarawi and W.W. Piegorsch (John Wiley & Sons, Ltd, Chichester, UK), pp. 544–552.

Tyack, P. L. (**1997**). “Development and social functions of signature whistles in bottlenose dolphins, *Tursiops truncatus*,” Bioacoustics **8**, 21–46.

Watkins, W. A. (**1981**). “Activities and Underwater Sounds of Fin Whales,” Scientific Reports of the Whales Research institute **93**, 83–117.

Watkins, W. A., Tyack, P., and Moore, K. E. (**1987**). “The 20-Hz signals of finback whales (*Balaenoptera physalus*),” Journal of the Acoustical Society of America **82**, 1901–1912.

Weirathmueller, M. J., Wilcock, W. S. D., and Soule, D. C. (**2012**). “Source levels of fin whale 20Hz pulses measured in the Northeast Pacific Ocean,” Journal of the Acoustical Society of America 133, 741–749.

Wiggins, S. M. (**2003**). “Autonomous acoustic recording package (ARPs) for long-term monitoring of whale sounds,” Marine Technology Society Journal **37**, 13–22.

Wiggins, S. M., Oleson, E. M., McDonald, A., and Hildebrand, J. A. (**2005**). "Blue whale (*Balaenoptera musculus*) diel call patterns offshore of southern California," Aquatic Mammals **31**, 161–168.

Wilcock, W. S. D. (**2012**). “Tracking fin whales in the northeast Pacific Ocean with a seafloor seismic network,” Journal of the Acoustical Society of America **132**, 2408–2419.

Zimmer, W. X. Z. (**2011**). *Passive Acoustic Monitoring of Cetaceans* (Cambridge University Press, New York, USA).

Zitellini, N., Mendes, L. A., Cordoba, D., Danobeitia, J., Nicolich, R., Pellis, G., et al. (**2001**). “Source of the 1755 Lisbon earthquake and tsunami investigated,” Eos **82**, 285–291.

ANNEX I - Examples of spectrograms of each class of signal

All spectrograms show 300 seconds of recording and were plotted with the following parameters: Frame size – 256 samples, 95% overlap, Hanning window, equalized, contrast: 300, brightness: -4.

20-Hz calls

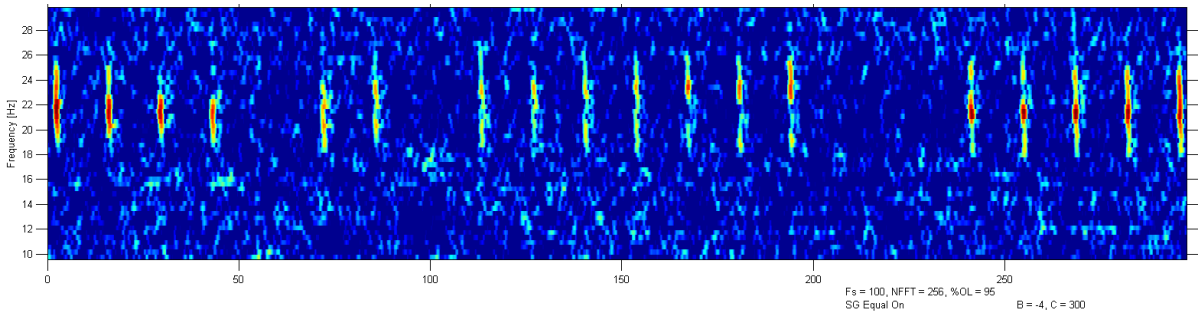

Figure A-I-1. Spectrogram of 5 minutes of the recording in OBS10, 13/10/2007, at 00:40:00, showing a range of signals that are assumed to be main 20-Hz calls.

Backbeats

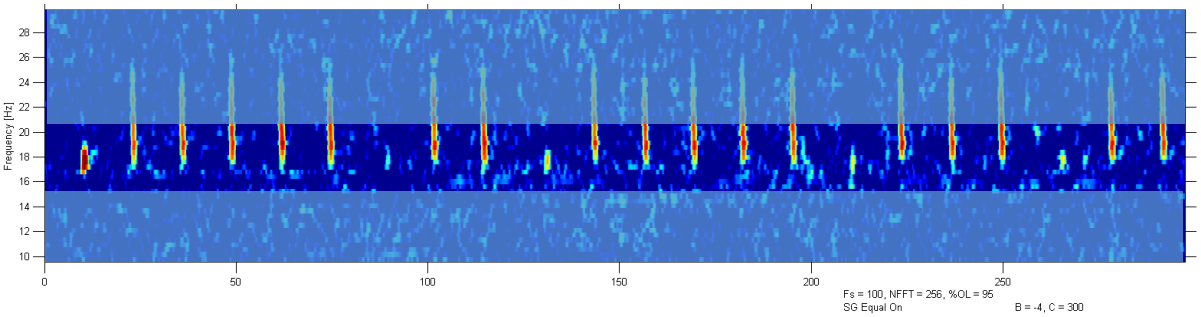

Figure A-I-2. Spectrogram of 5 minutes of the recording in OBS03, 8/12/2007, at 15:11:00, showing a range of signals that are assumed to be main backbeats.

Auxiliary

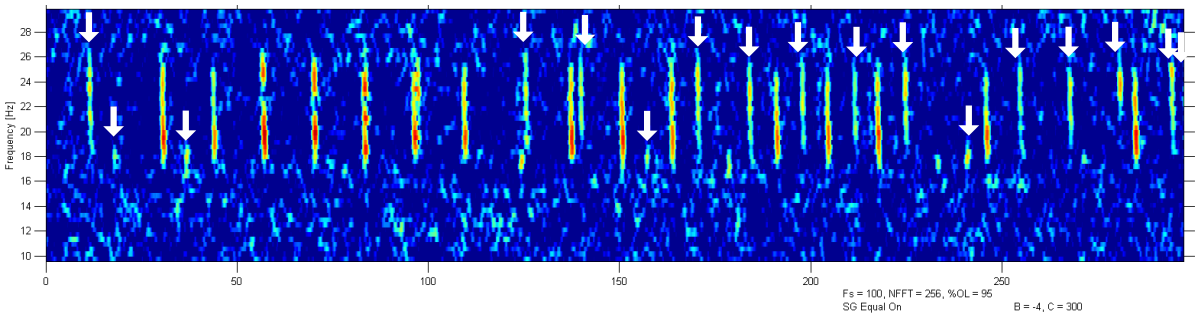

Figure A-I-3. Spectrogram of 5 minutes of the recording in OBS20, 4/01/2008, at 10:36:30, showing main 20-Hz calls with backbeats (the stronger signals) alternating with auxiliary calls (white arrows). The first two signals (20-Hz call followed by a backbeat) were considered auxiliary.

Multipath

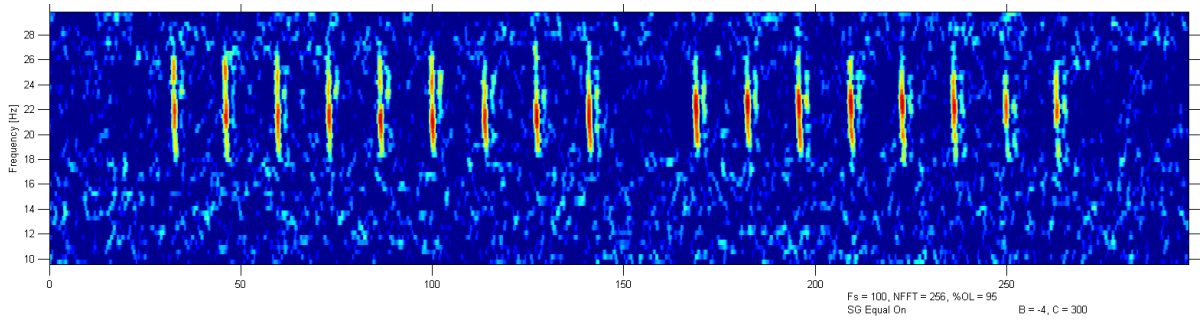

Figure A-I-4. Spectrogram of 5 minutes of the recording in OBS10, 13/01/2008, at 7:30:00, showing multipaths. When there was only one whale calling, faint signals that resemble 20-Hz/backbeats that were produced very close the main calls were considered multipaths.

Unsure

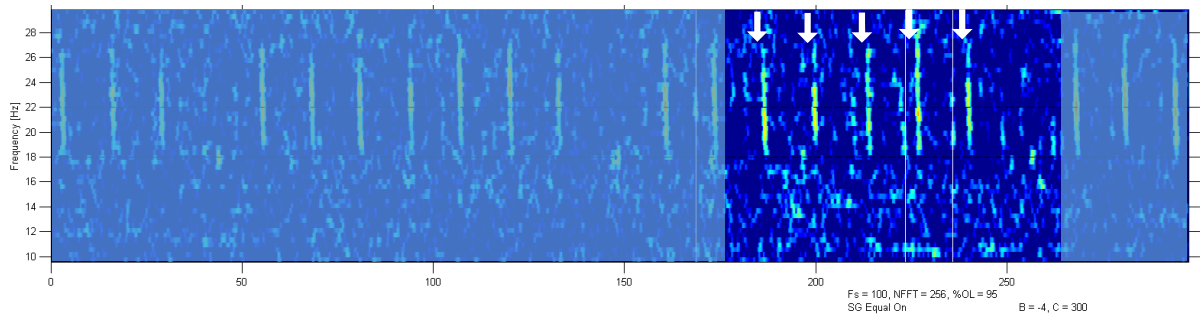

Figure A-I-5. Spectrogram of 5 minutes of the recording in OBS13, 22/01/2008, at 11:15:00, showing signals that had some resemblance with 20-Hz calls due to some spectral features or interval between a following signal. Unsure signals were identified with a vertical white line and 20-Hz calls and backbeats were identified with white arrows.

Other

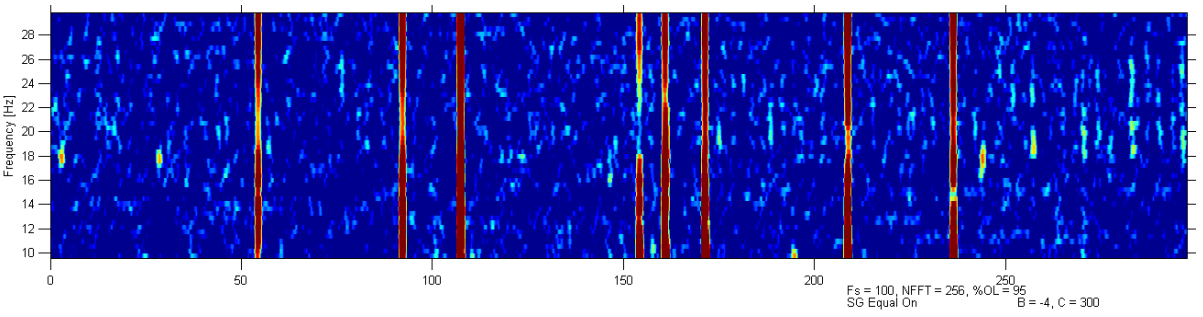

Figure A-I-6. Spectrogram of 5 minutes of the recording in OBS03, 17/17/2007, at 2:10:00, showing high intensity signals that are related with the OBS levelling.

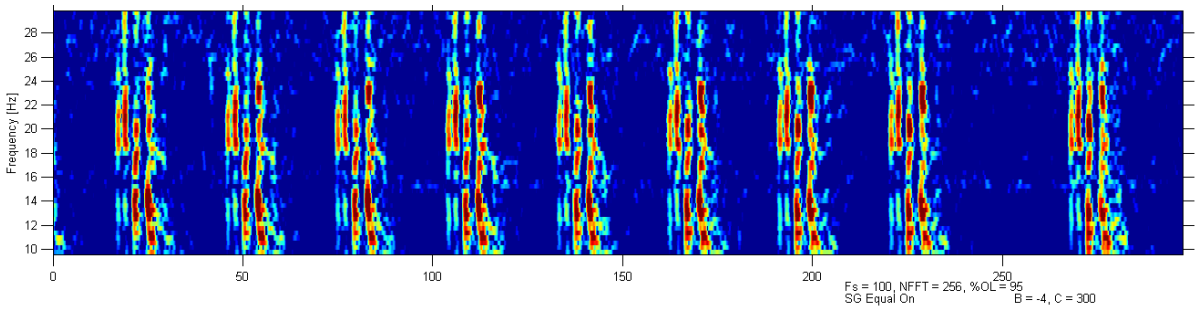

Figure A-I-7. Spectrogram of 5 minutes of the recording in OBS19, 02/09/2007, at 1:24:00, showing a series of air gun shots.

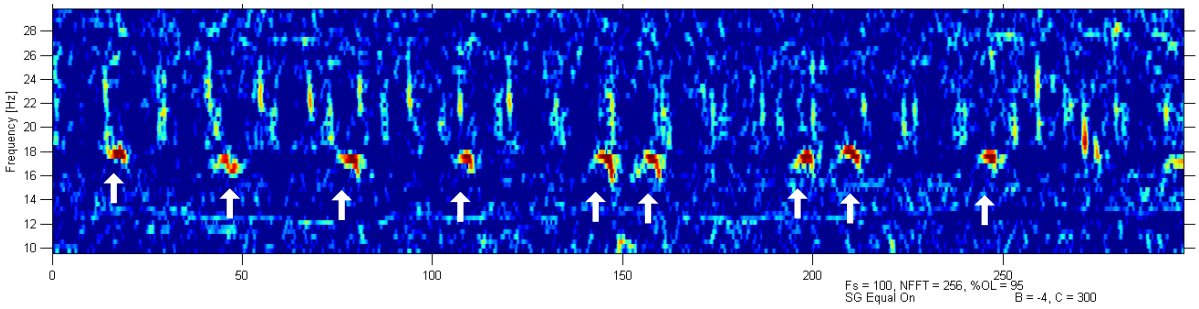

Figure A-I-8. Spectrogram of 5 minutes of the recording in OBS16, 10/12/2007, at 17:37:00, showing blue whale calls (higher intensity signals with white arrows) and fin whale calls (background signals).

ANNEX II – Number of detections of each detector

Table AII-I – Summary of detections of each detector in the 30-h subsample.

TYPE	MANUAL	1	2	3	4	4(0.1)	5	6	8	9
20-Hz	4 735	3 226	4 226	3 019	4 361	4 715	3 994	47 27	4 328	4 664
Backbeat	919	213	653	29	44	238	625	803	76	653
Auxiliary 20-Hz	983	520	777	318	615	926	728	953	726	932
Auxiliary backbeat	181	41	140	2	3	29	86	150	13	131
Multipath	192	27	126	1	25	114	120	151	12	116
Unsure	59	23	55	0	2	28	51	56	15	37
Other detections	NA	12 712	47 012	158	411	7 538	41 431	54 315	3 286	42 315
False positives	NA	13 016	47 986	190	485	8 873	42 313	55 475	4 128	44 184
Missed calls	NA	1 972	266	890	875	20	294	116	407	71
Total detections	**7 069**	**16 762**	**52 989**	**3 527**	**5 461**	**13 588**	**47 035**	**61 155**	**8 456**	**48 848**

Chapter 3

CLASSIFICATION OF 20-HZ FIN WHALE CALLS FROM OBS DATA OFF SOUTHWEST PORTUGAL FOR THE APPLICATION OF THE SINGLE-STATION LOCATION METHOD

3.1. INTRODUCTION

Usually, the detection process of signals of interest in large datasets is accompanied by classification, which involves deciding if the detections result from the desired signal(s) or not (Mellinger *et al.*, 2016). In this thesis, the classification was also related to the location technique employed because not only it was essential to decide if a detection resulted from the target signal but it was also necessary to decide if that detection was produced inside the range where the location technique works. Classification was considered to be the decision process with two states: 1) filtering of the false positives, described in Chapter 2 and 2) distinguishing 20-Hz fin whale calls that were produced inside the critical range from the ones that were emitted outside that range.

Passive acoustic location provides a non-intrusive approach to study movements and behaviour of animals, which can be less time consuming and less expensive than visual surveying. Instruments can record for extended periods of time during all hours of the day and through all seasons. For species with large scale movements, passive acoustic location allows the acquisition of spatial data that could otherwise be logistically challenging and expensive to obtain. The main negative aspect of passive acoustic location is that is only applicable to the acoustically active members of a stock. Location can be done at a small scale, with a fine spatial resolution and covering only a couple of kilometres, or at a scale of hundreds of kilometres in which the spatial resolution is more gross (Au and Hastings, 2008). There are several methods for passive acoustic location, but the application of a specific technique depends on the number and configuration of the recording instruments, the signal characteristics, the operational requirements, and the acoustic environment in which the signal propagates (Mellinger *et al.*, 2016).

Ocean-bottom seismometers (OBS) are designed to localize seismic events but they can also be used to localize any other signals that they are able to record, including baleen

whale sounds (e.g. Rebull *et al.*, 2006; Wilcock, 2012; Harris *et al.*, 2013). They provide a ranging estimate, i.e. a distance from the instrument and the sound source, and with their orientation and the relative azimuth of the sound source, they can also provide a location estimate. Various location methods have been adapted to localize and track blue and fin whales that are recorded in OBS. Differences in arrival times of the direct path (Harris *et al.*, 2013) and multipaths to a single OBS and/or several instruments have been applied (e.g. Rebull *et al.*, 2006; Dunn and Hernandez, 2009; Wilcock, 2012). However, multipath ranging with a single instrument does not allow the two-dimensional (2D) location of the sound source to be estimated, and multi-station techniques require a relatively close spacing between instruments, to a maximum of 10 to 15 kilometres (Matias and Harris, 2015). In addition, locating sound sources in the ocean is more laborious than in traditional crustal seismology due to the effects of oceanic sound velocity profiles on sound propagation (Matias and Harris, 2015). Harris *et al.* (2013) demonstrated the use of a single-station method that did not rely on multipath arrivals to localize fin whale calls at close ranges in a single day of the NEAREST acoustic recordings and with enough precision that the data could be used in animal density estimates. Matias and Harris (2015) further investigated the detection, classification and ranging of the 20-Hz fin whale calls with the single station method off southwest Portugal and compared the results with airgun data from the same area and a fin whale dataset from the Azores, in which positions could be estimated both with the single station method and multi-station techniques. With the single station method, when an acoustic signal is detected but is produced outside a critical range, the method returns spurious range estimates (Matias and Harris, 2015). Therefore, it is necessary to develop a classification scheme that retains detections that are inside the critical range and filters out the ones that are produced outside the critical range. Matias and Harris (2015) also showed the importance of the seabed and water properties to produce more accurate range estimates. Although Matias and Harris (2015) developed a classification scheme and provided information to improve the range estimation, the work used signals different from fin whale calls (air gun pulses) and only one day of fin whale data from the Azores.

In this chapter, the classification parameters developed by Matias and Harris (2015) were assessed using a representative subsample of the full dataset of the OBS that had all of the components of the seismometer working and therefore could provide a range estimate (localizing OBS). The potential of each parameter to 1) filter false positives from the detection process (stage 1 classification) and 2) identify fin whale calls inside the critical range of the single station method (stage 2 classification) was evaluated. Thresholds for the different parameters were identified and the resulting classification scheme was applied to the full dataset of the OBS. Although it was not possible to obtain exact locations of the calling whales,

the trends of some parameters with distance were assumed to give some indications of the validity of the ranging estimates. The true and false positives used in this chapter are related with the detection process and are the same as the ones identified in Chapter 2. The accuracy of the location method was improved by the application of corrections that account for the water and seabed properties.

3.2. METHODS

3.2.1. Subsample and dataset

In Chapter 2, a systematic random subsample of 30 hours was defined in order to assess the performance of several detectors (Table IV, Chapter 2). The detections used in this chapter were obtained with the most balanced detector identified in Chapter 2 (detector 4). Automatic detections were obtained for the detector and their trigger times were compared with times of signals that were registered from a manual inspection of the spectrograms of the subsample. Signals were grouped in different classes (Table III, Chapter 2) and only 20-Hz calls were considered true positives, i.e., correct detections. True positives were considered to be either 20-Hz fin whale calls produced from a main bout or an auxiliary bout. False positives were considered all detections from other types of acoustic signals or random acoustic noise. The assessment of the classification scheme, i.e. a set of rules for several parameters described below in section 3.2.4, was undertaken with only the subsampled hours that had all three-components of the seismometer working, allowing range estimates to be obtained for the detections. OBS that could provide a range estimate were designated as "localizing OBS" and OBS that did not have one or more of the seismometer components working and could not provide a range estimate were designated as "non-localizing" OBS. In the subsample, there was a total of 16 hours recorded on 8 localizing OBS (Table IV, grey rows, Chapter 2). After the identification of a classification scheme with the subsample, the same set of rules was applied to the full dataset of detections, obtained in Chapter 2.

3.2.2. The single station method

The recordings obtained from the set of OBS of the NEAREST monitoring project (see Fig. 1, Chapter 2) have been used in other studies that localized and estimated density of fin whale calls (Harris *et al.*, 2013; Matias and Harris, 2015). The main location method used to obtain a range estimate of the vocalizing fin whale calls has been the single-station method.

Multipath arrivals in the NEAREST recordings have shown very small amplitudes, which hinder their identification and the use of automated methods to obtain a range estimate from time differences of arrivals to a single instrument. A preliminary analysis of the propagation range of the 20-Hz fin whale calls detected in the hydrophone recordings showed that it was not possible to identify the same calls across different OBS (Pereira *et al.*, 2015). There were detections around the expected time of arrival of the call, considering a sound velocity in the water column of 1.5 km/s, but from the spectrograms they could not be confirmed as true positives, i.e., true fin whale calls. Therefore, the single station method (SSM) continues to be the most suitable location method for sparse networks of instruments deployed on soft sediments that do not generate strong multipaths, as it is the case for OBS in the NEAREST deployment area. This location method requires that all three components of the seismometer are working properly and a good knowledge of the propagation velocities in the shallowest seafloor layers for primary (P) and secondary (S) seismic waves. For classification purposes, Matias and Harris (2015) showed the utility of having also the simultaneous recording of pressure data by a hydrophone. Roberts *et al.* (1989) established the foundations in seismology of one method to calculate the location of seismic instrument-to-source azimuth and apparent incident angle at the surface from the recordings of 3-component seismic data. This method was applied to the OBS data to estimate the range and location of a sound source in the water column. The following description consists in an overview of the method and more details can be found in Harris *et al.* (2013).

Considering a fin whale that produces an acoustic signal, the pressure waves travel from the point source (PS) through the water column as a P-wave and reach the sea-floor with an incidence angle *i* (Fig. 1). Here the incident P-waves are reflected and transmitted as P and converted seismic waves (S-waves) that propagate through the sediments. SV waves are S-waves which the particle motion lies in the vertical plane, the plane that contains the P and S waves (Doyle, 1995). The OBS placed on the seafloor (OBS) registers the particle velocity caused by the seismic waves in its 3 channels of the seismometer (X, Y and Z). The apparent emergence angle i_{app} of the ray travelling in the sediments can be calculated by the decomposition of the seismic signal V_{seis} into its horizontal A_h and vertical A_z components:

$$i_{app} = tan^{-1}\left(\frac{A_h}{A_z}\right) \qquad \text{Eq. 1}$$

The azimuth of the acoustic signal ϕ can also be obtained from the horizontal components A_x and A_y:

$$\phi = tan^{-1}\left(\frac{A_y}{A_x}\right) \quad \text{Eq. 2}$$

The components A_x, A_y, A_z consist in the amplitudes of the channels X, Y, and Z and A_h is calculated with:

$$A_h = \sqrt{{A_y}^2 + {A_x}^2} \quad \text{Eq. 3}$$

If the height of the acoustic source above the sea-floor h_w is known, then with the incident angle in the water column i and the acoustic source azimuth ϕ, the horizontal range r and the coordinates of the acoustic source (a, b) can be calculated by trigonometry (disregarding the variations of sound speed in the water column):

$$r = h_w \times \tan(i) \quad \text{Eq. 4}$$

$$a = -r \times \sin(\phi) \quad \text{Eq. 5}$$

$$b = -r \times \cos(\phi) \quad \text{Eq. 6}$$

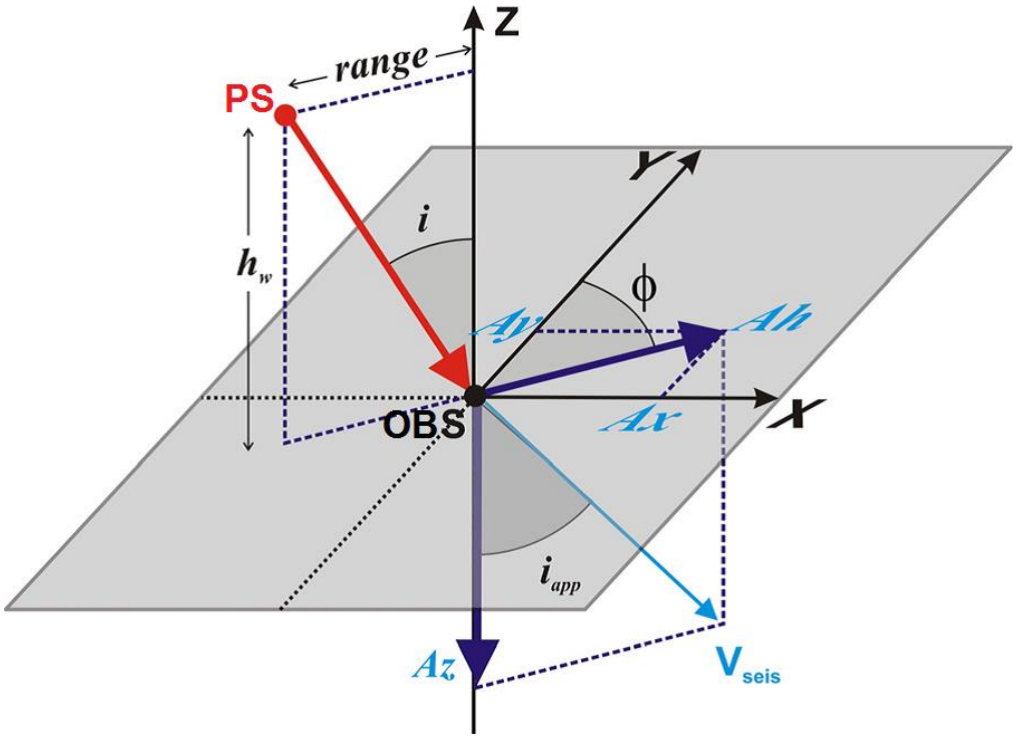

Figure 1. Geometry of the single-station location method as applied to an acoustic source (P) above the seismic sensor (S) at the sea-floor. Knowing the wave incident angle in the water layer (i) and the height above the sea-floor of the source (h_w) then the horizontal range between source and sensor can be computed (assuming a constant sound speed in the water layer). At the sea-floor the incident acoustic wave is reflected (not shown in the figure) and transmitted as P and SV converted seismic waves and the corresponding ground velocity (V_{seis}) are measured by the seismometer. The 3 components of ground velocity (A_x, A_y, A_z) define the apparent emergence angle in the sediments (i_{app}) and the azimuth of the whale call (ϕ), identified as the pressure wave source in the plot (P). Ah is the horizontal amplitude of the ground motion. by Harris et al., 2013, Applying distance sampling to fin whale calls recorded by single seismic instruments in the Northeast Atlantic," Journal of the Acoustical Society of America 134, 3522–3535. Copyright by the Acoustical Society of America.

It was possible to derive geographical positions of detections because Corela (2014) identified the true orientation of each OBS in the NEAREST deployment area. However, for this thesis only the range and relative location of the detections to the OBS was needed. The apparent emergence angle in the sediments i_{app} is one of the angles directly measured by the seismometer. The angle is designated as 'apparent' because the ground velocity in the sediments contains both P and SV waves that result from the transmission and conversion of the pressure waves at the water column-sediment interface. If the true emergence angle from the seafloor for the transmitted P-wave is known (i_2) then the incidence angle in the water column *i* can be calculated from the Snell's Law of refraction (Doyle, 1995). Snell's law states that the ratio of the sines of the angles of incidence and emergence is equal to the ratio of phase velocities in two media:

$$\frac{\sin i}{\sin i_2} = \frac{\alpha_w}{\alpha_s} \qquad \text{Eq. 7}$$

$$\Leftrightarrow$$

$$i = sin^{-1}\left(\frac{\alpha_w}{\alpha_s}\sin i_2\right) \qquad \text{Eq. 8}$$

Here α_w and α_s are the P-wave velocities for the water column and the sediments, respectively. The true emergence angle in the sediments i_2 can be derived from its relationship between the apparent emergence angle in the sediments i_{app}, using the Zoeppritz equations (described in Aki and Richards, 1980). These equations require knowledge of the properties of the water column and sediments, such as P-wave velocity in the water column and sediments, SV-wave velocity in the sediments, and water and sediment densities.

As in Harris *et al.* (2013), the initial calculation of the range estimate assumed that the apparent emergence angle in the sediments i_{app} was similar to the true emergence angle in the sediments i_2. Harris *et al.* (2013) conducted a simulation study to show that the difference between those two angles is determined by the velocity of the SV-wave. For the study area, there is no measurement available of the SV-wave velocities but the sediments are known to be water-saturated with P-wave velocities of about 1.8 km/s (Shipboard Scientific Party, 1972). The corresponding SV-wave velocity in a fluid-like marine sediment is estimated to be approximately 0.1–0.2 km/s (Buckingham, 1998). The simulation by Harris *et al.* (2013) showed that when SV-waves are slow, there is a close relationship between i_{app} and i_2, which confirms the use of i_{app} as an adequate proxy of i_2 for these particular conditions of the shallow seafloor structure.

For a P-wave that travels from a slow medium, in this case the water column, to a faster medium, the seabed sediments, there is a critical incidence angle i_c at which the three-component method becomes limited. At this angle, the emergence angle in the sediments i_{app} is equal to 90º and beyond the i_c the emergence angle in the sediments loses its geometrical meaning and the Zoeppritz equations results become complex numbers.

$$for\ \alpha_s > \alpha_w \qquad i_c = sin^{-1}\left(\frac{\alpha_w}{\alpha_s}\right) \qquad \text{Eq. 9}$$

In this way, the three-component method is limited to incidence angles smaller than i_c and ranges smaller than r_c

$$r_c = h_w \times \tan(i_c) \qquad \text{Eq. 10}$$

This equation is valid when the sound speed variations in the water column are disregarded. When an angle is larger than the critical incidence angle i_c, the 3 components of the signal suffer different phase shifts and the shape of the waveforms is modified, particularly for the Z channel. These considerations are the foundations for some of the parameters used for classification (stage 2).

Calculating apparent emergence angle in the sediments and azimuth from seismic data

Following Roberts *et al.* (1989), the ground velocity recorded by the 3 channels of a seismometer, X, Y and Z, over time t are defined by the vector $\vec{v}(t)$

$$\vec{v}(t) = \begin{bmatrix} \dot{x}(t) \\ \dot{y}(t) \\ \dot{z}(t) \end{bmatrix} \qquad \text{Eq. 11}$$

Each channel records a P-wave signal *P(t)* and noise *N(t)* that is assumed to be uncorrelated to the signal on a given channel and also uncorrelated with signals and noise on the other channels

$$\begin{aligned} \dot{x}(t) &= cP(t) + N_x(t) \\ \dot{y}(t) &= dP(t) + N_y(t) \\ \dot{z}(t) &= P(t) + N_z(t) \end{aligned} \qquad \text{Eq. 12}$$

Here *c* and *d* are constant coefficients for the incoming P-wave that is assumed to be linearly polarized in the ray direction. Those two constants depend on the azimuth and apparent emergence angle

$$\begin{aligned} c &= tan\left(i_{app}\right) \sin \phi \\ d &= tan\left(i_{app}\right) \cos \phi \end{aligned} \qquad \text{Eq. 13}$$

The apparent emergence angle in the sediments i_{app} and the azimuth ϕ are calculated by the cross correlation between the ground velocity of the X and Y channels and the Z channel

$$i_{app} = tan^{-1}\left(\frac{\sqrt{\langle \dot{x}, \dot{z} \rangle^2 + \langle \dot{y}, \dot{z} \rangle^2}}{\langle \dot{z}, \dot{z} \rangle - \langle N_z, N_z \rangle}\right) \quad \text{Eq. 14}$$

$$\phi = tan^{-1}\left(\frac{\langle \dot{x}, \dot{z} \rangle}{\langle \dot{y}, \dot{z} \rangle}\right) \quad \text{Eq. 15}$$

Where the cross-correlations are given by

$$\begin{aligned} \langle \dot{x}, \dot{z} \rangle &= c\langle P, P \rangle \\ \langle \dot{y}, \dot{z} \rangle &= d\langle P, P \rangle \\ \langle \dot{z}, \dot{z} \rangle &= \langle P, P \rangle + \langle N_z, N_z \rangle \end{aligned} \quad \text{Eq. 16}$$

The three-component analysis method of Roberts *et al.* (1989) is implemented in SEISAN (Havskov and Ottemöller, 1999), in a biased approach, because it does not consider the vertical noise contribution in Eq. 14 and 16. Harris *et al.* (2013) adjusted the three-component method routine in SEISAN to accommodate the noise autocorrelation using a window with the same size as the one from the detection event, just before the trigger time of a detection. Whenever a detection was registered, the three-component method was applied to derive estimated values for the relative azimuth, the apparent emergence angle, the incident angle range and (X, Y) location assuming a constant sound speed in the water column.

3.2.3. Adjustments to the range estimates

The initial run of the three-component method is a simplistic approach because it assumes the apparent emergence angle is similar to the true emergence angle and considers the water column as homogeneous. Matias and Harris (2015) showed the importance of the application of several adjustments to the range estimates that consider different wave velocities in the Zoeppritz equations, a velocity profile of the water column in the study area and a correction factor in the channel amplitudes. The values for each adjustments applied in this chapter were the same Matias and Harris (2015) identified as the values that resulted in the most accurate range estimates. Matias and Harris (2015) presented an extensive analysis of these adjustments and here only a brief description is given.

Zoeppritz equations

As mentioned above, the true emergence angle in the sediments can be obtained from its relation with the apparent emergence angle in the sediments. This relation can be derived by solving the Zoeppritz equations that depend on the elastic properties of the water column and the sediment layer (e.g. Aki and Richards, 1980). The new adjusted angles were calculated with the parameters by Matias and Harris (2015) (Table I).

Table I – Properties of the water column and sediment layer in the study area.

	Water column	**Sediment layer**
Density (g/cm^3)	1.0	1.4
P-wave (km/s)	1.5	1.7
S-wave (km/s)	0.0	0.3

Water layer structure

Because the ocean is stratified, ray paths in the water column from a near-surface source will curve considerably on their way down. For seismic instruments that are placed in deep water, this effect is expected to be large (Matias and Harris, 2015). Based on a simple ray propagation modelling it was possible to compute an adjusted range using the 1D sound speed profile of the study area (Fig. 2), the depth of each OBS and a fixed depth for the acoustic source (Fig. 3). Stimpert *et al.* (2015) found that high call production rates of fin whales were associated with depths between 10 and 15 m. For this reason, a fixed sound source depth of 15 m was used in the computation of the range. Ray tracing was performed integrating the propagation equations by a simple Euler rule from the seafloor to the acoustic source (Matias and Harris, 2015).

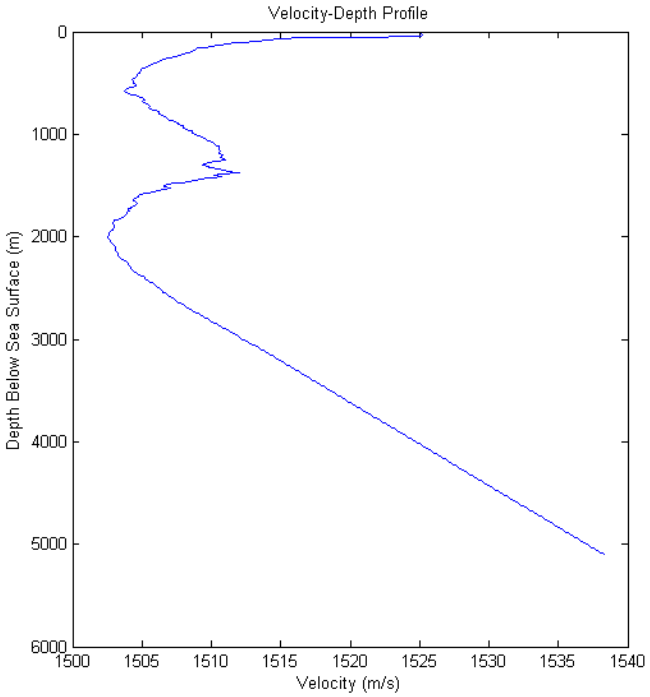

Figure 2. Sound speed profile acquired at a location close to OBS25 of the NEAREST seismic monitoring project (see Chapter 2, Fig. 1).

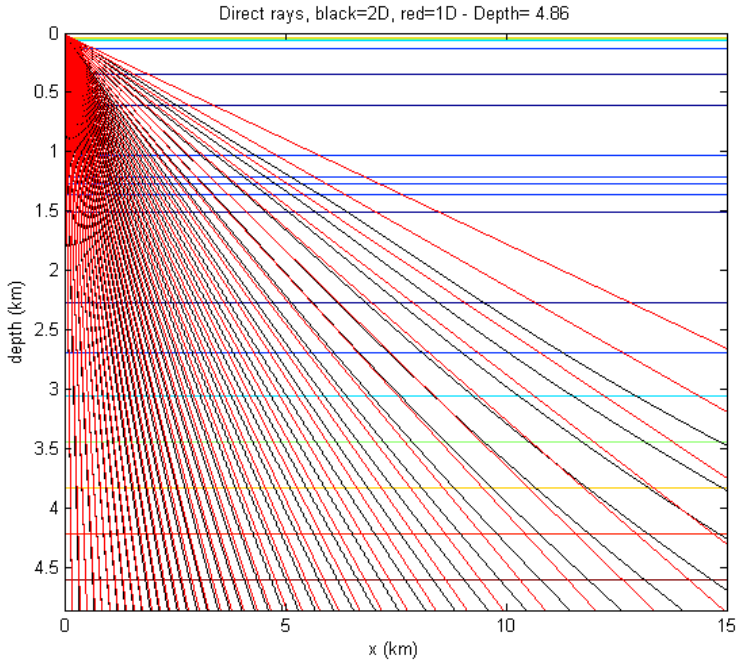

Figure 3. Example of the ray propagation model for OBS12, at a depth of 4 860 m and an acoustic source of 15 m. Red lines represent the straight path of a direct wave and black lines represent paths with ray bending.

Instrumental correction

A systematic bias in range estimates was observed in the southwest of Portugal and the Azores control datasets after the application of the range corrections for the water layer structure and the seafloor sediments properties, using the Zoeppritz equations. For a more detailed description see Matias and Harris (2015). Synthetic seismograms showed that when an OBS is just above the interface between the water layer and the sediments, the horizontal amplitudes are amplified. Therefore, a factor of 0.5 between vertical and horizontal amplitudes that partially corrected for the detailed interaction between the seismic waves and the soft bottom was deemed necessary and applied.

Summarizing, the use of the single station method for ranging and location of sound sources using OBS data requires 3 corrections to the first raw estimates produced by the detection algorithm: i) calculation of the true emergence angle with the Zoeppritz equations; ii) adjustment of range by accounting for the water layer structure, iii) application of a correction factor in the recorded signal amplitudes. Table II shows the critical ranges calculated with Eq. 10, considering a homogenous water column with a wave velocity in the water of α_w = 1.5 km/s and a wave velocity in the sediments of α_s = 1.7 km/s. The ray propagation modelling mentioned above provides a table with ranges and concurring incidence angles. Considering a wave velocity in the water of α_w = 1.5 km/s and a wave velocity in the sediments of α_s = 1.7 km/s, the critical angle i_c is 61.93º. The range associated with that critical angle for each OBS is obtained by polynomial interpolation from the results of the ray propagation modelling.

Table II – OBS depth and critical ranges for the single station method. The critical range with velocities only was calculated with Eq. 10 and with α_w = 1.5 km/s and α_s = 1.7 km/s. The second column of critical range was obtained by polynomial interpolation of the critical range considering the water layer structure.ΔCR is the difference between the two critical ranges.

OBS NO.	OBS DEPTH (km)	Critical range (velocities only)	Critical range (water layer)	ΔCR (km)
OBS 01	5.100	9.563	8.870	0.692
OBS 03	3.932	7.373	6.834	0.540
OBS 04	1.993	3.737	3.455	0.282
OBS 05	3.095	5.803	5.373	0.430
OBS 06	2.956	5.542	5.154	0.389
OBS 08	4.671	8.758	8.121	0.637
OBS 09	4.811	9.021	8.368	0.653
OBS 10	2.067	3.876	3.581	0.294
OBS 12	4.860	9.112	8.512	0.600
OBS 13	4.494	8.427	7.814	0.613
OBS 14	4.212	7.898	7.377	0.520
OBS 15	3.357	6.295	5.831	0.464
OBS 16	2.069	3.879	3.584	0.295
OBS 17	4.873	9.137	8.475	0.662
OBS 18	4.605	8.635	8.065	0.570
OBS 19	4.287	8.038	7.509	0.529
OBS 20	3.449	6.467	6.034	0.433
OBS 21	2.566	4.811	4.451	0.360
OBS 22	4.095	7.677	7.257	0.420
OBS 23	3.747	7.025	6.555	0.471
OBS 24	2.439	4.573	4.247	0.326
OBS 25	3.234	6.065	5.648	0.417

3.2.4. Classification

Classification was considered to be the decision process with two stages: 1) filtering of the false positives, described in Chapter 2 (stage 1), and 2) distinguishing 20-Hz fin whale calls that were produced inside the critical range from the ones that were potentially emitted outside that range (stage 2). The algorithm that detects and provides an estimated range to each detection also computes a number of parameters that can be used to assess the two stages of classification. The classification scheme was obtained by analysing the parameters related to the quality of the detected signal and others that showed potential in Matias and Harris (2015). In Chapter 2, stage 1 classification was initially assessed by characterizing the false positives in terms of their amplitude and SNR. In this chapter, that classification is further expanded. The stage 2 classification is undertaken by assessing parameters that aim to

identify detections that are generated at ranges less than the critical ones, adequate for the use of SSM for ranging and location. The normalized cross-correlation and signal-to-noise ratio were already described in Chapter 2. The full set of parameters considered for stage 2 classification were the following:

Coherency factor (Co)

Roberts *et al.* (1989) proposed one parameter to assess the quality of the angles calculated by the three-component method, the apparent emergence angle and the instrument-source azimuth. It evaluates the departure of the P-wave signal from the pure linear polarization model, using the 3 component signals. It stars by considering the ratio of the vertical to horizontal amplitudes measured by the cross-correlation

$$R = \frac{\langle \dot{z}, \dot{z} \rangle}{\sqrt{\langle \dot{x}, \dot{z} \rangle^2 + \langle \dot{y}, \dot{z} \rangle^2}} \qquad \text{Eq. 17}$$

Then, assuming a perfect linear polarization, the vertical movement can be predicted from the horizontal channels by

$$\dot{z_P}(t) = A\dot{x}(t) + B\dot{y}(t) + N_z, \qquad A = -Rsin\phi \; B = -Rcos\phi \qquad \text{Eq. 18}$$

A signal coherency *Co* is calculated by comparing the observed and predicted vertical movements with

$$Co = 1 - \frac{\langle (\dot{z}(t) - A\dot{x}(t) - B\dot{y}(t))^2 \rangle}{\langle \dot{z}, \dot{z} \rangle} \qquad \text{Eq. 19}$$

When the coherency is equal to 1, the signal is noise-free and linearly polarized. Otherwise, the value is smaller than 1. Beyond the critical incidence angle, because of the phase shifts and deformation of the signal, coherency should show a large decrease and even become negative A positive value of coherency generally identifies calls that are inside the critical range except in near vertical incidence, or near-zero range, where, due to the small amplitude of the horizontal channels, the coherency is poor (Fig. 4).

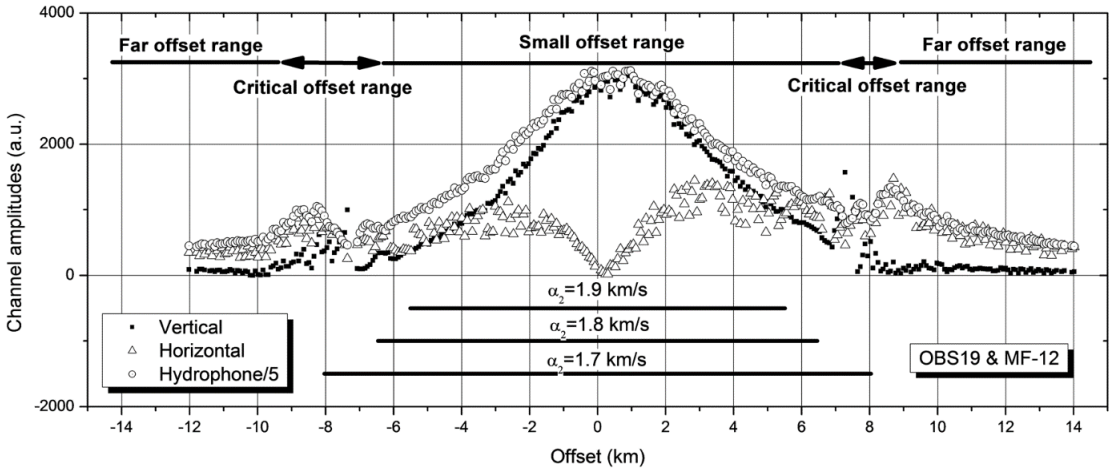

Figure 4. Variation of airgun shot amplitudes with range offset (negative to the west). Air gun shots were recorded around a single OBS, OBS19. The horizontal channels are merged into a single horizontal measure. The hydrophone was scaled (divided by five) so that it could be compared with the vertical channel. By Matias and Harris, 2015, A single-station method for the detection, classification and location of fin whale calls using ocean-bottom seismic stations," Journal of the Acoustical Society of America 138, 504–520. Copyright by the Acoustical Society of America.

Matias and Harris (2015) showed that when coherency is negative, detections could be produced outside the critical range or at very close ranges (Fig. 5). In the case of close ranges and in the presence of noise, when the amplitude of the horizontal particle velocity is small, Eq. 19 shows that coherency is not a reliable classification index and other parameters should be used instead. Matias and Harris (2015) identified a ‘protection radius’ of 250 m where all values of coherency were accepted.

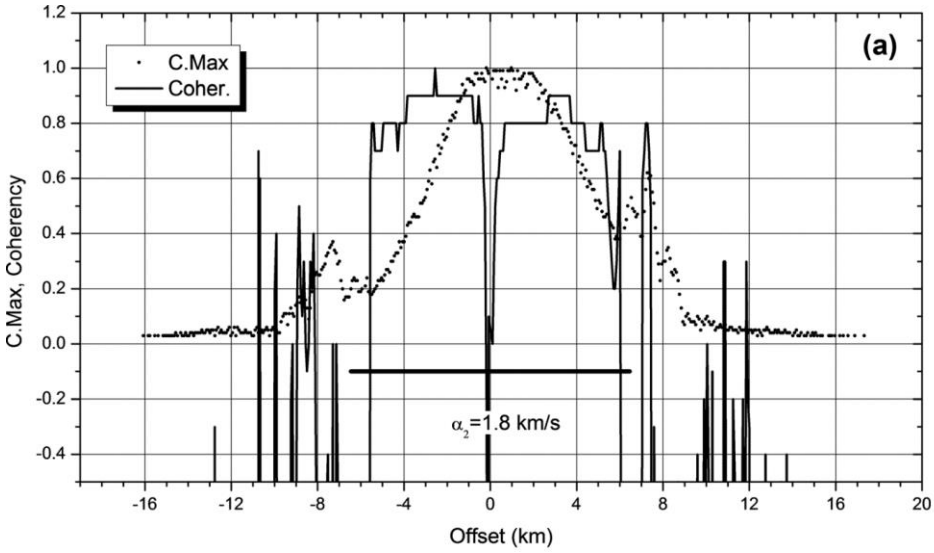

Figure 5. Variation of coherency factor (Co) with offset for direct paths of air gun shots inside a 16 km radius surrounding OBS19 (Fig. 1, Chapter 2). The maximum correlation that resulted from the detection process (C.max) is also shown. Direct wave arrivals were selected from OBS19 recording MF-12 line. By Matias and Harris, 2015, A single-station method for the detection, classification and location of fin whale calls using ocean-bottom seismic stations," Journal of the Acoustical Society of America 138, 504–520. Copyright by the Acoustical Society of America.

Cross-correlation between vertical and hydrophone channels (CZH)

This parameter represents the maximum normalized cross-correlation observed between the hydrophone and vertical channels at a lag time given by parameter iZH (described below). At incidence angles greater than the critical incidence angle, since the reflectivity coefficients are complex numbers, the three seismic channels will be differently deformed in shape and will also display different time shifts, particularly the Z channel, while the hydrophone signal will not be affected. Therefore, after the critical incidence angle, the correlation between hydrophone and vertical recordings is expected to be strongly degraded.

Lag between the vertical and hydrophone channel (iZH)

This parameter is the time lag (in samples) for which the CZH is observed. Due to the same reasons presented above, this lag should be large for rays with an incident angle larger than the critical one. At closer ranges this lag should be close to zero. The small lag observed maybe due to the difference phase instrumental response between the hydrophone and the seismometer.

Normalized cross-correlation (C.Max)

Correlation between the master template waveform and the recorded waveform, which goes up to 1. In Chapter 2, a modified normalized cross-correlation equation that degraded correlation values of signals that differed in amplitude with the template, even if they were perfectly correlated, was included in the detector. This modification avoided a large number of detections with small amplitudes that could potentially have been produced far away from the recording instrument outside the critical range and thus resulting in unreliable range estimates. It is expected that higher values of C.Max could potentially represent detections closer to the OBS and very similar to the template of the signal of interest in shape and amplitude. With increasing distance it is expected a decrease in this parameter due to the dissimilarity of the signals and the differences in amplitude (an extended discussion on this was provided in Chapter 2).

Signal-to-noise ratio (SNR)

Ratio of the RMS values for the detection and the RMS of the noise that precedes the trigger of the detection (measured across a time window defined by the master waveform). In Chapter 2, the detection results obtained with a modified normalized cross-correlation equation that degraded correlation values with amplitude levels showed that 20-Hz fin whale calls that were not detected had small channel amplitudes and low values of SNR. Although this parameter depends on sound propagation, i.e. the level of background noise that is affected by ship noise, seismic activity and environment, results from Chapter 2 suggested that high values of SNR could potentially represent detections closer to the OBS and low values of SNR could potentially represent calls further away from the instrument.

Classification requirements for distance sampling

Two of the main requirements of distance sampling, the chosen method to estimate animal abundance (see Chapter 5), are: 1) the range estimates need to be as accurate as possible and 2) detections produced at very close or at the top of the recording instrument must be detected with certainty (Buckland *et al.*, 2001). The first requirement was achieved by the application of several adjustments to the range estimates, mentioned above in 3.2.3. For the second requirement, the classification scheme started in Chapter 2 needed to be expanded in order to deal with the detections that produced unreliable range estimates. For instance, Fig. 5 above shows that there will be a proportion of negative coherency that result

in close ranges but are produced by detections outside the critical range (unreliable range) and there will also be a proportion of negative coherency from true close detections. Matias and Harris (2015) applied a spatial buffer of 250 m in order to accept detections with negative coherency, but there is a possibility that it was only adequate for that particular study because the sample used was very small. Therefore, it is assumed that the distance range of detections with negative coherency close to the instrument is unknown. The removal of all negative coherency detections will have an impact on the fitting of the probability detection function in distance sampling because it will affect the second requirement, as the probability of detection at close ranges will be lower than expected (g(0)<1, see Chapter 5). Therefore, the possibility of accepting all detections with negative coherency, regardless the range, based on thresholds of other parameters was assessed.

3.3. RESULTS

The run of detector 4 (identified in Chapter 2), for the 16-hour subsample of the 8 localizing OBS resulted in a total of 8 158 automatic detections (Table III). The correlation threshold was set to 0.1 in order to obtain as many detections possible to better assess the characteristics of the true positives and false positives of the detection process. The true positive rate for the 20-Hz fin whale call was 98.6% and the false positive rate was 61.7%.

Table III – Summary of automatic detections made for the 16-hour subsample of the 8 localizing OBS with detector 4 defined in Chapter 2.

Signal	Manual inspection	Automatic detections
Main 20-Hz	2 629	2 620
Main backbeat	433	163
Auxiliary 20-Hz	541	505
Auxiliary backbeat	71	20
Multipath	143	92
Unclear	44	18
Other	0	4 740
TOTAL	**3 861**	**8 158**

The first stage of the analysis was to apply each range adjustment to understand their impacts. According to Matias and Harris (2015), the coherency factor was the most appropriate parameter to decide if detections were inside the critical range of the three-component method or not. In that work only detections with positive coherency were considered to have trustworthy ranges. Therefore, only true positive detections with positive coherency were used to assess

the impact of the adjustments made to the range estimates. When the sound velocity profile in the water column and the elastic properties of the seabed are accounted separately in the range estimates, each correction resulted in an increase of the estimated ranges (Fig. 6). When all of the adjustments were applied simultaneously and the amplitude of the channel was corrected, the final estimated range showed a small decrease from the original one.

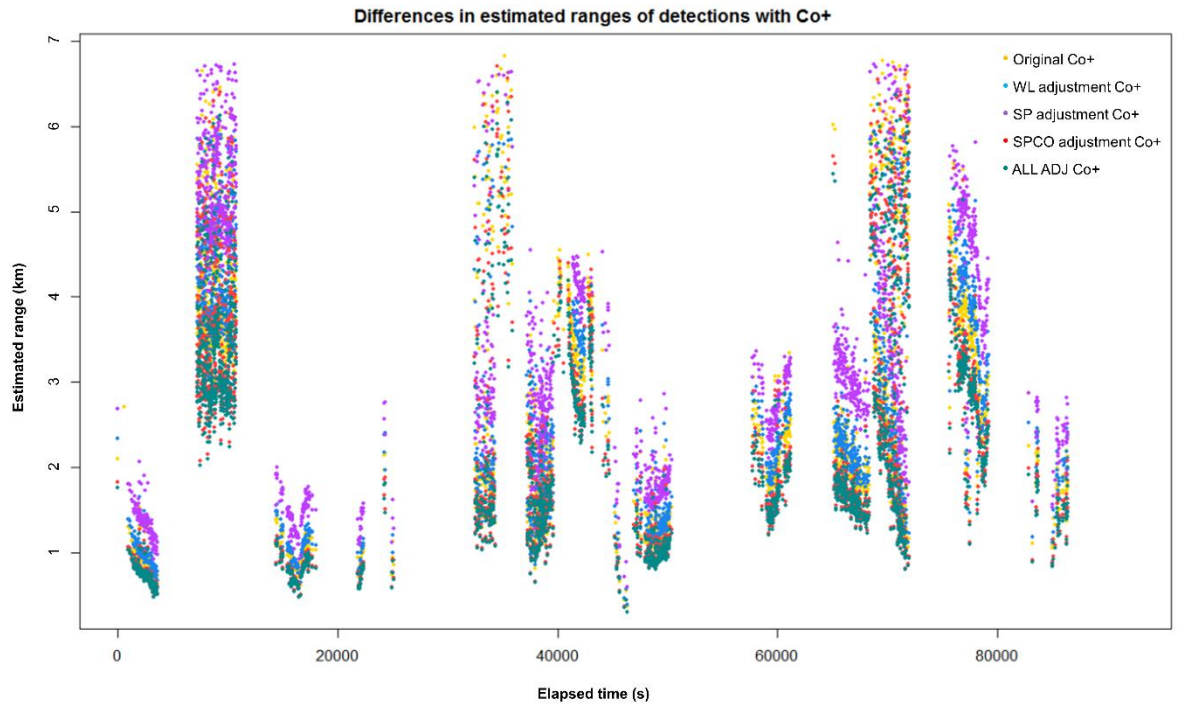

Figure 6. Estimated ranges for automatic detections confirmed as true positives of 20-Hz fin whale calls with positive coherency (Co+), obtained from the 16-h subsample of the localizing OBS, with the successive application of each range adjustment. Water layer (WL) refers to the use of a sound velocity speed profile; Sediment properties (SP) consists in the application of the elastic properties of the water column and sediment layer; Sediment properties+Instrument correction (SPCO) is the application of the elastic properties with an instrumental coupling correction; All (ALL) range adjustments are the combination of all adjustments.

After the assessment of each range adjustments, the next stage was to develop the stage 1 classification, i.e. remove as many false positives from the detection process as possible in order to minimize their impact in the assessment of the trends of the classification parameters. In Chapter 2, all automatic detections in the subsample were identified as either true positives, i.e. detections that were positively confirmed as 20-Hz fin whale calls, or false positives, i.e. detections that were not from 20-Hz fin whale calls. Regarding the stage 1 classification, SNR and C.Max revealed the highest potential for removing false positives, as observed in Chapter 2 (Fig. 7, A and B). A C.Max threshold of 0.2 and a SNR threshold of 2.0 removed almost all false positives while maintaining almost all true positives. The other two

parameters, CZH and iZH, showed a large overlap between the true and false positives, and it was not possible to identify a potential threshold that could be useful to the stage 1 of the classification scheme (Fig. 7, D and E). Similarly, a possible threshold or pattern that would distinguish true and false positives could not be determined from assessing the full range of coherency values (Fig. 5, C). The iZH, CZH and Co values were designed to assess if the range estimates were inside the critical range or not. They were not established to help in the identification of the 20-Hz fin whale calls. Therefore, the lack of any pattern in these values that could allow the distinction between true and false positives of 20-Hz fin whale calls was expected.

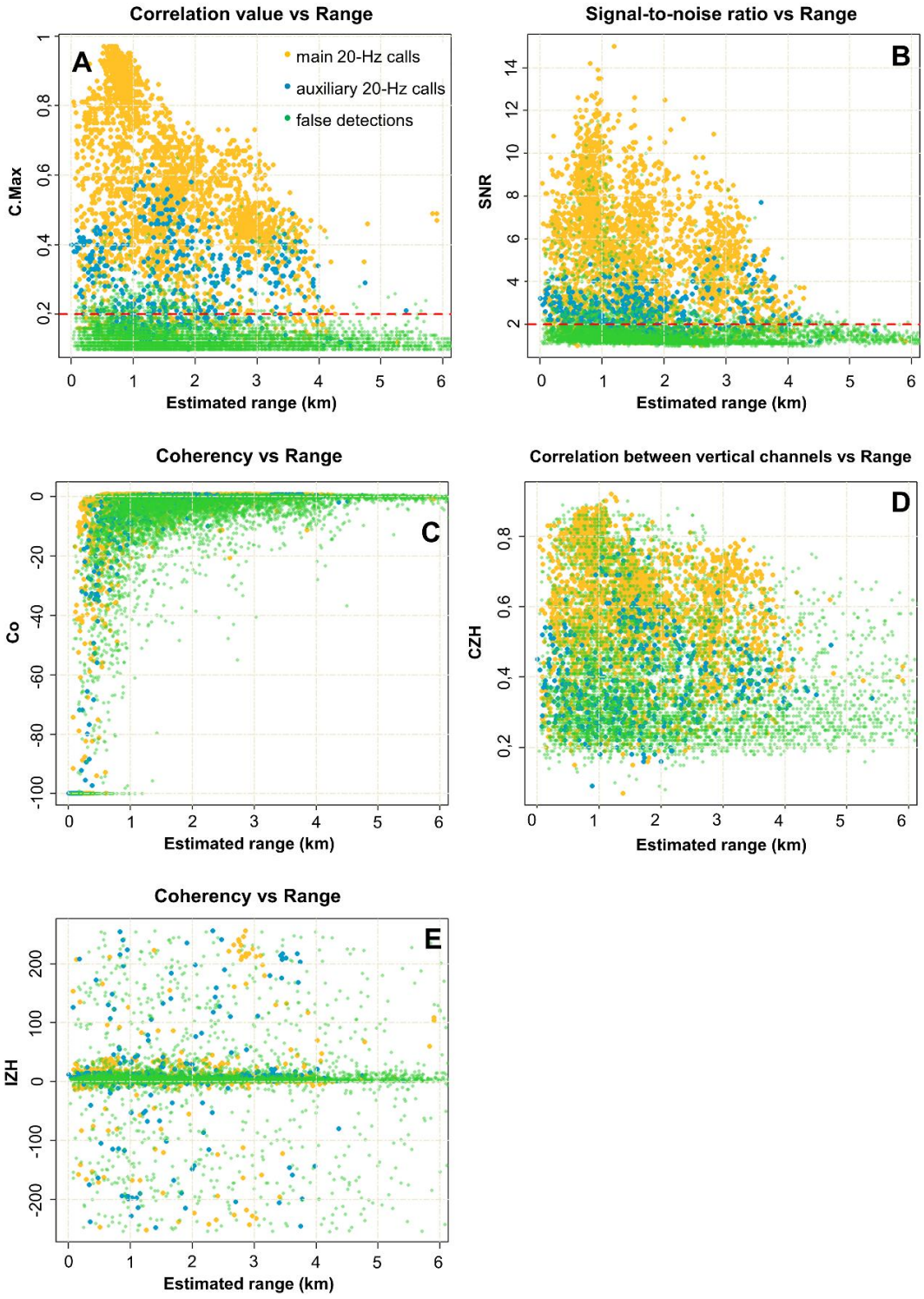

Figure 7. Comparison of each classification parameter versus estimated range computed by the SSM for the stage 1 of the classification scheme. Automatic detections were obtained for the 8 localizing OBS of the subsample (n = 8 158). True positives were considered as 20-Hz fin whale calls from a main or an auxiliary bout and all other types of signals were considered as false positives (see Chapter 2): A) Correlation values with range; B) Signal-to-noise ratio with range; C) coherency with range; D) correlation between vertical & hydrophone channels (CZH) with range; E) Lag in samples between vertical & hydrophone channels (iZH) with range. Red dashed lines in A and B identify the threshold for each parameter.

After the stage 1 classification, the assessment of trends in the classification parameters as a function of range was undertaken to identify calls inside the critical range, i.e., stage 2 of the classification. Only detections with positive coherency were considered in this analysis because they were considered to be the only detections with reliable ranges that could show a true pattern. As expected, there was a relationship between C.Max and distance for the detections with positive coherency of the subsample (Fig. 8, left). The maximum distance of true positives of 20-Hz fin whale calls with positive coherency did not show a considerable reduction from the detections with all coherency values (from 5.899 km with all coherency values to 5.262 km with only positive coherency). The relationship between SNR and distance was not so evident (Fig. 8, right).

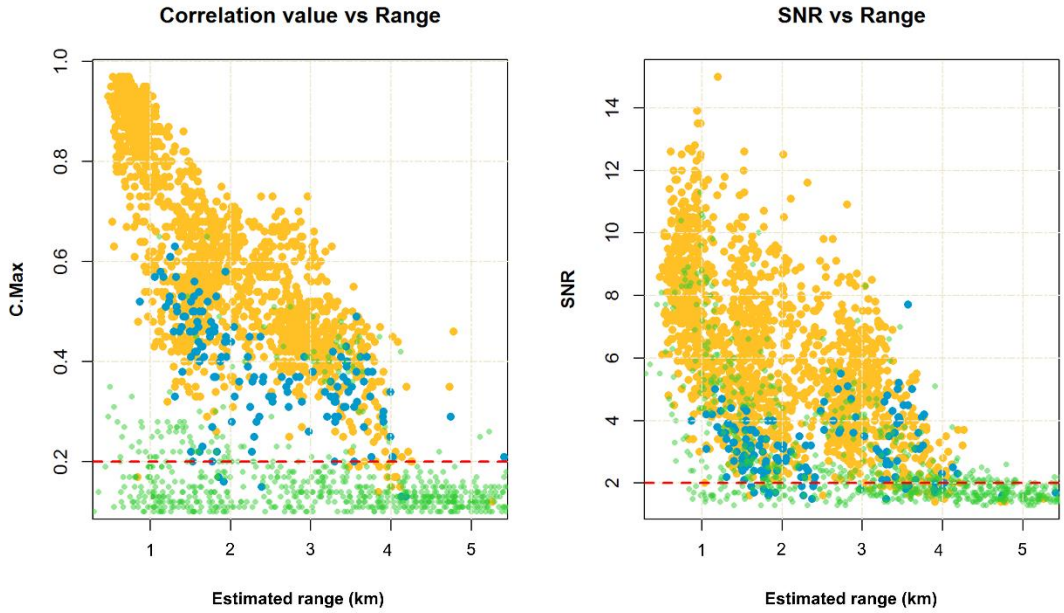

Figure 8. Correlation value (left) and SNR (right) of automatic detections from the subsample with positive coherency (n = 2 471). Yellow points are true positives of 20-Hz fin whale calls from a main bout, blue points are true positives of 20-Hz fin whale calls from auxiliary 20-Hz calls and green points are false positives. Dashed red lines are the thresholds identified in stage 1 of the classification.

The application of the overall classification scheme of C.Max≥0.2 and SNR≥2 (stage 1) and Co≥0 (stage 2) in the subsample kept a total of 53.6% true positives of 20-Hz fin whale calls, including main and auxiliary signals. The rate of false positives of 20-Hz fin whale calls decreased to 5.5%, with most of the false detections classified as “other” (e.g. mostly levelling of the OBS and noise). The accepted detections showed a variety of estimated ranges (Fig. 9). Furthermore, the classification scheme selected true positives of 20-Hz fin whale calls that

formed visible tracks when the relative locations were plotted (Fig. 9), which is a positive indication that the classification retained meaningful ranges for each bout.

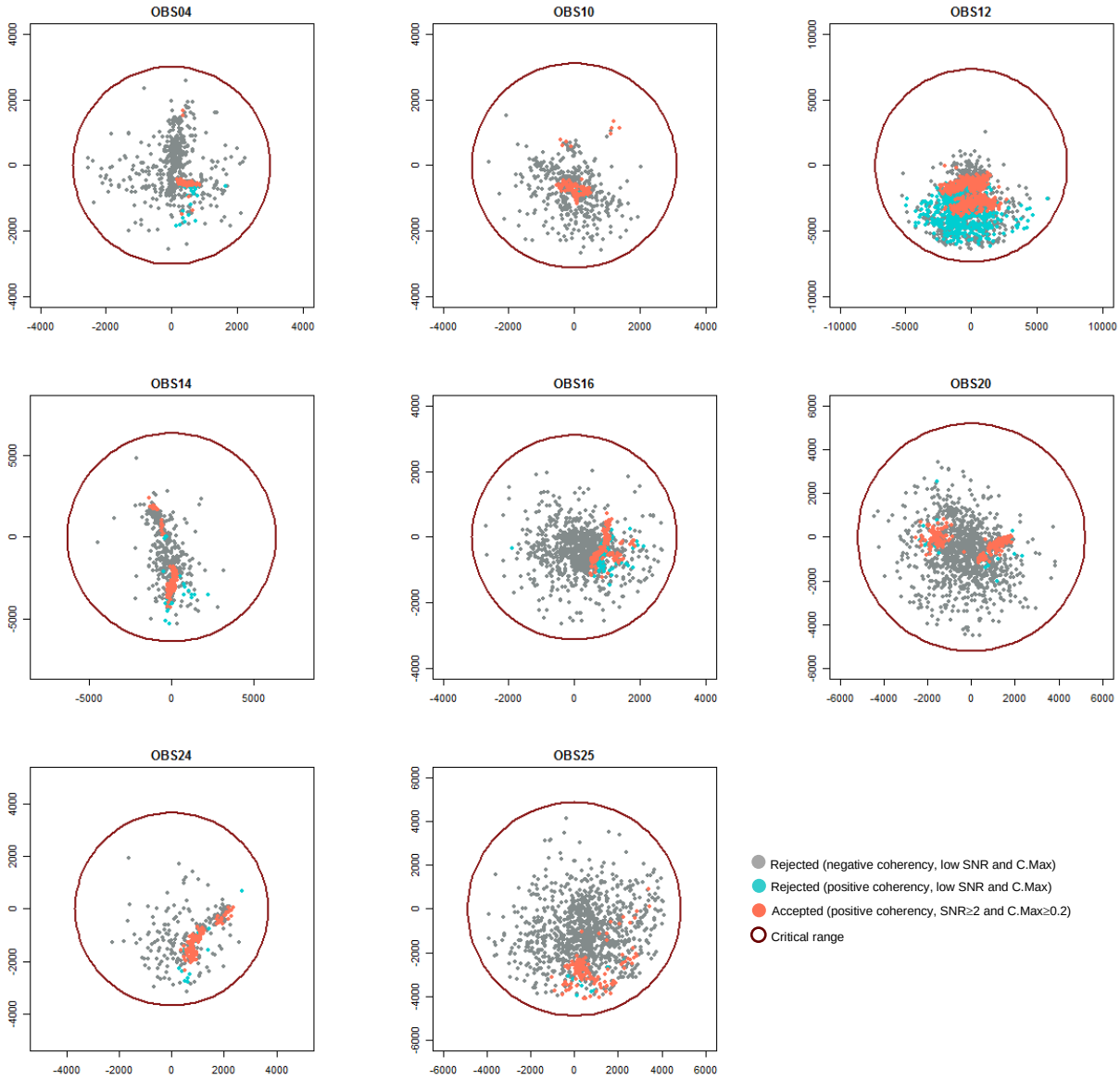

Figure 9. XY Plots of the relative locations of the automatic detections (true and false positives) of the subsample used in the classification analysis.

Applying the classification scheme to the full dataset for future analysis

The results of the two-stage (1 and 2) classification scheme described above determined thresholds of C.Max, SNR and Co that (1) removed false positives and (2) retained detections inside the critical range (though losing detections at close ranges to the OBS). Therefore, an overall classification scheme (C.Max≥0.2, SNR≥2 and Co≥0) was applied to the

full OBS dataset. The classification scheme was applied stepwise in the full dataset because it was not possible to apply the Co threshold to the non-localizing OBS. The first step consisted in applying the thresholds of the parameters that were common to localizing and non-localizing OBS, C.Max and SNR. A correlation threshold of 0.2 based was already defined in Chapter 2. The threshold was selected based on the performance analysis presented in Chapter 2 and produced a dataset large enough that could contain a high number of detections but could still be manageable. After the application of the SNR threshold on top of the application of the C.Max threshold to all OBS, 49.8% of the automatic detections in the dataset were maintained (Table IV). The second step was to apply the Co threshold to the localizing OBS. When the Co threshold was applied to the localizing OBS already filtered by C.Max and SNR, it was possible to retain 37.6% of the original localizing OBS detections. The final dataset with the detections of the non-localizing OBS filtered by C.Max and SNR, and the detections of the localizing OBS filtered by C.Max, SNR and Co, consisted of 37.9% of the original detections. The application of the coherency threshold of $Co \geq 0$ also resulted in the removal of the very close detections to the instrument (Fig. 10). The relative locations of the detections from OBS12 and OBS24 seemed to show a degree of bias as most locations were concentrated in a specific part of the area around the OBS. The reason for this was unknown.

Table IV – Summary of accepted automatic detections after the application of the classification scheme for each OBS. Grey lines are OBS that could not provide a range estimate because they did not have all the three components working in order to apply the SSM, i.e. non-localizing OBS. White lines are LOC or localizing OBS, i.e. instruments that had all 3 components of the seismometer working and could provide range estimates. OBS06 started recording without the three components working properly (NON LOC) but after February 2008 all the channels that enable a location of a detected signal were working (LOC).

								FILTER APPLIED TO LOC OBS ONLY
OBS NO.	**OBS Depth (km)**	**Critical Range (km)**	**Start date**	**Finish date**	**Number of days surveyed**	**Total number of detections C.Max≥0.2**	**Detections with SNR≥2**	**Detections with Co+ & SNR ≥ 2.0**
1	5.100	8.870	10-09-2007	12-06-2008	277	482 185	242 852	NA
3	3.932	6.834	10-09-2007	31-07-2008	326	122 488	101 918	NA
4	1.993	3.455	15-09-2007	25-06-2008	285	113 714	39 316	13 000
5	3.095	5.373	10-09-2007	23-06-2008	288	263 155	152 688	NA
6	2.956	5.154	14-02-2008	20-07-2008	158	7 327(LOC) + 145 338 (NON LOC)	3 416	1 199
8	4.671	8.121	10-09-2007	10-08-2008	336	48 975	41 545	NA
9	4.811	8.368	10-09-2007	29-04-2008	233	134 654	115 082	NA
10	2.067	3.581	10-09-2007	29-06-2008	294	141 885	457 29	16 210
12	4.860	8.512	10-09-2007	20-07-2008	315	151 924	102 447	59 455
13	4.494	7.814	10-09-2007	14-07-2008	309	107 506	77 177	NA
14	4.212	7.377	17-09-2007	20-07-2008	308	128 498	76 307	25 429
15	3.357	5.831	01-09-2007	07-04-2008	220	112	-	-
16	2.069	3.584	10-09-2007	07-07-2008	302	92 546	36 374	5 926
17	4.873	8.475	10-09-2007	28-05-2008	262	478 678	16 7574	NA
18	4.605	8.065	10-09-2007	17-07-2008	312	125 700	78 693	24 461
19	4.287	7.509	10-09-2007	17-07-2008	312	96 606	68 543	31 036
20	3.449	6.034	10-09-2007	12-07-2008	307	68 294	44 839	11 686
24	2.566	4.451	29-11-2007	11-08-2008	256	135 857	16 792	45 65
25	4.095	7.257	29-11-2007	11-08-2008	256	72 860	42 073	15 561
TOTAL	-	-	-	-	-	2 918 312 (1 135 211)	1 453 365 (554 529)	208 528

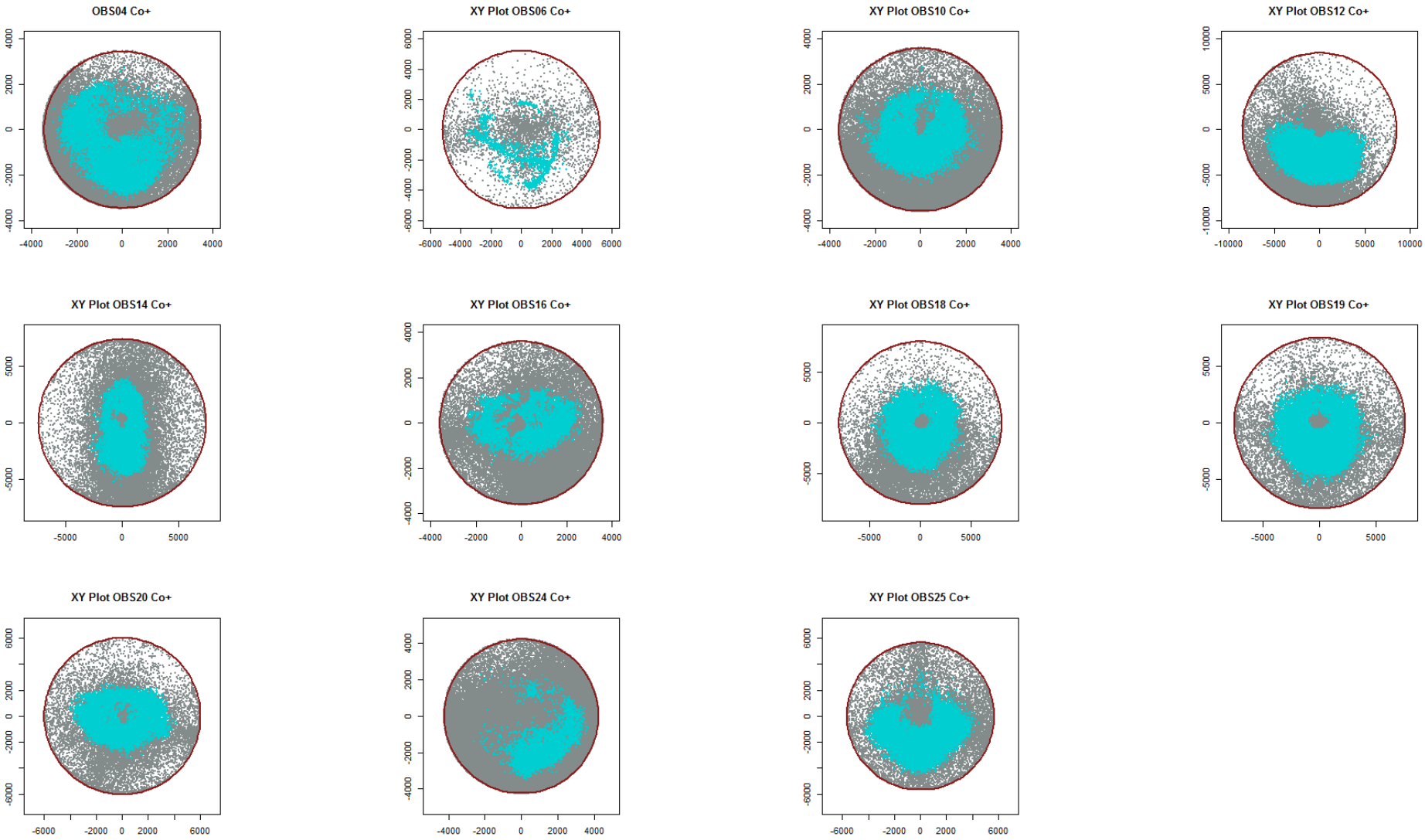

Figure 10. Relative locations of all detections obtained for the localizing OBS. Grey dots represent detections rejected by the classification scheme and the blue dots represent the ones that were accepted by the classification scheme (C.Max≥0.2, SNR≥2 and Co≥0).

Classification requirements for distance sampling

The full dataset that resulted from the application of the overall classification scheme, removing all negative coherencies, could be suitable for some studies, such as movement analyses as long as the direction and changes of tracks were registered. However, for distance sampling purposes it was necessary to find an additional rule in order to preserve the closer detections. In distance sampling analysis (the focus of Chapter 5), only detections from the localizing OBS were considered as the non-localizing OBS could not produce estimates of range with the single station method. In the dataset of all automatic detections of the localizing OBS with C.Max≥0.2 and SNR≥2, the application of the 250 m buffer identified in Matias and Harris (2015) resulted in an undesirable peak of detections around that distance (Fig. 11). For distance sampling, the distribution of ranges for point transects is expected to be as follows: as the radius increases from the centre of the point, the surveyed area also increases and, on average, there are more calls available to be detected. Therefore, there is an initial increase in the frequency of detections as a function of range from the centre of the point. However, as the distance between the point centre and the calls becomes larger, the probability of detecting those further away calls becomes lower. Therefore, at some range, the effect of reducing detectability is larger than the effect of increasing area. From that range, a decrease in the frequency of detections is expected. For more information about point transect methodology, see Buckland *et al.* (2001). The 250 m buffer produced a high number of detections at very close ranges, which is against the expected point transect theory. This result suggested that this buffer with this dataset maintained negative coherency detections with spurious ranges less than 250 m into the dataset. Therefore, another approach had to be taken to try to include the close range calls with true close ranges.

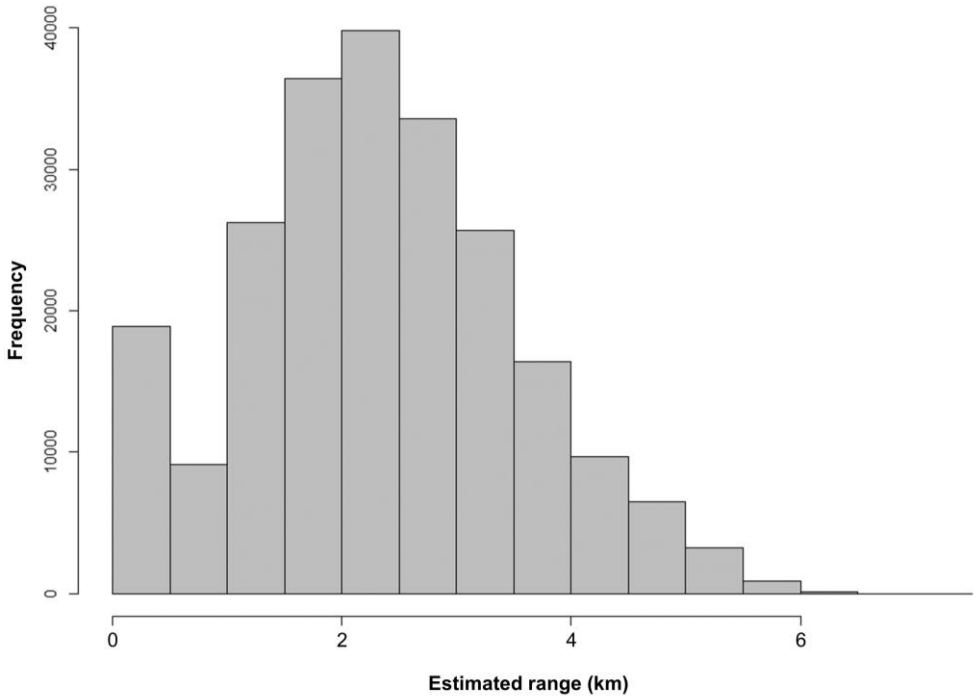

Figure 11. Distribution of ranges of the full dataset of the localizing OBS filtered with the overall classification scheme (C.Max≥0.2, SNR≥2) and a 250 m buffer where all values of coherency were accepted (n = 226 496).

Figure 8 showed that there was a trend between C.Max and distance, when detections showed positive coherency. Levels of correlation of 0.6 or above were only observed at ranges up to ~3.4 km and values of correlation 0.8 around ~1.8 km. If this relation is applicable to all detections, then true positives of 20-Hz calls with negative coherency and high correlation values should be produced at close ranges. Two classification schemes based on coherency were assessed in the full dataset of the localizing OBS: 1) detections with all values of coherency at a correlation threshold of 0.6 and SNR threshold of 2 (Fig. 12), and; 2) detections with SNR≥2, and C.Max≥0.6 if coherency was positive, and C.Max≥0.8 if coherency was negative (Fig. 13). For the classification scheme of C.Max≥0.6 and SNR≥2, estimated ranges for detections with negative coherency were between 7 m and 3.058 km and for detections with positive coherency were 169 m and 4.185 km. The estimated ranges for most detections with negative coherency values and C.Max≥0.8 and SNR≥2 were also the expected, around 1.8 km, based on the trend observed in Fig. 8. The maximum estimated range for detections with C.Max≥0.8 and negative coherency was 2.137 km.

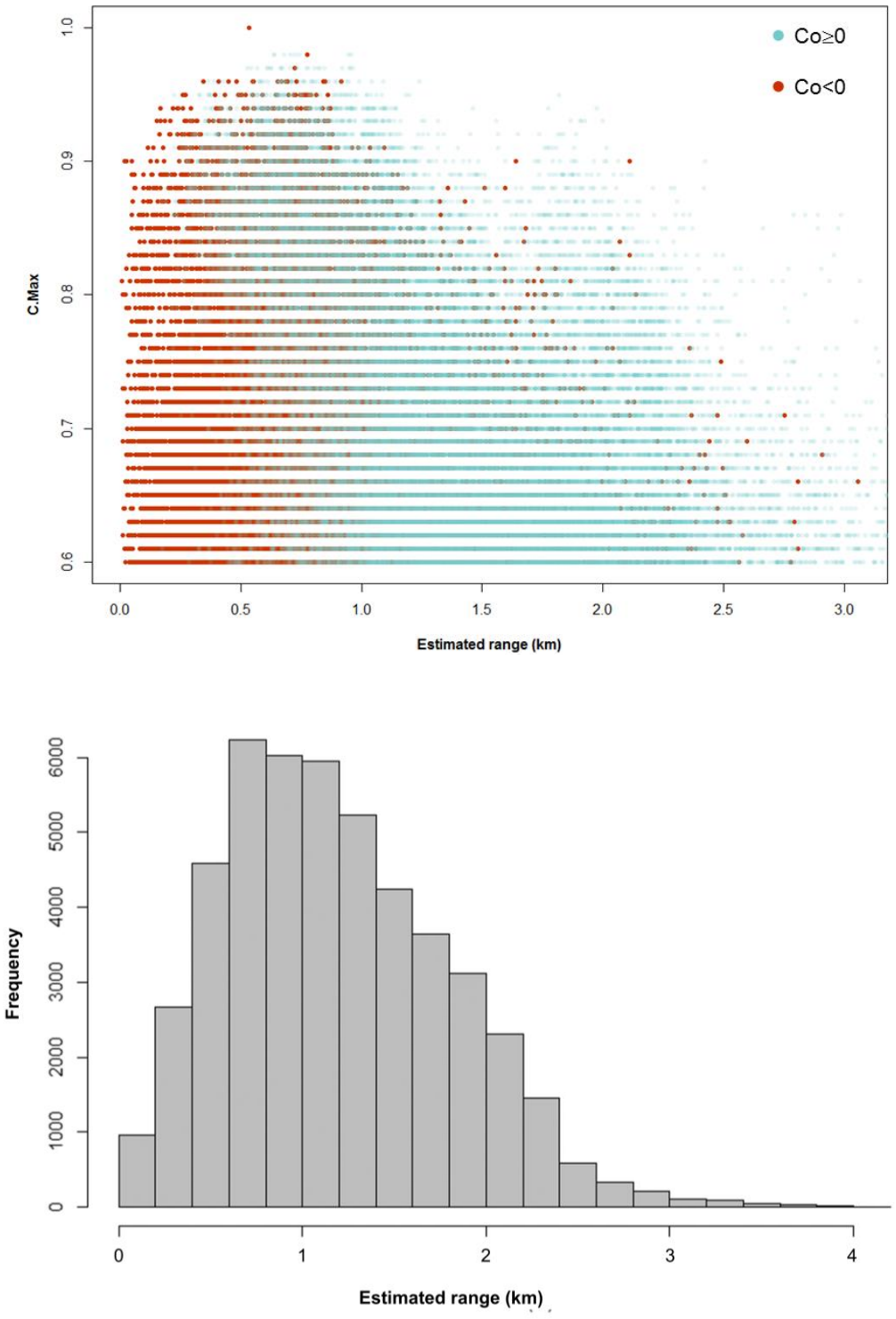

Figure 12. Correlation values above 0.6 with estimated range for positive and negative coherency values (top); Distribution of estimated ranges of the full dataset of the localizing OBS filtered with the classification scheme of C.Max≥0.6 and SNR≥2 (bottom) (n = 47 856).

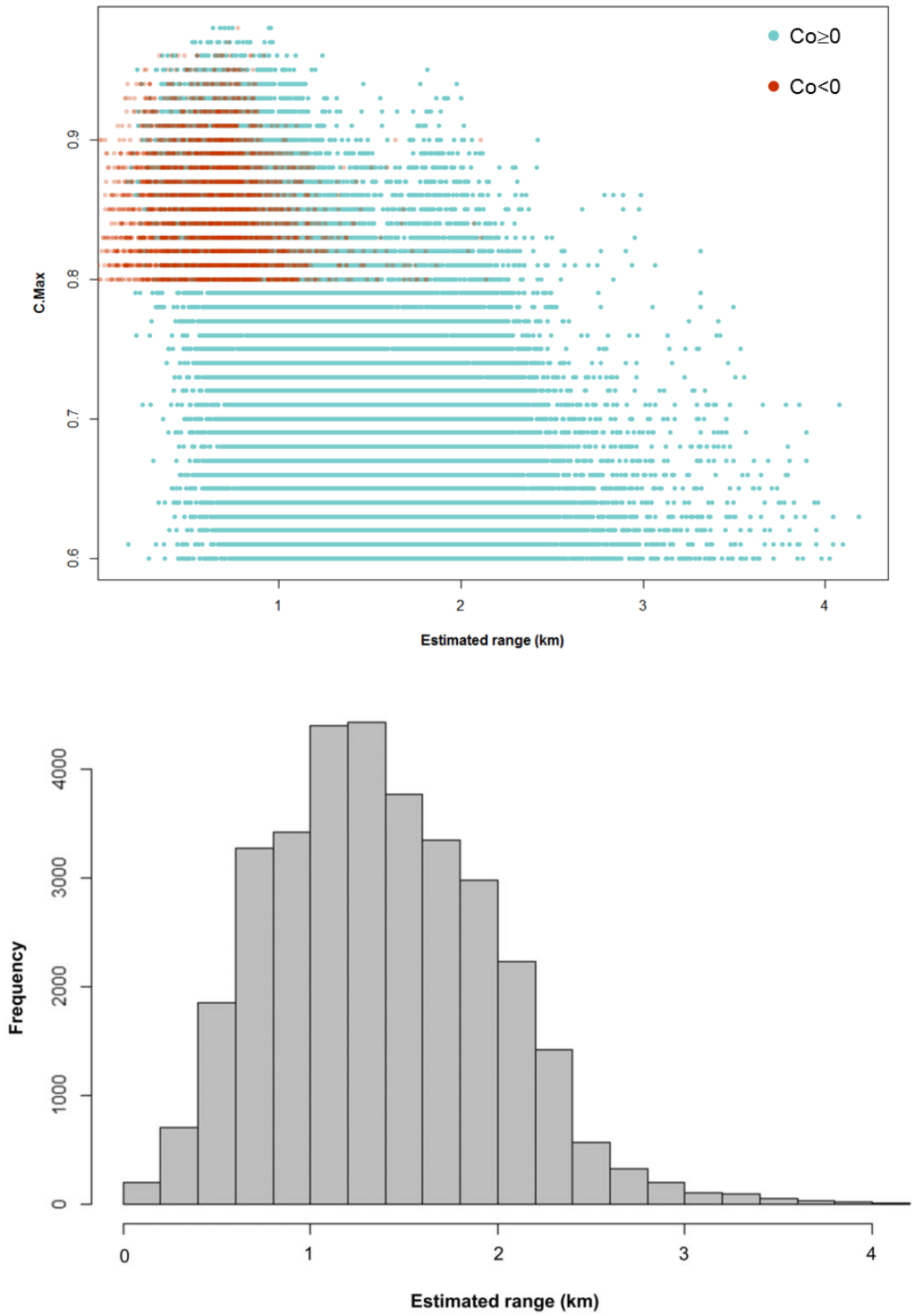

Figure 13. Correlation values with estimated range for detections with C.Max≥0.6 if coherency was positive and C.Max≥0.8 if coherency was negative (top); Distribution of estimated ranges of the full dataset of the localizing OBS filtered with the classification scheme of C.Max≥0.6+SNR≥2 if Co≥0 and C.Max≥0.8+SNR≥2 if Co<0 (bottom) (n = 33 404).

3.4. DISCUSSION

The classification scheme developed in this Chapter was divided into two stages: 1) stage 1, where several parameters calculated by the detection algorithm were used to filter out as many false positives as possible i.e., signals that were not 20-Hz fin whale calls; and 2) stage 2, where parameters related with distance where assessed to identify trends that help deciding if a 20-Hz fin whale call was inside the critical range or not. Although Matias and Harris (2015) conducted extensive work on the detection, classification and location of fin whale calls detected in the same set of OBS, they used a very small sample that might not be representative of all situations. This chapter used a larger fin whale acoustic dataset to identify a classification scheme related to the detection (stage 1) and the accurate ranging (stage 2) of the 20-Hz fin whale calls.

3.4.1. Range adjustments considerations

The use of the single station method for ranging and location of sound sources using OBS data requires three corrections to the first raw estimates produced by the ranging algorithm (Matias and Harris, 2015): i) calculation of the true emergence angle with the Zoeppritz equations; ii) adjustment of range by accounting for the water layer structure, iii) application of a correction factor in the recorded signal amplitudes.

The sound speed in the water varies from location to location and with environmental conditions, such as storms, currents, temperature of the water, among other parameters. There was only 1D sound speed profile available and was acquired in 24th August 2007 at 19:53:41 (UTC), at a location close to OBS25 (see Fig. 1, Chapter 2). For a more accurate adjustment regarding the water layer, several sound speed profiles should be acquired in order to include all types of environmental conditions. Although the use of a single sound speed profile could produce a bias in the adjustments, Matias and Harris (2015) also used the same sound speed profile measured around OBS25 to adjust ranges in OBS19 which were accurate. They estimated the ranges of air gun shots with the single station and adjusted the ranges with the same corrections applied in this Chapter. Then, they compared those adjusted estimates with true known locations of the air gun shots (Matias and Harris, 2015).

A correction factor of 0.5 in the recorded signal amplitudes was also necessary in order to improve the accuracy of the estimated ranges. Although there was no assessment of the requirement to apply the correction factor to all OBS in the study area, Matias and Harris (2015) observed this requirement at two different sites (southwest of Portugal and Azores), with two different seismic signals (fin whale calls and airgun shots in the ~20-Hz range),

recorded by two different types of instruments. In both cases, the estimated ranges were improved by the application of the same correction factor. Therefore, it seemed appropriate to apply the correction factor to all OBS in this study, though more research is needed to understand whether the amplitude correction factor is required in all OBS studies when using the single station method.

3.4.2. Classification of fin whale calls

In Matias and Harris (2015) the parameters that showed the most potential in removing false positives and identifying detections inside the critical range were the correlation between the vertical and hydrophone channels (CZH), the time lag between the vertical and hydrophone channels (iZH) and the coherency factor (Co). In that study, the true locations of the test datasets were known which eased the identification of several thresholds of the classification parameters. In the dataset investigated in this thesis, true locations of the automatic detections were not available, and the coherency factor was used as the main indicator whether detections were inside the critical range or not. In this chapter, the parameters that showed most potential in removing false positives (stage 1 classification) from a representative subsample of the dataset were the normalized cross-correlation (C.Max) and signal-to-noise ratio (SNR). Regarding the stage 2 of classification, the coherency (Co) was crucial for removing calls outside the critical range but additional parameters were required to re-introduce calls that may have been produced at close ranges but removed due to having negative coherency. The correlation threshold (C.Max) became important in this process. An overall classification scheme was identified and applied to the full dataset: C.Max$\geq$0.2, SNR$\geq$2 and Co$\geq$0. One advantage of this classification scheme over the CZH and iZH used by Matias and Harris (2015) is that the hydrophone that is deployed with the OBS was not needed. All three parameters, C.Max, SNR and Co were calculated using the channels from the seismometer. The correlation threshold was already established in Chapter 2, and therefore detections made for all OBS during the study period were obtained with C.Max$\geq$0.2 (see Chapter 2 for more details). The threshold of SNR was applied to OBS that could localize (localizing OBS) and could not localize (non-localizing OBS). However, because it was not possible to obtain coherency values for the non-localizing OBS, the threshold of Co$\geq$0 was only applied to the localizing OBS. With the application of the classification scheme to all OBS, the full dataset was prepared for further studies.

The removal of the detections of the subsample with negative coherency revealed a trend of correlation with range (Fig. 6). High correlation values (>0.8) were found at ranges

~1.8 km and decreased with range. This clear relationship between the C.Max threshold and range is linked to the equation of the matched filter used in the detection process, because it accounts for signal attenuation, i.e., calls that have small amplitudes and are probably produced far away from the recording instrument will result in small values of correlation.

3.4.3. Classification requirements for biological studies

The removal of all negative coherencies from the full dataset might not affect some types of biological study. For example, in a movement study assessing calling whale tracks, tracks of calling whales close to the OBS would be removed via the positive coherency classification criteria but would not necessarily impact the study. However, for animal abundance estimates that are based on distance sampling and assume a certainty in the detectability of calls at close distances (i.e., probability of detection at the point transect g(0)=1, see Chapter 5), close calls needed to be detected. The detector chosen in Chapter 2 was very selective. Based on a representative subsample with manual verification of the signals, the detector showed a high true positive rate and a low false positive rate. Considering that close calls needed to be retained, the goal was to obtain the simplest additional set of classification rules to the already established classification that could be applied to the full dataset. Matias and Harris (2015) used a relatively large list of parameters that in this chapter did not show the same thresholds. All results in this chapter suggested that SNR could be used to remove false positives and C.Max could be used to help in the decision of whether the detections were produced inside the critical range or not, along with the coherency factor.

3.4.4. Final considerations

The maximum estimated range for detections with a correlation threshold of 0.6 and SNR of 2 was 4.185 km for a positive coherency. This estimate were in the expected maximum range as the furthest critical range was 8.870 km for OBS01 and the closest 3.455 km for OBS04. In addition, Matias and Harris (2015) also showed that correlation values of air gun detections, with known locations, around 0.6 were observed at ranges up to 4 km (Fig. 5), which is in agreement with the result obtained in this Chapter. However, data with true known locations or estimates from other types of location methods, such as time difference of arrival, are still needed in order to validate the detection and classification scheme used on the localizing dataset.

Two datasets were generated for distance sampling in this chapter by including negative coherent detections in two ways. However, only one dataset was used for the analysis in Chapter 5. This is because 8 of the OBS deployed in the study area and which showed detections did not record the full set of seismometer components during some or the whole period of recording. As a result, it was not possible to obtain range estimates of their automatic detections with the single station method and coherency values of those detections were also not available. Therefore, most of the automatic detections could not be used in a straightforward approach for distance sampling. The final dataset chosen for distance analysis was the one that had all values of coherency and thresholds of correlation of 0.6 and SNR of 2. In Chapter 5, abundance estimates of fin whales were obtained with localizing OBS only. In future distance sampling analysis where the non-localizing OBS will also be used, the classification scheme needs to have the fewest parameters and ones that could be applied to all recording instruments.

Although the detection and classification processes investigated in this thesis showed a high true positive rate with the least amount of false positives regarding the detection process and the simplest set of rules in obtaining a suitable dataset for different types of studies, it would be useful to develop a validation study that could confirm the trend of correlation value obtained with this particular detector and distance. Because the true locations were not known and negative coherency values were accepted at all distances for detections with correlation values above or equal to 0.6, there was always a potential of having some proportion of unreliable range estimates (more details in Chapter 5). However, there was an effort to keep this number as small as possible. In order to better understand the ranges within the critical range at which the positive coherency changes to negative, a dedicated study where locations are known is also needed. In the recordings of this set of OBS, the multipaths displayed small amplitudes. However, in cases where they could be identified, the tracks obtained with a different location method could be compared with the locations obtained with the single-station method.

A four year project that involves the study of fin whales around the Azores in a multidisciplinary approach that includes the use of acoustic data acquired with OBS will start in October 2018. An expansion of the single station method to multipaths will be developed and a new location method that uses a sound propagation model will also be applied. The locations of the detections will be estimated by different methods that will help to improve the single station method.

3.5. REFERENCES

Aki, K., and Richards, P. (**1980**). *Quantitative Seismology, Theory and Methods* (Freeman and Company, San Francisco, CA), Vol. 1, 557 pp.

Au, W. W. L., and Hastings, M. C. (**2008**). *Principles of Marine Bioacoustics. Modern Acoustics and Signal Processing* (Springer-Verlag, New York), 679 pp.

Buckingham, M. J. (**1998**). "Theory of compressional and shear waves in fluidlike marine sediments," Journal of the Acoustical Society of America **103**, 288–299.

Buckland, S. T., Anderson, D. R., Burnham, K. P., Laake, J. L., Borchers, D. L., and Thomas, L. (**2001**). *Introduction to Distance Sampling* (Oxford University Press, Oxford, UK), 432 pp.

Corela, C. J. C. (**2014**). "Ocean Bottom Seismic noise: applications for the crust knowledge, interaction ocean-atmosphere and instrumental behaviour," Ph.D. dissertation, University of Lisbon, Lisbon, Portugal.

Doyle, H. (**1995**). *Seismology* (Wiley and Sons, Chichester, UK), Chap. 14, pp. 123–137.

Dunn, R. A., and Hernandez, O. (**2009**). "Tracking blue whales in the eastern tropical Pacific with an ocean-bottom seismometer and hydrophone array," Journal of the Acoustical Society of America **126**, 1084–1094.

Harris, D., Matias, L., Thomas, L., Harwood, J., and Geissler, W. H. (**2013**). "Applying distance sampling to fin whale calls recorded by single seismic instruments in the Northeast Atlantic," Journal of the Acoustical Society of America **134**, 3522–3535.

Havskov, J., and Ottemöller, L. (1999). "SeisAn Earthquake analysis software," Seismological Research Letters 70. http://www.seismosoc.org/publications/SRL/SRL_70/srl_70-5_es.html (Last viewed 12th February 2018).

Matias, L., and Harris, D. (**2015**) "A single-station method for the detection, classification and location of fin whale calls using ocean-bottom seismic stations," Journal of the Acoustical Society of America **138**, 504–520.

Mellinger, D. K., Roch, M. A., Nosal, E. M., Klinck, H. (**2016**). "Signal processing," in Listening in the Ocean: New Discoveries and Insights on Marine Life from Autonomous Passive Acoustic Recorders, edited by W.W.L. Au and M.O. Lammers (Springer-Verlag New York, New York, USA), pp. 359–409.

Pereira, A., Harris, D., Thomas, L., Tyack, P., and Matias, L. (**2015**). "Detection and propagation range of fin whale calls off Gulf of Cadiz," abstract presented at the 7th International DCLDE [Detection, Classification, Location, and Density Estimation] Workshop, 13-16 July, La Jolla, USA.

Rebull, O. G., Cusí J. D., Fernández M. R., and Muset J. G. (**2006**). "Tracking fin whale calls offshore the Galicia Margin, north east Atlantic ocean," Journal of the Acoustical Society of America **120**, 2077–2085.

Roberts, R. G., Christoffersson, A., and Cassidy, F. (**1989**). "Real time events detection, phase identification and source location estimation using single station component seismic data and a small PC," Geophysical Journal International **97**, 471–480.

Shipboard Scientific Party (**1972**). "Sites 135," in Initial Reports of the Deep Sea Drilling Project (U.S. Government Printing Office, Washington, DC), Vol. 14, pp. 15–48.

Stimpert, A. K., DeRuiter, S. L., Falcone, E. A., Joseph, J., Douglas, A. B., Moretti, D. J., et al. (**2015**). "Sound production and associated behavior of tagged fin whales (*Balaenoptera physalus*) in the Southern California Bight," Animal Biotelemetry **3**, 23.

Wilcock, W. S. D. (**2012**). "Tracking fin whales in the northeast Pacific Ocean with a seafloor seismic network," Journal of the Acoustical Society of America **132**, 2408–2419.

Chapter 4

ACOUSTIC CHARACTERISTICS OF THE 20-HZ FIN WHALE CALLS IN SEAS TO THE SOUTHWEST OF PORTUGAL

4.1. INTRODUCTION

Describing the variation of acoustic signals of a given species brings valuable insights about differences among populations. In acoustics, “geographical variation” is associated with differences between populations separated by large distances that do not normally mix (Mundinger, 1982). The word “dialect” is often used to describe observed differences in sound emission, such as differences in call features or songs, among neighbouring populations, which can potentially have some degree of interchange (Grimes, 1974). Dialects occur in many species of birds and they have also been observed in some species of mammals, such as tamarins (Maeda and Masataka, 1987), wild chimpanzees (Mitani *et al.*, 1992), and humans (Barbujani, 1991). In case of cetaceans, focused studies about dialects have been undertaken in killer whales (Ford, 1991), sperm whales (Weilgart and Whitehead, 1997) and bottlenose dolphins (Wang *et al.*, 1995). Although the word “dialect” has only been used for the three cetacean species mentioned above, acoustic data have been used to describe divergence across geographic regions in other species, such as humpback whales (e.g. Payne and Guinee, 1983), blue whales (e.g. McDonald *et al.*, 2006) and fin whales (e.g. Hatch and Clark, 2004). In the North Atlantic Ocean, fin whales have been differentiated by their inter-call interval (e.g. Delarue *et al.*, 2009), frequency bandwidth (e.g. Thompson *et al.*, 1992) and bout composition (e.g. Clark and Gagnon, 2002).

There has been some discussion about the significance of dialects in speciation (Maeda and Masataka, 1987). Nottebohm (1969) suggested that the occurrence of dialects among species that are distributed in a continuum over vast geographic areas may reduce the gene flow between breeding populations and allow a more efficient adaptation to local habitat conditions. Several researchers have tried to find links between genetic variance and acoustic variation among populations, but it is still a subject of debate. In studies of acoustic variation in birds, some show evidence that dialect variation reflect some amounts of genetic population structure (MacDougall-Shackleton and MacDougall-Shackleton, 2001), while others suggest the contrary (Lougheed *et al.*, 1993; Soha *et al.*, 2004).

In the seas to the southwest of Portugal there are two groups of fin whales, which were introduced in Chapter 1: the British Isles-Spain-Portugal, which is a stock of the North Atlantic fin whales, and the Mediterranean groups. The Mediterranean group is a subdivision of the British Isles-Spain-Portugal group. Although the Mediterranean fin whales seem to be resident, there is some evidence of a bidirectional movement between the North Atlantic Ocean and the Mediterranean Sea. Genetic studies and satellite-tag data suggest that the degree of interchange between the two groups seems to be small (Palsbøll *et al.*, 2004; Cotté *et al.*, 2009). In addition, there is also the question about whether the migrating whales are individuals from the North Atlantic returning to their main area. Castellote *et al.* (2011) found acoustic differences between bouts recorded in the Mediterranean Sea and in the North Atlantic Ocean, in relation to the inter-call interval and the frequency bandwidth of the 20-Hz call. The inter-call intervals and frequency bandwidth obtained for the Mediterranean fin whales were close to 15 seconds and 5 Hz, respectively. Bouts recorded in the North Atlantic Ocean showed inter-call intervals of 12-13 seconds and a frequency bandwidth around 6 Hz (Castellote *et al.*, 2011). These results suggest the existence of two dialects, one that was recorded in several locations between the North Atlantic Ocean and the western Mediterranean Sea and a second one that was restricted to the Mediterranean Sea. Given these previous studies, southwest Portugal constitutes a strategic area to study the movements and interchange of fin whales between the North Atlantic Ocean and the Mediterranean Sea.

In this chapter, 11 months of recordings off southwest Portugal were used to characterize the most common fin whale acoustic signal, the 20-Hz call. Several spectral and temporal features found in the literature were computed with a subsample of 20-Hz calls. This task required that the subsample of calls was large enough and was representative of all the whales recorded in the instruments. In order to avoid the presence of (a) false positives, (b) overlapping calls that could interfere in the measurement of the features and (c) the recording of the same whale multiple times, a set of rules was established during the detection process and the subsampling of calls. The measured spectral and temporal characteristics of the 20-Hz calls were then used in a hierarchical cluster analysis in order to assess the existence of dialects. Possible dialects identified in this analysis were then further validated by comparing their characteristics to other groups already established in the literature, more specifically the results of Castellote *et al.* (2011) for fin whales in the North Atlantic Ocean and the Mediterranean Sea. As already mentioned in Chapter 1, the inter-call interval is the call feature with most discriminatory power among fin whale groups. In a second stage of analysis, the temporal pattern of identified inter-call intervals was also assessed using the whole

dataset of detections. The aim of the analysis in this chapter was not to obtain a measure of call abundance, which is the main aim of Chapter 5, but instead an occurrence pattern. This was achieved by counting the occurrence of sequences of calls with the intervals found. In summary, this study identified dialects that occurred off southwest of Portugal and then assessed the temporal distribution of the inter-call interval in order to obtain a seasonality pattern of the different dialects.

4.2 METHODS

4.2.1. Data collection

Fin whale acoustic data used in this study were obtained between September 2007 and August 2008 with a network of 24 ocean-bottom seismometers (OBS) that was deployed off southwest Portugal (Fig. 1, Chapter 2). The main aim of the deployment of the OBS was to obtain data to study the microseismicity originating from potential tsunami sources. However, fin whale calls were also recorded during this time. A more detailed description of the deployment and recording instruments is found in Chapter 2.

4.2.2. Signal detection

The Z-channel of the seismometer was chosen as the main acoustic source because the signals had both higher amplitudes and signal-to-noise ratio (SNR) measurements than other channels (more details in Chapter 2). Fin whales produce a variety of sounds that were described in Chapter 1. The 20-Hz fin whale call was detected using an algorithm with a modified normalized cross-correlation equation with a matched filter of the signal waveform. Chapter 2 provides a description of the detection algorithm and detection process. As also mentioned in Chapter 2, backbeats were not detected. In the detection process, the normalized cross-correlation between the recording and a master template of a single call is calculated through time. When the normalized cross-correlation between these two time series reaches a threshold set by the researcher, a detection is recorded. The values of the normalized cross-correlation range from 0 to 1. At low correlation thresholds (generally smaller than 0.4), the signals detected might be weak signals or false positives that have a similar waveform (see Chapter 2 for examples of false positives). When the correlation

threshold is high (generally above 0.7), the detected signal has almost a perfect match with the template.

The template of the 20-Hz call used was obtained from the waveform of a well-defined 20-Hz call with high SNR that was observed during a manual inspection of the dataset. This template used with the settings of detector 4 (see Chapter 2) resulted in a true positive rate of 87%. The detection routine was applied to all OBS recordings with a low correlation threshold (0.2) and a buffer time of 3 seconds. These parameters were chosen in order to obtain as many calls as possible but with a decreased probability of detecting multiple whales calling at almost the same time, which would present a risk of overlapped calls. For each detection, several quality-related, spectral and temporal features were computed and are described below in 4.2.4.

4.2.2.1. Spectral cross-correlation

The detection routine included the calculation of the spectral cross-correlation, following the methodology of Mellinger and Clark (2000) with minor modifications. The initial detection was done using the waveform cross-correlation algorithm and the spectral cross-correlation was only applied when a detection was registered. After the detection process, the correlation values from the matched filter and the spectral cross-correlation were available in order to facilitate the choosing of the detections. In some occasions, where false-positives such as air guns, also show high values of the normalized cross-correlation, the spectral cross-correlation helps in filtering some of these detections. A detection with both high matched filter correlation and spectral cross-correlation would be a potential high quality and true call.

4.2.2.2. Constructing the spectrogram synthetic kernel

The spectrogram cross-correlation requires a spectrogram template of the target signal that is compared with the spectrogram of the recordings. The kernel spectrogram of the 20-Hz call was obtained by averaging the time and frequency characteristics of calls with large amplitude spectral values and high correlation signals given by the waveform matched filter. For example, in OBS04, in 21st December 2007, there were 39 20-Hz calls with a correlation value above 0.9 (see Fig. 1 for a sample of them).

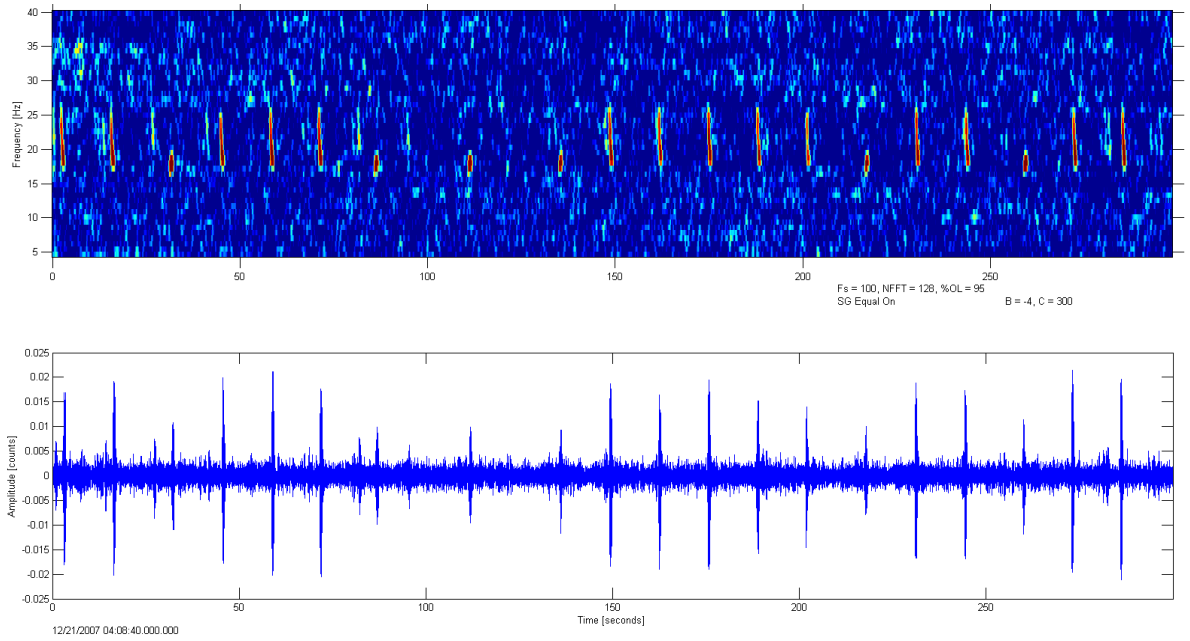

Figure 1. Spectrogram showing 5 minutes with some of the high quality calls that were used to establish the base of the spectrogram kernel. Recorded in OBS04, 21/12/2007 at 4:08:40. Spectrogram settings: Frame size – 128 samples, 95% overlap, Hanning window, equalized, contrast: 300, brightness: -4.

For each of these calls, the time of the median energy (definition below) was computed and saved as the signal arrival time. The kernel spectrum was extracted between 1.5 seconds before and 1.5 seconds after this reference time. The frequency limits were set between 12 and 31 Hz. Although from a visual inspection of the spectrograms, most 20-Hz calls have a shorter frequency range, these frequency limits were chosen in order to have a large frequency buffer, ensuring that the whole frequency spectrum of each call would be captured. After extraction, all 39 spectra were summed and averaged to obtain the base for the kernel. A final step was then required to produce the final kernel. The base kernel spectrogram only showed positive spectral amplitudes, but in Mellinger and Clark (2000) the discrimination between the signal of interest and noise and/or other interfering signals relies on the property that the kernel has equal positive and negative values so that the total sum is zero. Therefore, to obtain a final kernel, an amplitude level above which the spectrogram accumulated 90% of the amplitude was defined. This level was subtracted from the spectrogram. All negative amplitude values of the spectrogram were then given the same value so that the total sum of the kernel amplitudes was zero, as required by the method in Mellinger and Clark (2000). The final kernel obtained from this method was saved to use in the spectral cross-correlation analysis (Fig. 2).

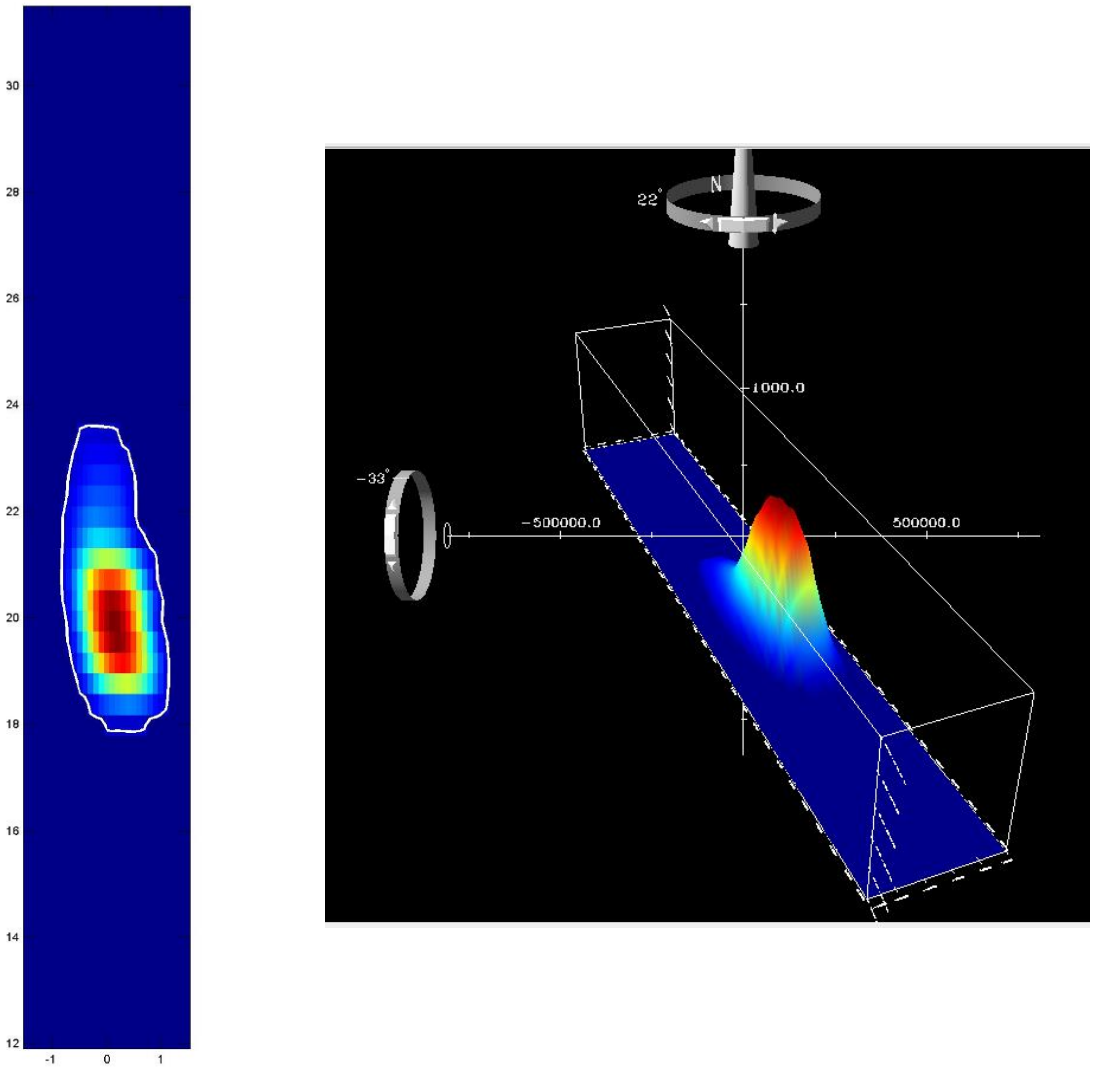

Figure 2. Spectrogram of the synthetic kernel that resulted from the averaging of the 39 20-Hz calls in 2D (left) and 3D (right) and further processing of the kernel base. On the left the white contour outlines the zero level. On the right the 3D axes are spectrogram frequency (y-axis), time (x-axis) and intensity (z-axis).

4.2.2.3. Spectrogram cross-correlation

When a detection was registered, the algorithm limited a time window starting 1 second before and extending 2 seconds after the trigger time. Every 0.1 seconds the algorithm extracted 256 samples (2.56 seconds at 100 Hz sampling rate) centred on the trigger time and computed the fast Fourier transform (FFT). Before doing that, to improve the resolution, the time series was windowed in both ends by a cosine taper, best known as the Hanning window. A slightly modified version was used by leaving the central 10% of the time series untouched. This meant that the Hanning window was applied only to 90% of the signal,

with a 45% taper at each end. At 100 Hz sampling rate, the frequency interval in the frequency domain is 0.39 Hz. Spectral values were saved between 12 and 31 Hz. Inside the investigation window (-1 to 2. seconds in time, and between 12 and 31 Hz in frequency), the spectral power (the square of the FFT amplitude) and the spectral cumulated power along the time and frequency axis were computed.

The spectrogram correlation was then computed, starting 1 second before the median time and ending 1 second after it. The correlation between the spectrogram kernel $k(t_0, f)$ and the spectrogram of the recording $S(t, f)$ was computed by the normalized correlation in time given by

$$\alpha_N(t) = \frac{\sum_{t_0,f} k(t_0,f)\, S(t-t_0,f)}{\sqrt{\sum_{t,f} k(t_0,f)^2 \sum_{t,f} S(t,f)^2}} \qquad \text{Eq. 1}$$

If the spectral window contained white noise (random data), then the normalized cross-correlation resulted in 0. For a perfect signal, 0 seconds outside the call and following the kernel, the normalized cross-correlation should be very close to 1, but not 1. The normalized cross-correlation can be negative for signals that are anti-correlated with the kernel. As in the waveform cross-correlation, a detection using the spectrogram is registered when the correlation value exceeds a defined threshold.

4.2.3. Signal sampling

A manual verification of the detections was needed in order to remove false positives and to assess if and how much acoustic interference was present in the detected calls. Examples of false positives were shown in Chapter 2. From the 401 days in the study period, 336 of them without considering duplicate days, had at least one detection with correlation values between 0.2 and close to 1. Due to time constraints it was not possible to verify all detections made in the entire dataset (2 918 312 detections) and instead a series of rules were established in order to obtain a subsample. A correlation of 0.5 and a SNR of 2.0 (both medium values) were used as thresholds to obtain a list of days with potentially good bouts of calls. Then, only days with a minimum of 250 automatic detections (with correlation values from 0.2 to close to 1) and at least 20 of them with high correlation values (≥ 0.7) were considered. From this list, a random sample of 5 days for each month was obtained (Table

I). There was no repetition of days and bouts were separated either by 24 hours or by a gap of 6 hours.

Table I – Summary of the days of each month with detections in the dataset, days with detections with correlation and SNR thresholds of 0.5 and 2.0 (days with potentially good bouts) and days considered for the random subsample of each month.

Year	Month	Days with detections	Days with potentially good bouts	Days considered in the random sample
2007	September	21	9	4
	October	31	26	16
	November	30	29	29
	December	31	31	31
2008	January	31	31	31
	February	29	24	24
	March	31	28	8
	April	30	25	5
	May	31	20	0
	June	30	27	0
	July	31	27	0
	August	10	4	0
TOTAL	**-**	**336**	**154**	**125**

Automatic detections of 20-Hz calls in the subsample were confirmed as true positives using spectrograms calculated with TRITON (Wiggins, 2010), a software package written in MATLAB (Mathworks, 2012). The bouts where the automatic detections were included were completed with the manual addition of the start times of false negatives of 20-Hz calls (missed detections) and backbeats.

There were rare occasions when days had more than one bout. In those cases, only the strongest was considered for the analysis. This was done to reduce the risk of detecting the same whale multiple times and therefore decrease the contribution of that individual to the overall call characteristics. However, it was not possible to determine if the same animal was detected more than once. The 20-Hz call is a fairly simple signal that does not show a pronounced individual characterization.

The strongest bout was defined as the one with the 20-Hz calls with highest SNR assessed visually. In some occasions, there was more than one whale calling which resulted in overlapping bouts. Because the inter-call interval showed low individual variability, it was often possible to follow a specific bout. Uncertainty was only present when the gap between

calls was larger than the inter-call interval for the calling whales. In those cases, the strongest bout was inspected and completed until it was not possible to identify the 'target' whale.

4.2.4. Spectral and temporal measurements

Based on Hatch and Clark (2004), several spectral features were extracted, and are described below (Fig. 3). The 90% of cumulated power window (between 5% and 95%) was chosen in order to give a more representative value of the frequency bandwidth and to mitigate the influence of noise inside the spectral window to be analysed (Fig. 4):

- Arrival time: The time of the median power;
- Starting frequency: The frequency in 5% of power along the frequency axis;
- Median frequency: The frequency corresponding to the median power, as measured along the frequency axis;
- Call duration: The time interval between 5% and 95% of power (time values were interpolated and rounded to 0.01 second resolution);
- Frequency bandwidth: The frequency interval between 5% and 95% of power along the frequency axis (frequency values were interpolated and rounded to 0.1 Hz resolution).

For measurements of the spectral features only the calls with highest SNR (≥ 3.0), high correlation values (≥ 0.75) and with no overlapping calls from other whales from each bout were used.

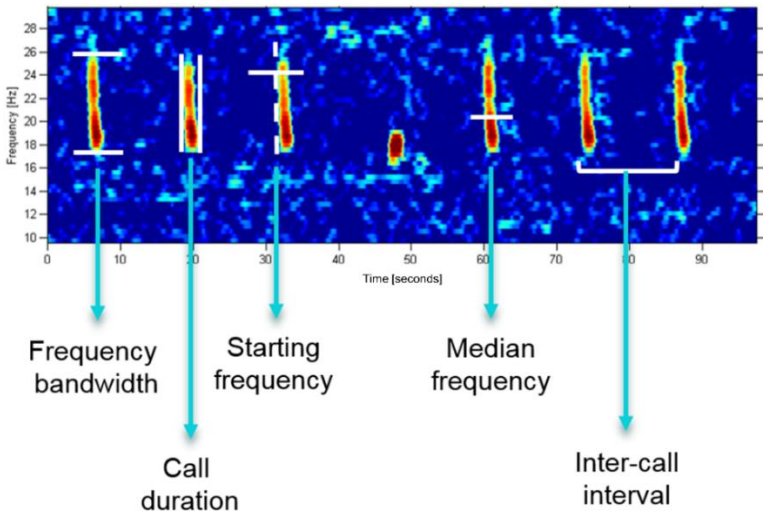

Figure 3. Spectrogram of 100 seconds of a fin whale sequence with 6 20-Hz calls and a backbeat (at ~50 seconds), showing the spectral features computed for 20-Hz calls. Spectrogram parameters: Frame size – 256 samples, 95% overlap, Hanning window, equalized. Adapted from Castellote et al., 2011, Fin whale (Balaenoptera physalus) population identity in the western Mediterranean Sea," Marine Mammal Science 28, 325–344. Copyright by the Society for Marine Mammalogy.

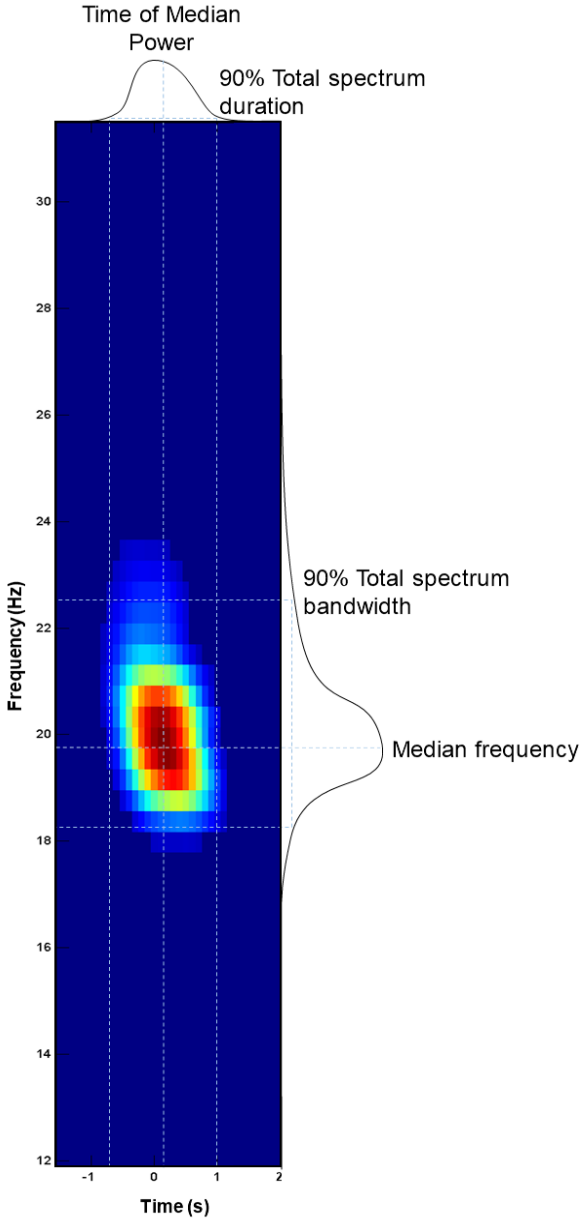

Figure 4. Representation of the measurements of fin whale call features from a spectrogram. Dashed lines represent the power limits used to compute the call features. The inset shows a representation of the distribution of the total spectrum power on the frequency and time axes. Frequency resolution was 0.39 Hz and temporal resolution was 0.1 seconds. Adapted from Hatch and Clark, 2004, Acoustic differentiation between fin whales in both the North Atlantic and North Pacific Oceans, and integration with genetic estimates of divergence, Paper presented to the IWC Scientific Committee, Sorrento, Italy, July, Paper No. SC/56/SD6, pp. 1–37. Copyright by the International Whaling Commission.

The inter-call interval is the most discriminatory call feature in fin whale bioacoustics (Hatch and Clark, 2004; Delarue *et al.*, 2009; Castellote *et al.*, 2011; Oleson *et al.*, 2014). The inter-call interval was calculated as the difference between trigger times obtained in the waveform cross-correlation detection process of each call. The trigger time based on the

waveform was preferred over the arrival time of the spectral measurements because it was more consistent. The arrival time based on the spectral measurements depends on the calculated power that is present in the investigation window. For the characterization of the 20-Hz call, only inter-call interval between 20-Hz calls was considered.

4.2.4.1. Inter-call interval occurrence pattern

According to the literature, it is possible that at least two acoustic groups of fin whales could occur in the study area. Castellote *et al.* (2011) found that these groups were differentiated mainly by the inter-call interval between 20-Hz calls. Because of the restrictions imposed in the subsample for the measurement analysis, the sample size might not allow a good representation of the presence of the different inter-call interval throughout the year. After finding one or more inter-call interval(s) in the subsample used for measurement analysis, an automatic search of the interval(s) through the dataset with all detections (correlation threshold of 0.2 and SNR $\geq$ 2.0) was undertaken. In this case, the main aim was not to obtain a measure of call abundance but instead a temporal pattern of each inter-call interval. Because inter-call interval is fairly consistent within bouts and it was calculated in the time domain, the variability was expected to be low. Therefore, the entire dataset was considered and there was no manual verification of the detections used in this analysis. Single (intervals between 20-Hz calls) or double (intervals when backbeats were between 20-Hz calls and therefore lasted double the time) inter-call intervals were considered. The pattern for inter-call interval(s) was obtained by the counts of sequences of at least 5 consecutive detections, with possible double inter-call interval. This rule allowed to minimize the occurrence of series of false positives that could show the same intervals.

Further validation of the occurrence pattern was taken by also counting the number of occurrences of 10 or more consecutive detections, with also possible double intervals.

4.2.5. Data analysis

This work aimed to find differences in the characteristics of the spectral (median frequency, call duration and frequency bandwidth) and temporal (inter-call interval) measurements made in 4.2.4. for the subsample of bouts obtained in 4.2.3., and therefore identify clusters. Cluster analysis has been used in cetacean bioacoustics to identify and classify different types of sounds (Chabot, 1988; Karlsen *et al.*, 2002; Nemiroff and Whitehead, 2009), assign sounds to social units (Rendell and Whitehead, 2003) and to

assess geographical variation in bout structure (e.g. Delarue *et al.*, 2009). In this study there was no pre-classification made of the 20-Hz calls, i.e., there was no class assignment of area or subpopulation. Therefore, a hierarchical cluster analysis was undertaken in order to identify different clusters using the *stats* package version 3.4.0 in R (R Core Team, 2015).

For cluster analysis, highly correlated variables need to be identified in order to assess a possible variable reduction. The linear correlation between spectral call features was evaluated by calculating the correlation coefficient *r* (Upton and Cook, 2014) using all high quality calls from each bout. This ensured a large enough sample size to assess relationships between variables. The coefficient *r* can take any value from -1 to 1, inclusive. If $r>0$, variables show a positive linear relation and if $r<0$ variables display a negative linear relation. When *r* is close to 0, it would indicate a weak linear relationship between the variables. If two variables were highly correlated ($r \geq 0.75$), the variable that was present in the least amount of references about acoustic characterization was removed from the cluster analysis (as suggested by Dawson and Trapp, 2004). The removal of the inter-call interval was not considered because it is the most discriminatory variable, based on the bibliographic review. Therefore, ICI was not used in this test.

Each bout was characterized by the median of the spectral and temporal features mentioned above in 4.2.4. Bouts were considered points in a coordinate space where the observed similarities of the points corresponded to metric distances between them. In some cases, when the variables have large differences in their units, rescaling of the data is performed to give equal importance to all variables. This is usually done by subtracting the mean of a particular variable from all measurements, and dividing by the standard deviation. In this study, the data were not scaled in order to preserve the higher influence of inter-call interval in the clustering process. The distance matrix of the bouts was calculated using the Euclidean distance. The distance *E* between two points x and y with N dimensions, in which points represent bouts and dimensions the number of variables, is given by:

$$\mathrm{E}(x, y) = \sqrt{\sum_{i=1}^{n} (x_i - y_i)^2} \qquad \text{Eq. 2}$$

The average linkage method was chosen as the amalgamation rule, in which the distance *L* between two clusters *r* and *s* is defined as the average distance between each point in one cluster to every point in the other cluster. The Euclidean distances *L* between all points were given by the distance matrix *D*

$$\mathrm{L}(r,s) = \frac{1}{n_r n_s} \sum_{i=1}^{n_r} \sum_{j=1}^{n_s} D\left(x_{ri}, x_{sj}\right) \qquad \text{Eq. 3}$$

To make an assessment of the clustering procedure the silhouette width (SW) was computed, which reflects the strength of the clusters (Rousseeuw, 1986) (Eq. 4). It uses the average distance from point *x* to all other points in *x*'s cluster (given by a_x) and b_x, which is the minimum average distance from point *x* to all points in another cluster:

$$SW_x = \frac{(b_x - a_x)}{max(a_x, b_x)} \qquad \text{, -1 < SWi < 1} \qquad \text{Eq. 4}$$

Kaufman and Rousseeuw (1990) give some guidance as to the desirable size of the silhouette width. A SW above 0.5 is considered a reasonable classification and a SW below 0.2 reflects a lack of substantial cluster structure. The optimal number of clusters was evaluated by calculating the average silhouette width (ASW) (Rousseeuw, 1986) using the R package *factoextra* version 1.0.4. (Kassambara and Mundt, 2017). Given the silhouette width of each cluster SW_r and the number of clusters *n*, the ASW is given by:

$$ASW = \frac{(\sum_r SW_r)}{n} \qquad \text{, 0 < ASW < 1} \qquad \text{Eq. 5}$$

It assesses the optimal ratio where the intra-cluster distance is minimized and the inter-cluster distance is maximized.

The visual results obtained by this traditional approach were compared with the results from the R package *pvclust* version 2.0.0 (Suzuki and Shimodaira, 2015). This package was developed to assess statistical significance in the hierarchical setting (Suzuki and Shimodaira, 2015) by calculating two types of probability values (p-values) for each cluster: an approximately unbiased (au) p-value, based on a multi-step bootstrap resampling procedure (Shimodaira, 2004), and a bootstrap probability (bp) p-value, calculated from ordinary bootstrap resampling (Efron *et al.*, 1996). The p-values are given in percent and represent the proportion of occurrence of a given cluster when a number of bootstrap replications (in this case 10 000) are performed. The following null hypothesis was tested at each node of the dendrogram (Suzuki and Shimodaira, 2015):

H_0: the cluster does not exist

H_1: the cluster exists

Based on a significance level of α = 0.10, a p-value > 90% suggested the rejection of the null hypothesis. The same distance matrix and the amalgamation rule were used for 10,000 bootstrap replications of the hierarchical clustering.

Non-parametric statistical tests, such as Kruskal-Wallis and post-hoc Wilcoxon-Mann-Whitney Rank Sum test with a Bonferroni correction (α = 0.05), were used to assess statistical differences of relevant spectral and temporal features between bouts. Kruskal-Wallis test was used to perform a comparison among all bouts. Wilcoxon-Mann-Whitney Rank Sum tests were used to compare two bouts at a time, if the Kruskal-Wallis test revealed statistical differences among bouts. The sample of each bout consisted of all calls suitable for reliable spectral and temporal measurements. The null hypothesis tested for the Kruskal-Wallis test was the following (Upton and Cook, 2014):

H_0: All of the *k* population distribution functions are identical

H_1: At least one of the k populations yields a different distribution function

Where *k* represents the number of bouts tested. The Wilcoxon-Mann-Whitney Rank Sum test compared pairs of bouts, following the null hypothesis:

H_0: The distributions of the two groups are identical

H_1: The distributions of the two groups are not identical

4.3. RESULTS

A total of 888 hours of sound recordings (37 days) was visually analysed which resulted in a total of 30 009 20-Hz calls identified and confirmed (Table II). This included automatic detections that were positively confirmed in the spectrogram and calls that were added to complete each bout. Calls that were manually added to the bouts were in the start and/or end of each bout and were missed by the detector because they showed low correlation value generally caused by low SNR. Backbeats were recorded in all bouts. Trigger times of a total of 7 216 backbeats were also stored for future analysis.

Although there were detections in almost every day of the recording period, days with potentially good bouts showed a seasonal occurrence. The 37 bouts considered in this study were produced between September 2007 and April 2008, which matches with the period of highest vocal activity mentioned in Chapter 1. Between May and August 2008 there was no day with potentially good high quality calls and automatic detections were reduced considerably. Five bouts (B6, B8, B16, B23 and B34) were omitted from all analysis. Although they showed a minimum of 250 automatic detections, they did not have enough high quality calls for them to be included in the measurement analysis (less than 20 calls with correlation ≥ 0.75 and SNR ≥ 3.0).

After applying all selection criteria and removing the five bouts, a total of 4 170 20-Hz calls were of high enough quality (SNR ≥ 3.0 and correlation values ≥ 0.75) to be considered for acoustic characterization. The median of the spectral and temporal features of the 20-Hz call (Table II – right) was used to characterize each bout in the hierarchical cluster analysis. Observing the standard deviation of the spectral features of each bout, the standard deviation was smaller or around the resolution in time (0.1 seconds) or frequency (0.39 Hz).

Table II – Summary of bouts showing median values and standard deviation of the spectral and temporal features of the 20-Hz fin whale call. Shaded bouts were not used in the analysis. represents bouts produced across days. 20-Hz calls with 20-20 and < 20 sec represents the interval between two 20-Hz calls less than 20 seconds.*

										Call features used in the hierarchical cluster analysis				
Bout ID	**Month**	**Day**	**OBS**	**Start**	**Finish**	**20-Hz calls**	**Backbeats**	**20-Hz calls with 20-20 and < 20 sec**	**20-Hz calls used for measurement**	**Call duration (s)**	**Starting frequency (Hz)**	**Median frequency (Hz)**	**Frequency bandwidth (Hz)**	**Inter-call interval (20-20) (s)**
B1	September	17/09/2007	3	06:44:33	12:39:37	548	396	215	146	1.47 (0.07)	19.10 (0.11)	20.20 (0.14)	3.10 (0.51)	14.83 (0.28)
B2		21/09/2007	3	06:41:03	21:11:20	1 099	672	449	166	1.42 (0.05)	19.30 (0.13)	20.70 (0.14)	3.40 (0.83)	14.32 (0.50)
B3		22/09/2007*	3	17:36:46	02:41:20	658	424	260	74	1.41 (0.03)	19.10 (0.10)	20.30 (0.16)	3.10 (0.26)	14.44 (0.73)
B4		29/09/2007	3	06:29:52	11:50:00	371	248	147	27	1.41 (0.02)	19.20 (0.12)	20.50 (0.09)	3.20 (0.23)	14.80 (0.73)
B5	October	13/10/2007	12	10:14:00	21:51:25	1 450	371	890	76	1.44 (0.06)	18.70 (0.23)	19.90 (0.27)	3.70 (0.51)	13.08 (0.91)
B6		18/10/2007	1	07:10:36	23:59:49	771	27	582	2	-	-	-	-	12.76 (1.20)
B7		21/10/2007	5	01:44:41	8:55:40	488	158	328	121	1.42 (0.09)	18.80 (0.20)	20.60 (0.23)	4.60 (0.96)	13.23 (0.42)
B8		26/10/2007*	3	22:48:18	01:08:23	381	150	298	18	-	-	-	-	13.57 (1.24)
B9		30/10/2007	5	10:20:15	17:22:21	1 018	146	621	74	1.49 (0.10)	19.10 (0.22)	21.00 (0.26)	4.80 (0.90)	12.49 (0.52)
B10	November	09/11/2007	1	14:01:40	20:22:06	846	59	696	101	1.64 (0.12)	19.20 (0.10)	20.60 (0.22)	5.00 (0.25)	12.94 (0.86)
B11		18/11/2007	13	15:48:04	23:04:51	1 235	56	1002	49	1.42 (0.03)	19.10 (0.09)	21.10 (0.18)	5.80 (0.42)	13.41 (0.68)
B12		20/11/2007	4	20:28:59	23:56:37	694	48	595	102	1.45 (0.21)	19.10 (0.66)	20.80 (0.26)	5.10 (1.46)	12.69 (0.40)
B13		27/11/2007	6	05:13:36	22:39:44	1 291	453	1011	446	1.58 (0.13)	19.20 (0.21)	20.80 (0.23)	4.90 (1.26)	13.00 (0.36)
B14		29/11/2007*	19	16:09:43	18:56:18	1 639	174	1090	24	1.53 (0.06)	19.20 (0.14)	20.70 (0.31)	4.45 (0.23)	13.21 (0.57)
B15	December	05/12/2007	19	03:21:09	14:39:45	1 027	832	549	263	1.63 (0.20)	19.20 (0.19)	20.70 (0.22)	4.30 (0.42)	13.22 (0.39)
B16		09/12/2007	24	14:59:56	17:12:20	215	130	136	5	-	-	-	-	14.82 (1.13)
B17		18/12/2007*	5	16:53:36	05:21:58	2 155	69	1660	417	1.49 (0.13)	18.90 (0.25)	20.70 (0.24)	4.90 (0.87)	12.94 (0.78)
B18		21/12/2007	4	00:00:13	09:40:56	929	227	697	146	1.52 (0.17)	18.40 (0.36)	20.15 (0.37)	4.70 (0.59)	13.15 (1.01)
B19		25/12/2007*	16	19:09:24	00:34:35	743	77	461	188	1.51 (0.16)	18.80 (0.12)	20.30 (0.29)	6.00 (0.77)	13.30 (0.57)
B20	January	04/01/2008	4	03:24:58	22:02:30	737	79	548	331	1.52 (0.18)	18.80 (0.19)	20.50 (0.21)	4.90 (0.42)	13.08 (0.53)
B21		07/01/2008*	16	20:54:59	01:01:20	296	150	348	106	1.50 (0.17)	18.80 (0.09)	20.20 (0.21)	4.70 (0.87)	13.32 (0.60)
B22		09/01/2008	12	00:05:45	04:28:06	454	205	298	104	1.59 (0.10)	18.50 (0.10)	19.80 (0.10)	4.00 (0.27)	12.97 (0.25)
B23		23/01/2008*	9	17:19:44	02:07:47	949	154	583	12	-	-	-	-	13.33 (0.94)
B24		31/01/2008	9	02:50:05	09:18:11	947	233	701	37	1.52 (0.22)	18.30 (0.28)	19.80 (0.19)	4.60 (0.45)	13.22 (0.90)
B25	February	11/02/2008	13	01:21:34	09:44:46	970	153	639	93	1.52 (0.09)	18.90 (0.10)	21.30 (0.17)	6.40 (0.58)	13.38 (0.35)
B26		16/02/2008	5	00:10:11	04:35:16	337	49	283	30	1.41 (0.07)	18.70 (0.13)	20.60 (0.13)	5.05 (0.43)	13.42 (0.54)
B27		22/02/2008*	1	23:56:52	06:19:20	880	249	624	52	1.71 (0.10)	19.00 (0.18)	20.00 (0.10)	3.75 (0.38)	13.51 (0.81)
B28		26/02/2008	12	03:00:18	13:05:37	1 335	166	895	53	1.40 (0.05)	18.60 (0.08)	20.10 (0.16)	4.80 (0.30)	13.14 (0.74)

Table II – Summary of bouts showing median values and standard deviation of the spectral and temporal features of the 20-Hz fin whale call (continuation). Shaded bouts were not used in the analysis. represents bouts produced across days. 20-Hz calls with 20-20 and < 20 sec represents the interval between two 20-Hz calls less than 20 seconds.*

Bout ID	Month	Day	OBS	Start	Finish	20-Hz calls	Backbeats	20-Hz calls with 20-20 and < 20 sec	20-Hz calls used for measurement	Call duration (s)	Starting frequency (Hz)	Median frequency (Hz)	Frequency bandwidth (Hz)	Inter-call interval (20-20) (s)
B29	March	01/03/2008	19	05:33:07	10:24:41	546	147	463	131	1.51 (0.09)	19.10 (0.12)	20.90 (0.19)	4.80 (0.26)	13.54 (0.63)
B30		03/03/2008	20	04:28:52	18:02:38	819	280	585	95	1.44 (0.05)	18.80 (0.09)	20.40 (0.14)	5.20 (0.30)	13.47 (0.71)
B31		07/03/2008	12	17:36:22	19:09:16	262	72	173	77	1.51 (0.07)	18.50 (0.10)	19.70 (0.10)	4.10 (0.28)	13.27 (0.16)
B32		10/03/2008	20	16:44:10	19:42:06	443	86	289	173	1.41 (0.03)	18.90 (0.09)	20.60 (0.12)	5.40 (0.20)	13.26 (0.24)
B33		12/03/2008	20	00:40:28	05:17:49	458	157	404	131	1.38 (0.04)	18.70 (0.11)	20.30 (0.16)	4.80 (0.37)	13.39 (0.36)
B34	April	09/04/2008	5	16:18:51	21:37:26	764	9	471	8	-	-	-	-	13.57 (0.39)
B35		15/04/2008	17	02:46:21	07:33:22	804	156	769	262	1.43 (0.08)	18.90 (0.22)	20.80 (0.21)	4.60 (0.35)	13.57 (0.17)
B36		20/04/2008	20	12:16:17	18:50:53	1146	62	915	35	1.40 (0.03)	19.10 (0.18)	21.00 (0.38)	5.20 (0.23)	13.12 (0.43)
B37		21/04/2008	12	20:37:41	22:34:56	304	95	328	40	1.47 (0.07)	18.80 (0.10)	20.10 (0.08)	3.95 (0.31)	13.47 (0.33)
TOTAL		-	-	-	-	**30,009**	**7 216**	**21 034**	**4 215**	-	-	-	-	-

Table III – Summary statistics of the spectral and temporal features of the 20-Hz call with all bouts pooled together. All bouts except B6, B8, B16, B23 and B34 were used (n = 4 170). STD refers to standard deviation.

Call features	Call duration (s)	Starting frequency (Hz)	Median frequency (Hz)	Frequency bandwidth (Hz)	Inter-call interval (s)
Minimum	1.38	18.3	19.7	3.1	12.49
Maximum	1.71	19.3	21.3	6.4	14.83
Delta	0.33	1.0	1.6	3.3	2.3
Average	1.49	18.9	20.5	4.6	13.4
Median	1.48	18.9	20.6	4.8	13.3
STD	0.08	0.26	0.40	0.78	0.52

Pairwise correlation tests with all high quality calls of each bout did not reveal significant correlation between spectral call features, as all correlation coefficients were below 0.75 (Table IV). Therefore, all spectral call features were maintained in the hierarchical cluster analysis.

Table IV – Pairwise correlation tests using all good calls from the fin whale bouts.

	Call duration (s)	Median frequency (Hz)	Starting frequency (Hz)	Frequency bandwidth (Hz)
Call duration (seconds)	1.00	0.01	-0.04	0.23
Median frequency (Hz)		1.00	0.52	0.30
Starting frequency (Hz)			1.00	-0.22
Frequency bandwidth (Hz)				1.00

Figure 5 shows the resulting dendrogram from the traditional hierarchical cluster analysis. The height of the dendrogram represents the distance between clusters in which larger distances are more conservative. The larger height of the dendrogram, 2.26, divided the bouts into two main clusters. The average silhouette width of 0.54 corroborated these two main clusters (Fig. 6). At smaller heights of the dendrogram, bouts could also be grouped into 3 (height of 1.65) or 4 (height of 1.31) clusters. However, the average silhouette width of 0.42 for a structure with 3 or 4 clusters was smaller than the one with 2 clusters. Therefore, the division of the bouts into two clusters was preferred.

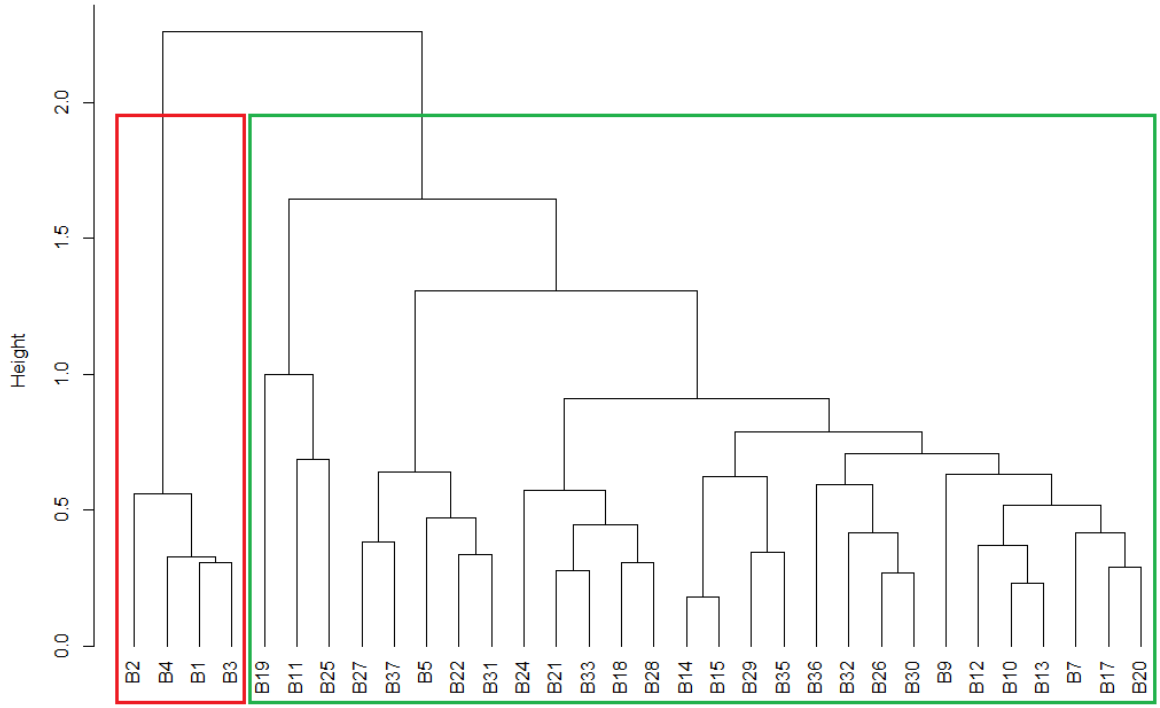

Figure 5. Dendrogram of fin whale bouts calculated using Euclidean distance and average linkage method. Red and green lines represent the two clusters validated by the average silhouette width.

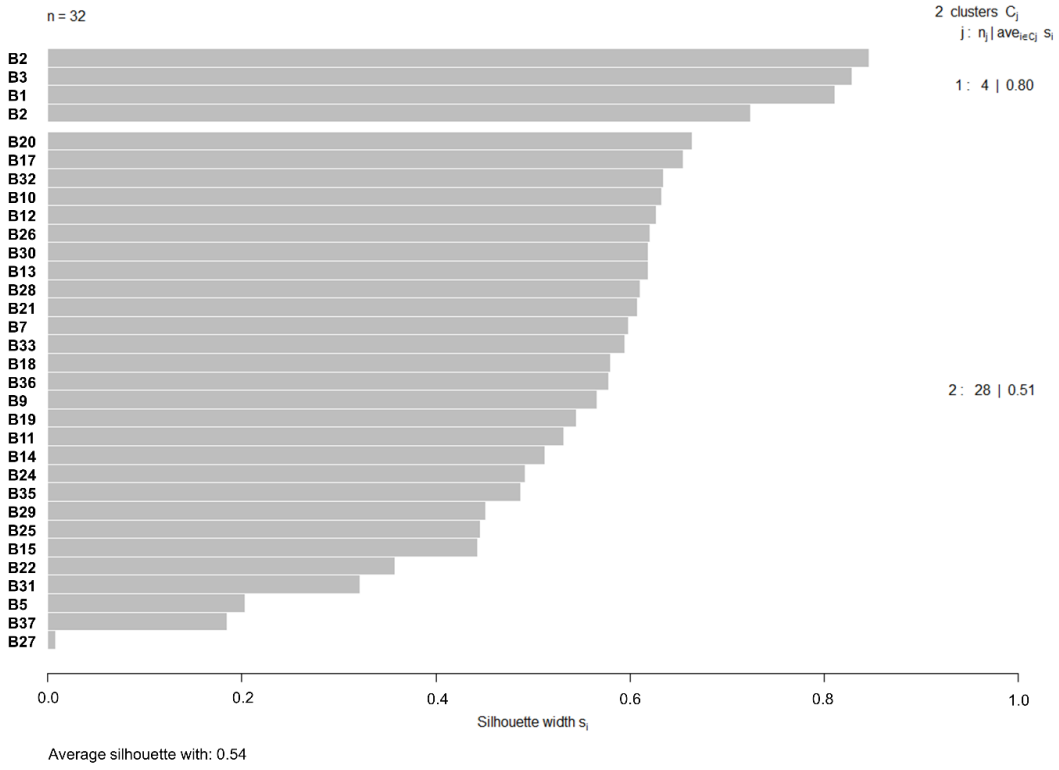

Figure 6. Silhouette plot for a 2-cluster solution for the fin whale bouts dataset. Values on the left represent the bout number. On the right side the values correspond to the identity of the cluster (1 and 2), the number of bouts and the silhouette width of each cluster.

The dendrogram that resulted from bootstrap sampling showed the same two main clusters (Fig. 7). The p-values (p>90%) for node 18 (Fig. 7, first left) indicated the existence of the same cluster of 4 bouts. The approximately unbiased (au) p-value showed that these 4 bouts were clustered in 100% of the occasions. The second cluster indicated by the node 30 showed lower p-values. The unbiased bootstrapping allocated the bouts in this second cluster 83% of the cases.

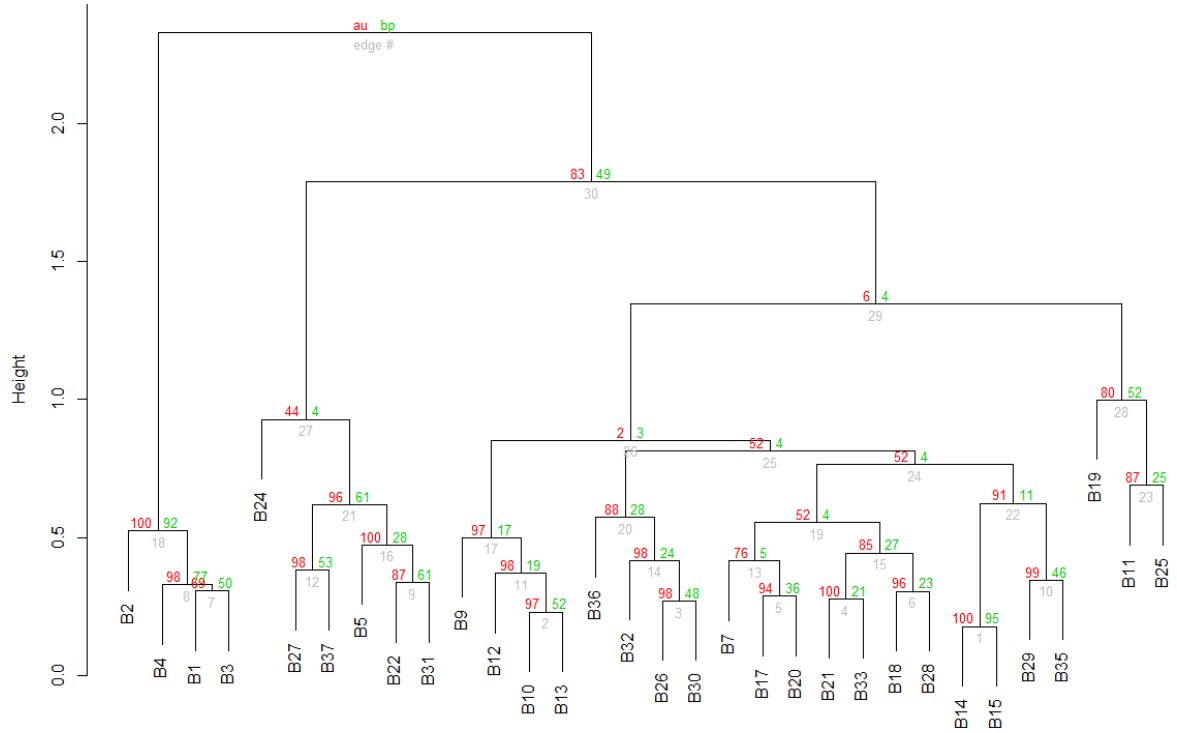

Figure 7. Dendrogram of fin whale bouts calculated using euclidean distance and average linkage method for 10 000 bootstrap replications. Red values represent the approximately unbiased (au) p-value and green numbers represent the bootstrap probability (bp) p-value. The gray numbers represent the node number.

Clustering analysis does not allow the researcher to determine which are the significant spectral/temporal measurements that might be contributing to the clustering, therefore further analysis was required An exploratory data analysis of the spectral and temporal features showed that inter-call interval (Fig. 8a) and frequency bandwidth (Fig. 8b) could be discriminatory features between bouts. Box-plots of the remaining spectral features are found in Appendix I. Kruskal-Wallis non-parametric tests showed statistical differences in relation to the inter-call intervals ($H = 1725.5$, $df = 31$, p-value $<< 0.05$) and frequency bandwidths ($H = 2407.4$, $df = 31$, p-value $<< 0.05$) between bouts. Regarding the inter-call intervals, the Wilcoxon-Mann-Whitney tests revealed that bouts 1-4 were statistically different from the rest of the bouts (p-values < 0.05, see annex II for all results). Bout B1 also showed

statistical differences between B2, but it was statistically similar to B3 and B4. Bouts B2, B3 and B4 did not show any statistical differences among them. Concerning the statistical comparison in relation to the frequency bandwidth between bouts, B1, B3 and B4 showed statistical differences between all the remaining bouts, even B2. Bout B2 was only statistically similar to B5.

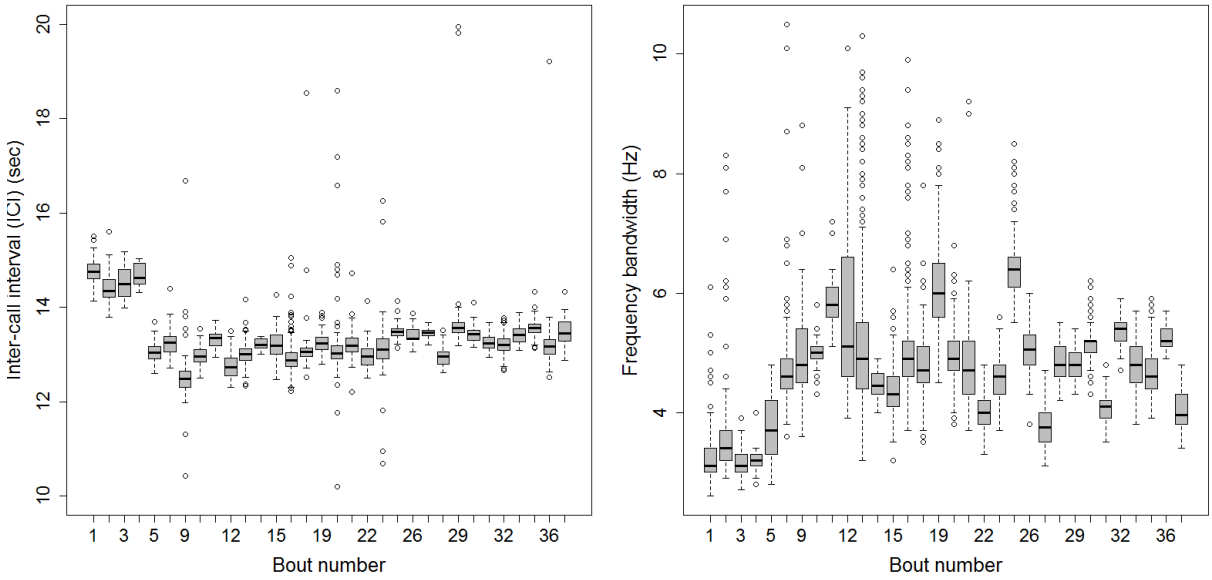

Figure 8. Box-plots of the inter-call interval (left) and frequency bandwidth (right) between bouts. Bouts 6, 8, 16, 23 and 34 were not included.

Figure 9 shows a sample of the “higher quality” bouts from each cluster. Bouts from cluster 1 were recorded only in September 2007 while bouts from cluster 2 were recorded during October 2007 – April 2008. Although this may seem to suggest seasonality in some of the characteristics of the bouts (inter-call interval and frequency bandwidth) it is important to note that there was one day where the two patterns were observed simultaneously (Fig. 10).

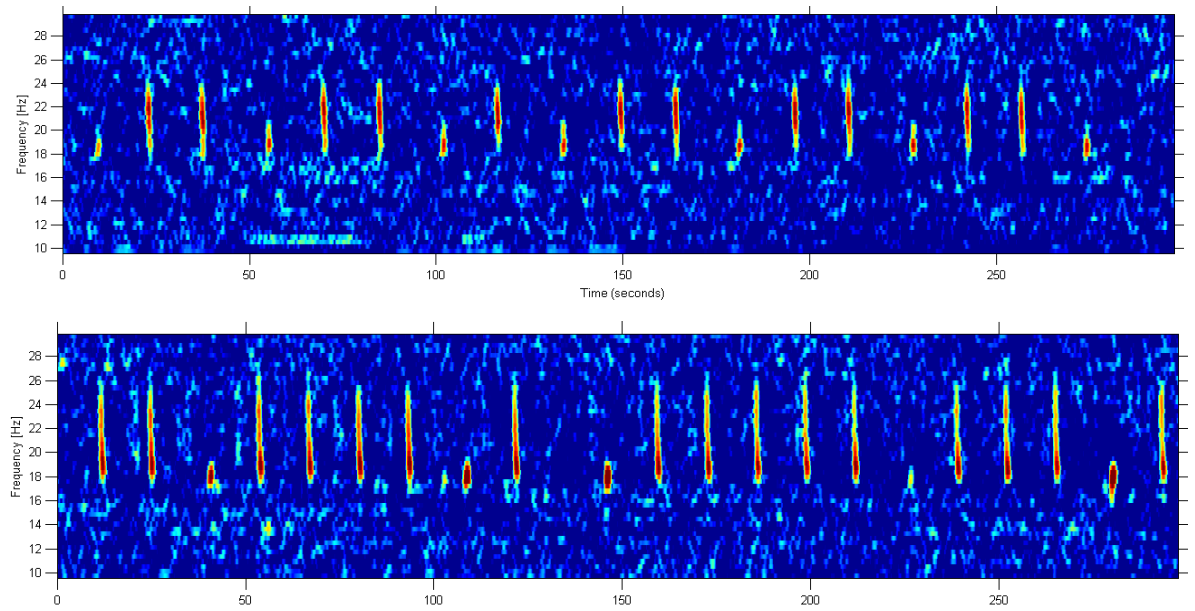

Figure 9. Spectrograms showing 5 minutes of the best fin whale bouts of each cluster identified in the hierarchical analysis. Top: cluster 1 (longer ICI, smaller FBW), recorded on 17/09/2007 at 08:37:20; Bottom: cluster 2 (shorter ICI, larger FBW), recorded on 21/12/2007 at 04:13:00. Spectrogram parameters: Frame size – 256 samples, 95% overlap, Hanning window, equalized.

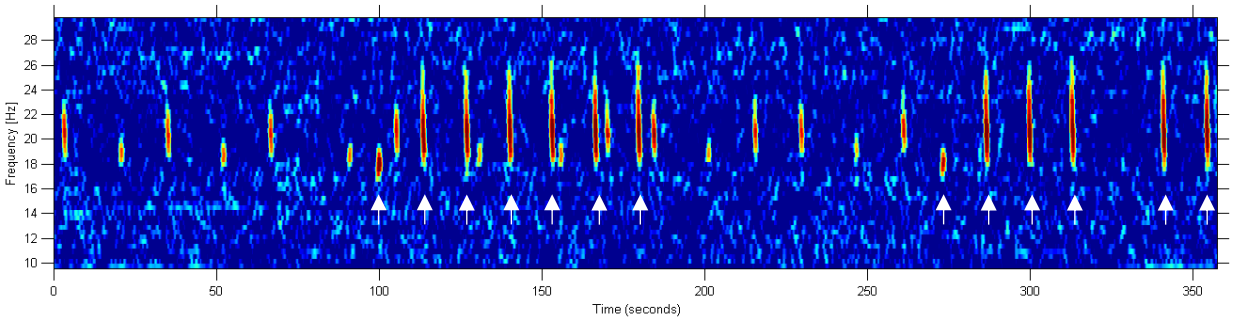

Figure 10. Spectrogram showing several minutes when two whales with distinct call features attributed to each cluster were calling at the same time. White arrows indicate the whale associated with cluster 2. The whales were recorded on 21/10/2007 around 01:00:00. Frame size – 256 samples, 95% overlap, Hanning window, equalized.

The hierarchical cluster analysis divided the bouts into two clusters of inter-call interval. Bouts with intervals around 14 seconds were grouped in cluster 1 and bouts with intervals about 13 seconds were grouped in cluster 2. A search in the whole dataset for the two types of inter-call interval was performed: intervals associated with cluster 1 (between 14 and 15 seconds) and intervals related with cluster 2 (between 12.5 and 13.5 seconds). The intervals had to occur in at least 5 consecutive detections in order to count one record of the presence of that interval. Because backbeats were produced in the middle of 20-Hz calls, an interval with double the time was also accepted (30 seconds for group 1 and 27 seconds for group 2). The count of the occurrence of series of at least 10 inter-call intervals was also

performed, in order to have a more conservative occurrence pattern. This conservative approach was helpful because detections featuring in this analysis were not manually verified. Therefore, this second and more refined search may have eliminated false detections that may have been included in the 5-detection rule. The search results revealed different occurrence patterns for each inter-call interval (Fig. 11 and 12). Series of 20-Hz calls with longer inter-call intervals showed a more stable occurrence after its peak while calls with shorter inter-call intervals showed a more pronounced seasonal pattern. The longer inter-call intervals occurred mostly in September 2007 (Fig. 11). The shorter inter-call intervals occurred mostly between November 2007 and January 2008 (Fig. 12).

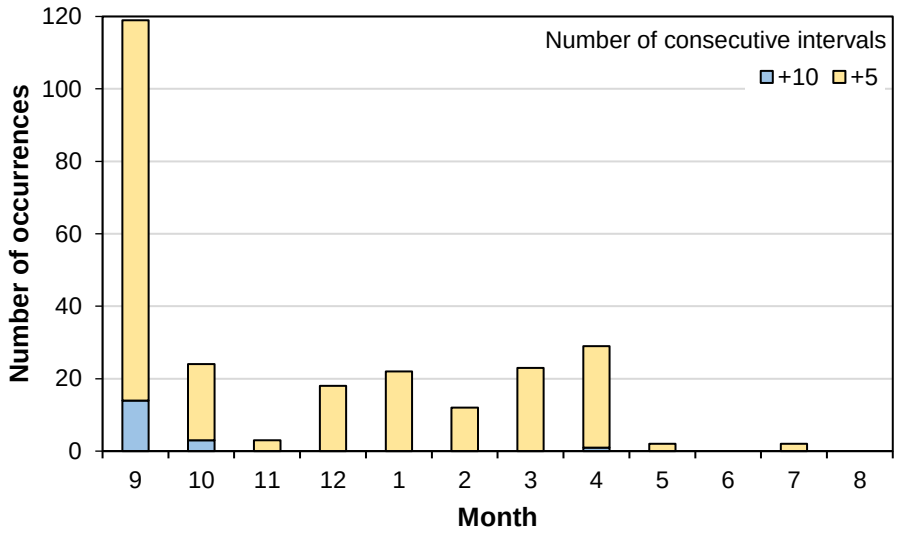

Figure 11. Distribution of the occurrence of series of 5 or more detections with intervals between 14 and 15 seconds, observed in cluster 1.

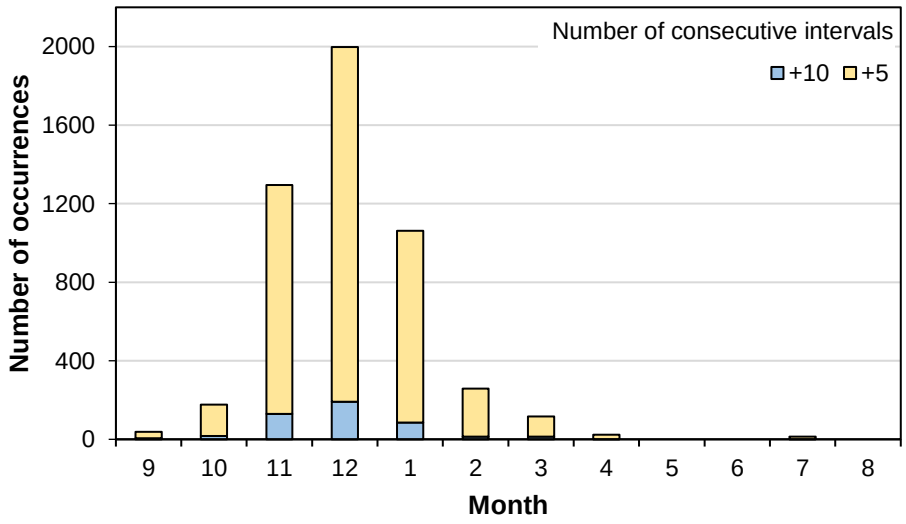

Figure 12 – Distribution of the occurrence of series of 5 or more detections with intervals between 12.5 and 13.5 seconds, associated with cluster 2.

4.5. DISCUSSION

Two clusters with different sets of acoustic characteristics of fin whales were identified in a subsample of the OBS recordings and they were distinguished by their inter-call interval and frequency bandwidth: a cluster showed a longer inter-call interval and shorter frequency bandwidth (cluster 1) and the other presented a shorter inter-call interval and a longer frequency bandwidth (cluster 2). Cluster 1 consisted of bouts manually verified in recordings of September 2007 and cluster 2 had bouts produced between October 2007 and February 2008 that were manually verified.

4.5.1. Occurrence of spectral and temporal call characteristics

The bouts grouped in cluster 1 were recorded during a 12 day period and could have been produced by a single animal that stayed close to OBS03 during that time. A bout with characteristics attributed to cluster 1 was also recorded and manually verified in 21st October 2007 while at the same time a bout from cluster 2 was being produced by another whale in the same area. Only the cluster 2 bout was formally analysed because of the established set of rules. An automatic search through the dataset of all automatic detections of the two types of intervals was undertaken without any post visual confirmation. The results revealed that two intervals were not temporally separated and the longer interval occurred also after September 2007. After the peak in September 2007, the longer interval occurred mostly between October 2007 and April 2008.

The call characteristic with the highest level of variance was the frequency bandwidth, with some bouts showing a standard deviation higher than 1 Hz (B12, B13). Ocean-acoustic interference, such as the Lloyd's Mirror effect, has been shown to cause accentuated changes in the frequency bandwidth and the median frequency of strong 20-Hz calls within a bout (Pereira *et al.*, 2016). The SNR and correlation threshold used in the sampling process prevented the selection of a high number of interference-altered calls. There was no variation of the frequency bandwidth across bouts from cluster 1 that was related to the Lloyd's Mirror effect. However, the variance in the two bouts from cluster 2 (B12, B13) could be related with the Lloyd's Mirror Effect, as some of the calls showed changes in their time/frequency characteristics.

4.5.2. Comparisons with other studies

The study of this Chapter found two similar clusters to the ones identified by Castellote *et al.* (2011). Both studies show the use of frequency bandwidth and inter-call interval to identify two different sets of acoustic characteristics in fin whales. In this chapter, cluster 1 was characterized by an interval around 14 seconds and a frequency bandwidth around 3 Hz. These values were close to those Castellote *et al.* (2011) assigned to "Mediterranean" fin whales; an interval close to 15 seconds and a frequency bandwidth of 5 Hz. Cluster 2 showed a longer inter-call interval and a larger frequency bandwidth than cluster 1; the interval was around 13 seconds the frequency bandwidth was close to 5 Hz. Castellote *et al.* (2011) recorded in the North Atlantic Ocean an inter-call interval of 12-13 seconds and a frequency bandwidth of 6 Hz. Although the frequency bandwidth of cluster 2 was smaller than the bandwidth recorded for the North Atlantic Ocean in Castellote *et al.* (2011), the inter-call interval was very close.

The differences between the study in this chapter and *Castellote et al.* (2011) do needed to be considered further. In addition to the variability of the data, the different values found for the North Atlantic Ocean could also be related to unreported details in the computation process, such as differences in the window size used to measure the features. However, the same trends were found in both studies: one cluster showed a longer inter-call interval and a smaller frequency bandwidth while the other showed a shorter inter-call interval and a larger frequency bandwidth. Some studies indicate intra-annual (Oleson *et al.*, 2014) and inter-annual (Morano *et al.*, 2012) differences in the inter-call interval. This could complicate its use as the main discriminatory feature of acoustic groups and its comparison between areas. Some of the data used in Castellote *et al.* (2011) were recorded in the same time period as this study. The recordings used in Castellote *et al.* (2011) in the Azores and Alboran basin were obtained between August 2007 and May 2008. This study used data recorded between September 2007 and August 2008. Therefore, although there were possible differences in the measurements of the 20-Hz call, inter-annual variability was potentially the same and the results could be comparable.

4.5.3. Implications of the existence of two dialects

The two clusters of acoustic characteristics further confirmed the existence of dialects that reflect acoustic differences between fin whales from the Mediterranean Sea and the North Atlantic Ocean, which is in line with the results found by Castellote *et al.* (2011). The

results of this study suggested that some individuals of the Mediterranean subdivision crossed the Strait of Gibraltar and entered the North Atlantic Ocean. Because only male fin whales are believed to produce bouts of calls (Croll *et al.*, 2002), this movement could only be attributed to males.

Cluster 1 was recorded in several months of the study, mostly between September 2007 and April 2008. However, the manual verification of the spectral and temporal characteristics was only done for detections obtained in September by OBS03, one of the most northern instruments and one of the most distant from the Strait of Gibraltar (Chapter 2, Fig. 1). One of the horizontal components of OBS03 was not working and therefore it was not possible to obtain estimates of locations or track direction. Considering the timing of the acoustic presence, it was possible that individuals of cluster 1 were potentially travelling towards a breeding area, possibly close to the African coast. Some authors suggest that areas close to the African coast might serve as potential breeding areas for Mediterranean fin whales (Notarbartolo di Sciara *et al.*, 2003).

The border used for management purposes of fin whales from the North Atlantic Ocean and the Mediterranean Sea is the Strait of Gibraltar (e.g. IWC, 2007; Panigada and Notarbartolo di Sciara, 2012). In Castellote *et al.* (2011), the dialect of the Mediterranean fin whales did not go that far and it was only recorded in the interior waters of this sea (Castellote *et al.*, 2011). This study confirmed the overlap between the two dialects observed in Castellote *et al.* (2011) and showed that the range of the Mediterranean dialect extends up to the southwest of Portugal. Future management actions should account for the growing evidence of overlap between fin whales from the North Atlantic Ocean and the Mediterranean Sea.

4.5.3. Final considerations and future work

In this Chapter, there were missed calls either because of the performance of the detector or because they were filtered by the set of rules established to obtain a high quality sample of calls for each bout. It was assumed that detectability of calls with the two different acoustic characteristics was the same (they were produced with the similar source levels), but there was no verification of this. Different detection probabilities could impact the results of the seasonality analysis but not the identification of the two acoustic groups.

The automatic detection was performed using a master template obtained from a 20-Hz call of the North Atlantic dialect. In addition, the kernel used in the spectrogram cross-

correlation was also obtained from the average of 20-Hz calls from the North Atlantic dialect. It could be possible that these templates were not the most suitable for the detection of 20-Hz calls of the Mediterranean dialect. The decision to subsample the detections based on SNR and correlation threshold was done assuming that the call characteristics did not vary as a function of these criteria. If the detection of 20-Hz calls from the Mediterranean dialect resulted in mostly low correlation thresholds, then most of them would have not been considered for the subsample. A dedicated automatic search for 20-Hz calls of the Mediterranean dialect could be be undertaken with appropriate time and frequency templates. For some months, the number of days considered for the subsample (days with a minimum number of calls with high correlation threshold and SNR) was reduced considerably from the list of days that could be used. From the visual inspection of the spectrograms of the recordings, there was evidence that the structure of the bouts was different between the two dialects. The dialect of the North Atlantic fin whales showed longer sequences of 20-Hz calls between backbeats. Further analysis could include a new set of rules that would increase the subsample and other variables related to bout structure, such as number of backbeats and diversity index.

The two dialects of fin whales recorded during this study showed spatial and temporal overlap. However, because the dialect from the Mediterranean fin whales is associated with resident animals and has not been previously reported in the literature as occurring outside the Mediterranean, it is important to understand if the results obtained from this acoustic dataset are consistent over the years. Although there is evidence of interchange between fin whales from the Mediterranean Sea and the North Atlantic Ocean, the extent of this is still debatable. The possibility of the recordings of cluster 1 being from one or few animals from the Mediterranean Sea should not be discarded.

OBS or other acoustic instruments could be deployed in two areas: 1) the same study area off southwest Portugal and 2) near the exit of the Mediterranean Sea, in the Alboran Sea. Acoustic data would be recorded in the same year and between the months of September and March, when the vocal activity is the highest. This task would provide further confirmation about the overlap and range of the two dialects. During the time of recording, satellite tags could also be attached to a number of fin whales in order to better understand the movements of the calling whales. Location estimates of the calling whales recorded in the acoustic instruments could be obtained from different types of location techniques, depending on the spacing of the instruments. A matching between the acoustic data and satellite telemetry could give insights about the migration routes Mediterranean and North Atlantic fin whales use and the area where breeding activities could occur. Biopsies of the tagged whales

would provide data to assess acoustic divergence with genetic differentiation between the Mediterranean and North Atlantic fin whales.

4.6. REFERENCES

Barbujani, G. (**1991**). "What do languages tell us about human microevolution? Trends in Ecology and Evolution," **6**, 151–156.

Castellote, M., Clark, C. W., and Lammers, M. O. (**2011**). "Fin whale (*Balaenoptera physalus*) population identity in the western Mediterranean Sea," Marine Mammal Science **28**, 325–344.

Chabot, D. (**1988**) "A quantitative technique to compare and classify humpback whale (*Megaptera novaeangliae*) sounds," Ethology **77**, 89–102.

Clark, C. W., and Gagnon G. J. (**2002**). "Low-frequency vocal behaviors of baleen whales in the North Atlantic: Insights from integrated undersea surveillance system detections, locations, and tracking from 1992 to 1996," U.S. Navy Journal of Underwater Acoustics **52**, 609–640.

Croll, D., Clark, C. W., Acevedo, A., Tershy, B., Flores, S., Gedamke, J., and Urban, J. (**2002**). "Only male fin whales sing loud songs," Nature (London) **117**, 809.

Dawson, B., and Trapp, R. G. (**2004**). *Basic and Clinical Biostatistics* (Lange Medical Books/McGraw-Hill, New York, USA).

Delarue, J., Todd, S. K., VanParijs, S. M., and DiIorio, L. (**2009**). "Geographic variation in Northwest Atlantic fin whale (*Balaenoptera physalus*) song: Implications for stock structure assessment," Journal of the Acoustical Society of America **125**, 1774–1782.

Efron, B., Halloran, E., and Holmes, S. (**1996**). "Bootstrap confidence levels for phylogenetic Trees," Proceedings of the National Academy of Sciences of the United States of America **93**, 13429–13434.

Ford, J. K. B. (**1991**). "Vocal traditions among resident killer whales (*Orcinus orca*) in coastal waters of British Columbia," Canadian Journal of Zoology **69**,1454–1483.

Grimes, L. G. (**1974**). "Dialects and geographical variation in the song of the splendid sunbird *Nectarinia coccinigaster*," Ibis **116**, 314–329.

Hatch, L. T., and Clark, C. W. (**2004**). “Acoustic differentiation between fin whales in both the North Atlantic and North Pacific Oceans, and integration with genetic estimates of divergence,” Paper presented to the IWC Scientific Committee, Sorrento, Italy, July, Paper No. SC/56/SD6, pp. 1–37.

International Whaling Commission, IWC. (**2007**). “Report of the Joint NAMMCO/IWC Scientific Workshop on the Catch History, Stock Structure and Abundance of North Atlantic Fin Whales, 23-26 March 2006, Reykjavík, Iceland,” Journal of Cetacean Research Management **9**, 451–68.

Karlsen, J., Bisther, A., Lydersen, C., Haug, T., and Kovacs, K. (**2002**). "Summer vocalisations of adult male white whales (*Delphinapterus leucas*) in Svalbard, Norway," Polar Biology **25**, 808–817.

Kassambara, A., and Mundt, F. (**2017**). factoextra R package http://www.sthda.com/english/rpkgs/factoextra/index.html (Last viewed 23rd January 2018).

Kaufman, L., and Rousseeuw, P. J. (**1990**) *Finding Groups in Data: An Introduction to Cluster Analysis* (Wiley-Interscience, New Jersey, USA).

Lougheed, S. C., Handford, P., Baker, A. J. (**1993**). “Mitochondrial DNA hyper diversity and vocal dialects in a subspecies transition of the rufous-collared sparrow,” Condor **95**, 889–895.

MacDougall-Shackleton, E., and MacDougall-Shackleton, S. A. (**2001**). “Cultural and genetic evolution in mountain white-crowned sparrows: song dialects are associated with population structure,” Evolution **55**, 2568–75.

Maeda, T., and Masataka, N. (**1987**). "Locale-specific Vocal Behaviour of the Tamarin (Saguinus I. labiatus)," Ethology **75**, 25–30.

Mathworks (**2012**). The Mathworks, Inc., Cambridge, U.K. http://www.mathworks.co.uk (Last viewed 31st January, 2018).

McDonald, M. A., Mesnick, S. L., and Hildebrand, J. A. (**2006**). “Biogeographic characterization of blue whale song worldwide: Using song to identify populations,” Journal of Cetacean Research and Management **8**, 55–65.

Mellinger, D.K., and Clark, C. W. (**2000**). “Recognizing transient low-frequency whale sounds by spectrogram correlation,” Journal of the Acoustical Society of America **107**, 3518–3529.

Mitani, J. C., Hasegawa, T., Gros-Louis, J., Marler, P., and Byrne, R. (**1992**). "Dialects in Wild Chimpanzees?," American Journal of Primatology **27**, 233–243.

Morano, J. L., Salisbury, D. P., Rice, A. N., Conklin, K. L., Falk, K. L., and Clark C. (**2012**). “Seasonal and geographical patterns of fin whale song in the western North Atlantic Ocean,” Journal of the Acoustical Society of America **132**, 1207–1212.

Mundinger, P. C. (**1982**). “Microgeographic and macrogeographic variation in the acquired vocalizations of birds,” in Acoustic Communication in Birds, edited by D.E. Kroodsma and E.H. Miller (Academic Press, New York, USA), pp. 147–208.

Nemiroff, L., and Whitehead, H. (**2009**). "Structural characteristics of pulsed calls of Long-finned Pilot Whales Globicephala melas," Bioacoustics **19**, 67–92.

Notarbartolo di Sciara, G., Zanardelli, M., Jahoda, M., Panigada, S. and Airoldi, S. (**2003**). “The fin whale *Balaenoptera physalus* (L. 1758) in the Mediterranean Sea,” Mammal Review **33**, 105–150.

Nottebohm, F. (**1969**). “The song of the chingolo, *Zonotrichia capensis*, in Argentina: Description and evaluation of a system of dialects,” Condor **71**, 299–315.

Oleson, E. M., Širović, A., Bayless, A. R., and Hildebrand, J. A. (**2014**). “Synchronous Seasonal Change in Fin Whale Song in the North Pacific,” PLoS ONE **9**, e115678.

Panigada, S. and Notarbartolo di Sciara, G. (**2012**). *Balaenoptera physalus*. in: IUCN 2017. IUCN Red List of Threatened Species. Version 2017.3, http://www.iucnredlist.org (Downloaded 31th January, 2018).

Payne, R. S., and Guinee, L. N. (**1983**). “Humpback whale (*Megaptera Novaeangliae*) songs as an indicator of ‘stocks’,” in Communication and Behavior of Whales, edited by R. S. Payne (Westview, Boulder, USA), pp. 333–358.

Pereira, A., Harris, D., Tyack, P. and Matias, L. (**2016**). "Lloyd's mirror effect in fin whale calls and its use to infer the depth of vocalizing animals," Proceedings of Meetings on Acoustics **27**, 070002.

R Core Team (**2015**). R: A language and environment for statistical computing, R Foundation for Statistical Computing, Vienna, Austria. http://www.R-project.org/ (Last viewed 31st January 2018).

Rendell, L., and Whitehead, H. (**2003**). "Vocal clans in sperm whales (*Physeter macrocephalus*)," Proceedings of the Royal Society B: Biological Sciences **270**,225–231.

Rousseeuw, P. J. (**1986**) "Silhouettes: a graphical aid to the interpretation and validation of cluster analysis," Journal of Computational and Applied Mathematics **20**, 53–65.

Shimodaira, H. (**2004**). "Approximately unbiased tests of regions using multistep-multiscale bootstrap resampling," The Annals of Statistics **32**, 2616–2641.

Soha, J. A., Nelson, D. A. and Parker, P. G. (**2004**). "Genetic analysis of song dialect populations in Puget sound white-crowned sparrows," Behavioral Ecology **15**, 636–46.

Suzuki, R., and Shimodaira, H. (**2015**). pvclust: Hierarchical Clustering with P-Values Via Multiscale Bootstrap Resampling. R package version 2.0-0 http://CRAN.R-project.org/package=pvclust (Last viewed 31st January 2018).

Thompson, P. O., Findley, L. T., and Vidal, O. (**1992**). "20-Hz pulses and other vocalizations of fin whales, *Balaenoptera physalus*, in the Gulf of Mexico," Journal of the Acoustical Society of America **92**, 3051–3057.

Upton, G., and Cook, I. (**2014**). *A Dictionary of Statistics* (Oxford University Press, Oxford, UK).

Wang, D., Wursig, B, and Evans, W. (**1995**). "Comparisons of whistles among seven odontocete species," in Sensory Systems of Aquatic Mammals, edited by R.A. Kastelein, J.A. Thomas, and A. Supin (De Spil Publishers, Woerden, The Netherlands), pp. 299–323.

Weilgart, L., and Whitehead, H. (**1997**). “Group-specific dialects and geographical variation in coda repertoire in South Pacific sperm whales,” Behavioral Ecology and Sociobiology **40**, 277–285.

Wiggins, S. M., Roch, M. A., and Hildebrand, J. A. (**2010**). “TRITON software package: Analyzing large passive acoustic monitoring data sets using MATLAB,” *Journal of the Acoustical Society of America* **128**, 2299.

ANNEX I – Boxplots of the spectral characteristics of the 20-Hz fin whale call

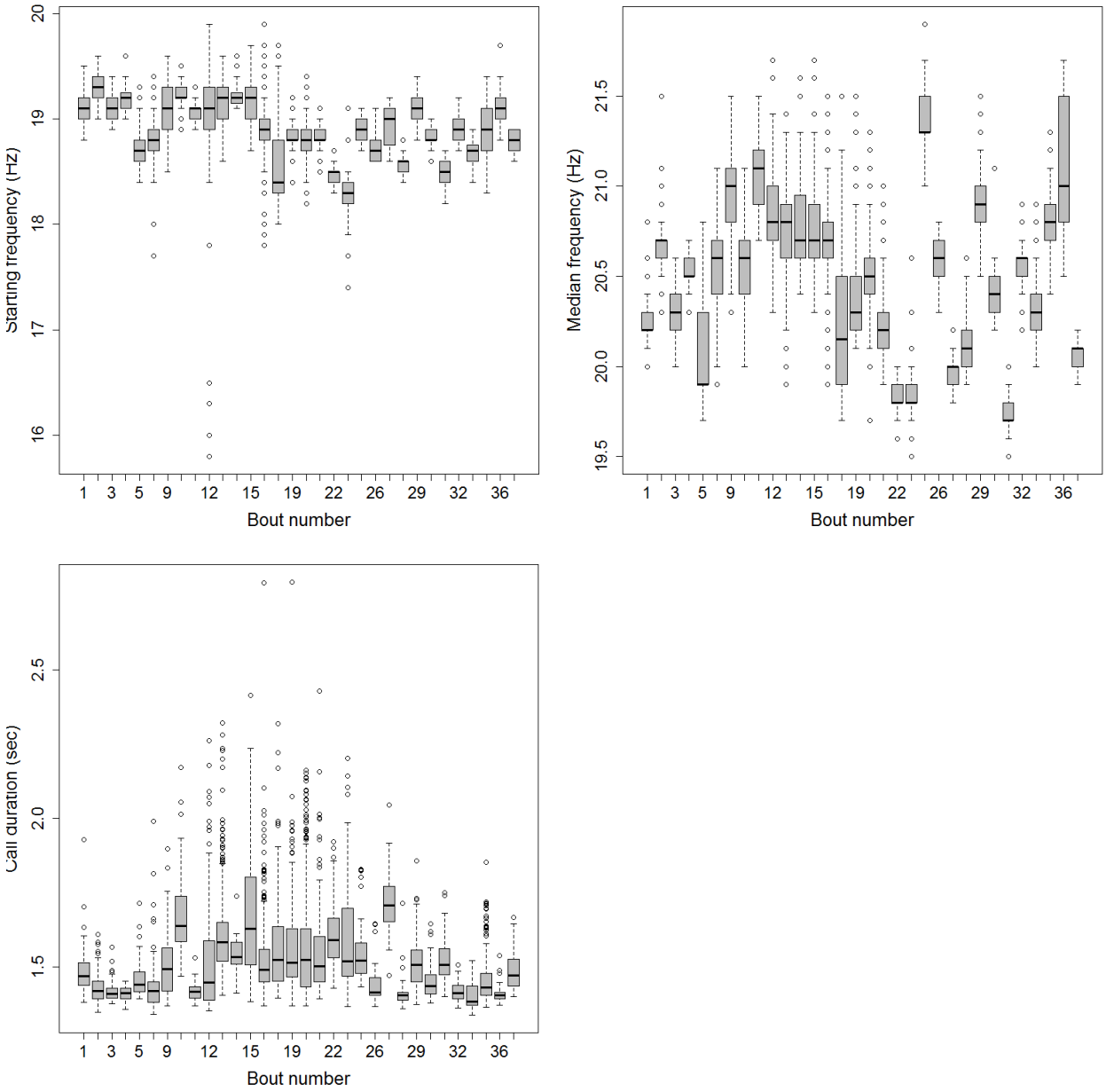

Figure 1 – Box-plots of the spectral features of each bout: a) Starting frequency; b) Median frequency; c) Call duration.

ANNEX II – Wilcoxon-Mann-Whitney Rank Sum test

Table I – Results of the Wilcoxon-Mann-Whitney Rank Sum test in regards to frequency bandwidth. Bouts were compared two at a time.

	B1	B2	B3	B4	B5	B7	B9	B10	B11	B12	B13	B14	B15	B17	B18	B19	B20	B21	B22	B24	B25	B26	B27	B28	B29	B30	B31	B32	B33	B35	B36
B2	**0.00**																														
B3	1.00	**0.00**																													
B4	1.00	**0.04**	1.00																												
B5	**0.00**	0.39	**0.00**	**0.00**																											
B7	**0.00**	**0.00**	**0.00**	**0.00**	**0.00**																										
B9	**0.00**	**0.00**	**0.00**	**0.00**	**0.00**	1.00																									
B10	**0.00**	**0.00**	**0.00**	**0.00**	**0.00**	**0.00**	1.00																								
B11	**0.00**	**0.00**	**0.00**	**0.00**	**0.00**	**0.00**	**0.00**	**0.00**																							
B12	**0.00**	**0.00**	**0.00**	**0.00**	**0.00**	**0.00**	1.00	1.00	0.42																						
B13	**0.00**	**0.00**	**0.00**	**0.00**	**0.00**	1.00	1.00	1.00	**0.00**	0.72																					
B14	**0.00**	**0.00**	**0.00**	**0.00**	**0.00**	1.00	0.45	**0.00**	**0.00**	**0.01**	1.00																				
B15	**0.00**	**0.00**	**0.00**	**0.00**	**0.00**	**0.00**	**0.00**	**0.00**	**0.00**	**0.00**	**0.00**	1.00																			
B17	**0.00**	**0.00**	**0.00**	**0.00**	**0.00**	**0.01**	1.00	1.00	**0.00**	0.35	1.00	**0.00**	**0.00**																		
B18	**0.00**	**0.00**	**0.00**	**0.00**	**0.00**	1.00	1.00	**0.01**	**0.00**	**0.01**	1.00	0.94	**0.00**	1.00																	
B19	**0.00**	**0.00**	**0.00**	**0.00**	**0.00**	**0.00**	**0.00**	**0.00**	1.00	**0.00**	**0.00**	**0.00**	**0.00**	**0.00**	**0.00**																
B20	**0.00**	**0.00**	**0.00**	**0.00**	**0.00**	**0.00**	1.00	1.00	**0.00**	1.00	1.00	**0.00**	**0.00**	1.00	**0.04**	**0.00**															
B21	**0.00**	**0.00**	**0.00**	**0.00**	**0.00**	1.00	1.00	0.42	**0.00**	0.09	1.00	1.00	**0.00**	1.00	1.00	**0.00**	1.00														
B22	**0.00**	**0.00**	**0.00**	**0.00**	**0.04**	**0.00**	**0.00**	**0.00**	**0.00**	**0.00**	**0.00**	**0.00**	**0.00**	**0.00**	**0.00**	**0.00**	**0.00**	**0.00**													
B24	**0.00**	**0.00**	**0.00**	**0.00**	**0.00**	1.00	1.00	**0.00**	**0.00**	**0.01**	1.00	1.00	1.00	0.14	1.00	**0.00**	**0.00**	1.00	**0.00**												
B25	**0.00**	**0.00**	**0.00**	**0.00**	**0.00**	**0.00**	**0.00**	**0.00**	**0.00**	**0.00**	**0.00**	**0.00**	**0.00**	**0.00**	**0.00**	**0.01**	**0.00**	**0.00**	**0.00**	**0.00**											
B26	**0.00**	**0.00**	**0.00**	**0.00**	**0.00**	**0.02**	1.00	1.00	**0.00**	1.00	1.00	**0.00**	**0.00**	1.00	0.54	**0.00**	1.00	1.00	**0.00**	**0.02**	**0.00**										
B27	**0.00**	**0.00**	**0.00**	**0.00**	1.00	**0.00**	**0.00**	**0.00**	**0.00**	**0.00**	**0.00**	**0.00**	**0.00**	**0.00**	**0.00**	**0.00**	**0.00**	**0.00**	**0.02**	**0.00**	**0.00**	**0.00**									
B28	**0.00**	**0.00**	**0.00**	**0.00**	**0.00**	1.00	1.00	1.00	**0.00**	1.00	1.00	**0.00**	**0.00**	1.00	1.00	**0.00**	1.00	1.00	**0.00**	0.81	**0.00**	1.00	**0.00**								
B29	**0.00**	**0.00**	**0.00**	**0.00**	**0.00**	0.93	1.00	**0.00**	**0.00**	**0.03**	1.00	**0.00**	**0.00**	1.00	1.00	**0.00**	**0.02**	1.00	**0.00**	0.98	**0.00**	**0.03**	**0.00**	1.00							
B30	**0.00**	**0.00**	**0.00**	**0.00**	**0.00**	**0.00**	0.24	**0.01**	**0.00**	1.00	0.13	**0.00**	**0.00**	**0.00**	**0.00**	**0.00**	**0.00**	**0.00**	**0.00**	**0.00**	**0.00**	1.00	**0.00**	**0.00**	**0.00**						
B31	**0.00**	**0.00**	**0.00**	**0.00**	**0.01**	**0.00**	**0.00**	**0.00**	**0.00**	**0.00**	**0.00**	**0.00**	**0.00**	**0.00**	**0.00**	**0.00**	**0.00**	**0.00**	1.00	**0.00**	**0.00**	**0.00**	**0.00**	**0.00**	**0.00**	**0.00**					
B32	**0.00**	**0.00**	**0.00**	**0.00**	**0.00**	**0.00**	**0.00**	**0.00**	**0.00**	1.00	**0.00**	**0.00**	**0.00**	**0.00**	**0.00**	**0.00**	**0.00**	**0.00**	**0.00**	**0.00**	**0.00**	0.06	**0.00**	**0.00**	**0.00**	**0.00**	**0.00**				
B33	**0.00**	**0.00**	**0.00**	**0.00**	**0.00**	0.92	1.00	0.23	**0.00**	0.16	1.00	**0.01**	**0.00**	1.00	1.00	**0.00**	1.00	1.00	**0.00**	0.61	**0.00**	1.00	**0.00**	1.00	1.00	**0.00**	**0.00**	**0.00**			
B35	**0.00**	**0.00**	**0.00**	**0.00**	**0.00**	1.00	0.29	**0.00**	**0.00**	**0.00**	**0.00**	1.00	**0.00**	**0.00**	1.00	**0.00**	**0.00**	1.00	**0.00**	1.00	**0.00**	**0.00**	**0.00**	**0.02**	**0.00**	**0.00**	**0.00**	**0.00**	**0.00**		
B36	**0.00**	**0.00**	**0.00**	**0.00**	**0.00**	**0.00**	0.18	**0.00**	**0.00**	1.00	0.77	**0.00**	**0.00**	**0.00**	**0.00**	**0.00**	**0.00**	**0.02**	**0.00**	**0.00**	**0.00**	1.00	**0.00**	**0.00**	**0.00**	1.00	**0.00**	1.00	**0.00**	**0.00**	
B37	**0.00**	**0.00**	**0.00**	**0.00**	1.00	**0.00**	**0.00**	**0.00**	**0.00**	**0.00**	**0.00**	**0.00**	**0.00**	**0.00**	**0.00**	**0.00**	**0.00**	**0.00**	1.00	**0.00**	**0.00**	**0.00**	1.00	**0.00**	**0.00**	**0.00**	1.00	**0.00**	**0.00**	**0.00**	**0.00**

Table II – Results of the Wilcoxon-Mann-Whitney Rank Sum test in regards to inter-call interval. Bouts were compared two at a time.

	B1	B2	B3	B4	B5	B7	B9	B10	B11	B12	B13	B14	B15	B17	B18	B19	B20	B21	B22	B24	B25	B26	B27	B28	B29	B30	B31	B32	B33	B35	B36
B2	**0.00**																														
B3	0.10	1.00																													
B4	1.00	0.80	1.00																												
B5	**0.00**	**0.00**	**0.00**	**0.00**																											
B7	**0.00**	**0.00**	**0.00**	**0.00**	0.10																										
B9	**0.00**	**0.00**	**0.00**	**0.00**	**0.00**	**0.00**																									
B10	**0.00**	**0.00**	**0.00**	**0.00**	1.00	**0.00**	**0.00**																								
B11	**0.00**	**0.00**	**0.00**	**0.00**	**0.00**	1.00	**0.00**	**0.00**																							
B12	**0.00**	**0.00**	**0.00**	**0.00**	**0.00**	**0.00**	**0.00**	**0.00**	**0.00**																						
B13	**0.00**	**0.00**	**0.00**	**0.00**	1.00	**0.00**	**0.00**	1.00	**0.00**	**0.00**																					
B14	**0.00**	**0.00**	**0.00**	**0.00**	1.00	1.00	**0.00**	**0.00**	1.00	**0.00**	**0.00**																				
B15	**0.00**	**0.00**	**0.00**	**0.00**	1.00	1.00	**0.00**	**0.00**	1.00	**0.00**	**0.00**	1.00																			
B17	**0.00**	**0.00**	**0.00**	**0.00**	0.10	**0.00**	**0.00**	0.50	**0.00**	**0.00**	**0.00**	**0.00**	**0.00**																		
B18	**0.00**	**0.00**	**0.00**	**0.00**	1.00	**0.00**	**0.00**	1.00	**0.00**	**0.00**	1.00	**0.00**	0.20	**0.00**																	
B19	**0.00**	**0.00**	**0.00**	**0.00**	**0.00**	1.00	**0.00**	**0.00**	1.00	**0.00**	**0.00**	1.00	1.00	**0.00**	**0.00**																
B20	**0.00**	**0.00**	**0.00**	**0.00**	1.00	**0.00**	**0.00**	1.00	**0.00**	**0.00**	1.00	0.10	**0.00**	**0.00**	1.00	**0.00**															
B21	**0.00**	**0.00**	**0.00**	**0.00**	0.40	1.00	**0.00**	**0.00**	1.00	**0.00**	**0.00**	1.00	1.00	**0.00**	**0.00**	1.00	**0.00**														
B22	**0.00**	**0.00**	**0.00**	**0.00**	1.00	**0.00**	**0.00**	1.00	**0.00**	**0.00**	1.00	**0.00**	**0.00**	1.00	1.00	**0.00**	1.00	**0.00**													
B24	**0.00**	**0.00**	**0.00**	**0.00**	1.00	1.00	**0.00**	1.00	1.00	**0.00**	1.00	1.00	1.00	0.10	1.00	1.00	1.00	1.00	1.00												
B25	**0.00**	**0.00**	**0.00**	**0.00**	**0.00**	**0.00**	**0.00**	**0.00**	**0.00**	**0.00**	**0.00**	**0.00**	**0.00**	**0.00**	**0.00**	**0.00**	**0.00**	**0.00**	**0.00**	**0.00**											
B26	**0.00**	**0.00**	**0.00**	**0.00**	**0.00**	1.00	**0.00**	**0.00**	1.00	**0.00**	**0.00**	1.00	1.00	**0.00**	**0.00**	1.00	**0.00**	1.00	**0.00**	1.00	1.00										
B27	**0.00**	**0.00**	**0.00**	**0.00**	**0.00**	**0.00**	**0.00**	**0.00**	1.00	**0.00**	**0.00**	**0.00**	0.10	**0.00**	**0.00**	**0.00**	**0.00**	**0.00**	**0.00**	**0.00**	1.00	1.00									
B28	**0.00**	**0.00**	**0.00**	**0.00**	1.00	**0.00**	**0.00**	1.00	**0.00**	**0.00**	1.00	**0.00**	**0.00**	1.00	0.90	**0.00**	1.00	**0.00**	1.00	1.00	**0.00**	**0.00**	**0.00**								
B29	**0.00**	**0.00**	**0.00**	**0.00**	**0.00**	**0.00**	**0.00**	**0.00**	**0.00**	**0.00**	**0.00**	**0.00**	**0.00**	**0.00**	**0.00**	**0.00**	**0.00**	**0.00**	**0.00**	**0.00**	0.20	1.00	0.10	**0.00**							
B30	**0.00**	**0.00**	**0.00**	**0.00**	**0.00**	**0.00**	**0.00**	**0.00**	1.00	**0.00**	**0.00**	**0.00**	**0.00**	**0.00**	**0.00**	**0.00**	**0.00**	**0.00**	**0.00**	**0.00**	1.00	1.00	1.00	**0.00**	**0.00**						
B31	**0.00**	**0.00**	**0.00**	**0.00**	**0.00**	1.00	**0.00**	**0.00**	1.00	**0.00**	**0.00**	1.00	1.00	**0.00**	**0.00**	1.00	**0.00**	1.00	**0.00**	1.00	**0.00**	1.00	**0.00**	**0.00**	**0.00**	**0.00**					
B32	**0.00**	**0.00**	**0.00**	**0.00**	**0.00**	1.00	**0.00**	**0.00**	0.10	**0.00**	**0.00**	1.00	1.00	**0.00**	**0.00**	1.00	**0.00**	1.00	**0.00**	1.00	**0.00**	0.30	**0.00**	**0.00**	**0.00**	**0.00**	1.00				
B33	**0.00**	**0.00**	**0.00**	**0.00**	**0.00**	**0.00**	**0.00**	**0.00**	1.00	**0.00**	**0.00**	**0.00**	**0.00**	**0.00**	**0.00**	**0.00**	**0.00**	**0.00**	**0.00**	**0.00**	1.00	1.00	1.00	**0.00**	**0.00**	1.00	**0.00**	**0.00**			
B35	**0.00**	**0.00**	**0.00**	**0.00**	**0.00**	**0.00**	**0.00**	**0.00**	**0.00**	**0.00**	**0.00**	**0.00**	**0.00**	**0.00**	**0.00**	**0.00**	**0.00**	**0.00**	**0.00**	**0.00**	0.10	1.00	0.20	**0.00**	1.00	**0.00**	**0.00**	**0.00**	**0.00**		
B36	**0.00**	**0.00**	**0.00**	**0.00**	1.00	1.00	**0.00**	0.20	1.00	**0.00**	0.10	1.00	1.00	**0.00**	1.00	1.00	1.00	1.00	0.30	1.00	**0.00**	1.00	**0.00**	0.10	**0.00**	**0.00**	1.00	1.00	**0.00**	**0.00**	
B37	**0.00**	**0.00**	**0.00**	**0.00**	**0.00**	0.30	**0.00**	**0.00**	1.00	**0.00**	**0.00**	1.00	0.90	**0.00**	**0.00**	0.10	**0.00**	0.40	**0.00**	0.60	1.00	1.00	1.00	**0.00**	1.00	1.00	0.70	**0.00**	1.00	1.00	1.00

Chapter 5

DENSITY ESTIMATES OF FIN WHALE OFF SOUTHWEST PORTUGAL USING PASSIVE ACOUSTIC CUE COUNTING

5.1. INTRODUCTION

The effective conservation and management of wildlife, either by the assessment of the importance of an area or the status of a stock, involve the acquisition of some measure of the number of animals. By obtaining this measure over a period of time it is possible to assess trends in the stock, i.e., if the stock is stable or if there should be concern in some geographical areas. When the stock is small, a complete census can be possible but, in general, it is not possible to count the absolute number of animals of a stock. A simple approach to estimate animal abundance is to survey plots randomly placed within a study area and count all the animals in the selected plots (Buckland *et al.*, 2001). The density estimate, $\widehat{D}$, number of animals per unit area, is given by the number of animals counted divided by the total area surveyed (sum of the surveyed plots). The animal abundance estimate in the study area, $\widehat{N}$, can be obtained by multiplying this estimated density by the area of the larger study region (Buckland *et al.,* 2001).

The count of animals usually involves observing the number of animals or some kind of 'trapping' method (either physically or by using animal markings to re-identify individuals). In some cases, animal cues (for example the blow of a whale at the surface, animal droppings and several types of acoustic signals produced by animals, such as song units, echolocation clicks, and several other types of calls) might be easier to detect instead of the animals themselves. As long as the cue rate, average number of cues produced per individual animal over a defined period of time, is known, cue abundance and/or density can be transformed into animal abundance/density. In the ocean, visual surveys are affected by different factors such as number of daylight hours, sea state, conspicuity of the animals and observer experience. Alternatively, acoustic signals of cetaceans are being used to understand their distribution and also to give abundance estimates (e.g. Marques *et al.,* 2009, 2011). Passive acoustic monitoring (PAM), which consists of obtaining acoustic data by an instrument that passively records and does not produce any sounds itself, has been the main approach to obtain acoustic data for cetacean studies (Mellinger *et al.,* 2007). PAM is not restricted to

daylight, is less weather dependent and it works even when animals spend large portions of time underwater (while they are vocalizing) (Marques *et al.,* 2013).

One of the most common methods to estimate animal abundance is distance sampling (Buckland *et al.,* 2001). A general description will be given next, but more information about specific details of surveys and methods can be found in Buckland *et al. (*2001). Marques *et al. (*2013) provides an overview of using passive acoustic monitoring and various methods, including distance sampling, to obtain animal abundance.

One form of distance sampling is line transect sampling, where line transects are placed randomly throughout the study area and are traversed by an observation platform, which can be a ship, an aircraft or an autonomous vehicle, such as an ocean glider. In the case of point transect sampling, another form of distance sampling, the observer, human or recording instrument, stay at a fixed point for a period of time. In both surveying situations, all animals or cues are recorded along with their perpendicular distance, for lines, or radial distance, for points, from the transect. When recording instruments are being used, it may be possible to estimate distances afterwards with location methods (Mellinger *et al.,* 2007). The probability of detecting an animal or a cue decreases with distance, as close animals/cues are likely to be detected with certainty and further away animals/cues will be harder to detect. Because only a proportion of animals/cues are detected, a probability of detection needs to be estimated, which is used to correct the number of detected animals/cues for those animals/cues that are missed during the survey. In distance sampling, the distribution of distances acquired during a survey is used to estimate an average probability of detection that is then used to estimate animal density. In the case of acoustic cue sampling, two other parameters are needed to estimate animal abundance: false positive proportion, c, and cue rate, r. When detections of the cues are made with 100% certainty that the sound is from the species of interest, then the false positive proportion will be zero i.e., $c = 0$. However, most passive acoustic monitoring relies on automated methods to detect animal sounds. The false positive proportion is obtained by manually verifying a sample of detections and counting the number of detections that are not the sound of interest (Marques *et al.,* 2009). The cue rate is more difficult to obtain. The ideal approach is to obtain a cue rate from the study area and during the time period when the main study is being conducted. From a representative sample of animals, individual animals are followed, either visually or by deploying an animal-borne tag. During a period of time the animal being followed is recorded with a separately deployed recording system, or via the tag. Every cue of interest produced by the focal animal is recorded (Marques *et al.,* 2009). The alternative approach is to use a cue rate estimate from published work elsewhere (e.g. Kusel *et al.,* 2011). However, this approach will likely produce a biased

density/abundance estimate if the cue rate is not representative of that stock and/or period of time.

Fin whales were extensively hunted during the 19th and 20th centuries and the numbers of the global population decreased considerably (Reilly *et al.,* 2013). As a result, the IUCN attributed a global conservation status of 'Endangered' to fin whales. The IWC divides fin whales in the North Atlantic into 7 stocks (Donovan, 1991): Nova Scotia; Newfoundland-Labrador; West Greenland; East Greenland-Iceland; North Norway; West Norway-Faeroe Islands; British Isles-Spain-Portugal. The estimate for the British Isles-Spain-Portugal is 17 355 animals (CV = 0.27) obtained in 1989 (Buckland *et al.,* 1992). No recent abundance estimates are available. The conservation status of fin whales around Europe is considered "Near Threatened", although there are still no recent quantitative data that could support this (IUCN 2007). Historical data show that fin whales were an abundant species and were observed throughout the year in the south of the Iberian Peninsula (Sanpera and Aguilar, 1992). During the 1920s, hunting activities in the south of the Iberian Peninsula resulted in the removal of 7 000 fin whales from the area (Reilly *et al.,* 2013). Although hunting activities ceased in 1986 after the IWC moratorium, based on past and present sightings data, it seems that the numbers of fin whales in the area are still small, compared to the past abundance (Clapham *et al.*, 2008).

In Portugal, fin whales have a national conservation status of "Endangered" but there are no data that support this, other than the global assessment (Queiroz *et al.,* 2006). In the Azores and Madeira archipelagos fin whales are seen throughout the year, but are more common during spring and summer, probably as they travel to their northern feeding grounds (Silva *et al.,* 2013; Queiroz *et al.,* 2006). Off continental Portugal, sightings are sparser because of fin whale pelagic occurrence and the logistics of studying this species. Fin whales prefer pelagic waters and the large extension of the continental shelf off mainland Portugal makes it difficult to conduct surveys in preferred fin whale habitat. The south of continental Portugal is a strategic area to study the interactions between fin whales from the North Atlantic population and fin whales from the Mediterranean subgroup. The latter group is considered a subdivision of the British Isles-Spain-Portugal stock and is classified as "Vulnerable" by the IUCN (Panigada and Notarbartolo di Sciara, 2012). Because movements between the North Atlantic and the Mediterranean fin whales seem seasonal (Geijer *et al.,* 2016), it is possible that in some periods of time the abundance of whales off the south coast of Portugal could be higher. However, without a baseline abundance it is not possible to assess this trend.

OBS deployed off southwest Portugal recorded data to study potential earthquake and tsunami sources (NEAREST project, see Chapter 2) as well as fin whale acoustic data during 11 months of monitoring. The fin whale acoustic dataset of the NEAREST project was used in multiple studies that involved the detection, classification, location of fin whale calls (Matias and Harris, 2015) and the use of estimated ranges in animal abundance estimates using distance sampling (Harris *et al.,* 2013). Both works were part of a larger project, the Cheap DECAF: Density Estimation for Cetaceans from Acoustic Fixed Sensors Using Separate, Non-Linked Devices, conducted between 2011 and 2014 that aimed to demonstrate the utility of using separate non-linked recording instruments to monitor cetacean density (Harris *et al.,* 2014). During the project one of the tasks was to use multiple covariate distance sampling (adding variables to the detection function model that could potentially affect detectability) to investigate spatial and temporal patterns in density of fin whales off southwest Portugal during the 11 months of recording of the NEAREST project.

The initial distance sampling analysis with the OBS data from the NEAREST project included in the Cheap DECAF project was undertaken by Harris *et al. (*2013). In this study, a day of the fin whale acoustic dataset of the NEAREST project was used to: 1) demonstrate the potential of the single station method in estimating ranges to fin whale calls and 2) use the estimated ranges of detected fin whale calls to obtain an average probability of detection, using distance sampling analysis. Multi-covariate distance sampling using depth as a covariate was then conducted and a spatio-temporal model of fin whale call densities was developed. Other tasks of the Cheap DECAF project included the development of a density estimation method that used the total energy present in the fin whale frequency band as the statistic upon which a density estimate was made (Mellinger, 2014). Matias and Harris (2015) also improved the accuracy of the estimated ranges obtained by the single station method, but their adjustments were not used in the distance sampling analyses included in the Cheap DECAF project.

The aim of this chapter was to obtain an estimate of the average density and abundance of fin whales over 11 months, between September 2007 and August 2008, off southwest Portugal. In this analysis, the estimated ranges by the single station method were improved by the adjustments developed by Matias and Harris (2015), which was described in Chapter 3. Prior to the distance sampling analysis, there was an initial assessment of the suitability of two datasets developed in Chapter 3. One of the main assumptions of distance sampling, which are described in more detail in the methods, is that cues (when using cue-counting) produced at or near the recording transect are detected with certainty (Buckland *et al.,* 2001). Although there are several approaches to overcome this issue (Buckland *et al.,* 2001), in this thesis efforts were made to maximize the detection of those calls. Therefore,

two datasets with different approaches to retain close calls generated from the detection process and classification scheme (Chapter 3) were tested in the distance sampling analysis. The dataset with the best fitting of a detection probability model (assessed from visual inspection and goodness of fit tests, described in the Methods) was the one used to produce the final distance sampling results in this chapter. In summary, the steps involved in animal abundance estimation using passive acoustic monitoring with distance sampling are: 1) detecting acoustic signals of the animal of interest, *n*; 2) estimating distances of the detections; 3) estimating an average probability of detection, $\hat{p}$, with the estimated distances; 4) estimating a false positive rate of detections to correct the number of detections, $\hat{c}$; 5) obtaining a production rate of the acoustic signal identified that transforms the acoustic signal density estimates into animal density estimates, $\hat{r}$; 6) transforming animal density estimates $\widehat{D}$ into animal abundance estimates $\widehat{N}$, by dividing $\widehat{D}$ by a study area *A* specified by the researcher.

5.2. METHODS

5.2.1. Acoustic dataset

A set of 24 OBS was deployed off southwest Portugal, between September 2007 and August 2008 (Fig. 1, Chapter 2). Although their main task was to obtain data to study local seismicity, they also recorded fin whale sounds. Instrument characteristics and deployment details were described in Chapter 2. The 20-Hz fin whale call was detected in an automated approach using a modified cross-correlation equation with a waveform template. The full description of the detection process was given in Chapter 2. Ranges for detected calls were estimated with the single-station method, which was described in Chapter 3. This method is a well-known location method in seismology and it only requires data from a single instrument, as long as the three-components of the seismometer are working. In addition, this method only works well in an area that is defined by a critical range, which in turn is a function of the depth of the recording instrument. Beyond this critical range, the estimated ranges are unreliable. A classification scheme with two stages (also described in Chapter 3) that removed most false positives (stage 1 of classification) of the detection process and filtered out detections outside the critical range of the single-station method (stage 2 of classification) was applied. This classification scheme included a parameter crucial to select calls closer to the instrument, called the coherency factor (Co). Matias and Harris (2015) showed that very close calls to the recording instruments had negative coherence. However, calls outside the

critical range also showed negative values of coherence. In Matias and Harris (2015), there were other parameters that helped filter out detections outside the critical range with negative coherence. However, the analysis presented in Chapter 3 showed that the application of such parameters was not so straightforward. Therefore, the classification scheme defined in Chapter 3 relied only on two simple parameters that showed the expected trends with distance: i) the correlation value between the detected signal and the template (C.Max) and; ii) the signal-to-noise ratio (SNR). Higher values of both parameters were observed at closer distances and decreased with distance. From the results shown in Chapter 3, both parameters were useful in removing false positives and identifying detections that were potentially produced outside the critical range of the single station.

Two datasets were generated from the detection process and classification scheme, each dealing with the coherency parameter differently. The first dataset consisted of detections with correlation values equal or above 0.6, SNR equal or above 2.0 and all values of coherence. The estimated distances in this dataset ranged from 7 m to 4.185 km. The second dataset included detections with negative coherence that were only accepted if they showed a level of correlation equal or above 0.8 and a SNR equal or above 2.0. Detections with positive coherence were accepted at a correlation threshold of 0.6 and SNR of 2.0. The estimated distances in the second dataset ranged from 7 m to 2.137 km when Co<0, C.Max≥0.8 and SNR≥2 and from 169 m to 4.185 km when Co≥0, C.Max≥0.6 and SNR≥2. More details about both datasets can be found in Chapter 3. Both datasets were analysed using distance sampling.

5.2.2. Distance sampling method

A point transect cue counting analysis was conducted in order to obtain a density of fin whale calls throughout the study period (Buckland *et al.,* 2001). The cues used in this analysis were the 20-Hz fin whale calls detected in Chapter 2 and classified in Chapter 3 and the estimated distances were obtained with the single-station method, also described in Chapter 3. Fin whale density was calculated with

$$\widehat{D} = \frac{n(1-\hat{c})}{k\pi w^2 \widehat{P}_a T_k \hat{r}} \qquad \text{Eq. 1}$$

where ^ denote an estimated quantity and:

n = number of detected cues

$\hat{c}$ = proportion of false positive detections

k = number of point transects sampled

w = right truncation distance

$\widehat{P_a}$ = average probability of detection

T_k = time monitored in the k points

$\hat{r}$ = cue rate

There are five main assumptions needed for distance sampling analysis to work (Buckland *et al.,* 2001, 2015):

1. Cues made on or near the point must be detected with certainty (g(0) = 1, in which g(r) represents the detection probability, which is described below). This implies that all calls made directly above each OBS must be detected. In this thesis, close calls were characterized by having a negative coherency factor and results from Chapter 3 suggested they were also characterized by having high values of correlation (C.Max). Both datasets were obtained with classification parameters that minimize the possibility of missing close calls with negative coherency (see Chapter 3). However, there are different approaches to address the violation of this assumption, either by using mark-recapture methods to estimate g(0) (Laake and Borchers, 2004) or left-truncating the data to a distance at which detection is believed to be certain or by fitting a detection function only to data beyond that distance and extrapolating back to distance zero (Buckland *et al.,* 2001).

2. Distances to cues are measured accurately. Matias and Harris (2015) showed that the single-station method provides accurate estimates of distances. In the dataset used by Matias and Harris (2015), in which the true locations of the signals were compared with the range estimates obtained with the single station method, the average error in estimated distance was 273 m but at distances smaller than 3 km from the OBS the error in estimated distance was less than 50 m.

3. Cues are detected at their initial location, prior to any movement in response to the observer. This assumption is always valid when using cues because cues are produced at an instant in time and, therefore, cannot be subject to movement.

4. Detections of cues are independent from one another. Fin whales generally produce 20-Hz calls in sequences that in turn form bouts which can last for hours. Therefore, because calls from the same bout are detected, this assumption will be violated. Both datasets

have large sample sizes with several bouts and also distance sampling is robust to dependent detections (Marques *et al.*, 2013).

5. Animals/cues are distributed independently of the transects. It is assumed that, on average, animals are distributed according to a triangular distribution with respect to distance from the point so that the distribution of distances $\pi(r) = 2r/w^2$. This is a key assumption as this distribution is used in the estimation of the detection function. Using a survey design where points are placed in the study area randomly ensures that this assumption is met. The deployment of the OBS was independent from the distribution of the fin whales in the study area which meant they were placed randomly in regards to fin whale distribution.

5.2.3. Parameters for fin whale density estimation

Each parameter needed to calculate fin whale density is described below:

n – number of detected cues:

In this Chapter, the 20-Hz fin whale call was chosen as the main cue. The detection process of this signal was presented in Chapter 2. The estimate of the distances and further classification was presented in Chapter 3. Distances of the detected cues were obtained for the 11 OBS that had all of the three-components of the seismometer working, which meant these instruments were the only ones that could provide estimates of the location of the detected acoustic signals with the single-station method (localizing OBS) (see Chapter 3). Two datasets of distances were created, which were described above and in Chapter 3.

$\hat{c}$ – proportion of false positive detections:

A false positive was considered an instance where an automated detection of a 20-Hz fin whale call was registered but it was caused by another signal instead. The false positive proportion is incorporated in Eq. 1 by multiplying the number of detections by (1-ĉ), the proportion of true positives. This correction scales down *n*, if false detections occurred. It was not possible to visually check if all detections registered were true positives or not and therefore the proportion of true positives was estimated from a sample. A systematic random subsample was determined in order to visually check at least 100 detections per month (Table I). For months where the number of detections was smaller than 100 (April-August, 2008), all detections were visually checked. In months with relatively large sample sizes (October-December 2007 and January-February 2008), every 30th sample was checked, with a random starting point between 1 and 30. For other months, every 5th (March-April 2008) or every 4th

(September 2007) detection was checked, with a random starting point between 1 and 4 or 5. The visually checked sample of the true positives across the months represented ~3.8% of the data.

Table I – False positive sample and results from the manual inspection of the detections selected for the assessment of the proportion of false positives. Total detections are the results from the automated process from Chapter 2 with C.Max≥0.6, SNR≥2 and all Co values for the localizing OBS. False positive sample is the systematic random subsample described in the text above. False positives were detections that were not from 20-Hz fin whale calls and true positives were detections positively confirmed as 20-Hz fin whale calls.

Month	Total detections	False positive sample (n_{FP})	False positive	True positive
1	33 469	1 116	5	1 111
2	7 073	236	3	233
3	960	192	9	183
4	544	109	4	105
5	10	10	9	1
6	33	33	33	0
7	18	18	18	0
8	3	3	3	0
9	454	114	1	113
10	3 625	121	1	120
11	14 556	485	2	483
12	28 070	936	1	935
TOTAL	**88 815**	**3 373**	**89**	**3 284**

k – number of points sampled:

The number of detections resulted from the recordings of 11 OBS (identified hereafter referred to as the "localizing OBS").

w – Right-truncation distance:

In some cases, detections with large distances are difficult to model and extra effort in the fitting process may increase the variance in density estimates (Buckland *et al.,* 2004). The truncation of data removes outliers and facilitates modelling of the data. The shortest critical range of the instruments, 3.455 km for OBS04, was chosen as the truncation distance. t. Therefore, distances larger than 3.455 km were not considered in the analysis. The covered area around each OBS was πw^2 = 37.50 km^2.

$\widehat{P_a}$ – average probability of detection:

This is the probability of detecting a cue given that it is produced within the truncation distance w. In order to estimate the average probability of detection, a detection function is

fitted to the recorded distances of the automated detections, $g(r)$ (Eq. 2), which represents the probability of detecting a cue given that the animal which produced it is at a distance r from the instrument.

$$\widehat{P_a} = \int_0^w g(r)\pi(r)dr \qquad \text{Eq. 2}$$

Where π(r) is the distribution of distances to all cues, detected or not from the point, already mentioned above (Buckland *et al.,* 2015). A set of possible candidate parametric models for $g(r)$ were tested (known as key functions) and series of expansion terms were also added for additional flexibility. The R package *Distance* version 0.9.7 (Miller, 2017) was used to fit these models to the data. Conceptually, the model $g(r)$ is given by the general form:

$$g(r) = key(r)[1 + series(r)] \qquad \text{Eq. 4}$$

Where key(r) gives the basic model shape and can include one of the following forms: half-normal, hazard-rate or negative exponential model (Fig. 1). The detection function models can have parameters that define their scale, σ*,* and shape, β. The scale parameter σ affects how quickly the probability of detection falls with distance from the line or point (Buckland *et al.,* 2015). Because the detection of the cues remains certain for small distances from the point, it is expected that the detection function shows a 'shoulder' near the point, which is given by the scale parameter (Buckland *et al.,* 2001). The shape parameter β provides more flexibility to the model (Buckland *et al.,* 2015). The uniform and negative exponential key models have no parameters. The half-normal model has a scale parameter. The hazard-rate model has both shape and scale parameters. Each of the parameters are unknown and are estimated from the distance data of the detections using maximum likelihood methods (Buckland *et al.,* 2001).

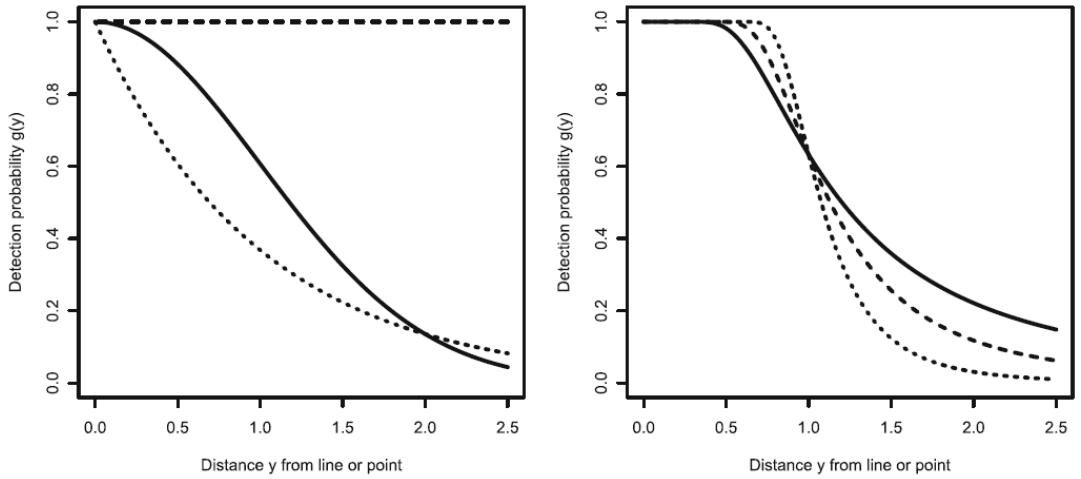

Figure 1. Plots of the key functions available in Distance. Left plot: uniform model (dashed line); half-normal model σ = 1 (solid line); negative exponential model with σ = 1 (dotted line). Right plot: hazard-rate model with σ = 1 and β = 2 (solid line), β = 3 (dashed line) and β = 5 (dotted line). In each case, truncation distance w = 2.5. The three hazard rate models show a 'shoulder' of the detection function that extends to a distance of 0.5 for the solid model and to a distance ~0.8 for the dotted model. In: Buckland et al. (2015). Distance sampling: methods and application (Springer International Publishing, Cham, Switzerland). Copyright by Springer International Publishing.

The expansion series of Eq. 4 is given by the general form:

$$Series(r) = \alpha_1 \times term_1 + \alpha_2 \times term_2 + \cdots + \alpha_n \times term_n \qquad \text{Eq. 5}$$

Where each term can be one of the following series adjustment: cosine, simple polynomials and Hermite polynomials (Buckland *et al.,* 2015). The α_n terms are parameters that are estimated.

In this analysis, half-normal and hazard rate detection functions were used as key functions, with only cosine series expansion terms considered to improve model fit. The maximum number of series expansion terms allowed in the model selection process was manually set to 1 to avoid improbable fits (e.g. non decreasing detection functions at distances further from the point). For each expansion term, an additional parameter is estimated.

Additional covariates were included in the model because they were believed to influence the detection process (Marques *et al.,* 2007). The covariates with potential influence in the detectability of a cue were: season (Table II), instrument depth and ambient noise. Temporal variation in detection probability was considered at a seasonal level rather than at a monthly level, because some months showed small detection numbers. Instrument depth was added because it was expected that detectability of a cue would be linked to OBS depth

because the critical range of each OBS is determined by depth of the instrument. Covariates are included in the model by altering the scale parameter σ of the key function (Marques *et al.,* 2007):

$$\sigma(y) = \exp(\beta_0 + \beta_1 Z_1 + \beta_2 Z_2 + \cdots + \beta_q Z_q) \quad \text{Eq. 6}$$

where β values indicate the intercept *(β_0)* and the slopes of each level of the covariate. *Z* values are indicator values, i.e., they take values 0-1 to indicate which level of the covariate is being considered.

The inclusion of covariates in the detection function model is not required for distance sampling to work, but their inclusion can potentially result in an improvement of the model fit and thus in more efficient estimates of abundance (Buckland *et al.,* 2004).

Table II – Temporal limits of each season for the study period. The beginning of each season corresponds to their equinoxes (astronomical seasons). In: https://www.timeanddate.com/

Season	**Start**	**Finish**
Spring	20th March	20th June
Summer	21st June	22nd September
Autumn	23th September	20th December
Winter	21st December	19th March

The choice of the best fitted model was based on the minimum Akaike Information Criterion (AIC), which provides a relative measure of fit. The absolute goodness of fit of the models was assessed by visually inspecting the fit of the models to the data and the quantile-quantile (Q-Q) plot. Points lining up on a 1:1 line on the Q-Q- plot suggest a good fit. The results of the Komogorov-Smirnov and Cramer-von Mises tests were also considered. The null hypothesis of those tests was that the fitted model is the true model (Buckland *et al.,* 2004). If p-value < 0.05, the null hypothesis is rejected.

T_k – time monitored:

Summation of the time periods in each of the k instruments.

$\hat{r}$ – cue rate:

Average number of cues per unit time that converts cue density into animal density. A 20-Hz call production rate was determined from Stimpert *et al. (*2015). The aim of the study

by Stimpert *et al. (*2015) was to describe the swimming behaviour and social context corresponding with calling in individually tagged fin whales in the summer and fall in the Southern California Bight. Fin whales were tagged between 2010 and 2013 as part of the Southern California Behavioural Response Study (SOCAL BRS) that aimed to investigate the effects of Navy sonar on cetaceans (Southall *et al.,* 2012). Periods of time (during and after) when some of the tagged animals were exposed to controlled exposures of simulated Navy sonar were excluded from the analysis, so that only natural behaviour data were analysed (although the authors could not rule out that behaviour may have been influenced by tag deployment, tag attachment, or presence of research vessels during the experiment). Deployment duration and number of calls recorded were reported for 18 digital acoustic recording tag (DTAGs, Johnson and Tyack, 2003) records. Ten animals were tagged with a version of the DTAG (v3) that enables calls from the tagged animal to be identified from other calls made by non-tagged conspecifics (Table III). It is crucial when estimating call production rate that only calls from the focal animal are included in the analysis, so the other 8 animals tagged with v2 DTAGs were omitted from the analysis.

Table III – Amount of data collected for each tagged whale (in hours and number of calls identified) excluding periods during or after experimental sound exposure, but including silent control trials. No tags contained calls that only occurred during and/or after an experimental exposure period. Whale ID indicates species ('bp'), year ('10'), Julian day of deployment ('236'), and the number deployment within that day ('a'). Tag type indicates DTAG version 2 or version 3 (version 3 included the faster sampling accelerometer sensors). In Stimpert et al., 2015, Sound production and associated behavior of tagged fin whales (Balaenoptera physalus) in the Southern California Bight," Animal Biotelemetry 3, 23. Copyright by BioMed Central Ltd.

Date	Whale ID	Tag type	Baseline tag duration (h)	Number of calls identified (produced by tagged animal)
8/24/2010	bp10_236a	2	2.5	0
8/24/2010	bp10_236b	2	2.1	0
8/27/2010	bp10_239a	2	2.8	0
9/1/2010	bp10_244a	2	2.9	0
9/1/2010	bp10_244b	2	2.3	288 (n/a)
9/2/2010	bp10_245a	2	1.0	0
9/4/2010	bp10_247a	2	2.2	44 (n/a)
8/4/2012	bp12_217a	2	2.9	0
10/20/2012	bp12_294a	3	3.1	372 (338)
5/19/2013	bp13_139a	3	1.6	0
8/4/2013	bp13_216a	3	2.3	0
9/14/2013	bp13_257a	3	2.4	0
9/14/2013	bp13_257b	3	3.0	33 (23)
9/15/2013	bp13_258a	3	5.9	0
9/15/2013	bp13_258b	3	5.5	515 (419)
9/15/2013	bp13_258c	3	6.3	1,237 (942)
9/16/2013	bp13_259a	3	2.1	0
9/22/2013	bp13_265a	3	3.7	0

5.2.4. Variance of the density estimates

The variance of the density estimate (Eq. 1) can be approximated by the delta method (Seber, 1982) assuming that the random components of the density estimator are independent:

$$\widehat{var}\left(\widehat{D}\right) = \widehat{D^2}\left[CV^2(n) + CV^2\left(\widehat{P_a}\right) + CV^2(\hat{c}) + CV^2(\hat{r})\right] \quad \text{Eq. 7}$$

where the CV denotes the coefficient of variation of the estimate, i.e., the standard error of the estimate divided by the estimate.

The variance of n, also known as the encounter rate, was obtained as the empirical variance of the number of detected calls per unit time by each OBS. Variance in the detection probability $\widehat{P_a}$ was calculated using the inverse of the information matrix resulting from the maximum likelihood estimation of the detection function parameters (Buckland *et al.,* 2015). Variance in the false positive proportion was calculated using a binomial variance with a finite population correction (Upton and Cook, 2016).

The estimate is defined as a success which is that a detected call is correctly a 20-Hz fin whale call. The probability of success is defined by pc and the variance is given by:

$$var(\widehat{c}) = n_{FP}p(1 - pc) \quad \text{Eq. 8}$$

Where n_{FP} is the number of detected cues used in the false positive sample (Table I), *pc* is the probability of a detection being a true positive.

The finite population correction:

$$FPC = \frac{var(\hat{c})}{n_{FP}}\left(1 - \frac{n_{FP}}{N_{FP}}\right) \quad \text{Eq. 9}$$

Where N_{FP} is the total number of detected cues, also used in Eq. 1

The standard error of the false proportion using the finite population correction is given by

$$SE = \frac{\sqrt{FPC}}{p} \quad \text{Eq. 10}$$

Having obtained $\widehat{D}$ and $\widehat{var}(\widehat{D})$ and assuming that $\widehat{D}$ is log-normally distributed, a $100(1-2\alpha)\%$ confidence interval is given by (Buckland *et al.,* 2001)

$$\left(\widehat{D}/C\,, \widehat{D}\cdot C\right) \quad \text{Eq. 11}$$

where

$$C = exp\left[z_\alpha \cdot \sqrt{\widehat{var}\left(ln\widehat{D}\right)}\right] \quad \text{Eq. 12}$$

and

$$\widehat{var}\left(ln\widehat{D}\right) = ln\left[1 + \frac{\widehat{var}\left(\widehat{D}\right)}{\widehat{D}^2}\right] \quad \text{Eq. 13}$$

The z_α is the upper α point of the N(0,1) distribution. For a 95% confidence interval $z_\alpha = z_{0.025} = 1.96$.

5.2.5. Fin whale abundance in the study area $\widehat{N}$

The study area *A* was defined as an area that surrounded the OBS, which was 62 601 km^2 (Fig. 2). The number of fin whales in this study area is given by Eq. 14

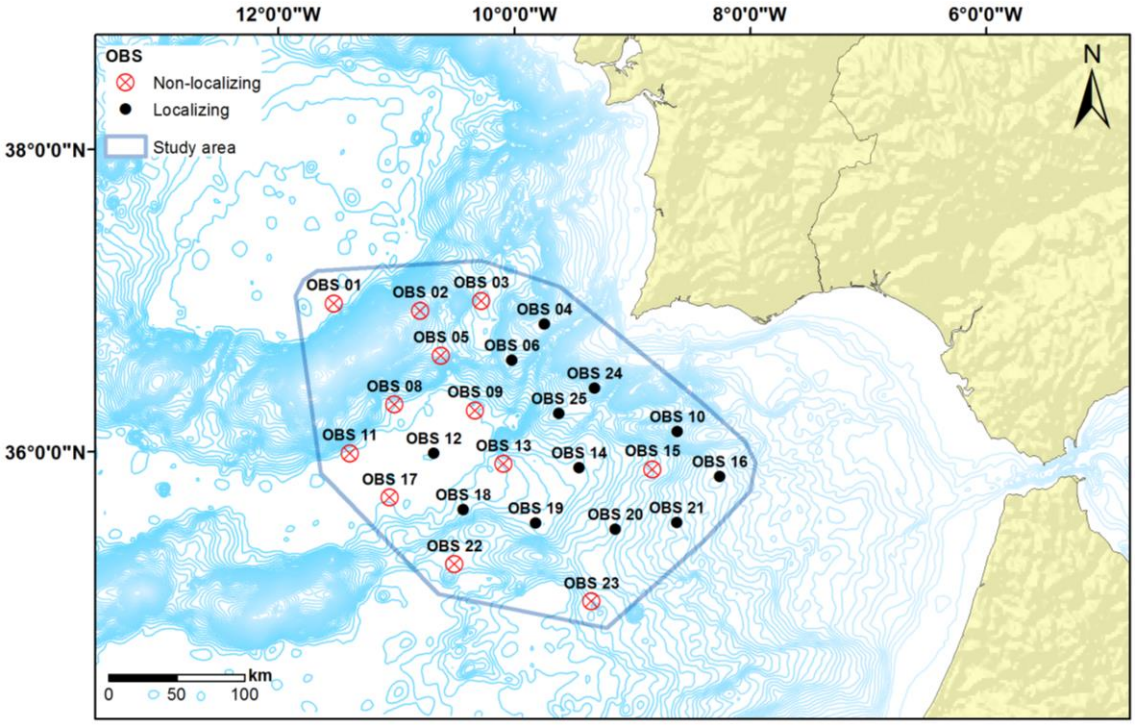

Figure 2. Study area defined for fin whale density purposes.

$$\widehat{N} = \widehat{D} \times A \qquad \text{Eq. 14}$$

where $\widehat{D}$ is the fin whale density calculated using Eq. 1.

5.3. RESULTS

5.3.1. Number of detections

During the 74 880 hours of monitoring time in the 11 localizing OBS, there was a total of 47 856 automatic detections with correlation values equal or above 0.6, SNR equal or above 2.0 with all values of coherence (dataset 1). The second dataset consisted of 33 404 detections with an SNR threshold of 2.0, and varying correlation thresholds depending on coherency: detections with negative coherence and a correlation threshold of 0.8 and detections with positive coherence and a correlation threshold of 0.6. Dataset 2 was defined in order to avoid false range estimates close to the instruments. Both datasets were presented in Chapter 3. After right truncation, dataset 1 had a total of 47 764 detections and an average encounter rate of 0.64 calls per hour (standard error, SE=0.13) with a CV of 20.98%. After

truncation, dataset 2 consisted of 33 312 detections with an average encounter rate of 0.44 calls per hour (SE=0.10) with a CV of 21.77%. Dataset 1 (Table IV) was the preferred one to continue with further analysis because it showed a better fit of the detection function, as shown later in the detection probability section (Section 5.3.2).

Table IV – Summary of acoustic data used in distance sampling analysis. Number of calls after truncation of data at 3.455 km are shown inside parenthesis.

OBS NO.	OBS DEPTH (km)	START	FINISH	Duration (h)	No. Of calls	Encounter rate (calls/h)
OBS 04	1.993	14-09-2007	25-06-2008	6864	6 655(6 655)	0.97
OBS 06	2.956	14-02-2008	20-07-2008	3792	288(288)	0.08
OBS 10	2.067	10-09-2007	29-06-2008	7056	10 933(10 933)	1.55
OBS 12	4.860	10-09-2007	20-07-2008	7560	1 240(1 153)	0.16
OBS 14	4.212	10-09-2007	20-07-2008	7560	7 455(7 455)	0.99
OBS 16	2.069	10-09-2007	07-07-2008	7248	4 579(4 579)	0.63
OBS 18	4.605	10-09-2007	17-07-2008	7488	5 197(5 196)	0.69
OBS 19	4.287	10-09-2007	17-07-2008	7488	5 901(5 899)	0.79
OBS 20	3.449	10-09-2007	12-07-2008	7368	2 927(2 927)	0.40
OBS 24	2.439	29-11-2007	11-08-2008	6168	487(487)	0.08
OBS 25	3.234	24-11-2007	11-08-2008	6288	2 194(2 192)	0.35

Three covariates were considered to affect detectability of fin whale calls: season, OBS depth and ambient noise. Figures 3-5 indicates that there is some effect of these covariates on the distances at which detections were recorded. In general, deeper OBS recorded detections at larger estimated ranges (Fig. 3), which is related with their larger critical range (see Chapter 3).

There was also a seasonal effect on the number of recorded detections and their estimated ranges (Fig. 4): there was an increase during autumn, which peaked in winter, and then there was a decrease during spring and summer. As expected, with increasing levels of noise, there was a small number of detected calls and shorter estimated ranges (Fig. 5).

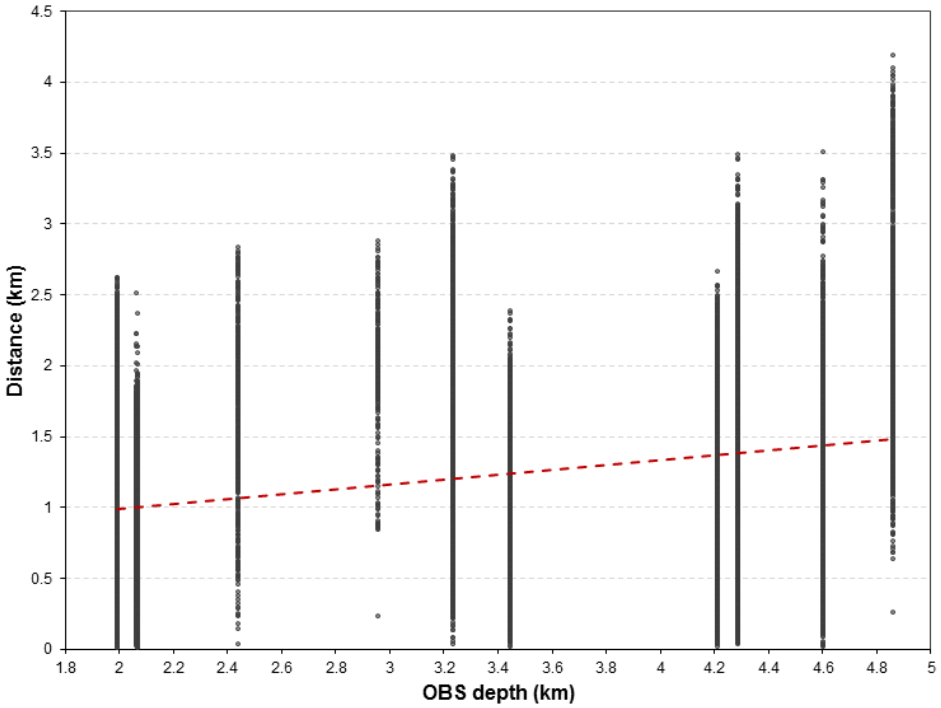

Figure 3. Exploratory data analysis for the effects on distance of OBS depth. Dashed lines indicate the fit of a simple linear model ($y = \beta_0 + \beta_i X_i + \varepsilon_i$) through the data in order to assess any general trends. Distance is the dependent variable, y, β_0 is the intercept, i.e. distance at the origin, β_i is the slope of each variable and ε_i represents the error terms.

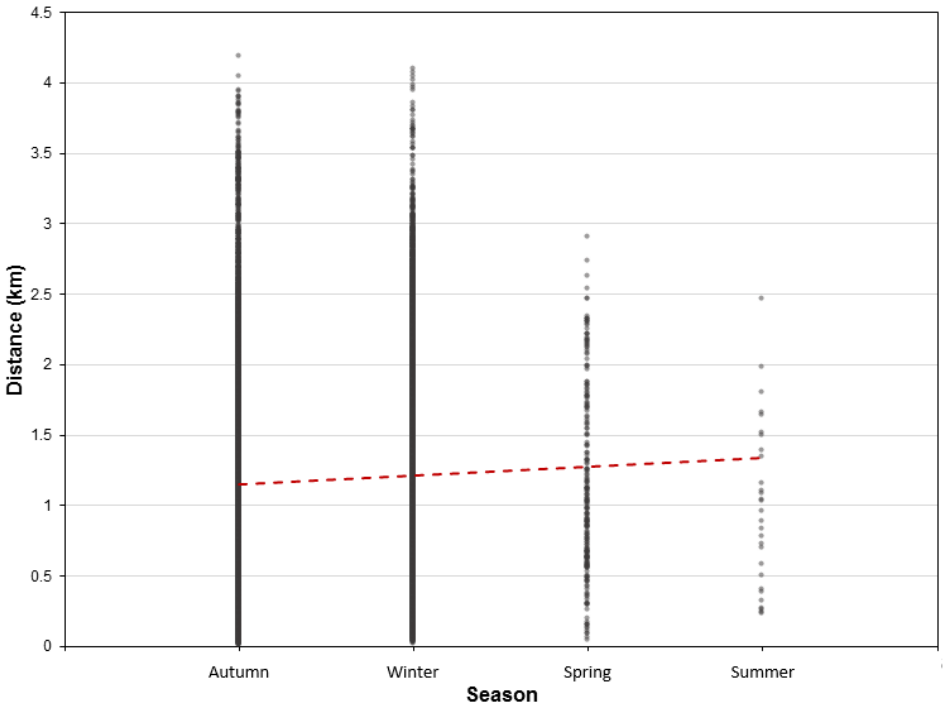

Figure 4. Exploratory data analysis for the effects on distance of season. Dashed lines indicate the fit of a simple linear model (similar to Fig. 3) through the data in order to assess any general trends.

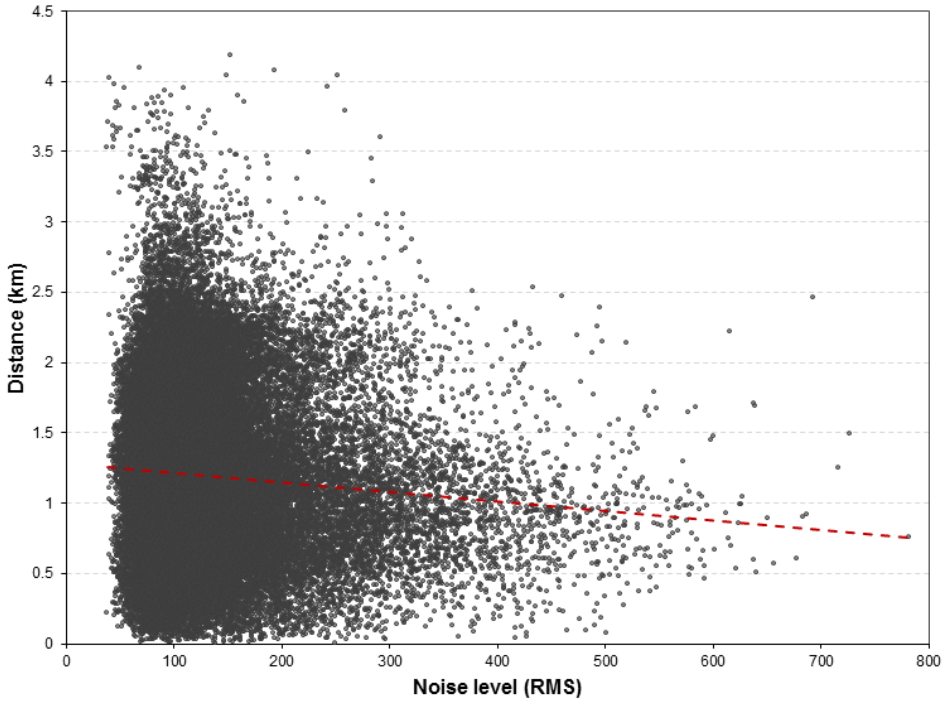

Figure 5. Exploratory data analysis for the effects on distance of ambient noise. Dashed lines indicate the fit of a simple linear model (similar to Fig. 3) through the data in order to assess any general trends.

5.3.2. Detection probability

An initial fit of a half-normal and a hazard-rate detection functions with no adjustments, no covariates and a truncation distance of 3.455 km was undertaken for dataset 1 (Fig. 6) and dataset 2 (Fig. 8). Dataset 1 showed a better fit of the probability density function plots when using the half-normal model, which was also confirmed by the quantile-quantile plots (Figure 7). The goodness of fit tests had a p-value<0.05 for both models of dataset 1 (Table V), suggesting that there was strong evidence to reject the null hypothesis. For dataset 2, the p-value for Komogorov-Smirnov tests were p-value<0.05 and for Cramer-von Mises tests were p-value>0.05 (Table VI). However, such goodness of fit tests are sensitive to large datasets and so can suggest a bad model fit, even when the fit is adequate (Buckland *et al.,* 2015). Based on visual inspection of the detection function fit to the distance data and the QQ plots, further analysis was undertaken with dataset 1.

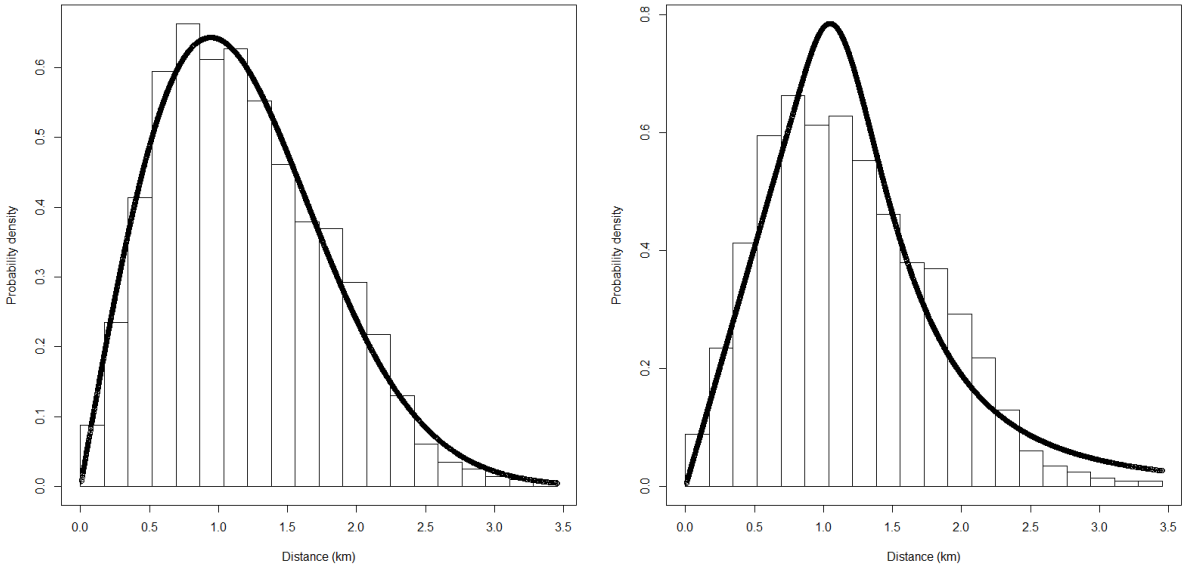

Figure 6. Fit of the half-normal (left) and a hazard-rate (right) detection functions to the dataset 1 (n = 47 764) with a truncation distance of 3.455 km: estimated probability density function (PDF) of detected distances superimposed over the histogram of estimates of distances for detections of dataset 1.

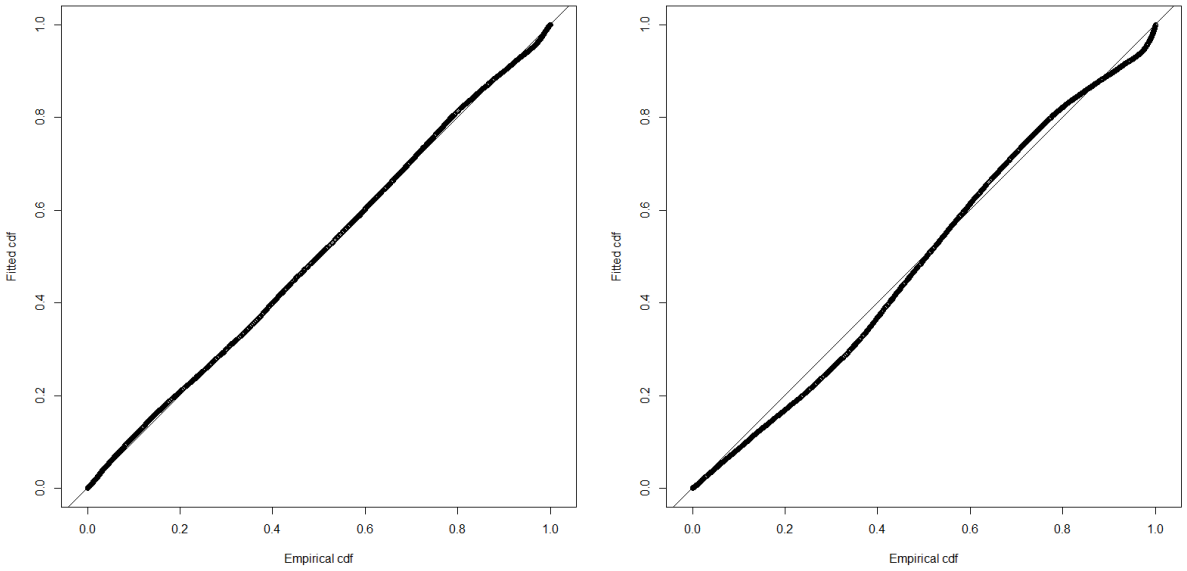

Figure 7. Quantile-quantile (QQ) plot to assess the goodness of fit of the detection function model for dataset 1: QQ plot of the half-normal model (left) and QQ plot of the hazard-rate model (right).

Table V – Goodness of fit tests for the half-normal and hazard-rate with null adjustments a truncation distance of 3.455 km for dataset 1. If p-values<0.05, the null hypothesis (H_0: the model tested is the true model) is rejected.

	Kolmogorov-Smirnov	Cramer-von Mises
Half-normal	1.282e-09	1.118e-06
Hazard-rate	4.741e-80	0.042

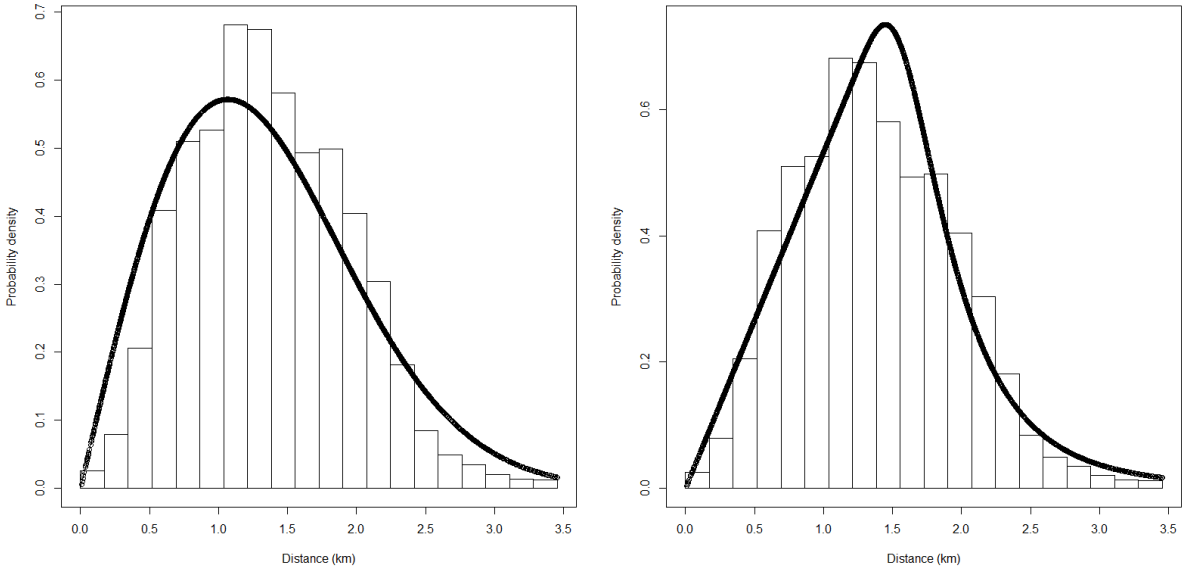

Figure 8. Fit of the half-normal (left) and a hazard-rate (right) detection functions to the dataset 2 (n = 33 312) with a truncation distance of 3.455 km: estimated probability density function (PDF) of detected distances superimposed over the histogram of estimates of distances for detections of dataset 2.

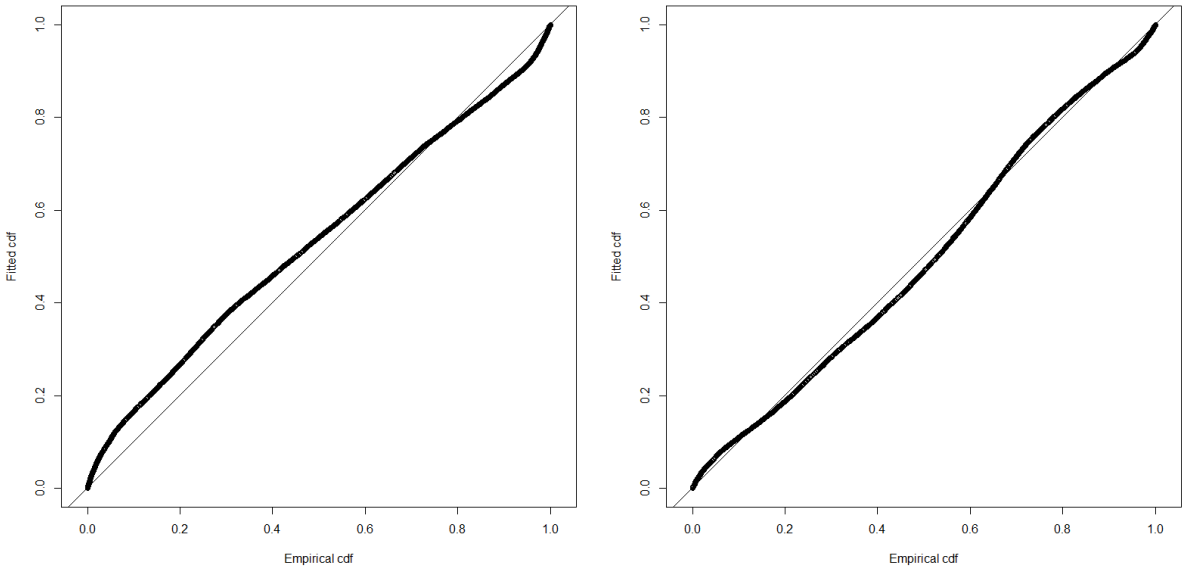

Figure 9. Quantile-quantile (QQ) plot to assess the goodness of fit of the detection function model for dataset 2: QQ plot of the half-normal model (left) and QQ plot of the hazard-rate model (right).

Table VI – Goodness of fit tests for the half-normal and hazard-rate with null adjustments a truncation distance of 3.455 km for dataset 2. If p-values<0.05, the null hypothesis (H_0: the model tested is the true model) is rejected.

	Kolmogorov-Smirnov	Cramer-von Mises
Half-normal	1.764e-170	0.145
Hazard-rate	8.094e-36	0.006

A second stage of the analysis consisted in fitting several detection functions to dataset 1, with and without covariates (Table VII). Depth of the OBS and season were important contributors to the detectability, with deeper depths and winter and spring resulting in an increase in the detection probability (Table VIII). Although the addition of the noise covariate decreased the Akaike's Information Criterion, the relationship between detectability was not the expected: probability of detection was higher with increasing levels of noise Therefore, a model with only depth and season as covariates was preferred over the ones with noise as a third covariate, as the relationship between noise and detection probability required further investigation. In conventional distance sampling (without covariates), series adjustment terms can improve model fit. However, in the case of multiple-covariate distance sampling the inclusion of series adjustment terms may lead to implausible fit in the detection function because there are no monotonicity constraints (improbable increase in the detection at further distances than expected can occur) (Buckland *et al.,* 2015). Therefore, the preferred model was a half-normal with no adjustments and with OBS depth and season as covariates. Visual inspection (Fig. 10) of the model and QQ plot (Fig. 11) confirmed the suitability of the model. The p-values of the two other goodness of fit tests (Fig. 11) suggest the rejection of the null hypothesis. As stated in previous results, this could be because the large sample size does detect small departures from the assumed model (Buckland *et al.,* 2015). The average probability of detection was estimated to be 0.14 with a CV of 0.5%.

Table VII – Results of the detection fitting process with Akaike's Information Criterion (AIC) and differences between each candidate model AIC and the model with the lowest AIC value. Key functions are half normal (HN) or hazard-rate (HR). Adjustment terms are cosine (Cos) and - means that no adjustment term was used. CV is the coefficient of variation of the average probability of detection.

Key	Adjustment terms	Covariates	# param.	AIC	ΔAIC	$\widehat{P_a}$	Cv($\widehat{P_a}$)
HN	-	-	1	82 456.87	-5 295.55	0.15	0.005
HN	cos	-	2	82 410.26	-5 248.94	0.16	0.010
HR	-	-	2	84 835.36	-7 674.03	0.20	0.005
HR	cos	-	3	82 346.78	-5 185.46	0.14	0.006
HN	-	Depth, season	5	77 807.93	-6 46.61	0.14	0.005
HN	cos	Depth, season	6	77 161.32	0	0.17	0.011
HR	-	Depth, season	6	78 214.32	-1 053	0.20	0.005
HR	cos	Depth, season	7	78 210.06	-1 048.74	0.19	0.010
HN	-	Depth, season,noise	6	77 778.19	-616.867	0.14	0.005
HR	-	Depth, season,noise	7	No fit	-	-	-

Table VIII – Summary of the coefficients estimated for the scale parameter of the selected half-normal model with the truncation distance of 3.455 km, following Eqn 5. Autumn was considered as the intercept of the model.

	estimate	se
(Intercept)	-0.119	0.004
depth	0.156	0.003
Spring	0.100	0.036
Summer	-0.080	0.103
Winter	0.125	0.006

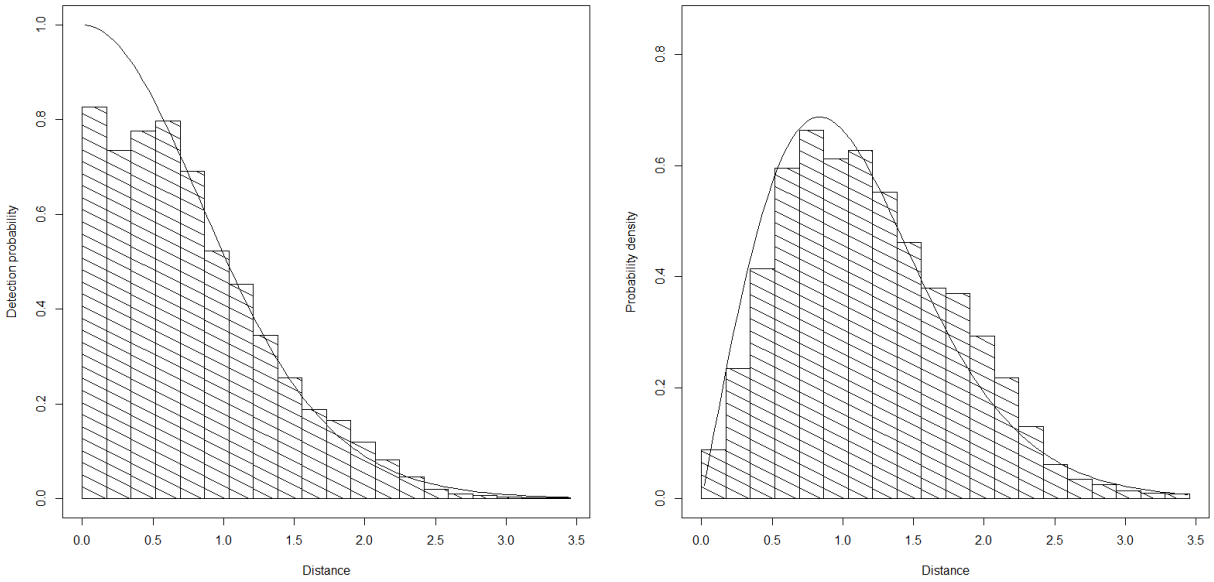

Figure 10. Estimated distances of detected fin whale calls and the fit of the chosen model (half-normal with no adjustments with season and depth as covariates and truncation distance of 3.455 km): detection function (left); probability density function (right).

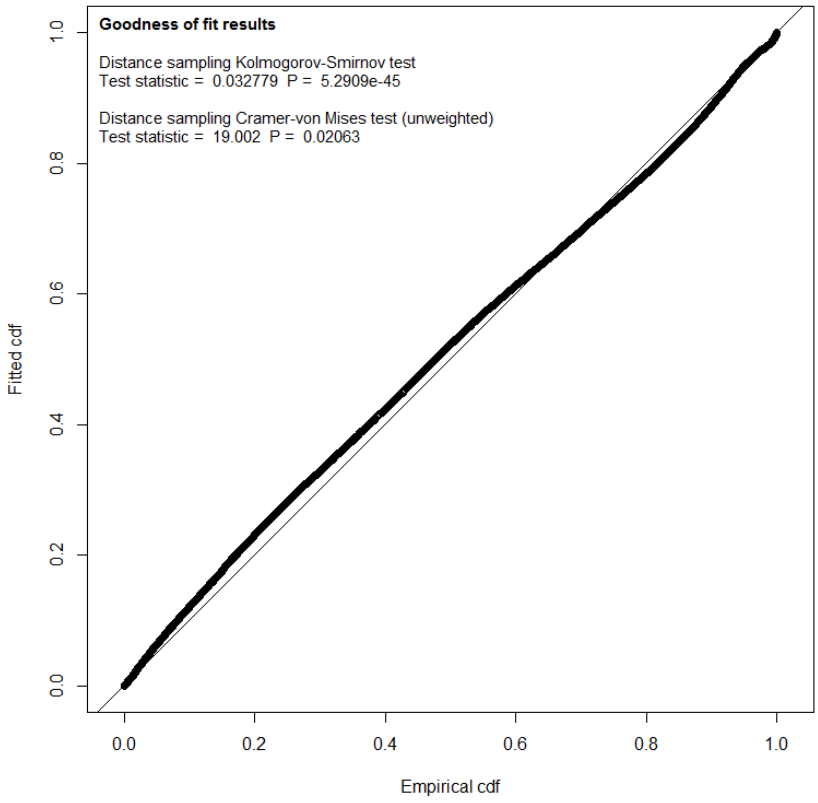

Figure 11. Quantile-quantile plot to assess the goodness of fit of the chosen detection function model.

5.3.3. True positive rate

The false positive proportion calculated from the subsample shown in Table I was $\hat{c}$ 0.026. The proportion of true positives was 0.97 with a standard error of 0.15 and a CV of 16.15%.

5.3.4. Cue rate

Cue production rate and its associated standard error were calculated with the number of calls presented in Stimpert *et al. (*2015). The v3 DTAGs were deployed between 1.60 and 6.30 hours (Table III). Six tags did not record any calls, while the number of calls produced by the remaining four tagged whales ranged between 23 and 942. The weighted mean call production rate using the ten tags was 45.08 calls.hr-1 (standard error: 22.31) and the CV was 49.49%.

5.3.5. Density and abundance

Applying Eq. 1, during the study period, there was an overall average density of 0.245 fin whales per 1 000 km^2 (CV% = 56.13, 95% CI 0.088-0.68). Assuming that this density estimate is representative of the area around the OBS (62 601 km^2), the estimated average fin whale abundance for the area was 15 whales (95% CI 5-43). The largest contributor to the variance of the density estimate was the cue rate (49.49%), followed by the encounter rate (20.98%) and true positive rate (16.15%) (Table IX). The variance attributed to the detection function (0.54%) was very small.

Table IX – Summary of the values derived for each parameter needed to estimate density of fin whales off southwest Portugal and their associated CVs.

Parameter	Value	%CV
Detected calls *n*	47 764	20.98
True positive rate *(1-ĉ)*	0.97	16.15
Right truncation distance *w*	3.455	-
Estimated probability of detection $\widehat{P_a}$	0.136	0.54
Monitoring period (hours) T_k	74 880	-
Average cue rate $\hat{r}$	45.08	49.49
OBS *K*	11	-

5.4 DISCUSSION

The overall density of fin whales per 1 000 km^2, obtained from the area surveyed by the OBS and during the 11 months of the monitoring period, was 0.245 animals (CV% = 56.13, 95% CI 0.088-0.68). Although Mellinger (2014) provided a spatial density of fin whales in the same study area and using the same extension of the study period of this thesis' for the Cheap DECAF project, the results obtained in this chapter are within the same interval of values (0.05-0.3 calling whales per 1000 km^2). However, Mellinger (2014) only estimated the density of the calling fin whales and used a different method from the one used in this chapter. By using a cue rate which considers both vocalizing and non-vocalizing fin whales (there were tags that did not record any call from the tagged whale, see details below), the density estimate obtained in this chapter refers to all fin whales from the surveyed area.

Although the OBS provided data to assess fin whale stock status at an abundance level, there were some considerations that needed to be highlighted and addressed in future work.

5.4.1. Dataset

For a standard distance sampling analysis, the certainty of probability of detection of cues at very close ranges to the transects (g(0)=1) is crucial to obtain unbiased density estimates (Buckland *et al.,* 2001). In the case of using estimated ranges obtained with the single-station method in distance sampling, special considerations had to be made about g(0)=1. The use of the single-station method to obtain range estimates of the detections meant that some assumptions had to be made about whether calls with associated range estimates were produced inside the critical range of each OBS or not. Calls produced outside the critical range would produce false range estimates in the dataset. Coherency was identified as a potentially useful parameter to identify whether or not calls were produced within the critical range (Matias and Harris, 2015). Positive coherency was indicative of calls produced inside the critical range but not for calls that were produced at or near the OBS. Calls produced at close distances to an OBS had negative coherency value but calls produced outside the critical range had also negative coherency. Removing calls produced outside the critical range based on coherency meant that close calls would also be removed and g(0)<1.

There are different approaches to take if g(0)=1 is not possible: 1) using mark-recapture methods to estimate g(0) (Laake and Borchers, 2004) or 2) left-truncating the data to a distance at which detection is believed to be certain or by fitting a detection function only to data beyond that distance and extrapolating back to distance zero (Buckland *et al.,* 2001).

In mark–recapture distance sampling methods, the object (animals/cues) is recorded more than once, i.e. is “captured” and “recaptured”. It is necessary that once the object is detected for a first time, i.e. it is “captured”, some of its features then allow for a subsequent detection, i.e. a “recapture”. During a mark–recapture distance sampling trial, two observers (humans or recording instruments) survey transects and detect each object independently. The “capture history” of the objects is then used to estimate a probability of detection at g(0) that can be incorporated in distance sampling analysis (Borchers *et al.,* 2002). A preliminary analysis of the propagation range of the 20-Hz fin whale calls detected in the hydrophone recordings showed that it was not possible to identify the same calls across different OBSs (Pereira *et al.,* 2015). There were detections around the expected time of arrival of the call, considering a sound velocity in the water column of 1.5 km/s, but from the spectrograms they could not be confirmed as true positives, i.e., true fin whale calls. Therefore, mark–recapture distance sampling methods could not be used in this chapter.

Left-truncation can be performed by deciding a specific distance at which detection is believed to be certain and by fitting a detection function from that point (Buckland *et al.,* 2001). However, if this point is not well known then there is a possibility of missing the shoulder (described in the methods) of the detection function and therefore cause a bias in the estimated average probability of detection. In this chapter, the left truncation distance could be considered as a turning point where the number of negative coherency detections at smaller ranges is reduced and thus have less contribution to the distribution of ranges. Several tests (not shown here) were undertaken in order to identify this turning point for each OBS with varying correlation thresholds. With this approach each OBS would have its own left truncation distance. However, the turning point varied with correlation values and it was not a function of depth, which was unexpected. Therefore, it was not possible to identify a left-truncation distance, neither a general left-truncation distance nor OBS specific.

In Chapter 3, positive coherency detections revealed a relationship between C.Max and distance: higher levels of correlation were observed at close estimated ranges and decreased with distance. This relationship was used to obtain two datasets with different approaches to retain close calls, and therefore used different levels of correlation depending on coherency.

In dataset 1, all coherence values were accepted to avoid losing detections very close to the OBS and maintaining the key assumption of distance sampling of g(0)=1. Because all levels of coherency were accepted, there was a possibility that detections produced outside the critical range were maintained in dataset 1. This would result in a higher number of detections estimated to occur within the critical range of each OBS, likely causing a bias in

the average probability of detection, as well as an inflated encounter rate. However, the occurrence of such detections was minimized by the high level of correlation threshold applied.

The classification of the dataset 2 was more selective and included two levels of correlation threshold that depended on the coherence values. The use of a correlation threshold for positive coherence and another higher correlation threshold for negative coherence. The results from Chapter 3 showed that levels of correlation C.Max>0.8 for positive coherency detections were only observed up to 1.8 km. Although the true locations of the detections used in this thesis are unknown, Matias and Harris (2015) showed that estimated ranges with positive coherency are accurate. Therefore, the use of C.Max≥0.8 could potentially minimize the occurrence of ranges produced by detections outside the critical range. However, the point closer to the recording instrument where coherence changes from negative to positive is unknown and there was also a possibility that this dataset filtered too many detections at close ranges. The C.Max≥0.8 threshold could be too selective and remove detections with lower correlation values (between 0.6 and 0.8) with negative coherency that could potentially be produced from close ranges. Choosing dataset 2 over 1 would result in a decrease of the encounter rate, since fewer detections are being used. Dataset 2 showed worse results in the goodness-of-fit tests of the fitted detection function and also showed a higher average probability of detection, which might suggest a possible higher level of bias in dataset 2.

Therefore, since mark-recapture distance sampling methods could not be applied and left truncation distances could not be determined, abundance estimation was undertaken with dataset 1 as it had the most simple classification criteria and a straightforward distance sampling analysis could be performed.

5.4.2. Effects of covariates

The addition of the three covariates, OBS depth, season and ambient noise decreased the AIC value of the detection function model. However, the relationship between noise and detectability was not expected as the resulting model showed a positive scale parameter (which meant that the probability of detection increased with higher levels of ambient noise). As a result, a model with only OBS depth and season was preferred for the abundance analysis presented here, though future work should explore the apparent positive relationship between ambient noise and detection probability. The positive relationship between detection and OBS depth was expected, as deeper OBS have larger critical ranges and, therefore, show a larger range of detection distances. There was also a seasonal relationship in

detectability of the calls, with spring and winter showing the highest values of detectability. The differences in detectability could be related with different sound source levels or differences in the acoustic propagation conditions. Future work could include assessing oceanographic conditions to look at whether changes to sound propagation could be driving this relationship.

5.4.3. Cue rate and false positive rate

Cue rate had the highest contribution to the variance of the density estimate, with 49.49%. It is recommended that cue rate is estimated during the study period and in the same study area with a large and random sample of animals (Marques *et al.,* 2013). Cue rates vary over time and space and some variation could also be dependent on sex or behavioural state. Obtaining a cue rate concurrently with the acquisition of detections and distances over a large sample of animals ensures that the cue rate estimate is representative of the study period, area and animals surveyed. In this chapter, the cue rate was obtained by extracting the number of calls from a study undertaken in the Southern California Bight during between 2010 and 2013 (Stimpert *et al.,* 2015). A total of 10 fin whales were tagged with a version of DTAG that enables to identify the calls produced by the tagged animal: 1 whale in autumn of 2012, 1 whale in spring of 2013 and the remaining 8 whales during summer of 2013. The study provided samples of both vocalizing and non-vocalizing animals as only four tags recorded calls and six tags did not did not record any calls. Seven years of acoustic data, between 2006 and 2012, in the Southern California Bight, showed that fin whale 20-Hz calls occurred year-round, with the highest values of occurrence between September and December, with a peak in November (Širović *et al.,* 2015). It is not clear whether this continuous presence is a result of a resident population, a rotating migration through the area, or a combination of the two (Širović *et al.,* 2015).

Fin whale density obtained in this chapter is likely to contain bias caused by an incorrect cue rate. Cue rate was obtained from a different ocean basin, different population and different monitoring time. Genetic results (Berubé *et al.,* 1998) and acoustic data (Hatch and Clark, 2004) show differences among fin whales of the North Atlantic Ocean and the North Pacific Ocean. In the study area, preliminary monthly call densities obtained during the Cheap DECAF project showed that there was a clear temporal pattern in call densities, with a peak in calling in December and January (Harris *et al.,* 2014). This pattern was different from the one obtained by Širović *et al. (*2015) for the area of the tagged whales, the Southern California Bight. In addition, the sample size of the whales that were tagged was very small (only 10 animals). Nonetheless, there is little information about fin whale calling rate and at

the time of this analysis, Stimpert *et al. (*2015) was the only study that provided data to obtain an estimate of the call production rate of the 20-Hz call.

5.4.4. Fin whale occurrence

It is possible that in some areas there were environmental conditions more favourable to the occurrence of fin whales than others, such as more pelagic waters and higher density of prey. Although it is assumed that fin whales occurring in this study area might feed at high latitude areas (Kellogg, 1929), feeding activities have been observed around the Gorringe Bank (F. Martinho 2015) which is very close the study area. It is possible that some surveyed areas could had more detections, due to a higher number of calling fin whales occurring in particular areas. However, the deployment of the OBS was independent from the distribution of the fin whales in the study area which meant they were placed randomly with regards to fin whale distribution. A random survey design ensures that the average density/abundance across the study area should be unbiased, despite possible spatial variation in the distribution of fin whales within the study area. (Buckland *et al.,* 2015). In distance sampling analysis, the data are pooled in order to provide an overall density estimate of the surveyed area. The next step is to produce density surfaces, which do explore the spatial changes in fin whale density throughout the study area. During the Cheap DECAF project this task was explored with two approaches: 1) using detections without adjusted ranges and distance sampling (Harris *et al.*, 2014) and 2) an energy-based detection process of the 20-Hz fin whale call (Mellinger, 2014).

The 20-Hz fin whale call is a fairly simple signal that does not allow for a recognition at an individual level. It is possible that on some occasions, the same individual was detected more than once as it travelled through the surveyed area. However, because the density/abundance estimate was obtained by counting cues, this was not a factor contributing to possible bias.

5.4.5. Decreasing variance - using non localizing OBS and estimating abundance for each season

The next immediate task would be to estimate fin whale call density for each season. In this case, using the cue rate from Stimpert *et al. (*2015) to transform the cue density into animal density might produce different levels of bias as the temporal resolution in next distance sampling analysis would be seasonal. The cue rate obtained Stimpert *et al. (*2015) included data from three seasons but mostly calls produced during summer, which is the

season with the lower preliminary call density in the study area (Harris *et al.,* 2014). Density/abundance estimates produced for the same seasons during which the cue rate was obtained would show less bias than the other seasons where no cue data was obtained.

The encounter rate had one of the highest contributions to the overall variance of the density estimate. Adding the detections of the non-localizing OBS should decrease the variance of the encounter rate. Although it is not possible to estimate distances of detections made for these OBS, the parameters used to filter detections are available (correlation threshold using the Z-channel and SNR) and can be used to filter them in the same way as in the localizing OBS. There were 13 OBS with detections that were not working properly (12 were not working properly during their whole monitoring period and OBS06 did not work properly during part of its monitoring period) and their detections did not have a distance estimate. Results from Chapter 3 showed that when coherency was positive there was a relationship between the correlation value and distance, for the localizing OBS. At closer ranges the correlation value was high and it decreased with range. It is expected that non-localizing OBS show similar trends to the localizing-OBS and so it is likely that the detections remaining after filtering for correlation threshold and SNR occur at similar ranges to those recorded on the localizing OBS. However, detections used for the distance sampling analysis showed ranges up to 4.185 km but were truncated at 3.455 km. Therefore, a similar proportion of calls need to be truncated from the non-localizing OBS. The number of detections for the non-localizing OBS that are beyond the right-truncation distance can be estimated by calculating the probability density function (pdf) of the detection function for each OBS and predicting the number of calls occurring between 3.455 km and the maximum detection distance (the critical range) for each OBS. Further, the detection function obtained in this Chapter contained depth as a covariate, so the OBS-specific average probability of detection (and associated detection function) for each of the non-localizing OBS could be estimated using the key function equation with the relevant covariates.

Although the abundance estimate obtained in this Chapter could be refined in several ways as discussed above, it provides an initial value that could be used as a baseline for future studies. Efforts to make the best use of OBS data for marine mammal studies are being developed and they will improve the abundance estimate already obtained. Future work will also assess abundance at a finer temporal scale.

5.5. REFERENCES

Borchers, D. L., Buckland, S. T., and Zucchini, W. (**2002**). *Estimating animal abundance: closed populations* (Springer, London, UK).

Buckland, S. T., Anderson, D. R., Burnham, K. P., Laake, J. L., Borchers, D., and Thomas, L. editors (**2004**). *Advanced Distance Sampling* (Oxford University Press, Oxford, UK), 416 pp.

Buckland, S. T., Anderson, D. R., Burnham, K. P., Laake, J. L., Borchers, D. L., and Thomas, L. (**2001**). *Introduction to Distance Sampling* (Oxford University Press, Oxford, UK), 432 pp.

Buckland, S. T., Cattanach, K. L. and Lens, S. (**1992**). “Fin whale abundance in the eastern North Atlantic, estimated from Spanish NASS-89 data,” Reports of the International Whaling Commission **42**, 457–460.

Buckland, S. T., Rexstad, E. A., Marques, T. A., and Oedekoven, C. S. (**2015**). *Distance sampling: methods and application* (Springer International Publishing, Cham, Switzerland).

Clapham, P. J., Aguilar, A., and Hatch, L. T. (**2008**). "Determining spatial and temporal scales for management: lessons from whaling," Marine Mammal Science **24**, 183–201.

Donovan, G. P. (**1991**). A review of IWC stock boundaries. Report of the International Whaling Commission **13**, 39–68.

Geijer, C. K. A., Notarbartolo di Sciara, G., and Panigada, S. (**2016**). "Mysticete migration revisited: are Mediterranean fin whales an anomaly?," Mammal Review **46**, 284–296.

Harris, D. V., Matias, L., and Thomas, L. (**2014**). Cheap DECAF: Density Estimation for Cetaceans from Acoustic Fixed Sensors Using Separate, Non-Linked Devices Final project report, http://www.dtic.mil/docs/citations/ADA610894 (Last viewed 21st April 2018). 17 pp.

Harris, D., Matias, L., Thomas, L., Harwood, J., and Geissler, W. H. (**2013**). “Applying distance sampling to fin whale calls recorded by single seismic instruments in the Northeast Atlantic,” Journal of the Acoustical Society of America **134**, 3522–3535.

Hatch, L. T., and Clark, C. W. (**2004**). “Acoustic differentiation between fin whales in both the North Atlantic and North Pacific Oceans, and integration with genetic estimates of

divergence," Paper presented to the IWC Scientific Committee, Sorrento, Italy, July, Paper No. SC/56/SD6, pp. 1–37.

Kellogg, R. (**1929**). "What is known of the migrations of some of the whalebone whales," Smithsonian Institution Annual Report **1929**, 467–494.

Kusel, E. T., Mellinger, D. K., Thomas, L., Marques, T. A., Moretti, D., and Ward, J. (**2011**).Cetacean population density estimation from single fixed sensors using passive acoustics," Journal of the Acoustical Society of America **129**, 3610–3622.

Laake, J. L. and D. L. Borchers (**2004**). "Methods for incomplete detection at distance zero," in Advanced Distance Sampling, edited by S.T. Buckland, D.R. Anderson, K.P. Burnham, J.L. Laake, D.L. Borchers, and L. Thomas (Oxford University Press, Oxford, UK), pp. 108–189.

Marques, T. A., Munger, L., Thomas, L., Wiggins, S. and Hildebrand, J. A. (**2011**). "Estimating North Pacific right whale (*Eubalaena japonica*) density using passive acoustic cue counting," Endangered Species Research **13**, 163–172.

Marques, T. A., Thomas, L., Fancy, S. G., and Buckland, S. T. (**2007**). "Improving estimates of bird density using multiple covariate distance sampling," Auk **124**, 1229–1243.

Marques, T. A., Thomas, L., Martin, S. W., Mellinger, D. K., Ward, J., Moretti, D., Harris. D., and Tyack, P. (**2013**). "Estimating animal population density using passive acoustics," Biological Reviews **88**, 287–309.

Marques, T. A., Thomas, L., Ward, J., DiMarzio, N., and Tyack, P. L. (**2009**). "Estimating cetacean population density using fixed passive acoustic sensors: An example with Blainville's beaked whales," Journal of the Acoustical Society of America **125**, 1982–1994.

Matias, L., and Harris, D. (**2015**) "A single-station method for the detection, classification and location of fin whale calls using ocean-bottom seismic stations," Journal of the Acoustical Society of America **138**, 504–520.

Mellinger, D. K. (**2014**). Cheap DECAF: Density Estimation for Cetaceans from Acoustic Fixed Sensors Using Separate, Non-Linked Devices, project report http://www.dtic.mil/docs/citations/ADA618005 (Last viewed 21st April 2018). 7 pp.

Mellinger, D. K., Stafford, K. M., Moore, S. E., Dziak, R. P., and Matsumoto, H. (**2007**) "An Overview of Fixed Passive Acoustic Observation Methods for Cetaceans," Oceanography **20**, 36–45.

Miller, D. L. (**2017**). Distance: Distance Sampling Detection Function and Abundance Estimation version 0.9.7, https://cran.r-project.org/web/packages/Distance/index.html (Last viewed 21st April 2018).

Panigada, S. and Notarbartolo di Sciara, G. (**2012**). *Balaenoptera physalus*. in: IUCN 2017. IUCN Red List of Threatened Species. Version 2017.3, http://www.iucnredlist.org (Downloaded 31th January, 2018).

Pereira, A., Harris, D., Thomas, L., Tyack, P., and Matias, L. (**2015**). "Detection and propagation range of fin whale calls off Gulf of Cadiz," abstract presented at the 7th International DCLDE [Detection, Classification, Location, and Density Estimation] Workshop, 13-16 July, La Jolla, USA.

Queiroz, A. I., Alves, P. C., Barroso, I., Beja, P., Fernandes, M., Freitas, L., et al. (**2006**). "*Balaenoptera physalus* Baleia-comum," in Livro Vermelho dos Vertebrados de Portugal edited by M.J. Cabral, J. Almeida, P.R. Almeida, T. Dellinger, N. Ferrand de Almeida, M.E. Oliveira et al. (Instituto da Conservação da Natureza/Assírio & Alvim, Lisboa, Portugal) pp. 511-512.

Reilly, S. B., Bannister, J. L., Best, P. B., Brown, M., Brownell Jr., R. L., Butterworth, D. S., et al. (**2013**). "*Balaenoptera physalus*," in IUCN 2017. IUCN Red List of Threatened Species. Version 2017.3, http://www.iucnredlist.org (Downloaded 31th January, 2018).

Sanpera, C., and Aguilar, A. (**1992**). "Modern whaling off the Iberian Peninsula during the 20th century," Reports of the International Whaling Commission **42**, 723–730.

Seber, G. A. F. (**1982**). *The Estimation of Animal Abundance* (The Blackburn Press, London, UK).

Silva, M. A., Prieto, R., Jonsen, I., Baumgartner, M. F., and Santos, R. S. (**2013**). "North Atlantic blue and fin whales suspend their spring migration to forage in middle latitudes: building up energy reserves for the journey?," Plos One **8**, e76507.

Širović, A., Rice, A., Chou, E., Hildebrand, J. A., Wiggins, S. M., and Roch, M. A. (**2015**). “Seven years of blue and fin whale call abundance in the Southern California Bight,” Endangered Species Research **28**, 61–76.

Southall, B., Moretti, D. J., Abraham, B., Calambokidis, J., Deruiter, S., and Tyack, P. (**2012**). Marine mammal behavioral response studies in Southern California: advances in technology and experimental methods,” Marine Technology Society Journal **46**, 48–59.

Stimpert, A. K., DeRuiter, S. L., Falcone, E. A., Joseph, J., Douglas, A. B., Moretti, D. J., et al. (**2015**). "Sound production and associated behavior of tagged fin whales (*Balaenoptera physalus*) in the Southern California Bight," Animal Biotelemetry **3**, 23.

Chapter 6

LLOYD'S MIRROR EFFECT IN FIN WHALE CALLS AND ITS USE TO INFER THE DEPTH OF VOCALIZING ANIMALS

6.1. INTRODUCTION

The acoustic repertoire of large cetaceans is differentiated at species and population levels, which can be useful for management purposes (McDonald *et al.*, 2006). Some calls are highly stereotyped and are produced in repeated sequences, which aids automated sound detection. Fin whales produce calls between 15 and 142 Hz (Watkins *et al.*, 1987; Hatch and Clark, 2004), but the most common and best studied call is the "20-Hz call" (Hatch and Clark, 2004). This signal is a ~1 second, downward sweeping tone between 30 and 15 Hz (Watkins *et al.*, 1987). Usually fin whales produce sequences of 20-Hz calls that are separated by two types of periods of silence: rests, which can last between 1–20 minutes, and longer gaps, lasting between 20 minutes and 2 hours (Watkins *et al.*, 1987; Delarue *et al.*, 2009; Soule and Wilcock, 2013). These sequences form bouts that are separated by periods of silence greater than 2 hours. Other types of low frequency sounds, such as Backbeats, can be produced within sequences (Clark *et al.*, 2002). Backbeats are relatively constant in frequency (between 18 and 20-Hz) and last ~0.8 second (Clark *et al.*, 2002). Several studies have found variation in some temporal (e.g., inter-call interval, call duration) and spectral features of the 20-Hz call (e.g. frequency bandwidth, median frequency) that seem to reflect geographic differences (Hatch and Clark, 2004; Delarue *et al.*, 2009; Castellote *et al.*, 2011). However, variability of call measurements may also be caused by acoustic interference. When a sound source emits a signal, the pressure waves can travel through both direct and reflected paths (in water, signals can reflect off both the seafloor and sea surface). Depending on sea state and signal frequency, the ocean surface can generate a reflected pressure signal with the phase reversed by 180 degrees. The interference between the direct path and this surface reflected signal is called the Lloyd's Mirror effect (hereafter LME) by analogy with optical interference. This results in alternating signal peaks caused by constructive interference, with signal nulls, caused by partial or complete cancellation. The LME is more prominent within the interference field, which is limited by the following ranges (Etter, 2013) that are a function of the source depth, Z_S, receiver depth, Z_R, and signal wavelength, λ:

$$Lower\ \ range\ limit \approx 2\sqrt{Z_s Z_r} \quad \text{Eq. 1}$$

$$Higher\ \ range\ limit \approx \frac{4\pi \cdot Z_S Z_R}{\lambda} \quad \text{Eq. 2}$$

For a shallow source (100 meters) and an acoustic sensor at 4 000 m, the lower and upper ranges estimated by these expressions are 1 250 and 67 000 m, respectively, considering a 20-Hz monochromatic wave. Since the particle displacement is free at the ocean surface, the reflected displacement and velocity signal (which are those recorded by geophones in a seismometer) will have the same polarity as the direct signal, but the pressure signal recorded by a hydrophone will be phase-reversed. As a consequence, hydrophone and geophone recordings will show different interference patterns. The seafloor also generates a reflected signal but we will not consider its effect. Ocean-bottom seismometers (OBS) record pressure and particle velocity at a location that is essentially at the seafloor for low frequencies. Therefore, the effect of the surface reflection is expected to dominate. The surface reflection will affect the time and frequency structure of signals, thus changing the expected acoustic signal. This is evident in spectrograms where frequency-dependent interference patterns can be observed. Although the tendency of the LME to affect time/frequency measurements of acoustic signals may be detrimental to some analyses, it can also provide opportunities to obtain data. The LME can be used to provide an estimate of either source depth or range from a receiver, if an *a priori* estimate of one of these variables is available. Using a sample of 20-Hz fin whale calls recorded by one OBS and with estimated ranges from the receiver, this study aimed to: 1) show and analyse differences of call features due to the LME; and 2) estimate the depth of the vocalizing whale.

6.2. METHODS

6.2.1. Recording instruments and dataset

Between August 2007 and July 2008, 24 OBSs were deployed southwest of Portugal to study potential tsunami sources (Fig. 2, Chapter 2). During this time, fin whale calls were also recorded, which have been the target of various studies (Harris *et al.*, 2013; Matias and Harris, 2015). Depths of the recording instruments ranged from 1.993 km to 5.100 km. A

description of the deployment, data recorded, and details about the instruments can be found in Harris *et al.* (2013).

Only the 20-Hz call type was considered in this study. Bouts of 20-Hz fin whale calls were viewed as spectrograms that were calculated with TRITON (Wiggins, 2010). During visual exploratory data analysis of these bouts, high signal-to-noise ratio calls with different spectral features were. It was hypothesized that these differences could be the result of surface interference. One bout was selected and analysed in more detail (taken from OBS12, on November 9th 2007, between 01:00 and 03:00) (Fig. 1).

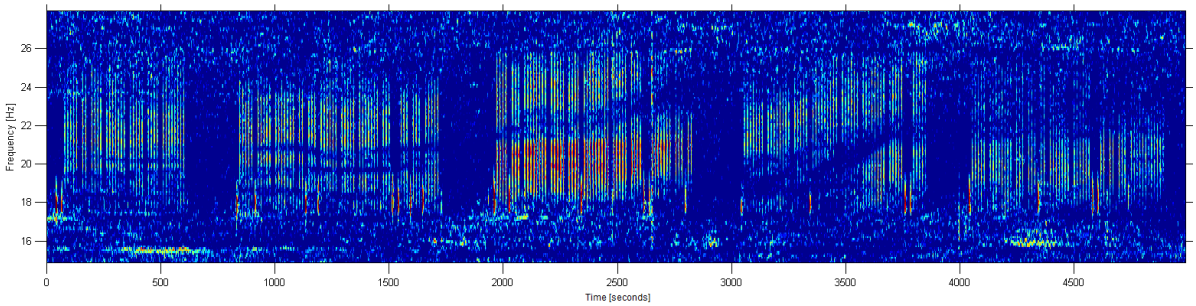

Figure 1. Spectrogram showing 01h23m19s of a fin whale bout where spectra consistent with frequency dependent interference patterns potentially due to LME were pronounced. The complete bout was produced during 3h20m. Backbeats (signals around 18 Hz) were also observed, but were not considered for the analysis. Spectrogram parameters: Frame size – 1 024 samples, 95% overlap, Hanning window, equalized.

6.2.2. Measuring call characteristics

The 20-Hz fin whale calls were identified using a modified normalized cross-correlation equation with a matched filter of the signal waveform, described in detail in Chapter 2. The detection routine also included the calculation of spectral cross-correlation, following the methodology of Mellinger and Clark (2000), described in Chapter 4. A two-dimensional spectrogram synthetic kernel was constructed based on the sound of interest. One day of the dataset when there were 20-Hz calls with high signal-to-noise ratio and high waveform cross-correlation values was selected. The kernel base was derived by summing and averaging the spectra of these calls. The recorded time series was analysed by its cross-correlation with the kernel. This produced a recognition function, which represented the likelihood at each point in time that the sound of interest was present. A threshold was then applied to both the waveform cross-correlation and the spectra function to obtain discrete detection events, times when the sound of interest was likely to be present. For each detection, several spectral and

temporal features were computed based on Hatch and Clark (2004), namely frequency bandwidth, starting frequency, median frequency and signal duration (see Chapter 4 for a full description of each feature). The variation of these features throughout the bout (including when the LME pattern was observed) was assessed by calculating derivatives of the smoothed original data. The resulting derivatives were smoothed again using an average smoothing method.

6.2.3. LME observations

To better examine the spectral differences between calls, the periods of silence between calls were extracted and the calls as individual waveform traces side-by-side along the time axis were plotted (Fig. 2).

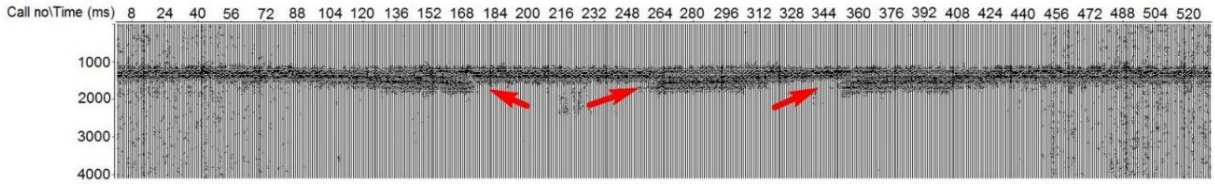

Figure 2. Individual trace of the waveform of each 20-Hz fin whale call of the bout (displayed vertically) through time.

A composite spectrogram of the bout without the periods of silence for the vertical channel (Z-channel) of the OBS was also computed (Fig. 3). Both the plotted waveforms and spectrogram clearly showed an interference pattern. The 20-Hz calls are highly stereotyped. Therefore, when they are produced in sequences both the waveforms and the composite spectrogram show a relatively stable stripe. However, call signals are changed when the surface-reflected path superimposes with the direct path of the call. This results in visible curved interference patterns both in the waveforms and spectrograms, which create a symmetrical “U” shape characteristic of the LME pattern (Hudson, 1983). In order to compare the observed interference pattern with modelled data curves were manually fitted by eye to the interference observed in the composite spectrogram. These curves represented the interpretation of the researcher of the LME pattern. Image dimensions were kept as constant as possible in order to avoid distortions of the interference patterns.

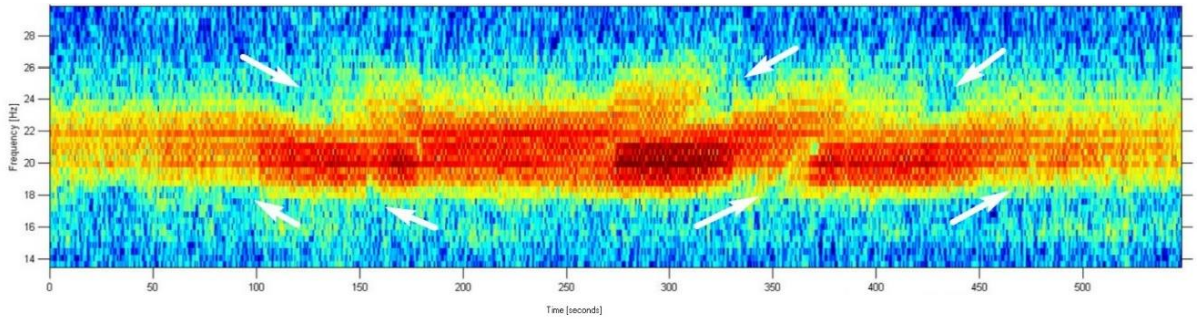

Figure 3. Composite spectrogram of the fin whale bout without periods of silence. Arrows show the features that were interpreted as LME interference patterns. Spectrogram parameters: Frame size – 256 samples, 95% overlap, Hanning window, not equalized. Y-axis, frequency (Hz), x-axis, time (seconds).

The effects of surface reflection on the shape of a 20-Hz call were simulated. For this, a MATLAB code was developed where two synthetic identical pulses were added with an increasing delay that could be caused by a variable depth or by a variable distance between source and receiver. Figure 4 shows the synthetic signals side by side which show a similar interference pattern to the one in Fig. 2.

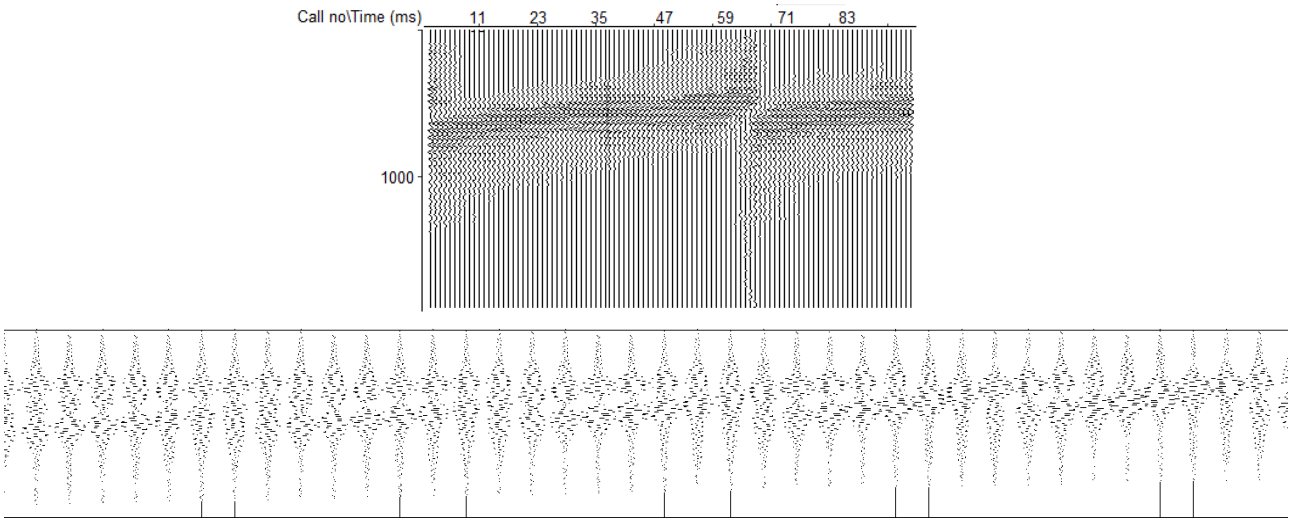

Figure 4. Superposition of two synthetic and identical fin whale 20-Hz calls with a decreasing delay, plotted side by side. Top) General pattern observed in a sequence of calls; Bottom) Zoom in to a group of calls.

6.2.4. Sound source range estimation

A variety of methods have been used to estimate ranges to vocalizing whales from OBS data, including the single-station method (SSM) (Harris *et al.*, 2013), multipath-based

techniques (Wilcock, 2012) and time difference of arrival (TDOA) approaches (Dunn and Hernandez, 2009). Range estimates of each 20-Hz call were obtained considering the difference between the arrival times of the direct signal and the multipath to the same OBS. The majority of the calls within the bout considered for this work were close to, or outside of, the critical range of the SSM (Matias and Harris, 2015) so the SSM was not applicable in this case. Multipath arrivals in this dataset had very small amplitudes, therefore a methodology to enhance the signals using the seismic software SPW was developed (Parallel Geoscience, 1999). The main processing steps were: i) Computation of the envelope of the waveforms using the Hilbert transform. This step transformed the 20-Hz call waveform into a smooth half-sine curve. ii) Signal filtering to enhance all envelopes with a ~0.8 s duration. iii) Since the direct path of the several calls of the bout were not perfectly aligned in time, the cross-correlation between each trace and a "pilot" trace was used to correct the small misalignments. This is a process identified as "residual statics" in seismic processing jargon. iv) An amplitude equalization was applied by automatic gain control to facilitate the picking of the low amplitude multipaths of the 20-Hz calls. The arrival times for the direct path and multipath were picked as smooth continuous lines across the display (Fig. 5). The time difference between the direct path and multipath was converted to a range.

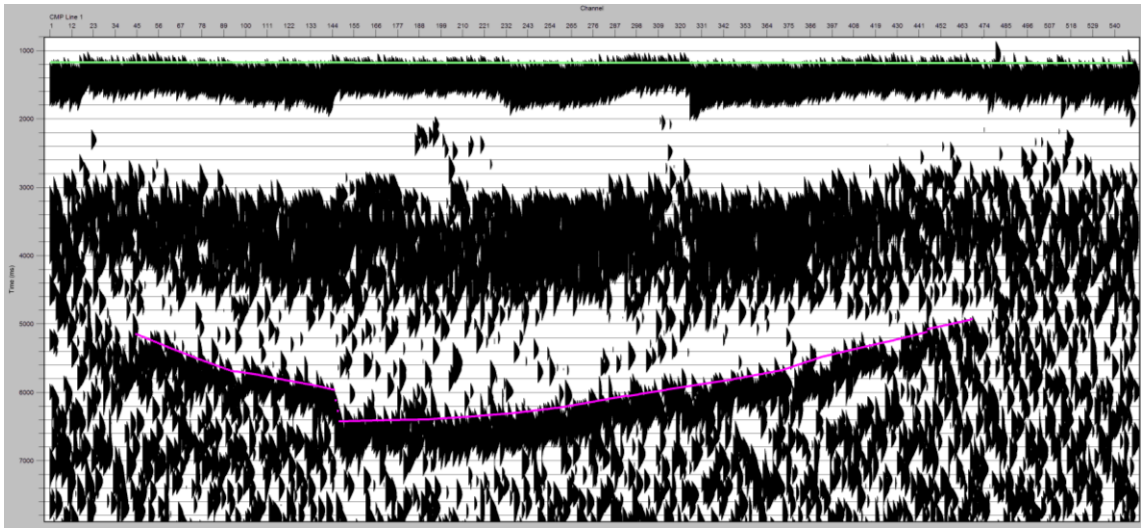

Figure 5. Display of the fin whale bout by SPW after computing the trace envelope and applying a band-pass filter and amplitude equalization. The green trace represents the direct pick times and the pink trace represents the multipath pick times.

All ranges of the fin whale calls in the sampled data were well inside the range where LME was predicted to occur and far from the boundaries defined using Eqns. 1 and 2.

6.2.5. LME modelling

Since the fin whale acoustic data used in this chapter had a range estimate for each individual call, the LME was used to estimate the depth of the vocalizing whale. Considering a whale that produced sequences of 20-Hz calls near a smooth reflecting sea surface, the geometry of the LME is given in Fig. 6.

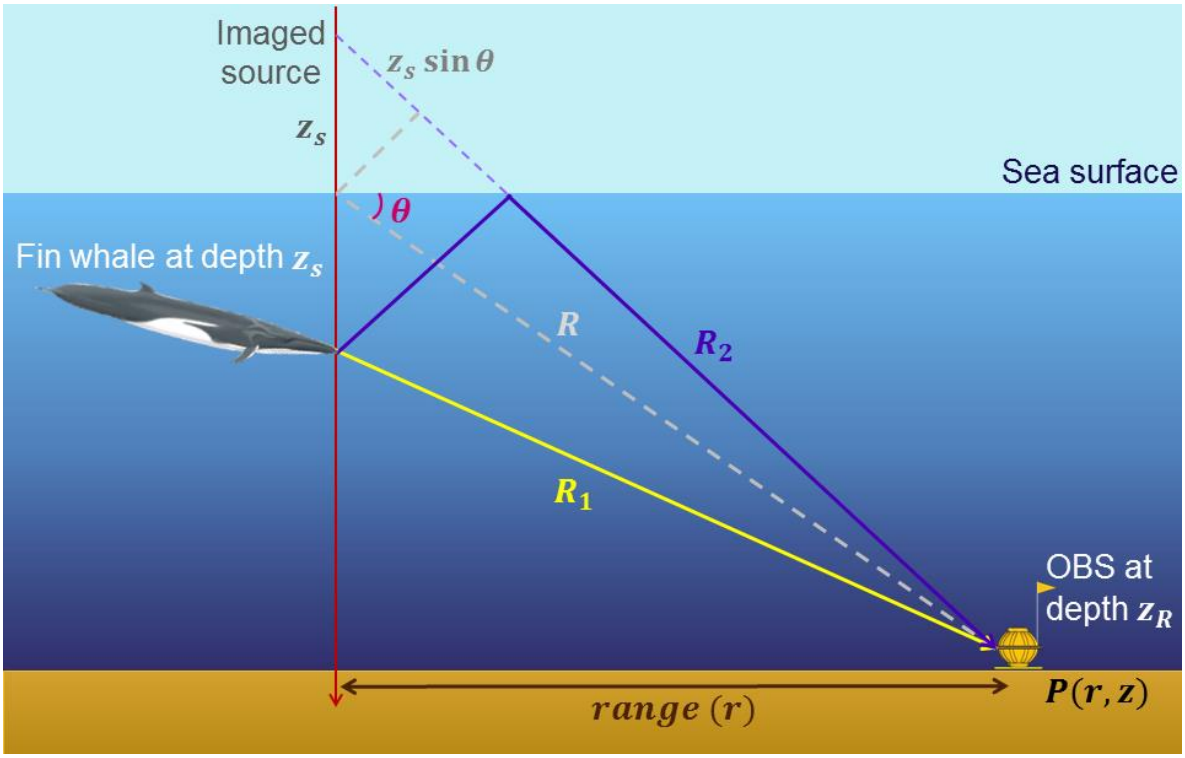

Figure 6. LME geometry with a fin whale as a sound source and the OBS as the receiver instrument. P(r,Z): Total amplitude of a signal at range r and received at depth Z. R1 represents the direct signal path and R2 shows the surface-reflected path.

The travel distances of the direct path, R_1, and the surface-reflected path, R_2, were calculated using Eq. 3 and 4 (Jensen *et al.*, 2011):

$$R_1 = \sqrt{r^2 + (z_R - z_s)^2} \qquad \text{Eq. 3}$$

$$R_2 = \sqrt{r^2 + (Z_R + z_s)^2} \qquad \text{Eq. 4}$$

The total signal amplitude was calculated as the sum of the two sound sources. For a monochromatic wave, this amplitude is given by:

$$P(r,Z) = \frac{e^{ikR_1}e^{-\alpha R_1}}{R_1} + \mu\frac{e^{ikR_2}e^{-\alpha R_2}}{R_2} \quad \text{Eq. 5}$$

Where k is the wave number of a monochromatic wave of wavelength λ (Eq. 6),

$$k = \frac{2\pi}{\lambda} \quad \text{Eq. 6}$$

and α is the frequency-dependent attenuation coefficient (Eq.7) (after Brekhovskikh and Lysanov, 1982):

$$\propto = 3.3 \times 10^{-3} + \frac{0.11f^2}{1+f^2} + \frac{44f^2}{4100+f^2} + 3.0 \times 10^{-4}f^2 \ \ (f \ in \ kHz) \quad \text{Eq. 7}$$

The symbol μ represents the reflection coefficient at the surface. For pressure signal and a perfect reflector μ = -1. For particle velocity signal and a perfect reflector $\mu = 1$.

The transmission loss (TL) due to LME as applied to a fin whale call generated close to the surface and recorded at the seafloor by an OBS was calculated using Eq. 8 and considering a reference pressure of P_{ref} = 1 µPa:

$$TL(r,Z) = -20log\left(\frac{P}{P_{ref}}\right) \quad \text{Eq. 8}$$

For each trial source depth, Eq. 8 was used to compute the TL for all frequencies and ranges of interest and the resulting synthetic spectrogram was plotted. TL models and figures were made using a modified version of the MATLAB code presented in Thompson (2009). The original code modelled TL using a regular range spacing and the altered code used the range estimates of the 20-Hz fin whale calls of this Chapter. Because fin whale calls have a limited frequency band, a cosine taper between 18 and 24 Hz was applied to generate synthetic calls. To make the figures more realistic some random noise was added to the modelled synthetic calls and the colour scale was adjusted in order to generate an image as close as possible to the observations. Synthetic transmission loss models were developed for a sound source (Z_s) varying in depth between 10 and 500 m every 10 m. In order to compare the observed LME pattern with the modelled data, the curves that represented the observed LME pattern were overlaid on each synthetic spectrogram. Depth of the vocalizing whale was estimated by a visual assessment of the fit between the modelled data and the observed LME pattern considering: i) the whole bout; ii) only the most visible part of the interference pattern;

and iii) the most visible part of the interference pattern with altered ranges. For the first analysis, it assumed that the entire bout was produced at a constant depth and the complete interference pattern was compared with the modelled data. To examine if the depth estimate of the first analysis was adequate, then depth was estimated using only the most conspicuous features of the interference pattern. The use of multipaths to estimate range to the calls required a large amount of manual data selection i.e., identifying multipath arrivals. Therefore, the estimated ranges could contain some error. The potential effect of such error on the results was assessed by both increasing and decreasing the estimated ranges by 500 m and re-running the restricted analysis.

6. 3. RESULTS

6.3.1. Analysis of LME changes in call characteristics

During the fin whale bout an LME pattern was interpreted and had three sections where there was a considerable change in the waveform of the 20-Hz calls: at calls #168, #260 and #350 (approximately) (Fig. 3). Those sections corresponded to three periods of the composite spectrogram where the curvatures of the LME pattern occurred: ~150, 300 and 350 seconds (Fig. 3). The smoothed derivative of the call features showed three main areas of change that coincided with the three sections of the LME pattern (Fig. 7). These areas were more pronounced in the signal quality related features. The spectral features were more variable but the smoothed derivative showed an accentuated change in the frequency bandwidth and median frequency. The large variation of the spectral features at the start and end of the bout coincided with the largest estimated ranges between the whale and the sensor and so is likely to be range-related.

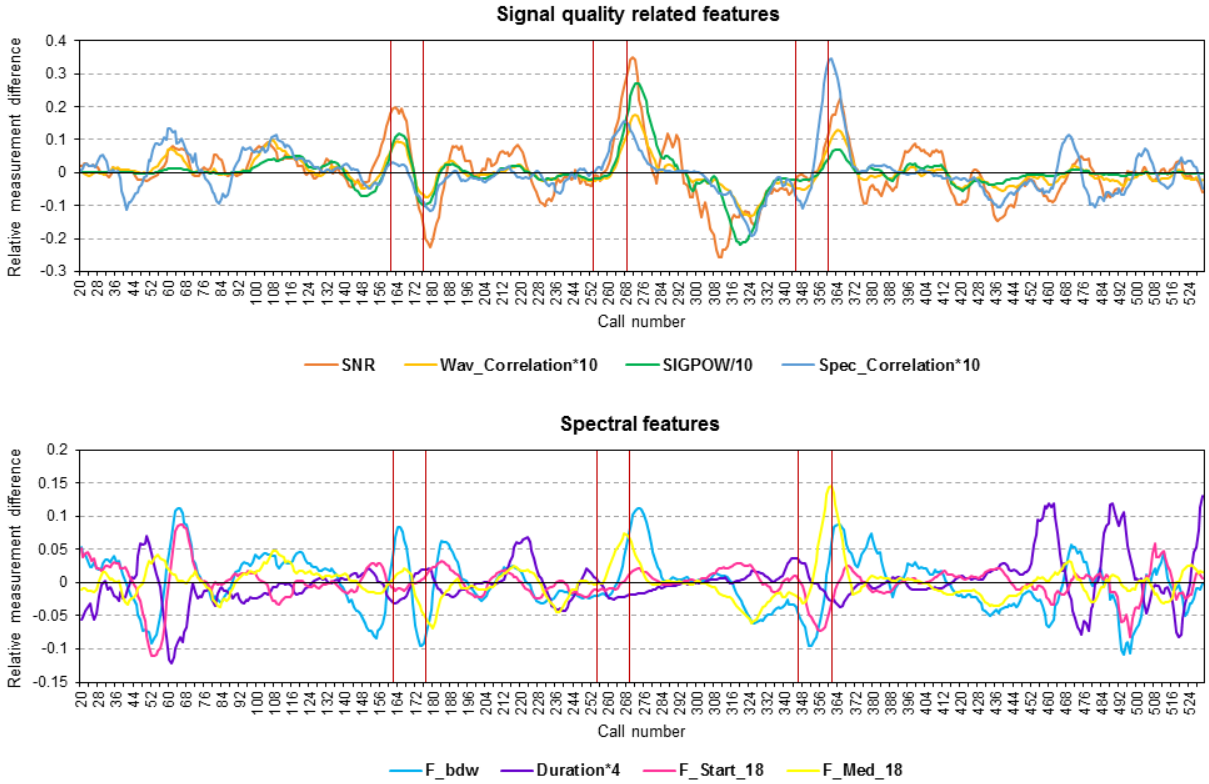

*Figure 7. Smoothed derivative of the features of the 20-Hz fin whale calls. All features except signal-to-noise ratio (SNR) and frequency bandwidth (F_bdw) were scaled to fit in the same plot. Top) Signal quality related features: SNR – Signal-to-noise ratio; Wav_Correlation*10 – Waveform cross-correlation value multiplied by 10; SIGPOW/10 – Signal power divided by 10; Spec_Correlation*10 – Spectrogram correlation value multiplied by 10. Bottom) Spectral features: F_bdw – Frequency bandwidth; Duration*4 – Call duration multiplied by 4; F_Start_18 – Starting frequency, difference to 18 Hz; F_Med_18 – Median frequency, difference to 18 Hz. Vertical red lines represent the areas where the three curves of the interference pattern occurred. When the original data showed peaks the derivative is 0. When the curve of the derivative is positive there was an increasing tendency in the original data. If it is negative then there was a decreasing tendency.*

6.3.2. Inference of depth of the vocalizing whale

Even after the signal enhancement and additional processing treatment with the seismic software SPW, not all multipaths of the calls could be identified. Therefore, further analysis of the LME was restricted to the individual traces where range could be estimated, and a new composite spectrogram was created (Fig. 8). Despite removing parts of the bout (e.g., Fig. 8 at 125 s), there was a clear symmetry in the pattern displayed.

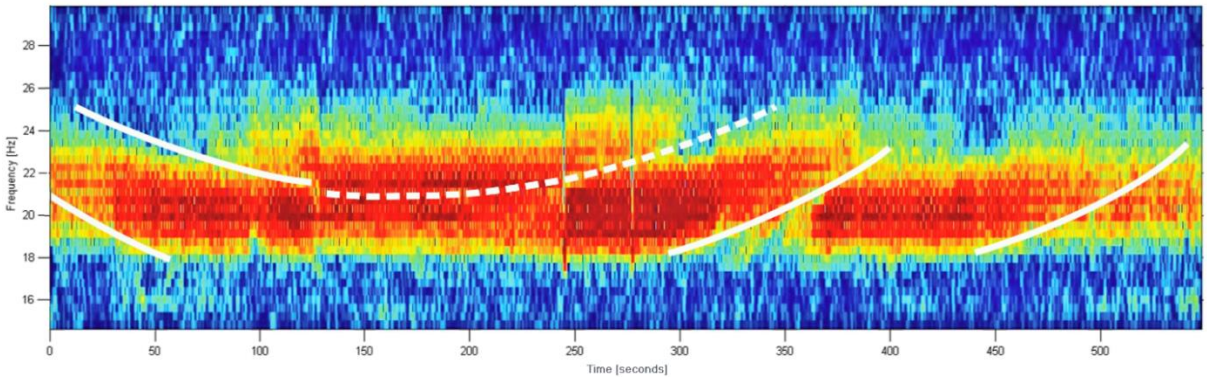

Figure 8. Composite spectrogram of the fin whale bout without 20-Hz calls that had no range estimate. White curves represent our interpretation of the LME interference pattern fitted by eye. Thick curves represent our most certain interpretation of the interference pattern. Dashed curve represent uncertainty in the continuity of the thick curve. Spectrogram parameters: Frame size – 256 samples, 95% overlap, Hanning window, not equalized.

The closest synthetic transmission loss models to the observations were the ones with a source depth between 330 and 350 m (Fig. 9, right). Models with shallower depths did not show very prominent interference patterns (Fig. 9, left).

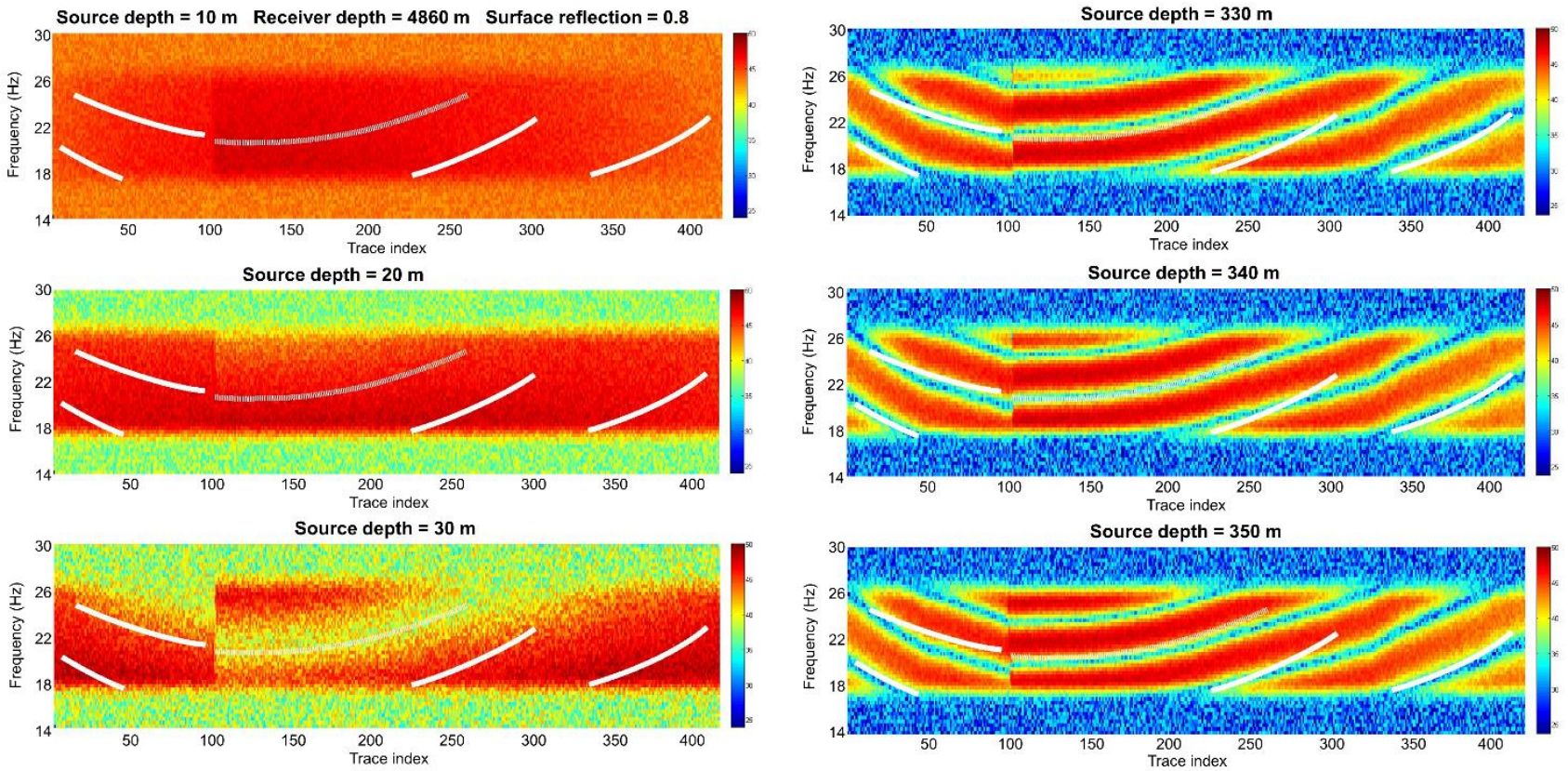

Figure 9. TL models for the LME with a varying source depth with the interference patterns identified in the composite spectrogram of the fin whale calls (white lines). Left from top to bottom) transmission loss models for source depths of 10, 20 and 30 m respectively; Right from top to bottom) transmission loss models for source depths of 330, 340 and 350 m respectively.

6.3.3. Depth estimation using part of the bout with the most visible interference

In this second analysis, the depth of the vocalizing whale was estimated at ~40 m (Fig. 10, left). The model with an estimated depth of ~340 m no longer matched the observed lower curve (Fig. 10, right).

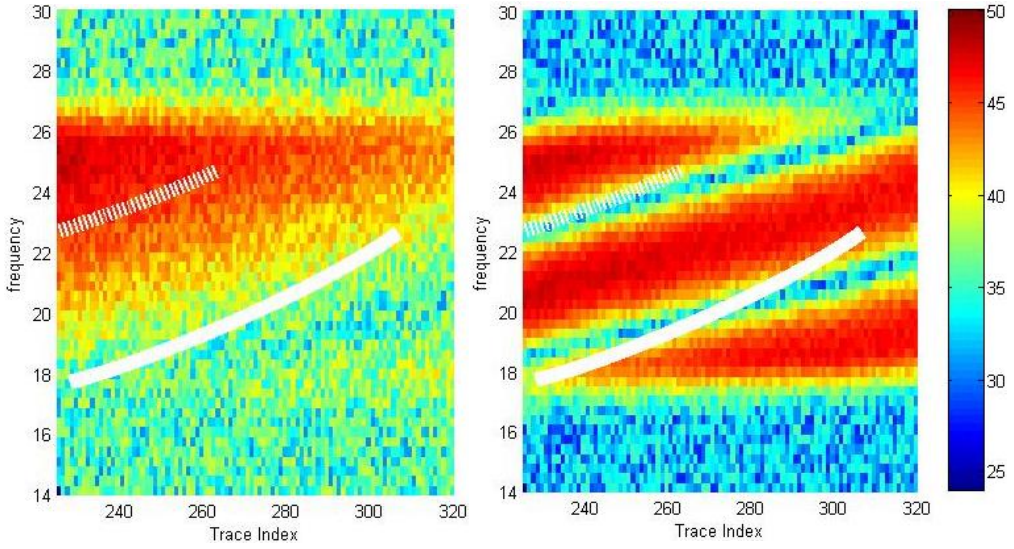

Figure 10. Best visual fit obtained by comparing the most prominent part of the interference pattern identified in the composite spectrogram of the fin whale calls (thick white line) with a transmission loss model for the LME with a source depth of 40 m (left) and 340 m (right). The dashed line starting at 23 Hz represented part of the interference pattern that was not considered for this part of the analysis because of its uncertainty.

The TL models calculated with altered ranges obtained for shallow source depths (up to 30 m) did not match the observed interference pattern. There were no significant changes in the interference patterns and the models with depths around 35-45 m retained the best fit (Fig. 11).

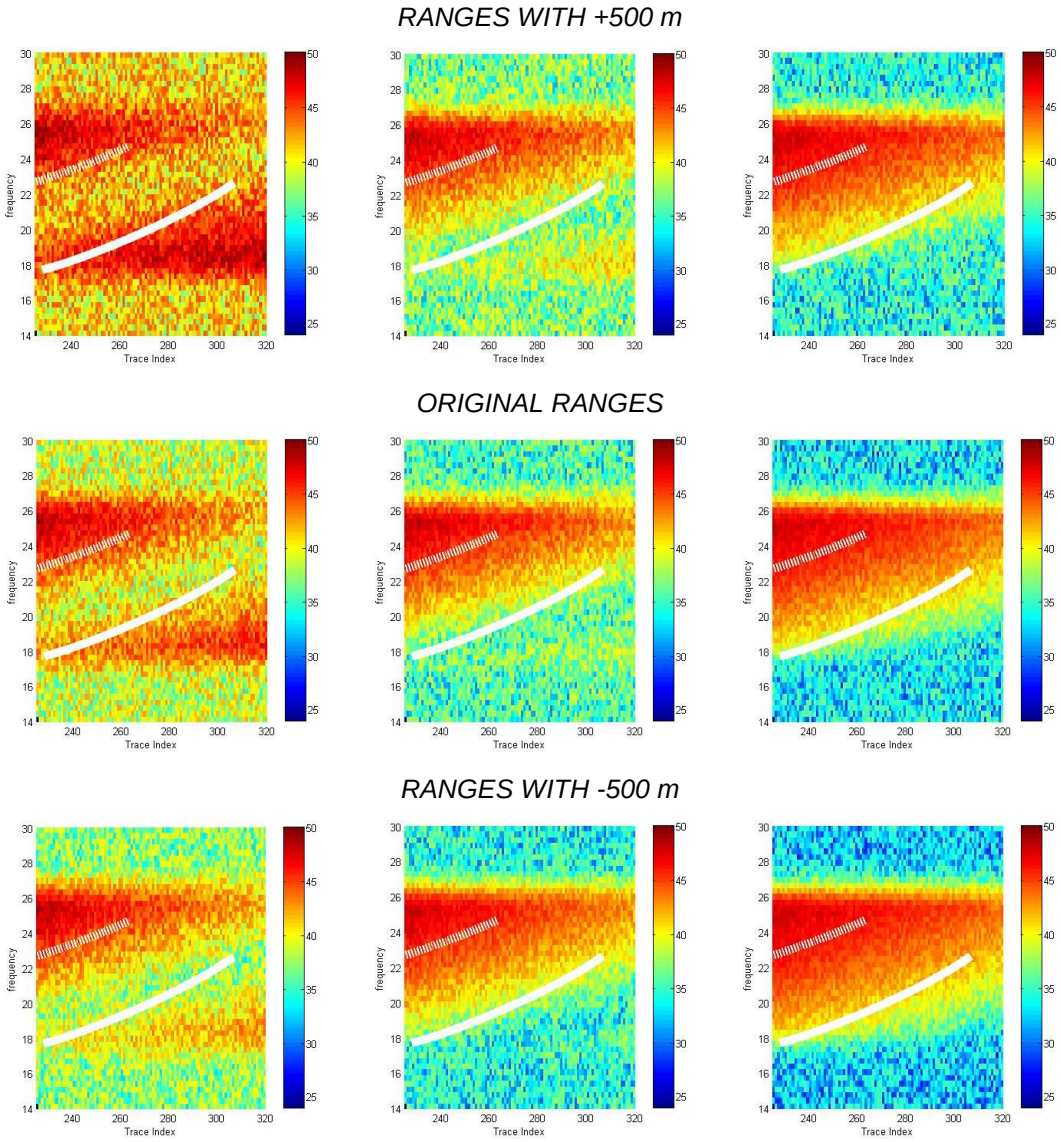

Figure 11. Best visual fit models obtained by comparing the most prominent part of the interference pattern (thick white lines) with a transmission loss model for the LME with a sound source depth of 35 m (left), 40 m (center) and 45 m (right) and a deviation of 500 m from the original estimated ranges. The dashed line represented part of the interference pattern that was not considered for this part of the analysis because of its uncertainty.

6.4. DISCUSSION

An understanding of acoustic propagation of biological signals in the ocean is crucial for studies of marine mammal sounds that rely on high quality and accurate characterization of the signals. Some characteristics associated with biological factors might be artefacts of propagation. For example, Premus and Spiesberger (1996) demonstrated that multipath propagation could explain the production of the 20-Hz doublets by fin whales in the Gulf of California. Measurement error might also occur due to interference caused by propagation. For example, inaccurate estimates of sound source levels have been related with the occurrence of LME (Charif *et al.*, 2002). Here, accentuated changes in the frequency bandwidth and median frequency occurred at the same time as curved patterns in the spectrogram, characteristic of the "U" shape of the LME fringes. These results further suggested that LME can cause signal change and thus alter signal features that can be used to investigate spatiotemporal variation in stereotyped marine mammal vocalizations. The frequency of occurrence and the extent of impact of the LME on studies that characterize signals of cetaceans remains unknown.

From the initial approach of estimating the depth of the entire bout, a depth of ~340 m was obtained, which is in agreement with the current knowledge of diving behaviour of fin whales but not with their vocal activity. Aroyan *et al.* (2000) argue that the depth at which baleen whales call is limited by the volume of air required to produce the sound, a volume which decreases with depth due to increasing hydrostatic pressure. Fin whales can dive up to 470 m (Panigada *et al.*, 1999) and the deepest dives are typically feeding dives (Goldbogen *et al.*, 2006). However, vocal activity of fin whales is thought to occur at shallower depths. Tagged fin whales off Southern California showed that individuals called at depths down to approximately 15-20 m (Stimpert *et al.*, 2015). Behavioural descriptions from Watkins *et al.* (1987) reports depths of ~50 m for vocalizing whales. For the 340 m estimated vocalizing depth, it was assumed a constant depth for the entire bout, which is likely to be an unrealistic assumption. When the depth of only the most visible interference pattern was estimated, the best fit model was the one with depths around 35-45 m, which is in the range of previously estimated vocalizing depths for fin whales. None of the models supported a depth between 10-30 m.

There were sources of potential bias and uncertainty in these analyses that require discussion. Firstly, the transmission loss models depended on the estimated ranges of the calls. All ranges of the fin whale calls in the data used in this Chapter were well inside the range where LME was predicted to occur and far from the boundaries defined using Eqns 1 and 2. A bias in the estimated ranges could occur because of small processing errors in the

manual part of the methodology. However, the tests with a 500 m deviation in range showed that TL models did not change significantly. These results suggested that the models may tolerate some level of measurement error in the range estimates, though a more thorough investigation is required. Secondly, the interference curves were identified by eye and no quantitative model fitting routine was implemented to find the model with the best fit to the observed interference patterns. A more developed analysis with automated identification of interference curves and model fit, in addition to a review of the transmission loss model, should be undertaken in order to verify the results about the LME in fin whale calls and its use to infer the depth of vocalizing whales.

6.5. REFERENCES

Aroyan, J. L., McDonald, M. A., Webb, S. C., Hildebrand, J. A., Clark, D., Laitman, J. T., and Reidenberg, J. S. (**2000**). “Acoustic models of sound production and propagation,” in Hearing by Whales and Dolphins, edited by W.W.L. Au, A.N. Popper, and R.R. Fay (Springer, New York, USA), pp. 409–469.

Brekhovskikh, L., and Lysanov, Y. (**1982**). *Fundamentals of Ocean Acoustics* (Springer-Verlag, Berlin, Germany).

Castellote, M., Clark, C. W., and Lammers, M. O. (**2011**). “Fin whale (*Balaenoptera physalus*) population identity in the western Mediterranean Sea,” Marine Mammal Science **28**, 325–344.

Charif, R. A., Mellinger, D. K., Dunsmore, K. J., Fristrup, K. M., and Clark, C. W. (**2002**). “Estimated sound source levels of fin whale (*Balaenoptera physalus*) vocalizations: adjustments for surface interference,” Marine Mammal Science **18**, 81–98.

Clark, C. W., Borsani, J. F., and Notarbartolo-di-Sciara, G. (**2002**). “Vocal activity of fin whales, *Balaenoptera physalus*, in the Ligurian Sea,” Marine Mammal Science **18**, 281–285.

Delarue, J., Todd, S. K., VanParijs, S. M., and DiIorio, L. (**2009**). “Geographic variation in Northwest Atlantic fin whale (*Balaenoptera physalus*) song: Implications for stock structure assessment,” Journal of the Acoustical Society of America **125**, 1774–1782.

Dunn, R. A., and Hernandez, O. (**2009**). “Tracking blue whales in the eastern tropical Pacific with an ocean-bottom seismometer and hydrophone array,” Journal of the Acoustical Society of America **126**, 1084–1094.

Etter, P. C. (**2013**). *Underwater Acoustic Modeling and Simulation* (CRC Press, Taylor and Francis Group, Boca Raton, USA).

Goldbogen, J. A., Calambokidis, J., Shadwick, R. E., Oleson, E. M., McDonald, M. A., and Hildebrand, J. A. (**2006**). "Kinematics of foraging dives and lunge-feeding in fin whales," Journal of Experimental Biology **209**, 1231–1244.

Harris, D., Matias, L., Thomas, L., Harwood, J., and Geissler, W. H. (**2013**). “Applying distance sampling to fin whale calls recorded by single seismic instruments in the Northeast Atlantic,” Journal of the Acoustical Society of America **134**, 3522–3535.

Hatch, L. T., and Clark, C. W. (**2004**). “Acoustic differentiation between fin whales in both the North Atlantic and North Pacific Oceans, and integration with genetic estimates of divergence,” Paper presented to the IWC Scientific Committee, Sorrento, Italy, July, Paper No. SC/56/SD6, pp. 1–37.

Hudson, R. F. (**1983**). “A Horizontal Range vs. Depth Solution of Sound Source Position under General Sound Velocity Conditions using the Lloyd's Mirror Interference Pattern,” M.Sc. dissertation, Naval Postgraduate School, Monterey, USA, pp. 1–67.
Jensen, F. B., Kuperman, W. A., Porter, M. B., and Schmidt, H. (**2011**). *Computational Ocean Acoustics* (Springer Science+Business Media, New York, USA).

Mathworks (**2012**). The Mathworks, Inc., Cambridge, U.K. http://www.mathworks.co.uk (Last viewed 31st January, 2018).

Matias, L., and Harris, D. (**2015**) "A single-station method for the detection, classification and location of fin whale calls using ocean-bottom seismic stations," Journal of the Acoustical Society of America **138**, 504–520.

McDonald, M. A., Mesnick, S. L., and Hildebrand, J. A. (**2006**). “Biogeographic characterization of blue whale song worldwide: Using song to identify populations,” Journal of Cetacean Research and Management **8**, 55–65.

Mellinger, D. K., and Clark, C. W. (**2000**). “Recognizing transient low frequency whale sounds by spectrogram correlation,” Journal of the Acoustical Society of America **107**, 3518–3529.

Panigada, S., Zanardelli, M., Canese, S., and Jahoda, M. (**1999**). "How deep can baleen whales dive?," Marine Ecology Progress Series **187**, 309–311.

Parallel Geoscience. (**1999**). SPW - Parallel Seismic Processing, Incline Village, USA http://www.parallelgeo.com/?q=product&p=SPW (Last viewed 207th September 2016).

Premus, V., and Spiesberger, J. L. (**1997**). “Can acoustic multipath explain finback (*B. physalus*) 20-Hz doublets in shallow water?” Journal of the Acoustical Society of America **101**, 1127–1138.

Soule, D. C., and Wilcock, J. S. (**2013**). “Fin whale tracks recorded by a seismic network on the Juan de Fuca Ridge, Northeast Pacific Ocean,” Journal of the Acoustical Society of America **133**, 1751–1761.

Stimpert, A. K., DeRuiter, S. L., Falcone, E. A., Joseph, J., Douglas, A. B., Moretti, D. J., et al. (**2015**). "Sound production and associated behavior of tagged fin whales (*Balaenoptera physalus*) in the Southern California Bight," Animal Biotelemetry **3**, 23.

Thompson, S. R. (**2009**). “Sound propagation considerations for a deep-ocean acoustic network,” M.Sc. dissertation, Naval Postgraduate School, Monterey, USA, pp. 1–82.

Watkins, W. A., Tyack, P., and Moore, K. E. (**1987**). “The 20-Hz signals of finback whales (*Balaenoptera physalus*),” Journal of the Acoustical Society of America **82**, 1901–1912.

Wiggins, S. M., Roch, M. A., and Hildebrand, J. A. (**2010**). “TRITON software package: Analyzing large passive acoustic monitoring data sets using MATLAB,” *Journal of the Acoustical Society of America* **128**, 2299.

Wilcock, W. S. D. (**2012**). “Tracking fin whales in the northeast Pacific Ocean with a seafloor seismic network,” Journal of the Acoustical Society of America **132**, 2408–2419.

CHAPTER 7

GENERAL DISCUSSION

Ocean-bottom seismometers (OBS) are designed to locate earthquakes and to study the earth's structure (Frank and Ferris, 2011). Depending on the instrument configurations and recording parameters, some can provide acoustic recordings over long periods of time and cover large geographical areas. The low sampling rate at which these long-term instruments record, which can be between 40 and 100 Hz (Havskov and Ottemoller, 2010), enables them not only to record their target data but also to record low frequency biological sounds, such as baleen whale sounds (Mellinger *et al.*, 2007). Baleen whales, more specifically fin and blue whales, are species that have extensive geographic distribution ranges and occur during some part of the year in pelagic waters (Aguilar, 2002), which makes them difficult to study with traditional, often ship-based, methods. OBS can provide valuable information for the study of large cetaceans that would otherwise be difficult to obtain due to economic and logistic reasons. With the large amount of OBS deployed across the world's oceans, there are still many seismological datasets potentially useful for the study of baleen whales left to explore.

Fin whales have a conservation status of 'Endangered' at a worldwide (Reilly *et al.*, 2013) and Portuguese (Queiroz *et al.*, 2006) level. They were one of the main targets of modern whaling and some populations were severely depleted by intensive hunting activities (Clapham and Baker, 2002; Reilly *et al.*, 2013). Although in some areas populations show signs of recovery, the status of recovery on other populations is still uncertain (Reilly *et al.*, 2013). One of these cases is the south of the Iberian Peninsula, where fin whales were once abundant and showed a year-round occurrence (Sanpera and Aguilar, 1992). Recent records suggest that abundance is still small compared with the relative abundance recorded during the whaling period between the 19th and 20th centuries (Clapham and Baker, 2002). Therefore, it is crucial to gather information about fin whale spatial and temporal patterns in order to better assess its status.

The main goal of this thesis, which was to demonstrate the use of acoustic datasets, such as seismic datasets, that were not collected for biological studies, to study fin whales, was fully accomplished. The NEAREST project that aimed to study potential tsunami sources from a set of 24 OBS deployed off southwest Portugal (Silva *et al.*, 2017), provided data that

were used to study different aspects of fin whale ecology in the study area, during a 11 month period.

In Chapters 2 and 3, a software program (SEISAN) and location method (the single station method), which were developed for seismic studies, were useful tools to detect the main call produced by fin whales, the 20-Hz call and to estimate the ranges to the calling fin whales. Chapter 4 provided the first results about the acoustic presence of fin whales with 11 months of data off southwest Portugal and showed the occurrence of two different acoustic groups. In Chapter 5, the work initiated with the Cheap DECAF project regarding fin whale abundance estimates was further expanded and an animal abundance estimate was obtained using distance sampling. Chapter 6 showed the use of the pattern caused the Lloyd's Mirror Effect, an acoustic interference in the 20-Hz calls, to infer the depth of the calling whale.

The routine implemented in *SEISAN* to detect fin whale calls, in Chapter 2, had better performance than the detection process included in the software *Ishmael*, which is a software widely used by bioacousticians (Mellinger, 2002). The detector could be adapted depending on the purpose of the detection results. If, for example the aim of the study is to detect the presence of a rare species, then the detector should be developed with settings that maximizes the detection of the signal of that species, even if that meant a high proportion of false positives. In studies where the aim is to track a calling animal, it may not be necessary to have the highest proportion of true positives, as long as the direction and the changes of tracks are being well represented. However, an effort to reduce the proportion of false positives should be made in order to avoid the potential bias caused by false positives. The final result of Chapter 2 showed that a balanced detector, which resulted in a high number of true positive detections (although not the maximum) with the least number of false positives produced a dataset that was suitable for different types of studies that were developed in the following chapters. The task included in this thesis which aimed to develop a detection process of the 20-Hz fin whale call was achieved. One future task would be to evaluate a routine that identifies sequences of 20-Hz fin whale calls. A routine that classifies earthquake aftershocks, i.e. a smaller earthquakes that occur after a previous large earthquake, was modified in order to extract sequences of fin whale calls (Matias, 2015). The detections made from the detection algorithm were grouped based on the time interval between detections. Another aspect that needs to be considered and it is not part of the routine yet is the possibility of simultaneous calling whales. In this case, in addition to the time interval between detections, the similarity between the amplitude of calls and their spectral parameters could be helpful. This routine was not included in any part of the analysis of this thesis and only preliminary tests have been made so far. This routine will provide an automated process that groups 20-Hz fin whale calls into sequences, which will be very helpful in studies of acoustic

characterization, where sequences are used to evaluate characteristics of the signals, and studies about animal movement, which is evaluated using extended bouts. Another future task would be to evaluate other detection techniques to detect backbeats. Backbeats are low frequency narrow-band signals between 15 to 18 Hz that are almost always produced in between 20-Hz calls (Watkins, 1981). Although not presented in Chapter 2, a detection routine based on the matched-filtering technique presented in Chapter 2 for backbeats was also undertaken. However, because backbeats vary considerably in amplitude, the detection routine worked less well (low number of true positives with high number of false positives) as it worked for the 20-Hz fin whale call. The detection process of the backbeat was not completed and could be included in future work. A detection of backbeats based on energy sum or spectrogram cross-correlation could be evaluated. After the acquisition of a large enough sample of backbeats, an assessment of its characteristics, as it was done in Chapter 4 for the 20-Hz call, will be possible.

The single-station method applied in Chapter 3 provided relative locations of the calling fin whales that formed distinct tracks. The classification scheme developed in that Chapter was used to decide if: 1) a call was a true positive (detection from the 20-Hz call), state a, and 2) a detection was produced inside the range where the single-station method worked correctly (within the critical range), state b. The classification scheme was initiated by Matias and Harris (2015) and was further assessed in this thesis. However, the classification scheme needs further work. Although the classification of state a was accomplished, there were several uncertainties regarding classification state b. The classification scheme developed by Matias and Harris (2015) was not optimal for the classification of detections of the representative subsample used in Chapter 3. In Matias and Harris (2015) the sample used in the analysis was very small and it was not representative of all conditions. Because the true locations of fin whales in this thesis were unknown, the classification type b was based on some assumptions of the relationship between cross-correlation (C.Max) and distance from the instruments. C.Max consisted in the cross-correlation between a template of the target signal of detection and the waveform of the acoustic recordings. Another parameter that was crucial for the classification scheme and distance sampling analysis was the coherency factor (Co). This factor reflects the quality of the angles calculated by the three-component method, the apparent emergence angle and the instrument-source azimuth (Roberts *et al.*, 1989). By doing this, it also provides an indication of whether the detections are inside the critical range or not. Matias and Harris (2015) showed that detections with positive values of coherency values were inside the critical range of the single station. When detections showed negative values of coherency, theythey could have been produced very close or above the OBS or outside the critical range. The point inside the critical range where

negative coherency at close ranges changes to positive is still unknown. Results from Chapter 3 suggested that detections with higher correlation values were potentially produced at close ranges, while detections with lower values were potentially produced further away. However, it is worth noting that this relationship was based on detections that showed positive coherency. A validation study with a sample of detections with known true locations is needed in order to confirm the relationship between C.Max and distance, and to assess the variation of coherency inside the critical range. Additional parameters based on the polarization measurements of the signal evaluate .its linearity. These parameters have been added to the latest version of the algorithm and their potential in classifying close detections where the coherency is less useful needs to be evaluated with a representative sample.

Future studies about deciding if a call is inside the critical range of the single station or not are probably the most necessary because accurate fin whale abundance estimates based on distance sampling analysis are influenced by the classification scheme applied, when using the single station method.

The acoustic characterization presented in Chapter 4 showed the presence of two acoustic groups with characteristics identified by Castellote *et al.* (2011) as 'North Atlantic' fin whales and 'Mediterranean' fin whales. Although there is an increasing amount of evidence of the division between these two groups (see Chapter 1), the degree of geographical overlap and interchange between them is still subject of great discussion. The results of Chapter 4 provided results of acoustic presence throughout a year of fin whales off southwest Portugal and also contributed to the understanding of the acoustic overlap between the two groups mentioned above. The acoustic presence of 'Mediterranean' fin whales was not only extended from the range already observed, but there was also an extension of the overlap between these two groups, as on one occasion both groups of acoustic characteristics were recorded simultaneously. The 'Mediterranean' acoustic group was detected with a 20-Hz call template based on 'North Atlantic' characteristics. Future work could include running the detector with a template from the 'Mediterranean' acoustic group in the 11 months of recording in order to better assess the presence of this group. An analysis of the movements of both groups would also give crucial information about the spatial patterns of these whales.

Efforts to obtain a fin whale abundance estimate with the NEAREST OBS dataset was initiated by the Cheap DECAF project (Harris *et al.*, 2014). The final report of the project focused more on the spatial density and, because a cue rate was not available at the time, it was not possible to obtain an animal abundance based on distance sampling analysis. At the time of this thesis, adjustments to the ranges calculated with the single-station had been developed by Matias and Harris (2015) and a cue rate calculated with the data available in

Stimpert *et al.* (2015) was also available. The results in Chapter 5 expanded the work of the Cheap DECAF project by including these two aspects in the distance sampling analysis. An average fin whale abundance was estimated in Chapter 5 but it is likely to contain bias caused by different aspects of the analysis, mostly from aspects of the classification scheme and application of a cue rate from another study site and time periodThe most recent fin whale abundance estimates were obtained at a European scale and for a particular time of the year (e.g. SCANS III, Hammond *et al.*, 2017). For projects with such a large scale that aim to obtain abundance estimates for several species, it is logistically and economically difficult to obtain data for different seasons and particular groups of a species. Future work would be to obtain a fin whale abundance for all the seasons of the OBS recordings used in this thesis. The inclusion of the number of detections of the non-localizing OBS in the abundance estimates, in order to reduce variance, could also be considered. Results like those presented in Chapter 5 constitute valuable sources of information for habitat modelling to predict distribution and critical habitats of a species.

Chapter 6 showed that acoustic interference can cause changes to acoustic signals, but can also be used to infer the depth of the calling whales. The frequency of the changes caused by the Lloyd's Mirror Effect is unknown, but results from Chapter 6 show that it is an aspect that needs to be considered when characterizing an acoustic signal. This is of special importance when the characteristics of these signals are being used to assess acoustic variation that may reflect differences in geographical areas. Future work on this matter could include a large sample to assess the occurrence of the Lloyd's Mirror Effect. Furthermore, automated methods to perform the matching of the transmission loss models with the spectrograms of the recordings could be undertaken. This task would enable the processing of more data and would reduce the possible bias caused by the manual processing.

The NEAREST OBS data provided information about the acoustic characteristics and presence of the fin whale off southwest Portugal. It also provided data that were used to obtain an abundance estimate of fin whales and to understand their calling behaviour. These aspects are crucial to evaluate the status of a stock and to assess the importance of a geographical area to a species. Although some results of this thesis contain potential bias, they provide novel information about an endangered species that is poorly studied in Portuguese waters. The large spatial and temporal coverage of OBS and the types of data that can be obtained by their recordings show that these instruments are valuable tools to the conservation of cetaceans. This thesis showed how OBS data can be used in different types of studies about fin whales and provide valuable information for their conservation. This thesis also established

the foundations on which future work can be developed to profit from the opportunistic recordings of whale vocalizations made by OBS, particularly from sparse networks of instruments.

REFERENCES

Aguilar, A. (**2002**). “Fin whale (*Balaenoptera physalus*),” in Encyclopedia of Marine Mammals, edited by W.F. Perrin, B. Würsig, and J.G.M. Thewissen (Academic Press, San Diego, USA), pp. 435–438.

Castellote, M., Clark, C. W., and Lammers, M. O. (**2011**). “Fin whale (*Balaenoptera physalus*) population identity in the western Mediterranean Sea,” Marine Mammal Science **28**, 325–344.

Clapham, P. J. and Baker, C. S. (**2002**). “Modern whaling,” in Encyclopedia of Marine Mammals, edited by W.F. Perrin, B. Würsig, and J.G.M. Thewissen (Academic Press, San Diego, USA), pp. 1328–1332.

Frank, S. D., and Ferris, A. N. (**2011**). "Analysis and location of blue whale vocalizations in the Solomon Sea using waveform amplitude data," Journal of the Acoustical Society of America **130**, 731–736.

Hammond, P. S., Lacey, C., Gilles, A., Viquerat, S., Börjesson, P., Herr, H., et al. (**2017**). Estimates of cetacean abundance in European Atlantic waters in summer 2016 from the SCANS-III aerial and shipboard surveys," Research report, St. Andrews, UK, https://synergy.st-andrews.ac.uk/scans3/- (Last viewed 24th April 2018).

Harris, D. V., Matias, L., and Thomas, L. (**2014**). Cheap DECAF: Density Estimation for Cetaceans from Acoustic Fixed Sensors Using Separate, Non-Linked Devices Final project report, http://www.dtic.mil/docs/citations/ADA610894 (Last viewed 21st April 2018). 17 pp.

Havskov J., Ottemöller L. (**2010**). *Routine Data Processing in Earthquake Seismology* (Springer Science+Business Media B.V., Dordrecht, The Netherlands).

Matias, L. (2015) personal communication.

Matias, L., and Harris, D. (**2015**) "A single-station method for the detection, classification and location of fin whale calls using ocean-bottom seismic stations," Journal of the Acoustical Society of America **138**, 504–520.

Mellinger, D. K., Stafford, K. M., Moore, S. E., Dziak, R. P., and Matsumoto, H. (**2007**) "An Overview of Fixed Passive Acoustic Observation Methods for Cetaceans," Oceanography **20**, 36–45.

Mellinger D. K. (**2002**) ISHMAEL: Integrated system for holistic multi-channel acoustic exploration and location. Pacific Marine Environmental Laboratory, Newport, OR. http://www.bioacoustics.us/ishmael.html (Last viewed 12th February 2018).

Queiroz, A. I., Alves, P. C., Barroso, I., Beja, P., Fernandes, M., Freitas, L., et al. (**2006**). "*Balaenoptera physalus* Baleia-comum," in Livro Vermelho dos Vertebrados de Portugal edited by M.J. Cabral, J. Almeida, P.R. Almeida, T. Dellinger, N. Ferrand de Almeida, M.E. Oliveira et al. (Instituto da Conservação da Natureza/Assírio & Alvim, Lisboa, Portugal) pp. 511-512.

Reilly, S. B., Bannister, J. L., Best, P. B., Brown, M., Brownell Jr., R. L., Butterworth, D. S., et al. (**2013**). "*Balaenoptera physalus*," in IUCN 2017. IUCN Red List of Threatened Species. Version 2017.3, http://www.iucnredlist.org (Downloaded 31th January, 2018).

Roberts, R. G., Christoffersson, A., and Cassidy, F. (**1989**). "Real time events detection, phase identification and source location estimation using single station component seismic data and a small PC," Geophysical Journal International **97**, 471–480.

Sanpera, C., and Aguilar, A. (**1992**). "Modern whaling off the Iberian Peninsula during the 20th century," Reports of the International Whaling Commission **42**, 723–730.

Silva, S. D. M. M. F. (**2017**). "Strain partitioning and the seismicity distribution within a transpressive plate boundary: SW Iberia-NW Nubia," Ph.D. dissertation, University of Lisbon, Lisbon, Portugal.

Stimpert, A. K., DeRuiter, S. L., Falcone, E. A., Joseph, J., Douglas, A. B., Moretti, D. J., et al. (**2015**). "Sound production and associated behavior of tagged fin whales (*Balaenoptera physalus*) in the Southern California Bight," Animal Biotelemetry **3**, 23.

Watkins, W. A. (**1981**). "Activities and Underwater Sounds of Fin Whales," Scientific Reports of the Whales Research institute **93**, 83–117.